Heavy Metal Incorporation into Benthic Foraminifera and Tropical Corals

Dissertation

zur Erlangung des Doktorgrades
Dr. rer. nat.

der Mathematisch-Naturwissenschaftlichen Fakultät
der Christian-Albrechts-Universität zu Kiel

vorgelegt von

Sarina Schmidt

Kiel, 2021

Erster Gutachter: Prof. Dr. Martin Frank

Zweiter Gutachter: Prof. Dr. Sigal Abramovich

Eingereicht am: 2. Dezember 2021

Erklärung

Hiermit erkläre ich des Eides statt, dass ich die vorliegende Abhandlung, abgesehen von der Beratung durch meine Betreuer, nach Inhalt und Form selbstständig erarbeitet habe und keine anderen als die von mir aufgeführten Quellen und Hilfsmittel verwendet wurden.

Diese Arbeit ist unter Einhaltung der Regeln guter wissenschaftlicher Praxis der Deutschen Forschungsgemeinschaft entstanden und wurde weder in Auszügen noch in ganzer Form an einer anderen Stelle im Rahmen eines Prüfungsverfahrens eingereicht.

Teile dieser Arbeit wurden zur Veröffentlichung in einer Fachzeitschrift eingereicht oder sind in Vorbereitung eingereicht zu werden.

Es wurde kein akademischer Grad entzogen.

Kiel, den 2. Dezember 2021

Sarina Schmidt

Abstract

Some heavy metals e.g., zinc, copper or manganese serve as micronutrients for eukaryotic life and play an important role for the cellular metabolism, growth of organisms, reproduction and enzymatic activity. However, other metals like mercury or lead are not known to have any beneficial effects for organisms and are believed to have a higher toxic potential. Heavy metals occur naturally in the environment. However, in higher concentrations, they become toxic and have hazardous effects on marine biota. Furthermore, they are highly persistent in the marine environment as they are not readily degraded by organisms. Pollution originating from anthropogenic sources, e.g., mining, industry and extensive land use, increased the heavy metal concentration in certain areas above a critical level. Especially temperate and tropical coastal environments act as natural catchment for anthropogenic pollutants because these areas are densely populated and highly affected by industry, agriculture and urban runoff. Therefore, it is vitally important to assess past heavy metal distributions, spatially and temporally and to compare those with recent pollution in order to evaluate contemporary emission reduction measures.

The chemistry of the tests of benthic foraminifera and the skeletons of scleractinian corals are widely used for the reconstruction of changes in past environmental conditions including temperature, salinity and carbonate system parameters. Recent studies further demonstrated that the trace metal concentration in the aragonite of corals and the calcite of foraminifera is linked to that in seawater. Therefore, the geochemical analysis of coral skeletons and foraminiferal tests offers the opportunity to gain insights into past heavy metal concentrations in seawater, which can in turn help to improve coastal management. However, it is important to understand distribution patterns, ecological and environmental factors influencing the organism itself and associated species in order to evaluate which species is suitable and representative for a certain area. Therefore, the living and dead foraminiferal assemblage along a transect in the German North Sea was investigated. The results of this study indicate that transport via tidal currents is the dominant environmental factor shaping the foraminiferal assemblages. *Haynesina germanica*, *Ammonia batava* and different *Elphidium* species from the living foraminiferal fauna depict a close linkage between open North Sea areas like Helgoland and the mainland. These species share an opportunistic behaviour and are able to occupy a variety of environments rendering them as possible proxy-carriers for heavy metal contamination in seawater. Nevertheless, an application of the heavy metal concentration in the calcium carbonate of both of the organism groups will only be possible after a calibration of this proxy. Therefore, benthic foraminifera from temperate environments (*Ammonia aomoriensis*, *Ammonia batava* and *Elphidium excavatum*) and tropical corals (*Porites lichen* and *Porites lobata*) were exposed to a mixture of dissolved chromium (Cr), manganese (Mn), nickel (Ni), copper (Cu), zinc (Zn), silver (Ag), cadmium (Cd), tin (Sn), mercury (Hg) and lead (Pb) over a wide concentration range. High frequency water monitoring in combination with laser ablation ICP-MS measurements of the calcium carbonate, which was precipitated during the culturing period, revealed the uptake of some of these metals mainly depends on its concentration in seawater, which is indicated by strong positive correlations between the metal concentration in seawater and in the calcium carbonate. All three foraminiferal species showed a strong positive correlation between Pb and Ag in the water and their calcite. *Ammonia aomoriensis* further revealed a correlation with Mn and Cu, *Ammonia batava* with Mn and Hg and *Elphidium excavatum* with Cr and Ni, and partially also with Hg. Zinc, Sn and Cd showed no clear trends in all three foraminiferal species studied, which in case of Cd may be due to the exposure to more than one metal at a time. The investigated coral species revealed a positive correlation between the trace metal concentration in seawater and in the coral skeleton for Cr, Mn, Ni, Zn, Ag, Cd and Pb. No correlation was found for Cu, Sn and Hg. The calculated partitioning coefficients (D_{TE}) allow a determination of the heavy metal concentrations in seawater. Therefore, the trace element concentration in benthic foraminifera and in scleractinian corals provides a promising tool for ecosystem status assessments in the future, which can serve as a deciding support for governments and environmental agencies.

Kurzfassung

Einige Schwermetalle, wie z.B. Zink, Kupfer oder Mangan sind in geringen Mengen essentielle Mikro-Nährstoffe für Organismen. Sie werden verwendet, um den Zellmetabolismus aufrecht zu erhalten, um das Wachstum oder die Vermehrung der Organismen zu ermöglichen und um enzymatische Aktivitäten zu koordinieren. Andere Schwermetalle, wie z.B. Quecksilber und Blei, nehmen keine essentielle Rolle im Zellmetabolismus ein und haben auch keine anderen positiven Effekte, weshalb diesen Metallen ein höheres toxisches Potential zugeschrieben wird. Die meisten Schwermetalle kommen in sehr geringen Mengen in der Umwelt vor und haben erst eine schädigende Wirkung auf marine Organismen, wenn höhere Konzentrationen erreicht werden. Sobald ein bestimmter Grenzwert überschritten wird, können Schwermetalle extreme toxische Wirkungen entfalten. Außerdem sind sie in der marinen Umwelt nur schlecht abbaubar und können auch von Organismen nur schwerlich ausgeschieden werden. Durch Menschen verursachte Verschmutzungen, die durch industrielle Produktion, extensiven Bergbau oder durch intensive landwirtschaftliche Nutzung erzeugt werden, haben dazu geführt, dass die Schwermetallkonzentration in vielen Gebieten ein kritisches Level überschritten hat. Vor allem küstennahe Regionen in tropischen und temperierten Klimazonen sind Gebiete, die stark unter menschenverursachten Schadstoffeinträgen leiden. Diese Gebiete werden sowohl von der Industrie also auch von Landwirtschaft und den städtischen Abwässern in der Nähe großer Ballungsgebiete beeinflusst. Dieser Umstand macht es umso wichtiger, dass räumliche und zeitliche Verbreitungsmuster der Schwermetalle identifiziert und mit den heutigen Schadstoffeinträgen verglichen werden, um bereits etablierte Emissionsminderungs-Maßnahmen zu beurteilen.

Die chemische Zusammensetzung der Gehäuse von benthischen Foraminiferen und der Skelette von Steinkorallen wird genutzt, um Veränderungen von Umweltparametern wie der Temperatur oder der Salinität in vergangenen Zeitaltern zu rekonstruieren. Studien deuten an, dass die Spurenmetallkonzentration im Aragonit der Korallen und im Kalzit der Foraminiferen von der chemischen Zusammensetzung des Meerwassers abhängt, was auch verschiedene Kontaminationsstufen einschließt. Aufgrund dessen können chemische Untersuchungen des Korallenskeletts und der Foraminiferengehäuse neue Möglichkeiten bieten, um Auskünfte über die Schwermetallkonzentrationen im Meerwasser der vergangenen Jahrhunderte zu erlangen. Dies wiederum kann dabei helfen, zukünftige Entwicklungen der Schwermetallkonzentrationen im Meerwasser zuverlässiger vorherzusagen. Auf der Grundlage dieses Wissens kann außerdem das Management eines Ökosystems verbessert werden. Vorab ist es jedoch unabdingbar, die Verteilungsmuster sowie die ökologischen und umweltbedingten Faktoren zu verstehen, die den untersuchten Organismus und assoziierte Arten beeinflussen. Auf Grundlage dessen kann entschieden werden, welche Spezies geeignete Indikatoren für ein bestimmtes Gebiet sind. Um dies herauszufinden, wurde die fossile und moderne Foraminiferenvergesellschaftung entlang eines Transekts in der deutschen Nordsee untersucht. Die Ergebnisse dieser Studie zeigen, dass Transportprozesse eine dominierende Rolle spielen und die Zusammensetzung der Foraminiferengemeinschaft maßgeblich beeinflussen. *Haynesina germanica*, *Ammonia batava* und verschiedene Arten der Gattung *Elphidium* aus der Lebendfauna zeigen eine enge Verbindung zwischen Gebieten der offenen Nordsee und dem Festland. Alle drei Arten haben eine opportunistische Lebensweise und können eine

Kurzfassung

Vielzahl verschiedener mariner Lebensräume besiedeln, was sie zu potentiellen Indikatoren für Schwermetallkontamination im Wasser macht. Bevor die Schwermetallkonzentration im Kalziumkarbonat der Organismen angewandt werden kann, ist eine Kalibrierung des Proxys zwingend erforderlich. Deswegen wurden im Rahmen dieser Studie tropische Korallen (*Porites lichen* und *Porites lobata*) und benthische Foraminiferen aus temperierten Gebieten (*Ammonia aomoriensis*, *Ammonia batava* und *Elphidium excavatum*) mit einer Mischung aus gelöstem Chrom (Cr), Mangan (Mn), Nickel (Ni), Kupfer (Cu), Zink (Zn), Silber (Ag), Cadmium (Cd), Zinn (Sn), Quecksilber (Hg) und Blei (Pb) über einen weiten Konzentrationsbereich kultiviert. Kontinuierliche Überwachung der Schwermetallkonzentrationen im Kulturmedium zusammen mit Laser Ablation ICP-MS Messungen des Kalziumkarbonats, welches während der Kultivierung gebildet wurde, erwiesen, dass die Aufnahme bestimmter Schwermetalle hauptsächlich von der Konzentration des jeweiligen Metalls im Meerwasser abhängt. Dies zeigte sich anhand einer positiven Korrelation der Schwermetallkonzentrationen im Meerwasser und im neu gebildeten Kalziumkarbonat. Die drei Foraminiferenarten zeigten eine signifikante Korrelation der Blei- und Silberkonzentration im Kalzit zum umgebenden Meerwasser. *Ammonia aomoriensis* wies zudem eine Korrelation für Mn und Cu, *Ammonia batava* für Mn und Hg und *Elphidium excavatum* für Cr und Ni, sowie teilweise auch für Hg auf. In allen drei Foraminiferenarten zeigten Zn, Sn und Cd keine klaren Trends. Bei den untersuchten Korallenarten zeigte sich eine positive Korrelation zwischen der Spurenmetallkonzentration im Meerwasser und im Skelett für Cr, Mn, Ni, Zn, Ag, Cd und Pb. Für Cu, Sn und Hg konnte keine Korrelation festgestellt werden. Die Ergebnisse dieser Studie ermöglichen damit die Rekonstruktion der Schwermetallkonzentrationen im Meerwasser für diejenigen Elemente, welche eine positive Korrelation zwischen Meerwasser und Kalziumkarbonat aufweisen. Die berechneten Partitionierungs-Koeffizienten (D_{TE}) erlauben eine Abschätzung der Schwermetallkonzentration im Wasser. Damit bietet die Spurenelementkonzentration in benthischen Foraminiferen und Steinkorallen ein sehr vielversprechendes Instrument, um den Zustand eines Ökosystems zu beurteilen. Dies kann Regierungen und Umweltbehörden als Entscheidungshilfe für notwendige Maßnahmen dienen. Außerdem können Vorhersagen der Entwicklung der Schwermetallkontamination durch chemische Analysen von Paläo-Archiven wie Korallen und Foraminiferen zukünftig besser eingeordnet werden.

Content

1. Introduction

1.1 Heavy Metals – Definition, application and threat

The term "heavy metal" was increasingly used in a multidisciplinary scientific context over the past two decades. The use of these metals in an industrial, domestic, agricultural, medical and technological context became vitally important over the past years (e.g., Bradl, 2005). They are usually present in trace amounts in various environments (e.g., Kabata-Pendias and Pendias, 2001), making the term "trace elements" synonymous. Furthermore, they are natural constituents of the Earth´s crust and are introduced in small amounts into the environment by various natural processes including meteorite impacts, erosion of rocks, weathering of minerals or volcanic eruptions. Heavy metals are often associated with pollution and toxicity although many metals, like copper (Cu), chromium (Cr), manganese (Mn), nickel (Ni) or zinc (Zn), are essential micro-nutrients for various biochemical and physiological processes and only become toxic at critical concentrations (Prothro, 1993). Elements like cadmium (Cd), lead (Pb) or mercury (Hg) are not essential for biological processes and do not have a physiological role, which makes them toxic even in small amounts (Nordberg et al., 2007). As a by-product of the expanded application of heavy metals, negative impacts on human health or on the environment occurred. Nevertheless, a uniform definition for the term "heavy metals" is not given, even though many authors tried to establish more specific definitions based on different criteria like chemical behaviour, physical properties or toxicity (Duffus, 2002; Pourret, 2018). Generally, heavy metals are a group of metals or metalloids with a relatively high atomic number (>23, Bennett, 1986; >40 Rand et al., 1995) and density (> 7 g/cm^3, Bjerrum, 1936; >5 g/ cm^3, Passow et al., 1961; >3.5 g/cm^3, Falbe and Regitz, 1996). A more biochemical way of defining metals is their behaviour as a Lewis acid, which is essential for the interaction of metallic elements with living material. Lewis acids are electron acceptors, which means that every elemental species with a positive charge behaves as a Lewis acid (Lewis, 1923). The classification of metals by their Lewis acidity into Class A, B and borderline indicates the form of bonding in organic complexes. Defining "heavy metals" in terms of toxicology would need to be based on chemical properties in combination with biological impacts on the organism exposed to the metals. This is at present not possible, because knowledge about the relationship between biological processes and linked toxicity is still poor and a more fundamental understanding would be necessary for a clear definition (Duffus, 2002). In summary, there are many different ways to define the term "heavy metal" and no definition is commonly accepted to date.

The most abundant heavy metals in the marine environment originating mainly from anthropogenic sources are chromium (Cr), manganese (Mn), nickel (Ni), copper (Cu), zinc (Zn), silver (Ag), cadmium (Cd), tin (Sn), mercury (Hg) and lead (Pb). These metals are used in different industrial and agricultural applications including mining and steel manufacturing, for the production of alloys, fertilizers, pesticides, fungicides and marine paint including antifouling treatments. They are also released by intensive animal farming, batteries, oil and gas production, cosmetics, dental and pharmaceutical industry, biomass burning in forest fires, and polymer production (Al-Rousan et al., 2007; Jaishankar et al., 2014; Richir and Gobert, 2016, Shah, 2021 and references therein). They can enter the marine environment through several different ways including riverine and wastewater discharge, dumping of sewage sludge, atmospheric transportation as dust, weathering processes, terrigeneous input via flash flooding, waste dumping or coal firing (Guzmán and Jiménez, 1992; Esslemont, 1999; Al-Rousan et al., 2007; Shah, 2021 and references therein).

Once heavy metals have reached the marine environment, they can enter the tissue of organisms through the respiratory track, digestion or by penetration through the skin (Darmono, 2001) and therefore pass through the food chain through various trophic levels (Das et al., 2013). Heavy metals can occur in the water column and in the sediments in different forms and speciations such as free ions, complexes, colloids, suspensions in the liquid phase or adsorbed to surfaces. They are highly persistent, tend to bioaccumulate and are poorly removable from the organism (Diagomanolin et al., 2004; Naser, 2013). Their toxicity depends on factors like chemical speciation, type, concentration, synergistic-antagonist effects, environmental conditions including pH, temperature, salinity and dissolved oxygen, the adaption of the organism to the metal exposure or their biological role and pathways (Ansari et al., 2004; Akan et al., 2010). Heavy metals can have different sub-lethal or even lethal effects and cause diseases in animals and the human body. Some metals cause damage of the kidneys, lungs, heart, nervous system, brain and can lead to the deformation of bones (Rieuwerts, 2015). Furthermore, heavy metals can cause the alteration of enzyme functions, lead to oxidative stress in the cell, inhibit reproduction, disrupt ion regulation and have mutagenic and carcinogenic effects (Natale et al., 2000; McGeer at al., 2000; Bielmyer-Fraser et al., 2018).

In summary, heavy metals become an increasing threat for biota and humans, which makes it essential to apply an adequate ecosystem management in order to inhibit heavy metal emissions to the environment and to evaluate current pollution measures.

1.2 Paleo-climate recorders

Reliable instrumental measurements of chemical seawater conditions are limited to the period after the industrialization (Woodruff et al., 2005). Environmental proxy records based on geological and biological archives provide an insight into paleo-climatic and environmental conditions. Various archives are used for unravelling the physical and chemical parameters of different environments over time and these include corals, ice cores, sediment cores, speleothems and tree rings. Information gained from paleo-archives is vitally important for the understanding of the Earth system before and after the influences of human activities. Furthermore, climate models are based on data from past environmental settings and an accurate prediction of the future will only be possible by testing the models under different boundary conditions including pre-impacted or pre-industrial conditions. Therefore, analysis and understanding of paleo-archives will help to improve today's ecosystem management and remediation.

Chemical, physical or biological materials that are preserved in the fossil record can be analysed and used as paleo-proxies because their composition is often correlated to climatic and environmental parameters. Many different proxies can be used to identify changes in the past climate and environmental system. For examples, physical parameters like sedimentary properties (e.g., the sediment composition, structure or the texture) facilitate a reconstruction of flow regimes of rivers, ocean currents or reveal ash from volcanic eruptions. Biological proxies include the assemblage composition of different organisms, for example foraminifera, their shell morphology and mode of life. The past distribution patterns of corals and other organisms reveals the environmental conditions of the past like temperature, salinity, nutrient availability or turbidity. Chemical proxies are based on the element or isotopic composition of biomineral material (e.g., calcite in foraminifera or aragonite in corals). This composition depends on the environmental conditions of the ambient seawater and can therefore be used for the reconstruction of parameters like temperature, salinity, carbonate system parameters and primary productivity. For example, the sodium-to-calcium ratio (Na/Ca) in foraminifera is correlated to the salinity in the seawater the foraminifera grew in (Wit et al., 2013; Mezger et al., 2016; Bertlich et al., 2018), or the strontium-to-calcium ratio (Sr/Ca) in corals is a function of seawater temperature (Shen et al., 1996; Marshall et al., 2002; Clarke et al., 2017). For the application of chemical proxies, a comprehensive understanding of the relationship between the element composition in the paleo-archive and the ambient seawater is crucial, which can be achieved by culturing experiments investigating the environmental parameter and organism of interest. Furthermore, ecological factors driving the distribution of the particular species and associated organisms may be revealed by the assessment of ambiental environmental parameters. Faunal analysis and correlation with the environmental parameters identify indicator species and faunal assemblages.

The anthropogenic heavy metal contamination of the oceans and other environments is now a serious issue. Therefore, monitoring of the development of this pollution is necessary for the future to support governmental decisions concerning ecosystem management. Models for the prediction of future development need paleo-data as a baseline enabling a comparison between pre-impacted and recent pollution levels. Chemical proxies stored in the calcite of foraminifera from sediment cores could deliver important insights into the development of heavy metal concentration in areas of interest. In particular benthic foraminifera are suitable indicators for anthropogenic pollution because they are known to incorporate heavy metals into their calcitic shell (e.g., Smith et al., 2020; Sagar et al., 2021a; Titelboim et al., 2021). Furthermore, some taxa are distributed all over the world (e.g., *Ammonia*, Figure 1.1), well preserved in the fossil record (McGann, 2008; Xiang et al., 2008) and have a short life cycle (Wefer, 1976; Murray, 1992), which enables them to react immediately to changes in environmental conditions such as contamination by varying heavy metal concentrations.

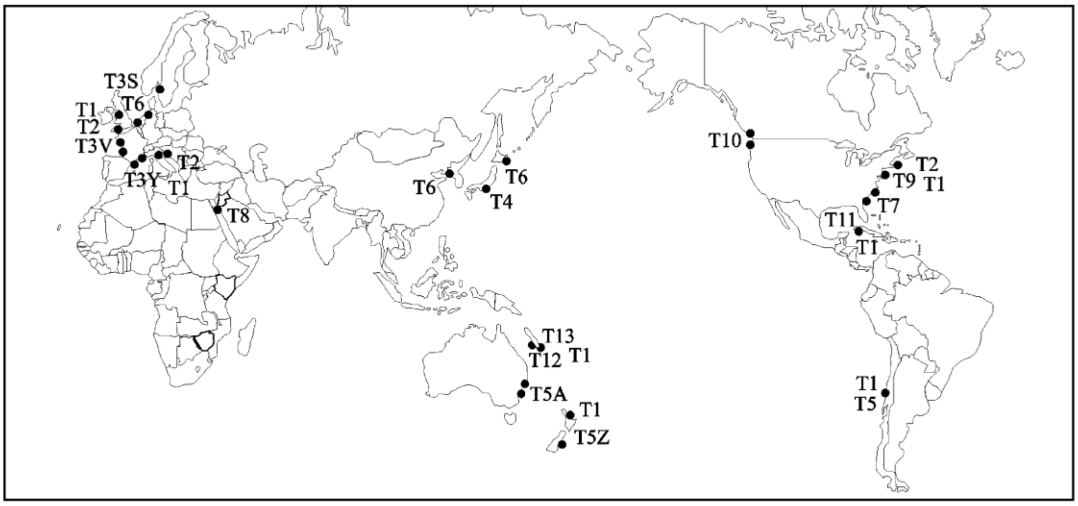

Figure 1.1: Global distribution of 13 *Ammonia* genotypes after Hayward et al. (2004).

Besides foraminifera, scleractinian corals have also a great potential as a tool for monitoring the heavy metal concentration in the environment. They are highly sensitive to chemical changes in their surrounding (Shen, 1996; David, 2003) and can survive high heavy metal concentrations (e.g., El-Sorogy et al., 2012). Furthermore, coral reefs are globally distributed in tropical regions between the 20 °C winter isotherms (see Figure 1.2). Corals have high growth rates, which allows determining the elemental composition in the coral skeleton at sub-annual resolution. Their size and growth rate creates environmental archives covering hundreds of years. Therefore, both groups of organisms are excellent candidates for monitoring the spatial and temporal distribution of heavy metals in seawater.

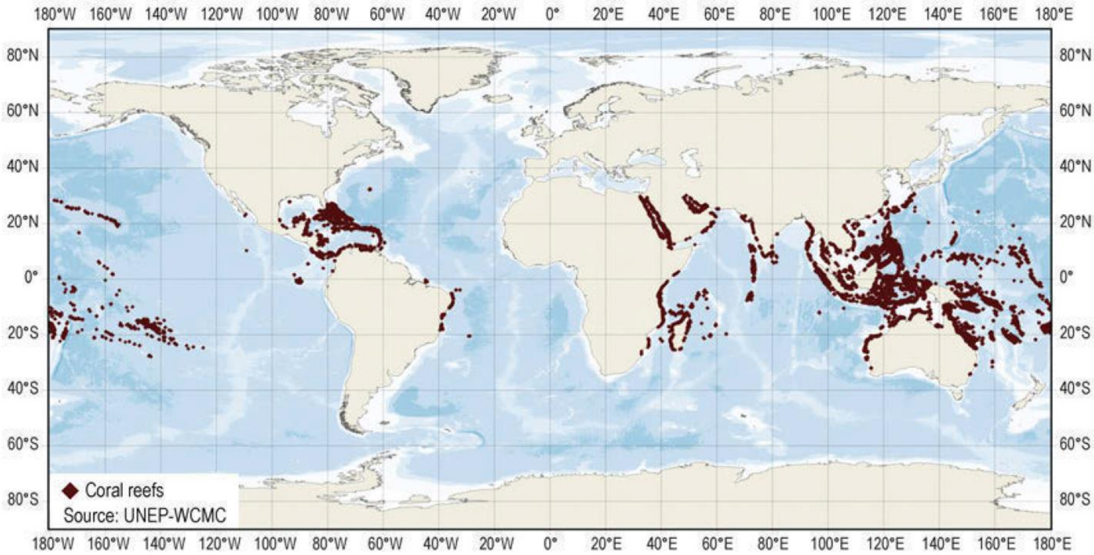

Figure 1.2: Global distribution of coral reefs after Cardini et al., 2015.

The metal-to-calcium-ratio in foraminiferal tests and coral skeletons have been widely applied for different purposes. The cadmium-to-calcium (Cd/Ca) and zinc-to-calcium ratio (Zn/Ca) in foraminifera for example is used for the reconstruction of dissolved Cd and Zn concentration in seawater (Bertram et al., 1995; Tachikawa and Elderfield, 2002) and as paleonutrient proxy for the investigation of past deep ocean circulation patterns (Boyle and Keigwin, 1982; Rosenthal et al., 1997; Marchitto and Broecker, 2006; Bryan and Marchitto, 2010). Cd/Ca in corals is applied for reconstructions of upwelling (Shen et al., 1987; Reuer et al., 2003; Matthews et al., 2008) and as a salinity proxy (Pretet et al., 2014). Cd/Ca and Zn/Ca are also used as tracers for anthropogenic pollution (Hanna and Muir, 1990; Ramos et al., 2004; Jiang et al., 2020). The lead-to-calcium ratio (Pb/Ca) of foraminiferal tests and coral skeletons is also used for the evaluation of recent and past pollution levels (Shen and Boyle, 1987; Kelly et al., 2009; Rumolo et al., 2009; Titelboim et al., 2018; 2021). Furthermore, the manganese-to-calcium ratio (Mn/Ca) in foraminifera correlates with the oxygen content of the seawater (e.g., Groeneveld and Filipsson, 2013; Guo et al., 2019), and Mn/Ca in coral skeletons serve as proxy for terrestrial input (Moyer et al., 2012; Lewis et al., 2018). This ratio can also be used for wind reconstruction (Sayani et al., 2021).

Culturing experiments enable the variation of only one environmental or chemical parameter while all other are kept stable. This removes much of the ambiguity associated with calibration by indirect means (Lea, 1999). Culturing experiments with foraminifera have been performed for more than 150 years now starting with the early works of Gervais (1847) and Schultze (1856). Most early works on foraminifera and corals focused on taxonomic and biological studies addressing for example the life cycle of the organism or optimal growth conditions. Delaney et al. (1985) were one of the first who performed chemical experiments on living foraminifera in the laboratory to investigate the dependency of elements in the foraminiferal test on its concentration in the culturing seawater. During the same time, Weil et al. (1981) investigated the influence of temperature and light on the stable isotope composition in coral skeletons. Since then, culturing techniques evolved a lot and culturing of foraminifera became an important tool to assess the trace element incorporation into their calcite and for the calibration of paleo-proxies (Nürnberg et al., 1996; Lea, 1999; Hintz et al., 2004; Linshy et al., 2007 and references therein; Filipsson et al., 2010; Koho et al., 2017; Sagar et al., 2021a; 2021b). Scientific approaches addressing the trace element concentration in corals are still mainly based on field sampling (Goreau, 1977; Shen and Boyle, 1988; Reichelt-Brushett and McOrist, 2003; Kumar et al., 2010; Jiang et al., 2020).

1.3 Biomineralization processes

The application of paleo-climate recorders like foraminifera and corals requires a deeper understanding of underlying biomineralization processes in order to assess the reliability of paleo-archives.

Perforate or rotaliid foraminifera build three-dimensional test in various configurations starting from simple one or few chambers and evolve to more complex forms like trocho- or planspiral tests (Erez, 2003). Porcelaneous or miliolid foraminifera build complex tests in rare cases only. Both groups have different calcification mechanisms. Porcelaneous foraminifera form high-Mg, needle-like calcite crystals in an intracellular space that are precipitated without orientation at the site of calcification (SOC) (Angell, 1980; Hemleben et al., 1986). Perforate foraminifera form a thin high-Mg layer at the base of the shell, and a thicker low-Mg calcite layer with a radial structure. They develop pores within their chamber walls and cover the pre-existing chambers with a newly formed calcite layer every time a new chamber is added. This leads to a lamination of the test (Reiss, 1957). An organic matrix forms the shape of the chambers in both types of foraminifera before a new chamber is built. The pseudopodial network is separating the SOC from the surrounding seawater, which enables a biological control on the calcification mechanism (Banner et al., 1973). Foraminifera are known to create a $CaCO_3$ supersaturated microenvironment from which they calcify from (Erez, 2003; Glas et al., 2012; Toyofuku et al., 2017). The required ions are taken up from the surrounding seawater and are pre-concentrated in order to enable calcification. For the concentration of ions, the foraminifera either need to extract Ca^{2+} and dissolved inorganic carbon or take up seawater and reduce the concentration of other ions that would inhibit nucleation like Mg (Zeebe and Sanyal, 2002). Another possible mechanism is the removal of protons from seawater taken up by endocytotic pathways. During both processes, ions are either transported directly to the SOC (Erez, 2003; Bentov and Erez, 2006) or they are intermediately stored in an internal pool (Ter Kuile and

Erez, 1988; de Nooijer et al., 2009). A direct transport can be performed passively via diffusion (Wolf-Gladrow et al., 1999) or actively through transmembrane channels (Nehrke et al., 2013). Another widely accepted concept for the uptake of ions into foraminifera is endocytosis. This mechanism involves special vesicles called vacuoles that transport the seawater into the cell of the foraminifera (Erez, 2003; de Nooijer et al., 2008, 2009; Bentov et al., 2009) where it is further processed. There is still an ongoing debate on which mechanism is predominant. The incorporation of trace metals into the foraminiferal tests after the uptake from seawater can be performed by Ca^{2+} substitution in the calcite lattice (Branson et al., 2013). Furthermore, trace metals can be bound to the organic matrix (Geerken et al., 2019) or they can be integrated into the calcite lattice in interstitial positions where the lattice has defects (Ishikawa and Ichikuni, 1984; Okumura and Kitano, 1986).

The coral skeleton is constructed from mineral aragonite and an organic matrix (Mitterer, 1978; Stolarski, 2003; Cuif and Dauphin, 2005). Similar to foraminifera, the organic matrix facilitates a microenvironment suitable for controlled biomineralization and provides a structural basis for crystal nucleation. The coral tissue is attached to the coral skeleton facing the outside of the animal and consists of two organic tissues, the oral tissue at the seawater side and the aboral tissue located at the side of the coral skeleton (e.g., Chevalier, 1987; Fautin and Mariscal, 1991). Within the aboral tissue, the calicoblastic epidermis (also calicodermis) is located, which is responsible for the formation of the coral skeleton (Von Heider, 1881; Galloway et al., 2007; Puverel et al., 2005). The submicrometric interface between the calicodermis and the skeleton is called the “extracellular calcifying medium” (ECM). This is the site of calcification and it is filled with a hydrogel (Cuif et al., 2004). The sub-calicoblastic ECM is isolated from the environment by an epithelium, which allows ions to access the site of calcification by creating a certain degree of permeability (Tambutté et al., 2011). The type of permeability determines the ion concentration at the site of calcification and is therefore fundamentally important for the degree of incorporation of ions into the coral skeleton. It is believed that corals control the composition of the ECM at least to a certain degree and it is suggested that an active transport mechanism is involved to enable an adequate supply of ions to the site of calcification (Allemand et al., 2011). pH investigations further suggested that the $CaCO_3$ precipitation from the ECM is affected by more factors than just the chemical behaviour of the ions and molecules (Al-Horani et al., 2003). The initial calcification takes place extracellularly and ions are transported to the ECM either paracellular or transcellular. Active uptake by a transcellular pathway involves that ions are transported through the calictodermis to the ECM inferring a tight biological control. Passive paracellular pathways can be diffusion of ions or direct diffusion of the seawater (Gagnon et al., 2012). In case of the diffusion of ions and molecules, the chemical properties like size and charge are decisive and the uptake of ions is selective. Direct diffusion of the seawater is non-selective (Tambutté et al., 2012). This suggest a paracellular pathway for seawater entering the ECM without any physical barrier and biological control (Cohen and McConnaughey, 2003). At present it cannot be clearly distinguished between an active or passive route, but it is likely that paracellular and transcellular pathways coexist and both pathways as well as the type of organic matrix contribute to the ion supply and therefore on the incorporation of elements into the coral skeleton (Allemand et al., 2011). This incorporation can be performed by different modes: (1) substitution of Ca^{2+} in the aragonite lattice, which depends on chemical properties like the effective ionic radius and the charge of the ion. Divalent metal ions similar to Ca^{2+} substitute more readily than ions with a divergent ionic radius. Nevertheless, it has also been reported that monovalent metal ions like Na^{+} or Li^{+}, rare earth elements (REE) (Shannon, 1976) with a 3+ charge and smaller (Amiel et al., 1973a; Shen and Boyle, 1988; Pingitore et al., 2002; Anu et al., 2007) or bigger (Inoue et al., 2004; Shen and Boyle, 1988) divalent ions are also substituting Ca^{2+} in the coral lattice. (2) The formation of complexes with the organic matrix have been found to contribute significantly to the overall trace metal budget in the coral skeleton. Amiel et al. (1973a, 1973b), Allison and Finch (2007) and Shen et al. (1991) found for example a high amount of Sr, Mg, Na, Mn and other trace metals connected to the organic compounds of the coral. (3) Trapping of particulate material like clay minerals, organic matter, colloids or microorganisms in skeletal pores of the coral was reported to play a role for turbid settings (Barnhard et al., 1974). (4) Trace metals could also adsorb to bare skeletal surfaces during stress periods when the coral tissue retracts, but should not influence the trace metal concentration in the coral skeleton during normal environmental conditions (Brown et al., 1991; Saha et 2016).

1.4 Thesis objectives and outline

The principal objective of this thesis was to investigate the heavy metal incorporation into benthic foraminifera and tropical corals as a potential proxy for the heavy metal concentration in seawater. Various areas all over the world are threatened by anthropogenic pollution and this study aims to establish a first step towards the application of foraminifera and corals as proxy-carrier for heavy metals in seawater in pristine and polluted areas. Earlier studies mostly addressed the impact of only one contaminant at a time, but in reality there is rarely only one metal polluting environments but instead a combination of several pollutant metals is usually found. This could lead to interactions between the metals and to synergetic effects and this is also why this study investigated the impact of a mixture of metals in seawater on the metal concentration in the calcium carbonate of foraminifera and corals. However, before the heavy metal concentration in one of these paleo-archives can be applied, the selection of a suitable species and the determination of factors influencing the respective distribution of this species is necessary and was examined for a region in the North Sea of Germany in this study. In detail this study addresses the following questions:

1. What is driving the ecology and distribution of benthic foraminifera around the supratidal sand Japsand, North Sea, Germany?
2. How and to which extent do benthic foraminifera and stony corals incorporate heavy metals into their calcium carbonate?
3. Does a mixture of different metals in seawater influence this incorporation?
4. Does the heavy metal concentration in the calcitic shell of benthic foraminifera and the aragonitic skeleton of stony corals monitor the heavy metal concentration in seawater?

This thesis comprises three main scientific chapters. Each chapter is an individual publication or is currently prepared to be submitted. Chapter 1 is published in *Helgoland Marine Research*. Chapter 2 is accepted for publication in *Biogeoscience* and chapter 3 is in preparation for submission to another peer-reviewed journal. The main chapters are wrapped up by a general introduction to the topic and an overall conclusion with outlook for possible future studies.

Chapter 1 introduces the ecology and distribution patterns of benthic foraminifera along a transect from the supratidal barrier sand Japsand to Hallig Hooge, North Sea, Germany. The living and dead foraminiferal assemblage was analyses and size distribution patterns gave information on the reproductive cycle of distinct foraminiferal species. Furthermore, key species revealed a connectivity and an active exchange between distant populations and areas. This chapter is published in *Helgoland Marine Research*.

Contribution to Chapter 1: Dr. Joachim Schönfeld and I designed this study. I collected the samples, processes them in the laboratory, analysed the living fauna, acquired, analysed and interpreted the data. Furthermore, I created the figures and plates. Dr. Joachim Schönfeld designed the work concept in part, analysed the foraminifera from the dead assemblage and contributed mainly to the taxonomic work of this manuscript. Both authors were equal contributors in writing and editing of the manuscript.

Chapter 2 presents the results from multi-element culturing experiments with three different foraminiferal species (*Ammonia aomoriensis*, *Ammonia batava* and *Elphidium excavatum*). The foraminifera were cultured with a mixture of dissolved chromium (Cr), manganese (Mn), nickel (Ni), copper (Cu), zinc (Zn), silver (Ag), cadmium (Cd), tin (Sn), mercury (Hg) and lead (Pb) in artificial seawater with a wide concentration range of these metals. The partitioning factor between seawater and the calcium carbonate of the foraminifera was constrained by continuous water monitoring and laser ablation ICP-MS measurements on newly grown foraminiferal calcite. A correlation between the heavy metal concentration within the culture medium and the foraminiferal calcite was found for some metals. This chapter is accepted to be published in *Biogeoscience*.

Contribution to Chapter 2: Dr. Ed Hathorne and Dr. Joachim Schönfeld proposed this study. I collected the samples, cultured the foraminifera, processed the samples in the laboratory, acquired, analysed and interpreted the water and foraminiferal data. Dr. Joachim Schönfeld helped with the design of the study and sampling logistics and the implementation of the culturing system. Dr. Ed Hathorne helped with the processing and analysis of the water samples. Furthermore, Dr. Ed Hathorne and Dr. Dieter Garbe-Schönberg adviced me with the laser ablation measurements of foraminiferal samples. As first author, I wrote the manuscript with all the co-authors contributing to the data interpretation, discussion and editing of the work. I submitted and revised the manuscript according to the comments and suggestions of two anonymous reviewers.

Chapter 3 addresses the relationship of heavy metal concentration in seawater and the coral skeleton of two different *Porites* species (*Porites lobata* and *Porites lichen*). Culturing experiments were similar to those described in Chapter 2 and exposed *Porites* spp. to a similar metal mixture. Continuous water monitoring in combination with laser ablation ICP-MS measurements of the coral aragonites revealed a positive correlation of Cr, Mn, Ni, Zn, Ag, Cd and Pb concentrations in the culturing medium and the coral aragonite. This chapter is in preparation for the submission to a peer-reviewed journal.

Contribution to Chapter 3: Dr. Ed Hathorne and Dr. Joachim Schönfeld proposed this study. I designed the experimental setup with input from Dr. Ed Hathorne and Dr. Joachim Schönfeld, cultured the corals, processed the samples in the laboratory, acquired, analysed and interpreted the water and coral data. Dr. Joachim Schönfeld organized the DNA analysis of the cultured coral colonies. Dr. Ed Hathorne helped with the processing and analysis of the water samples. Dr. Kathleen Gosnell performed the Hg measurements in the water samples. Furthermore, Dr. Ed Hathorne and Dr. Dieter Garbe-Schönberg supervised the laser ablation measurements of the coral samples. I wrote the manuscript and all co-authors contributed to the data interpretation, discussion, and editing of the manuscript

2. Scientific Chapter I. Living and dead foraminiferal assemblage from the supratidal sand Japsand, North Frisian Wadden Sea: Distributional patterns and controlling factors

Published in *Helgoland Marine Research* as: Schmidt, S., Schönfeld, J. Living and dead foraminiferal assemblage from the supratidal sand Japsand, North Frisian Wadden Sea: distributional patterns and controlling factors. *Helgoland Marine Research* **75,** 6 (2021). https://doi.org/10.1186/s10152-021-00551-2

Abstract.
Supratidal sands are vitally important for coastal defence in the German Wadden Sea. They are less affected by human activities than other areas as they are located far off the mainland shore, touristical and commercial activities are generally prohibited. Therefore, supratidal sands are of high ecological interest. Nevertheless, the faunal inventory and distribution pattern of microorganisms on these sands were studied very little. The composition of living and dead foraminiferal assemblages was therefore investigated along a transect from the supratidal sand Japsand up to Hallig Hooge. Both assemblages were dominated by calcareous foraminifera of which *Ammonia batava* was the most abundant species. *Elphidium selseyense* and *Elphidium williamsoni* were also common in the living assemblage, but *Elphidium williamsoni* was comparably rare in the dead assemblage. The high proportions of *Ammonia batava* and *Elphidium selseyense* in the living assemblage arose from the reproduction season that differed between species. While *Ammonia batava* and *Elphidium selseyense* just finished their reproductive cycles, *Elphidium williamsoni* was just about to start. This was also confirmed by the size distribution patterns of the different species.
The dead assemblage revealed 20 species that were not found in the living assemblage of which some were reworked from older sediments (e.g., *Bucella frigida*) and some were transported via tidal currents from other areas in the North Sea (e.g., *Jadammina macrescens)*. The living foraminiferal faunas depicted close linkages between the open North Sea and the mainland. Key species revealing exchange between distant populations were *Haynesina germanica*, *Ammonia batava* and different *Elphidium* species. All these species share an opportunistic behaviour and are able to inhabit a variety of different environments; hence, they well may cope with changing environmental conditions. The benthic foraminiferal association from Japsand revealed that transport mechanisms via tides and currents play a major ecological role and strongly influence the faunal composition at this site.

2.1 Introduction

The North Frisian supratidal sands Japsand, Norderoogsand and Süderoogsand are located at the seaward border of the German Wadden Sea and North Sea (Fig. 2.1a). They are highly significant for coastal defence because most of the energy of the incoming deep – water waves from the North Sea is dissipated along the seaward slope of these sands [1, 2]. Therefore, the sands are essential for the stability and protection of the North Frisian shoreline.

Besides their protective function, the North Frisian supratidal sands are uninhabited by humans and therefore ideal resting places for birds and seals. As such, the sands have a high ecological relevance. The faunal inventory and distribution pattern of smaller organisms on supratidal sands has attracted less attention though. In particular, little is known about benthic foraminiferal associations, their connectivity, i.e. relationship and exchange with faunas from the open North Sea and the intertidal zone [3], which both are well investigated [e.g., 4–8]. Foraminifera are an important constituent of the benthic meiofauna and play a key role in benthic biogeochemical cycles [e.g., 9, 10, 11]. The aim of this study was to address how foraminiferal communities were connected over a wide range of facies and distance. In this context, barrier sands like the Japsand act as connectors between the shelf sea environments and the intertidal zone at the coast and can reveal new insights into the interaction, i.e. linkage by exchange of different foraminiferal communities. Therefore, we investigated the foraminiferal assemblages from Japsand and compared them with associations from the open North Sea close to Helgoland and near shore associations from Schobüll and Bay of Tümlau (Fig. 2.1a).

A growing literature has demonstrated that benthic foraminifera were reliable indicators for environmental and paleoenvironmental conditions as well as for the ecosystem status in general [e.g., 12–22]. Furthermore, they are highly sensitive to small changes in critical environmental parameters like salinity [23, 24], temperature [25, 26] or carbonate system parameters [27–30]. Their short generation time and good preservation potential of dead, empty tests [31–33], render benthic foraminifera a prominent tool for reconstructing environmental parameters in the present and past [34]. This particularly holds true under the ongoing anthropogenic pressure, like global warming and pollution, as foraminiferal assemblage structures are going to change dramatically [35–38]. Even though the sensitivity living species for certain environmental parameters have been well constrained, the living fauna represents only a snapshot in time. Therefore, dead foraminiferal assemblages comprising multiple generations have often been used to calibrate palaeoproxies for the reconstruction of past environmental conditions, for instance the sea level [39–44]. However, dissolution [31, 45–47] or reworking [48] may well have biased the composition of the dead assemblage, hence making it possible that the living fauna and their driving environmental factors were not correctly mirrored anymore. A comparison of the living faunas and modern dead assemblages from Japsand was attempted to constrain processes that potentially have changed the foraminiferal assemblage composition on sand flats and near shore sands. Size distribution analyses of the most abundant species may reveal whether cohorts of juveniles are present in the living fauna, hence recent reproduction has taken place. Differences in size distribution of living and dead assemblages allow to constrain the timeframe that is necessary to transpose recent changes to the dead and subfossil assemblage composition.

2.2 Regional setting

The Wadden Sea covers an area of approximately 10.000 km^2 and extends from the city of Den Helder in the Netherlands up north to Blåvand headland in Denmark. The area is shaped by tides and currents, hosts a dynamic shallow water body variable in salinity and temperature, and sustains a high primary production and biodiversity. The German sector of the Wadden Sea is characterized by extensive tidal mud flats, numerous inlets, four major estuaries, sandy barrier islands and sands (Fig. 2.1a).

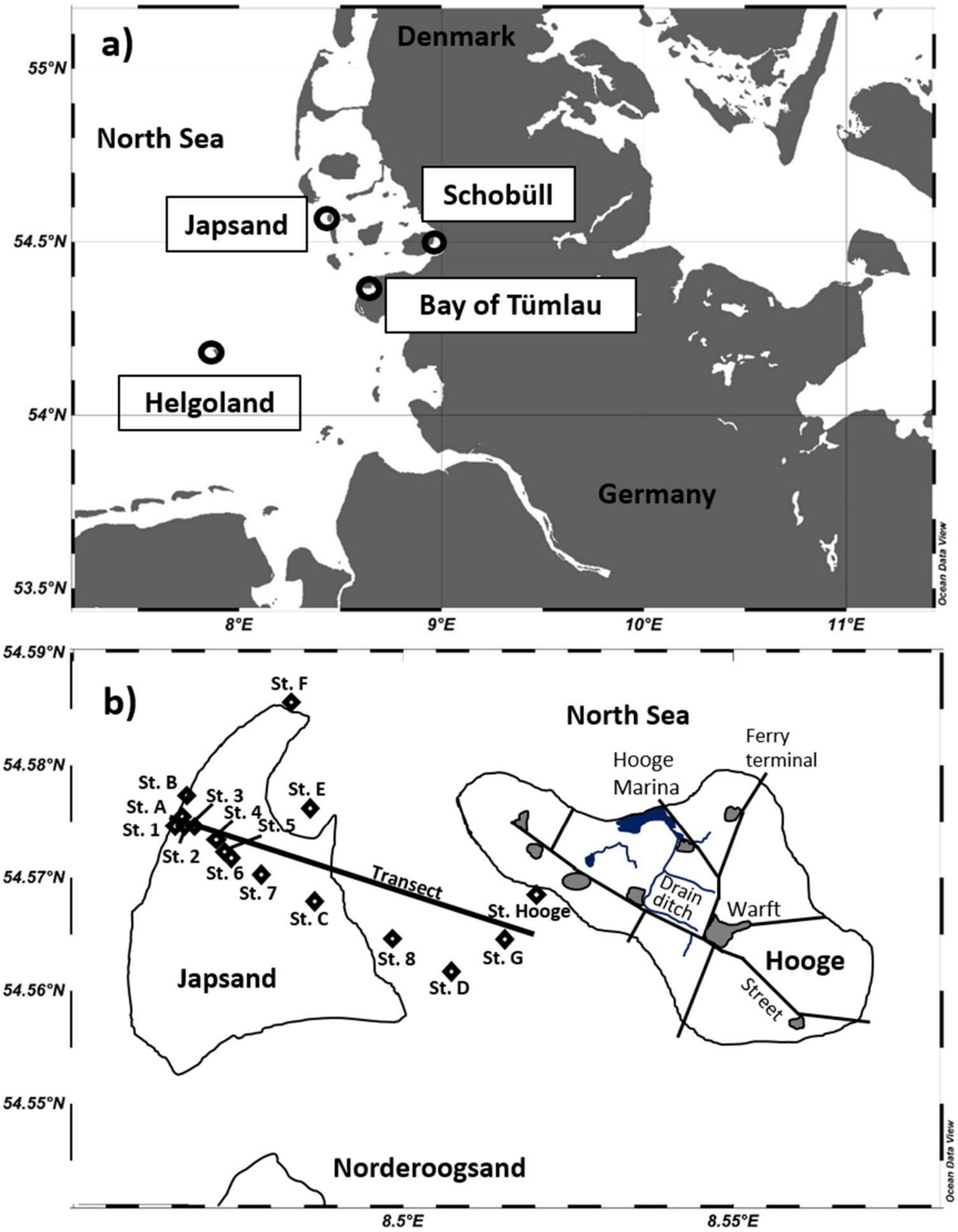

Fig. 2.1: Locations of the Japsand and comparative sites (Helgoland, Schobüll and Bay of Tümlau) in the German North Sea (a). Location of the individual stations in the study area (b). The outline of the Japsand represents the mean high water level. The map was drawn after

satellite images from 2019 and the geological map of Schleswig Holstein (1:250 000, ed. 2012 © Landesvermessungsamt Schleswig-Holstein) and personal observations.

This study focuses on Japsand, which is located 2 km west of Hallig Hooge island (Fig. 2.1b). Japsand, Norderoogsand and Süderoogsand form a chain of supratidal barrier sands with a north-south extension of ca. 19 km and a width ranging from 4 km in the South to 1 km in the North [1, 2]. Japsand is the smallest of these barrier sands, with a north-south extension of 3 km, a west-east extension of ca. 2 km at maximum and an area of ca. 3 km^2. All barriers moved continuously eastwards. The displacement velocity of Japsand has been estimated to 15-27 m a^{-1} [2] (Fig. 2.2a), an amalgamation with Hallig Hooge will hence take place in the future. The tidal channel Hooger Loch separates Japsand and Norderoogsand, and the strong tidal currents inhibited a merger of both barrier sands. Mean tidal range is approximately 2.7 m. Japsand is not regularly submerged during spring tides. The mean wave height is 0.75 m, the prevailing wind and wave directions are west to northwest [1]. Extensive storm floods during autumn and winter episodically caused a flooding of the whole area of the barrier sand.

2.3 Material and methods

Foraminiferal samples were collected at 16 stations along an east-western transect from Hallig Hooge to the western edge of Japsand on two sampling campaigns in Mai and July 2019 (Fig. 2.1b, Tab. 2.1). All stations were in the intertidal zone. They were either submerged or showed evidences for recent flooding in terms of wet diatom mats, macroalgae, or living macrofauna. The exact locations were chosen as being representative for the prevailing sedimentary environment that we observed at certain intervals of the transect. The surface structures, algae, macrofauna and sediment properties were described. The latter are of particular importance as different substrates may house different foraminiferal associations.

The surface sediment was sampled using a handheld push corer of 54 mm inner diameter. Supernatant water was carefully drained off, and the uppermost 1 cm of the surface sediment was sliced off using a graduated plastic ring and a cutting plate [49]. Analysing the 0-1 cm interval was common practice in foraminiferal surveys in the Baltic and in the North Sea [e.g., 4, 50–52]. Duplicates were taken for Station A to G within a 30 x 30 cm square. All samples were transferred into 100 ml PVC bottles (Kautex®). Vessels filled with muddy sediments were gently slewed, bottles with sand-rich samples were cautiously tottered until the surface levelled out and could be marked on the vials immediately after sampling [49]. Within a few hours after collecting, the samples were preserved and stained with a solution of 2 g rose Bengal per 1 litre ethanol (96 %, denaturised, technical quality). A preservative volume of at least 1.5 x the sample volume was added [49].

Temperature and salinity of seep waters were measured with a WTW 3210 conductimeter in nearby puddles or excavated holes in the vicinity, if possible. Precision of the conductimeter was ±0.5 % for conductivity and ±0.1 °C for temperature according to a manufacturer's test certificate. The conductimeter was calibrated using substandards of artificial seawater, which salinities were determined by using an OPTIMARE laboratory salinometer with a precision of

0.0001 permil. The accuracy of the WTW 3210 conductimeter equipped with a TetraCon 325 probe was ±0.13 units (1-sigma value).

Table 2.1: Geographical coordinates of sampling sites in the Japsand intertidal area, North Frisian Wadden Sea, Germany

Station	Sampling date	Latitude (°N)	Longitude (°E)
A	29.07.19	54°34'28.3"	8°27'52.0"
1	29.05.19	54°34'28.8"	8°27'54.7"
B	29.07.19	54°34'35.5"	8°27'57.1"
2	29.05.19	54°34'28.3"	8°27'56.3"
F	30.07.19	54°35'08.0"	8°28'58.0"
3	29.05.19	54°34'27.5"	8°28'02.2"
4	29.05.19	54°34'23.5"	8°28'16.0"
5	29.05.19	54°34'20.7"	8°28'19.4"
6	29.05.19	54°34'18.9"	8°28'22.9"
7	29.05.19	54°34'14.9"	8°28'40.2"
E	30.07.19	54°34'33.1"	8°29'07.9"
C	30.07.19	54°34'06.5"	8°29'10.5"
8	29.05.19	54°33'56.2"	8°29'54.7"
D	30.07.19	54°33'47.4"	8°30'27.4"
G	30.07.19	54°33'56.4"	8°30'58.6"
Hooge	29.05.19	54°34'11.0"	8°31'16.3"

Foraminiferal samples were kept in the rose Bengal staining solution for at least two weeks at ca. 8 °C in the dark to ensure that staining of the cytoplasm of formerly living foraminifera was pervasive [53]. Afterwards, the samples were processed following the procedure described by Wefer [54], Schönfeld et al. [55] or summarized by Lübbers and Schönfeld [56]. All samples were wet sieved using stacked 2000 µm and 63 µm sieves in order to remove larger particles or shell debris. The size fraction >2000 µm containing fragments of mussels, crabs, snails and seaweed was dried overnight at 50 °C, weighted and stored. The size fraction 63-2000 µm was also dried and weighed. After sample washing, the initial volume was determined by refilling the empty PVC vessel with tap water up to the mark on the outside. The water was transferred to a graduated cylinder and the volume was measured [49].

Due to the high amount of detrital sand and the low density of foraminiferal tests, a flotation with a high density liquid was required. Sodium polytungstate (SPT) solution with a density of 2.3 g cm^{-3} was applied following Parent et al. [57]. According to the authors, the recovery rate of foraminiferal tests was >95 % using a SPT solution with a density of 2.3 g cm^{-3}. The density of the fluid was checked after every use. Residues and flotates were rinsed with tap water several times after the treatment to ensure that foraminiferal test were not coated by SPT crystals or crusts after drying. Samples containing a large number of tiny clay lumps could not be treated with SPT (Stations 1, Station B and Station D). The complete residues of these samples were picked dry.

Rose Bengal stained foraminifera were recognized by a bright red or pink coloration of the cytoplasm [49, 55]. Only well-stained specimens were picked and considered for this study. They were picked wet. After the stained individuals were sorted out, the flotates were dried at 50°C. In order to investigate the assemblage composition of non-living foraminifera, aliquots were made with a Green Geological microsplitter from one sample per station. A target number of 200-300 dead foraminiferal specimens was aimed to [34, 49]. The split was picked for foraminiferal tests completely. If less than ca. 100 specimens were available in ½ split, the entire floatate was picked. Living and dead foraminifera were sorted separately by species in Plummer cell slides, fixed with glue and counted. The size distribution of the three-ranked species was assessed by measuring the maximum test diameter on all intact specimens of *Elphidium selseyense*, *E. williamsoni* and *Ammonia batava* collected in the cell slides. The measurements were made with Leica Wild (Leica Wild M60 and M80) stereomicroscopes at 60 X magnification by using an eyepiece reticle with a resolution of 12.5 µm.
Light microscopic images for species' documentation were taken with a Keyence VHX-700 FD digital microscope (living specimens) and a Keyence digital microscope VHX.7000 at the Institute of Geosciences, Kiel University. Statistical analysis of the census data, e.g., calculation of diversity indices, were performed with Past 4.0 [58].

2.4 Results

2.4.1 Hydrography

On-site measurements of temperatures and salinities at low tide and comparison with those recorded by the adjacent MARNET monitoring network stations are important to assess the diurnal, intertidal variability of these environmental parameters. The surface temperature varied from 19.4° C at Station 8 and 22.8° C at Station 3 in May 2019 (Table S2.1). The mean temperature was 21.3 (±1.4)° C. The mean salinity was 34.0 (± 4.5) and varied between 40.4 at Station 8 and 30.3 at Station 1. Temperatures in July ranged from 21.1° C at Station A to 26.3° C at Station E (Table S2.1). The mean temperature was 23.9 (±2.7)° C. The mean salinity in July was 34.8 (±1.7). The maximum salinity was 38.1 at Station E and the minimum salinity of 31.6 was measured at Station F. Overall, no pronounced trend in salinity or temperature was recognised along the transect.

The temperature and salinity measurements on seep waters or in little puddles were strongly influenced by evaporation and heating by the atmosphere and solar radiation during emergence at low tide. Near-surface water data from Station Hörnum of the MARNET monitoring network recorded water temperatures of 11°C in May and 18°C in July 2019 on average, i.e. lower by about 10 K in May and 3 K in July as compared to measurements for the present study on Japsand. Station Deutsche Bucht recorded salinities between 31.4 and 32.9 PSU in May, and between 32.7 to 33.1 PSU in July 2019. The averages of both ranges were about 2 units lower than the measurements on Japsand (https://www.bsh.de/DE/DATEN/Meeresumweltmessnetz/Jahreszeitreihen/jahreszeitreihen_node.html).

2.4.2 Sedimentology

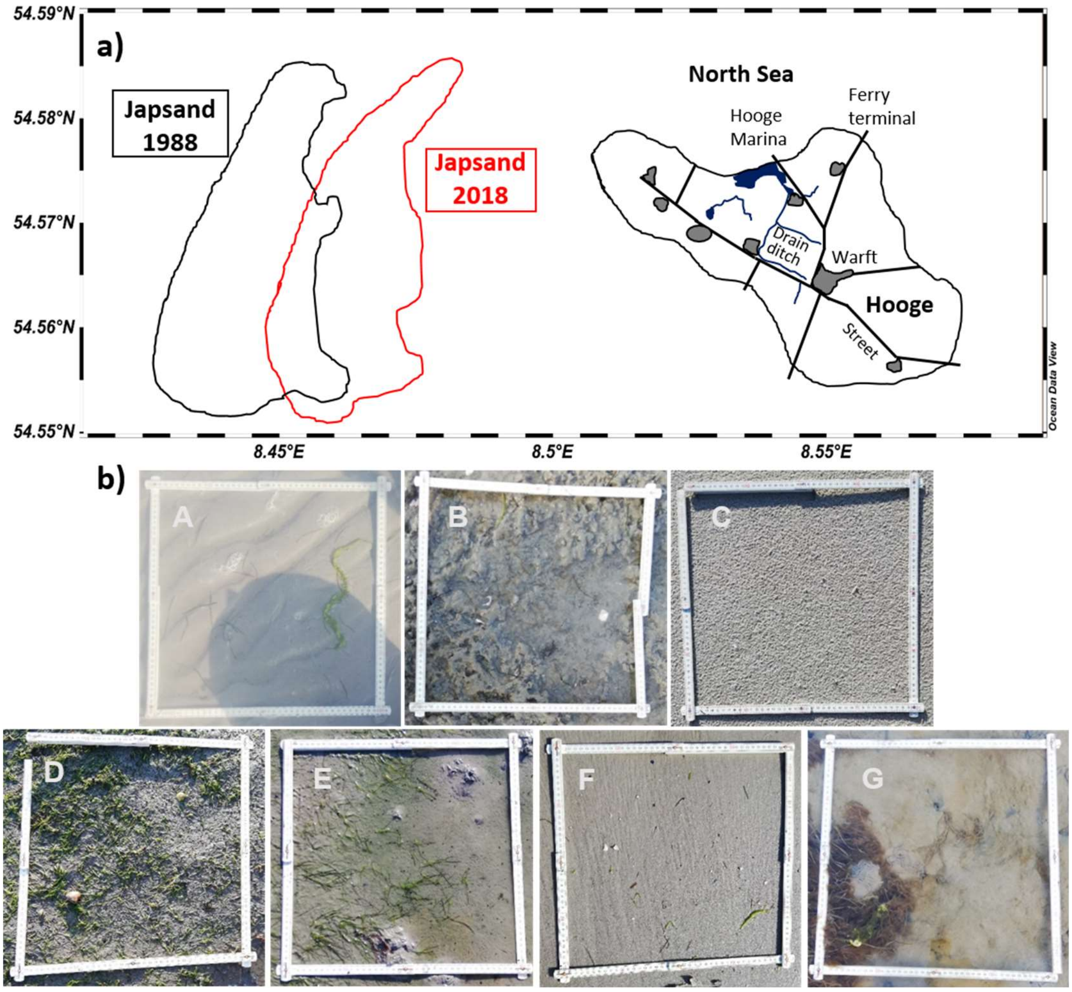

Fig. 2.2. Movement of the Japsand barrier sand towards Hallig Hooge. Comparison between 1988 indicated in black and 2018 indicated in red (a). The outline of the Japsand represents spring high water level. The map was drawn after the geological map from Schleswig Holstein (1:250 000, ed. 2012 © Landesvermessungsamt Schleswig-Holstein) and satellite images that were calibrated with two fix points at Hallig Hooge (coordinates: 54°33'56.5"N, 8°32'50.7"E; 54°34'28.8"N, 8°31'02.6"E). Sediment surface images from the individual sampling stations (A-G; 30.07.2019) (b).

Five stations (1-3, A, B) and Station F in the North were located on the seaward, western part of the Japsand. This area is mainly influenced by waves from the open North Sea. Two different surface sediments were recognised, sand and silty clay (Fig. 2.2b).

Stations 1 and B were the westernmost station closest to the average low tide level. An extremely slippery and stiff silty clay prevailed. Diatom mats and bivalve shells were recorded. The surface was extremely uneven and intersected by numerous erosional ditches. The sediment was most likely a glacial till or Eemian clay, which was exposed to the high wave energy at the seaward side (Fig. 2.2b).

Station 2, A and F showed a completely different sedimentological inventory. The surface sediment was a pure sand, wave ripple marks were common (Fig. 2.2b). The area characterizes the beach face and swash zone, particularly at low tide.

Station 3 was located at the highest part, above mean water level, at a berm crest built of bivalve shells. The sediment was sand, diatom mats were common and the surface of the sediment was perforated by aeration holes (Fig. 2.2b).

The area between Station 4 and Station 8, including Station 5, 6, 7 and C, was situated at the eastern, landward side of the Japsand. The sediment was predominately sand and drier than at Stations 2 and 3. Nevertheless, the area was frequently flooded, which reflected in the presence of bivalves and gastropods. Especially the surface of Station 7 was covered with ventilation holes for snails and other animals. The colour of the sediment surface was slightly brownish to black. Station E was located at the northeastern part of Japsand in an embayment with calm conditions and represented a mixed mud flat. The sediment was a silty sand and contained shells and fragments of bivalves and gastropods. Crabs and lugworms were common. Furthermore, the sediment showed a marked shift in colour from brown to grey at a few mm depth. Station 8 represented the transition between sand flats and mixed flats. The sediment was a silty sand in the uppermost cm, whereas the silt content increased and the colour darkened with depth. *Hydrobia* and their corresponding ventilation holes were recognised in large numbers.

Stations D and G were located on the mud flat near Hallig Hooge. Brown algae, seaweed, diatom mats, lugworm excrements as well as bivalves and gastropodes were recorded (Fig. 2.2b). Below 0.5 cm, the mud was anoxic as depicted by a shift of the sediment colour to darker tones.

Station Hooge was close to the jetty of “Volkerswarft”. The sediment was a stiff and consolidated silty sand (Fig. 2.2b).

2.4.3 Living foraminiferal faunas

Plate 2.1. Live rose Bengal stained foraminifera from the Japsand area, North Frisian Wadden Sea, Schleswig – Holstein, Germany. 1: *Elphidium williamsoni* (St. C) 1a: lateral view, 1b: side view. 2: *Haynesina germanica* (St. D), 2a: lateral view, 2b: side view. 3: *Saccamina sp*. (St. 2). 4: *Elphidium oceanense* (St. D), 4a: lateral view, 4b: side view. 5: *Haynesina depressula* (St. 2), 5a: lateral view, 5b: side view. 6: *Eggerelloides scaber* (St. 2). 7: *Bulliminella elegantissima* (St. D). 8: *Elphidium selseyense* (St. D), 8a: lateral view, 8b: side view. 9: *Elphidium gerthi* (St. 5). 10: *Ammonia batava* (St. D), 10a: spiral side, 10b: umbilical side, 10c: side view. The locations of the individual stations are indicated on Fig. 2.1b.

The living foraminiferal faunas from Japsand comprised 10 different species, of which two were agglutinated (*Eggerelloides scaber* and *Saccammina sp.*) (Plate 2.1, Table S2.1). Eight species were calcareous and belong to the genera *Ammonia*, *Elphidium* and *Haynesina*. *Ammonia batava*, *Elphidium selseyense* and *Elphidium williamsoni* were the three most common species with average proportions of 57%, 22% and 16%, respectively. Individual proportions at the different stations ranged between 15 and 100% for *Ammonia batava*, 8 and 100 % for *Elphidium selseyense* and 2 to 100 % for *Elphidium williamsoni* (Fig. 2.3). *Elphidium oceanense*, *Elphidium gerthi* and *Haynesina depressula* were rare.

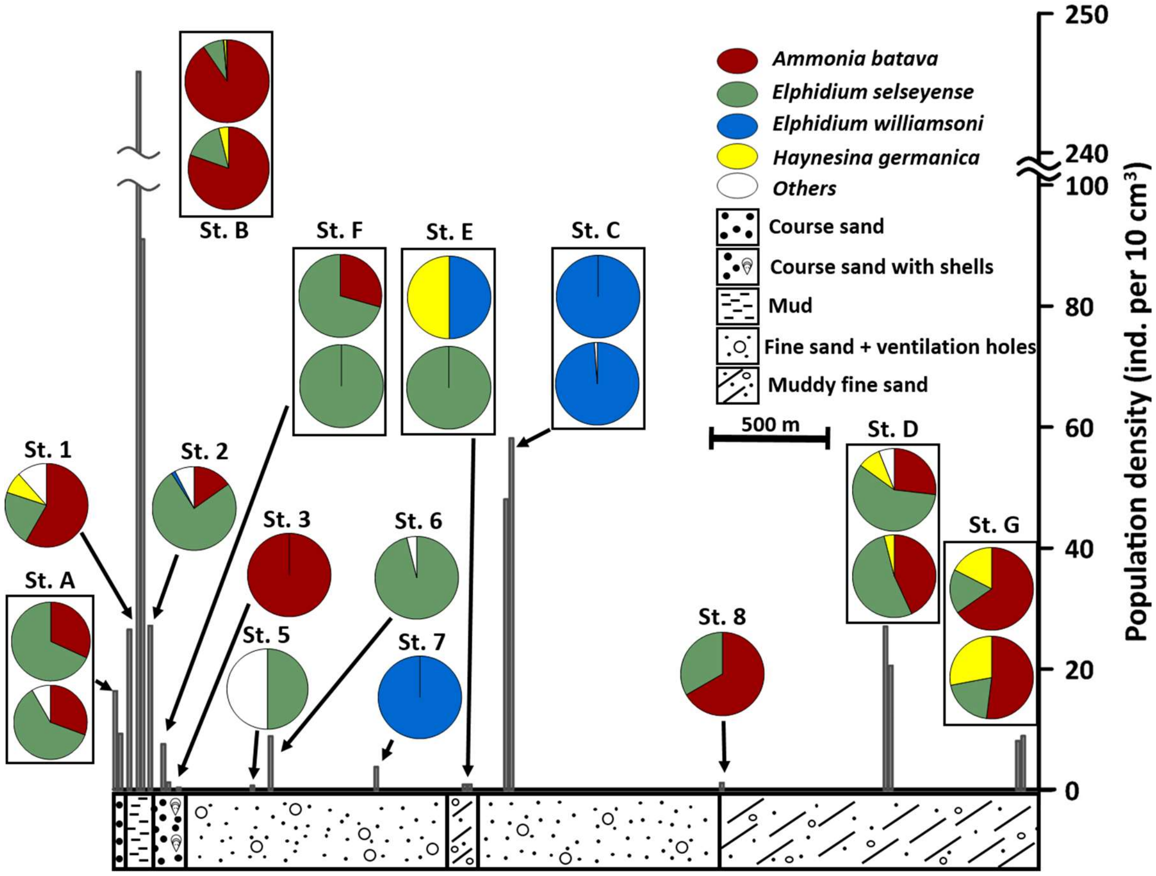

Fig. 2.3: Population density (individuals per 10 cm^3) of living rose Bengal stained foraminifera and sediment type from the Japsand area, North Frisian Wadden Sea, Germany. Pie charts show the proportion of individual species on the living fauna. Pie charts grouped within a rectangle represent duplicates at the same station where the upper pie chart represents sample 1 and the lower pie chart represents sample 2. Please note that the vertical axis is clipped and the horizontal axis is spread for the westernmost samples (St. A, 1, B and 2) for better visualization.

At three of 16 stations, i.e. Hooge, 8 and 4, no living foraminifera could be recovered. The foraminiferal population density hence varied between 0 and 246 individuals per 10 cm^3 (Fig. 2.3). The highest standing stock values were recorded at the outer part of Japsand. The population densities were very low or samples were barren between the luv side and the end of the lee side of Japsand. From the end of Japsand at the landward side up to Hallig Hooge, the foraminiferal population densities increased again. The Fisher´s alpha diversity index was generally very low and did not exceed 2.0 (Table S2.1). Surprisingly, the index displayed a distribution pattern matching the foraminiferal population density distribution. This is most likely due to the low population densities in that only the most frequent species were captured at the given sample size.

Among the individual species, *Ammonia batava* was common at the seaward side of the Japsand (Station A-Station 2) and re-appeared at two stations close to Hallig Hooge (Station D, G). *Elphidium selseyense* showed a similar distribution pattern though this species was additionally present at the landward extension of Japsand (Station 5, 6 and E) and at Station F in the northernmost part. *Elphidium williamsoni* showed a trend almost opposite to *Ammonia batava* and was found in substantial numbers at two stations only (Station 7 and C), which were located on the landward side of Japsand. *Haynesina germanica* sporadically occurred at stations where muddy fine sand or mud prevailed, and it was more common at the landward Stations D and G (Fig. 2.3).

Duplicate samples were taken at Stations A-G and analysed separately. The statistical significance of the similarity of the faunal composition of the duplicates was investigated with a non-parametric Wilcoxon Mann-Whitney test using the program PAST [58]. The p-values were all >0.05 (alpha = 5 %), indicating that the species proportions from the duplicates were not significantly different with a 95 % confidence level. The only exception was Station E with a p-value of 0.04, which demonstrated that the population of the two replicates at this station were significantly different from each other.

2.4.4 Dead foraminiferal assemblage

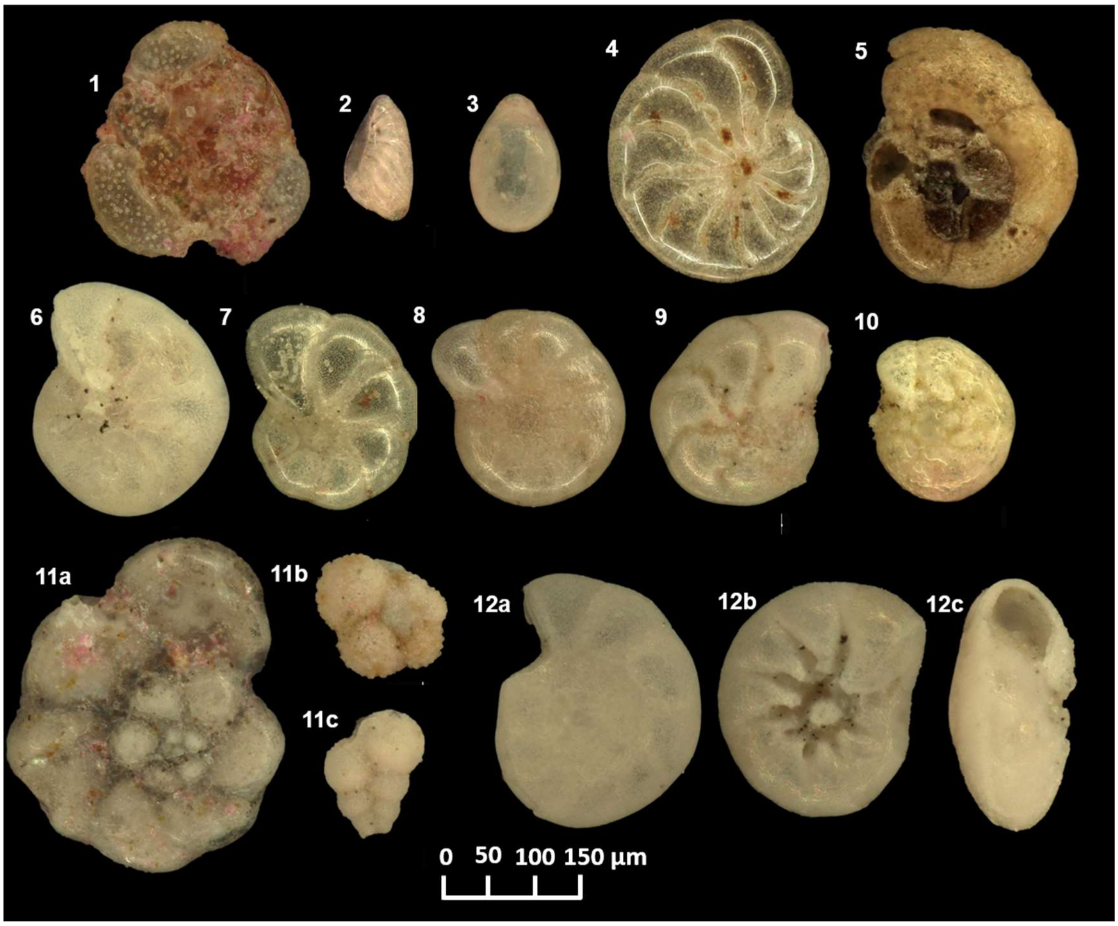

Plate 2.2. Selected foraminiferal species from the dead foraminiferal assemblage from the Japsand area, North Frisian Wadden Sea, Schleswig-Holstein, Germany. 1: *Planorbulina mediterranensis* (St. 6). 2: *Nonionella crassesuturalis* (St. B). 3: *Fissurina lucida* (St. B). 4: *Elphidium voorthuyseni* (St. D). 5: *Trochamina inflata* (St. 2). 6: *Elphidium incertum* (St. 8). 7: *Haynesina orbicularis* (St. 2). 8: *Elphidium waddense* (St. 8). 9: *Elphidium clavatum* (St. D). 10: *Elphidium oceanensis* (St. D). 11: reworked foraminifera from the Cretaceous, 11a: *Praeglobotruncana sp.* (St. 6), 11b: *Hedbergella sp*. (St. D), 11c: *Heterohelix sp*. (St. D). 12: *Ammonia aberdoveyensis* (St. 2), 12a: spiral side, 12b: umbilical side, 12c: side view. The locations of the individual stations are indicated on Fig. 2.1b.

The living fauna as described above represents only a snapshot in time, i.e. our sampling during summer. The dead foraminiferal assemblage is considered a perennial product of multiple generations, augmented by recent reproduction events and moulded by reworking and dissolution. In particular, the dead foraminiferal assemblages at Japsand comprised 26 different species of which 23 species were calcareous whereas only 3 species were agglutinating. *Elphidium* represented the most diverse genus with 9 different species (Plate 2.2, Table S2.2). The most abundant species were *Ammonia batava* (24%), *Haynesina germanica* (22.5%), *Elphidium selseyense* (13.8%) and *Elphidium waddense* (13%) (Fig. 2.4). These species were found in every sample. *Elphidium williamsoni* (9.2%) was only the fifth ranked species. In single samples, *E. williamsoni* represented more than 50 % of the assemblage (Station 7, Station C, smp. 1).

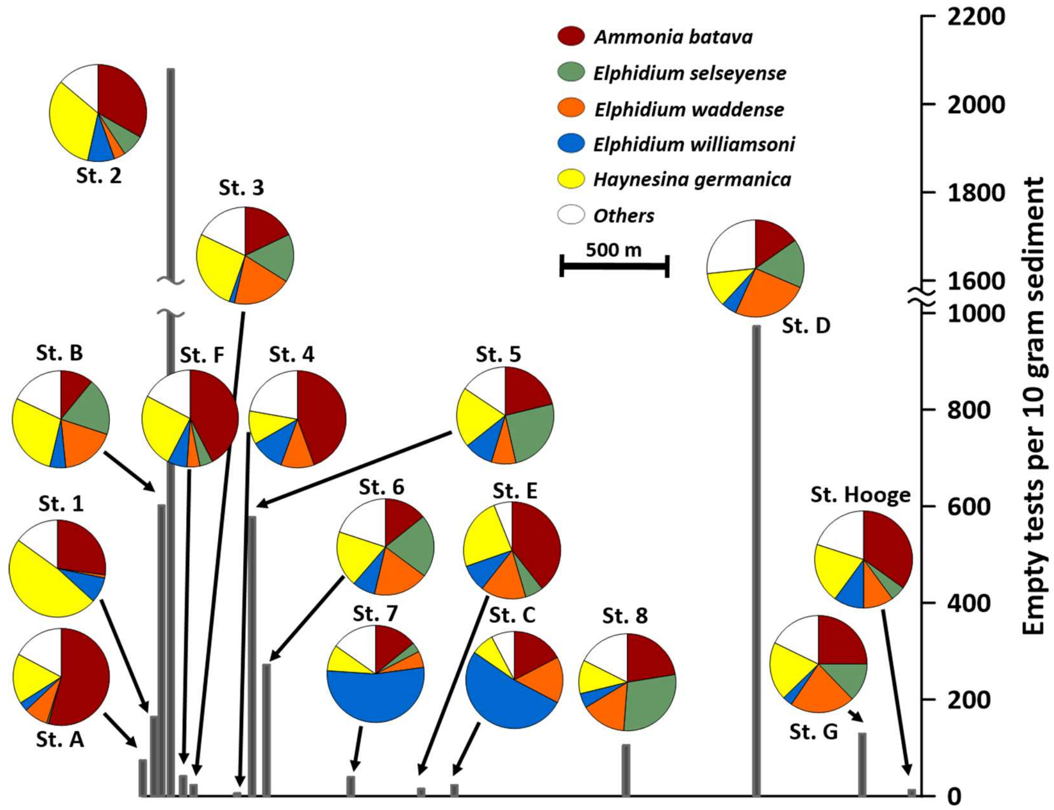

Fig. 2.4: Empty tests per 10 gram sediment of dead foraminifera from the Japsand area, North Frisian Wadden Sea, Germany. Pie charts show the proportion of individual species on the dead assemblage. Please note that the vertical axis is clipped and the horizontal axis is spread for the westernmost samples (St. A, 1, B and 2) for better visualization.

The abundances of empty tests were highest at the seaward side of Japsand with a maximum of 2079 tests per 10 cm^3 at Station 2 (Fig. 2.4). The test density strongly declined eastwards up to a minimum of 6 test per 10 cm^3 at the landward side of the barrier sand. Similar low values showed up at Station Hooge (12 empty tests per 10 cm^3) (Fig. 2.4).

The Fisher's alpha diversity index was with 4.94 highest at Station Hooge and lowest (2.22) at Station 1. The highest species richness was recorded at Station D, where 19 different species were found (Table S2.2).

2.4.5 Size distribution

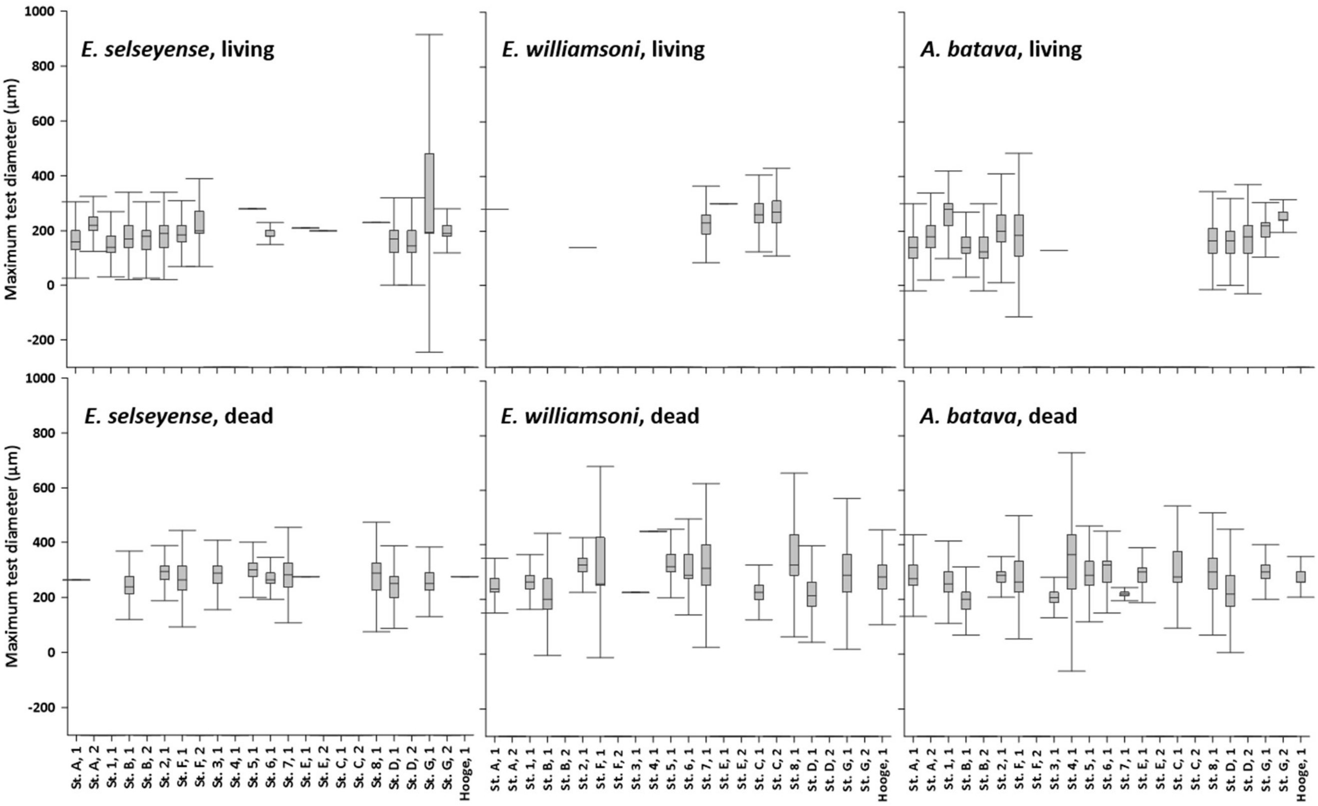

Fig. 2.5: Ranges of maximum test diameter of the most important foraminiferal species from the Japsand area, North Frisian Wadden Sea, Germany. top: living rose Bengal stained foraminifera and bottom: dead foraminifera. The vertical bar in the middle of the box represents the median, the box edges are the first and third quartil (also upper and lower quartil) and the whiskers represent 1.5 * IQR (Interquartil range = difference between lower and upper quartil).

Biometric measurements were performed to assess the growth state of the populations, and to identify cohorts of juveniles as indicator of recent reproduction events. The most abundant species of the living fauna, i.e. *E. selseyense*, *E. williamsoni* and *A. batava* were measured considering both, living fauna (Fig. 2.5, Fig. 2.6, Additional file 3: Table S2.3) and dead assemblage (Fig. 2.5, Fig. 2.6, Additional file 4: Table S2.4). The size distributions in terms of maximum test diameter of living *Elphidium selseyense* were quite uniform in the individual samples. According to the Wilcoxon Mann-Whitney test, the populations in duplicate samples were not significantly different with the exception of Station A. The size distributions of the dead assemblages were uniform as well (Fig. 2.5).

Elphidium williamsoni yielded a sufficient number of specimens only in three samples. The individual mean value of these samples was in the range of upper and lower quartile of the other samples (Fig. 2.5). The size distribution of Station C duplicates were almost identical.

Living *Ammonia batava* showed a large scatter in the size distributions of individual samples. Wilcoxon Mann-Whitney test revealed that the populations of duplicate samples of station A and C were not significantly different, while Station B and G show significant differences (St. B: p=0.004, St. G: p=0.03). The size distribution of the dead assemblages showed a large scatter among individual samples as well (Fig. 2.5).

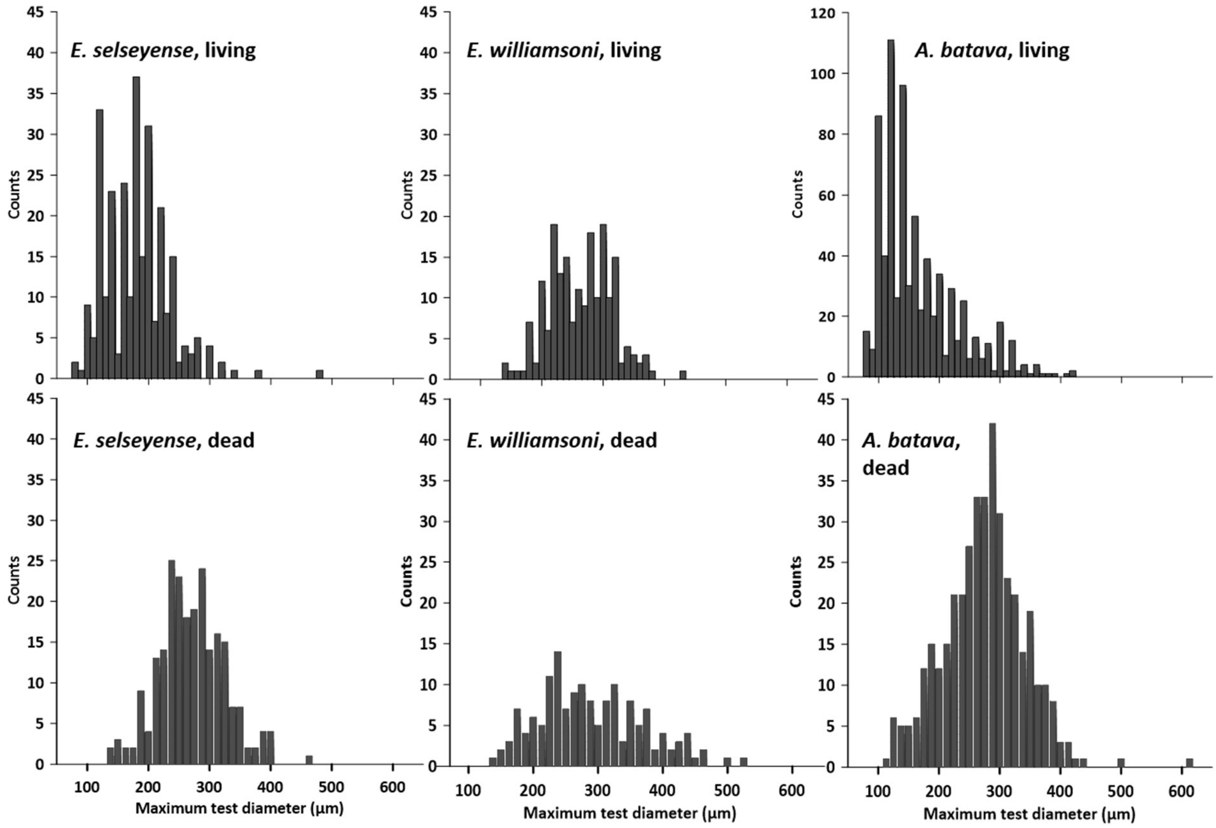

Fig. 2.6: Maximum test diameter distribution of the most important foraminiferal species from the Japsand area, North Frisian Wadden Sea, Germany. top: living rose Bengal stained foraminifera and bottom: dead foraminifera. Please note the different y-axis scale of *A. batava*, living. The interval size of 10 µm resembles the measurement accuracy, i.e. the resolution of the eyepiece reticle.

Once the biometric data from all samples were merged, *Elphidium selseyense* showed an asymmetric distribution in the living fauna, which appeared as a left skewed rather than log-normal distribution (Fig. 2.5). The size distribution of the entire dead assemblage was almost symmetrical. The mean value was 271 ±54 µm and thus substantially higher than in the living fauna (180 ±54 µm) (Fig. 2.6).

Elphidium williamsoni showed a symmetrical size distribution histogram in the combined living fauna with a mean value of 264 ±115 µm. In the dead assemblages, *E. williamsoni* showed much more scatter around a mean of 289 ±80 µm (Fig. 2.6). It has to be noted however, that the dead specimens from samples taken in July (Stations A through D), were consistently smaller.

The histogram of the entire *Ammonia batava* population showed a log-normal distribution pattern with a high number of small individuals and a low number of large specimens. The mean value was 165 ±65 µm. The size distribution of the entire dead assemblage showed a mean of 274 ±66 µm. The distribution was almost symmetrical and closely resembled a Gaussian curve (Fig. 2.6).

The cumulative size distribution of *Ammonia batava* and *Elphidium selseyense* were plotted on a log-probability scale (Fig. 2.7). The data pattern revealed that the living assemblage of both species was composed of two different subpopulations, each having an individual log-normal distribution that was displayed by a straight line (Fig. 2.7). The subpopulation of small specimens ranged from 80 to 120 µm test diameter in *E. selseyense* and 80-100 µm in *A. batava.*

2.5 Discussion

2.5.1 Reproductive state of the foraminiferal faunas

Reproductive events in intertidal or near-shore foraminifera may take place several times during the year [21, 54, 59], mainly depending on or triggered by the availability of fresh food [60, 61]. Even a continuous reproduction throughout the year has been suggested, though with lower rates during winter [62]. The biometric data of the present study were therefore explored to assess whether reproduction has recently taken place and how this may have influenced the assemblage composition.

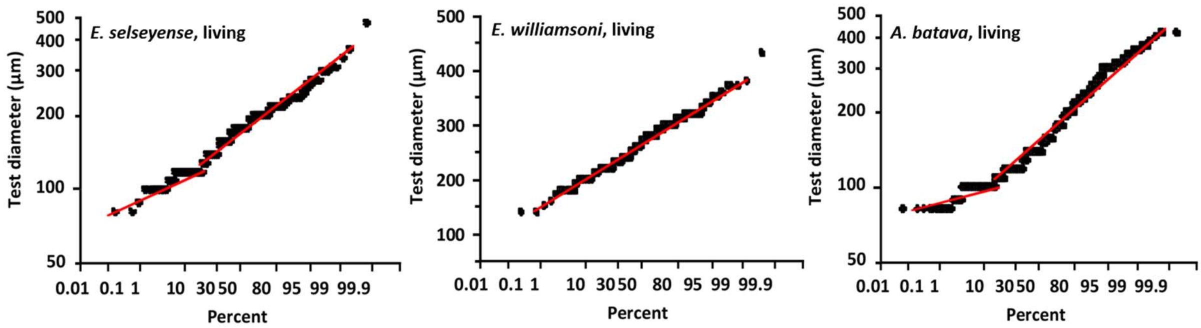

Fig. 2.7: Cumulative size distribution of the most abundant foraminiferal species in the living assemblage from the Japsand area on a log probability scale. A log-normal or normal distribution is depicted by a straight line [63]. Breaks of their slope indicate the limits of individual subpopulations [64].

The size distribution of living *Ammonia batava* and *Elphidium selseyense* revealed two different subpopulations, of which the subpopulation of small specimens comprise 18 and 15 % of the whole population only. If such small specimens were holding the majority of all living individuals, this may indicate the onset of the reproductive season, which mainly takes place in the summer months [e.g., 65]. During asexual reproduction, one single foraminifer may produce offspring of more than 100 very small juveniles [e.g., 6, 66]. It is evident that such a scaled phenomenon can strongly influence the living assemblage. *Elphidium williamsoni,* on the other hand, showed a straight line on log-probability plot (Fig. 2.7) indicating that only a single population was present. Reproduction might not have been started, the juveniles were too small to be captured by a 63-µm mesh, or they could have been displaced by currents or tides. At Station C, sample 1, however, the dead assemblage of *E. williamsoni* showed 23 well-preserved specimens very uniform in size, which contained spratty, unstructured remnants of cytoplasm. The sample has been taken in July. This observation corroborated the assumption that reproduction of *E. williamsoni* was just commencing. The mean diameter of living *E. williamsoni* was with ca. 263 ±51 µm slightly lower than 289 ±80 µm in the dead assemblage. The mean diameter of dead specimens displays the average size of the individuals when reproduction usually takes place. As such, the size difference of living and dead specimens indicates that the specimens would have to grow for some more time before reproduction maturity is reached. None-the-less, our sampling represents only two surveys in almost nine weeks and at least bi-weekly sampling is required to constrain the timing of reproductive events [62, 67].

2.5.2 Comparison of living and dead assemblages

The dead foraminiferal assemblage showed a species richness of 26 that was more than twice as high as the 10 species recorded in the living fauna. Furthermore, the foraminiferal test abundance of the dead assemblages exceed the abundance of living specimens by one order of magnitude, which is a common feature and often reported in the literature [e.g., 39, 68]. General patterns of abundance were uniform at the seaward side of Japsand in dead assemblages and living faunas up to Station 3. This similarity was changing on the landward side of Japsand. Especially at Stations 5 and 6, the dead assemblage showed much higher abundances and species richness values. This was also mirrored in the Fisher's alpha index, which was close to the maximum of all diversity index values in the dead assemblage and only slightly above the minimum of all index values in the living fauna (Table S2.1, Table S2.2).

Ammonia batava was the most abundant species in the living fauna and dead assemblage, even though its dominance was less pronounced. *Haynesina germanica* on the other hand, which was the second ranked species in the dead assemblage, was with a relative abundance of ca. 3 % on average comparatively rare in the living fauna. *Elphidium selseyense* was more common in the living fauna. *Elphidium williamsoni* was replaced by *Elphidium waddense* in the dead assemblage (13%) though still abundant. Several species were found in the dead assemblage and not found in the living fauna at Japsand.

Single specimens of *Fussurina lucida* were found in the dead assemblages of samples Station 1, B and 8. This stenohaline species was common in near shore and shelf environments in NW Europe [69, 70] and was scarcely recorded in intertidal environments of the North Sea [71]. *Planorbulina mediterranensis* was also found occasionally as single specimens. The species was preferentially living attached to plants or hard substrates in subtidal waters or turbulent shelf environments [e.g., 72-74]. The agglutinating species *Jadammina macrescens* and *Trochammina inflata* were recorded as one or two specimens in some samples. They were generally associated with salt marsh plants [5, 6, 75]. The Japsand area neither exhibited salt marshes nor deeper shelf environments. Therefore, these species must have been introduced into the system via different pathways. The landward side of the Japsand was submerged during high water and storm floods, and ebb currents may have transported foraminiferal tests from other parts of the North Sea to the Japsand area [e.g., 76]. These tests accumulated in sheltered areas, as the landward side of the Japsand [77, 78].

At the Stations 8 and D, *Cibicides lobatus* was present in the dead assemblage. This species was living in open marine areas attached to plants, seaweed and hard substrates [79]. Therefore, it was common in high-energy environments [80-82]. In the western Baltic Sea, small populations attached to red algae were reported [83]. Alve and Murray [75] suggested that small populations could enter more sheltered environments with adequate substrates and sufficient food supply. Therefore, it is conceivable that this species has been displaced to the Japsand area via currents. It is also possible that some individuals could recruit because the area is characterized by seaweed and shell fragments, which are adequate substrate for living *Cibicicides lobatulus*.

Bucella frigida was recorded at Stations 5, 6 and D. The species is known from water depth >15 m and colder environments [84], also from Eemian deposits [85–87]. *Ammonia aberdoveyensis* was common in the dead assemblage. This species is associated with warmer temperatures and higher salinities [88]. Many shells of this species found in the dead assemblages of the Japsand had a dull, whitish surface and the last chamber was often missing. This points to an alteration process the shells underwent during fossilisation, which in turn may be seen as an evidence for reworking from older sediments and redeposition, which lead to the influx of fossil foraminifera into the dead assemblage. This also applies to Cretaceous foraminifera that were reworked from Pleistocene glacial till, in which they have been incorporated when glaciers eroded Chalk bedrock [59, 89].

2.5.3 Connectivity of the foraminiferal faunas

Langer et al. [90] and Haake [71] proposed conceptual models for the horizontal distribution of foraminiferal species along a transect from the shoreline to the open sea, or from mud flats to sand flats. According to these models, *Haynesina germanica* and *Elphidium selseyense* were distributed nearly equally in all facies. *Elphidium williamsoni* was common on the mixed flats. *Ammonia batava* was restricted to sand flats according to Langer et al. [90], while Haake [71] found it more common on mud flats but not restricted to this environment. These models do only partly apply to the Japsand area. *Elphidium williamsoni* was found to be confined to the mixed flats (Fig. 2.3). Furthermore, *Elphidium selseyense* was common in all facies. *Ammonia batava* was frequent on the sand flats, common on the mud flat but almost absent on the mixed flat, which is in agreement with Haake [71] and Langer et al. [90]. Contrary to the conceptual models, *Haynesina germanica* was rare on the mixed flats and constituted only a small proportion of the fauna (Fig. 2.3).

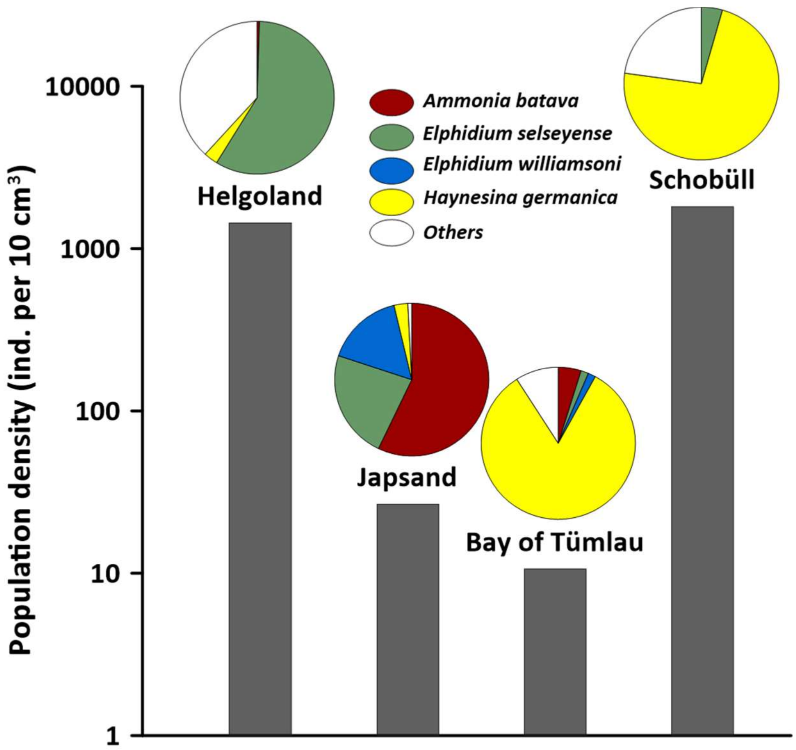

Fig. 2.8: Population density (individuals per 10 cm^3) of living rose Bengal stained foraminifera from the Japsand area, North Frisian Wadden Sea, Germany and comparative locations at Helgoland, the Bay of Tümlau [based on 4] and Schobüll. Pie charts show the proportion of individual species in the living fauna.

Due to the permanent redeposition of intertidal sands and the ubiquitous lateral displacement of foraminiferal tests, as explained above, it is necessary to assess the connectivity between different foraminiferal faunas in a wider geographical range. Helgoland inner port represents a first stage from the open sea to a more sheltered environment. The fauna showed several foraminiferal species that were normally found at greater depths around the island (e.g., *Hopkinsina pacifica*). The dominant species was *Elphidium selseyense* (58 %). *Ammonia batava, Ammonia tepida* and *Haynesina germanica* were rare (Fig. 2.8, Table S2.5). Agglutinating littoral species were not found. A connectivity between Helgoland and Japsand was clearly visible in the presence of *Elphidium selseyense*, *Ammonia batava* and *Haynesina germanica* even though proportions of the species were shifting towards a dominance of *Ammonia batava* (57.1 %) on the expense of *Elphidium selseyense* (22 %) (Fig. 2.8). Deep water species were not present anymore, but agglutinating species were in minority, which was due to the sandy environment and the strong hydrodynamics at Japsand [78]. Furthermore, *Elphidium williamsoni* appeared, which marked a first connection to the higher, intertidal environments.

The next step on the way from the open North Sea to the mainland is the Bay of Tümlau, near Westerhever [4]. The most common species in samples with a sand content of more than 40 % (see Table S2.6) from this area was *Haynesina germanica* (90.2 %). *Ammonia batava*, *Elphidium selseyense* (*Elphidium excavatum* in [4]) and *Elphidium williamsoni* were present with much lower proportions. This fauna was linking not only to Japsand but also to the tidal flats at Schobüll (Fig. 2.8, Table S2.7).

The marginal mudflats before the indigenous saltmarsh at Schobüll depicted that the connection between the different environments can be tracked further. The connecting species were *Haynesina germanica* (73 %) and *Elphidium selseyense* (4 %) (Fig. 2.8). *Ammonia batava* was replaced by *Ammonia tepida* (17 %), and *Elphidium williamsoni* disappeared, though it was occasionally found in the salt marsh here [6].

2.6 Conclusions

Ammonia batava was the most abundant species in the living fauna and dead assemblage at Japsand. *Elphidium selseyense* was more common in the living fauna. *Haynesina germanica* was rare in the living fauna but frequent in the dead assemblage. *Elphidium williamsoni* was common in the living fauna but rare in the dead assemblage. *Elphidium waddense* was only found in the dead assemblage. It is conceivable that the high proportions of living *Ammonia batava* and *Elphidium selseyense* were effected by reproduction. The size distribution curves of both species indeed provided corroborating evidence that reproduction had recently taken place, whereas reproduction of *Elphidium williamsoni* had probably just started (Fig. 2.5 and 2.6).

Several species were found in the dead assemblage and not found in the living fauna. Those species have been reported from other areas of the North Sea and North Atlantic. As they were comparatively rare, they were probably displaced to the Japsand area via tidal currents. Recent distribution and preservation of *Bucella frigida* and *Ammonia aberdoveyensis* revealed their reworking from older sediments. Therefore, fossil foraminifera could have a certain influence on the structure of the dead assemblage. An ubiquitous lateral displacement of foraminiferal tests at short distance certainly prevailed on Japsand, as evidenced by the uniform assemblage composition of the dead assemblages, and the same size distribution of empty tests of different species.

The conceptual model of Haake [71] and Langer et al. [90] on the distribution of sublitoral foraminifera was confirmed in the present study, with the exception of *Elphidium williamsoni*. It is a matter of further investigations whether this may be due to the specific ecological requirements of this species, as it holds and sequesters chloroplasts [91, 92].

A connection between the open North Sea environment and the mainland can be tracked in the living fauna of benthic foraminifera (Fig. 2.8). Species depicting this link at most were *Haynesina germanica*, *Ammonia batava* and different *Elphidium* species. They are known to have a wide range of distribution and also an excellent ability of adapting to different environments [93–95] thus, they can be classified as opportunistic species. While major vectors for the transoceanic transport of foraminifera were ships' ballast water [96–98] or the digestive pathway of fish [99, 100], the proliferation of foraminifera and their propagules in intraoceanic settings like the North Sea was mainly effected by suspended load via currents and tides [76, 101]. Our results indicated that the latter of the before mentioned processes were dominant environmental factors shaping in particular the dead foraminiferal assemblages in the Japsand area.

2.7 Supplementary information

Additional file 3: Table S2.3. Biometric measurements of the most important foraminiferal species from the living fauna, Japsand, German Wadden Sea.

Additional file 4: Table S2.4. Biometric measurements of the most important foraminiferal species from the dead assemblage, Japsand, German Wadden Sea.

2.8 Availability of data and materials

All data generated or analysed during this study are included in this chapter and its appendices or are available in the online version of the published manuscript at https://hmr.biomedcentral.com/articles/10.1186/s10152-021-00551-2#Sec16 (Additional file 3 and 4).

2.9 Acknowledgments

We want to thank the team from the "Schutzstation Wattenmeer" at Hallig Hooge for their support by giving the opportunity to join a guided tour to the Japsand. Furthermore, they let us use their facilities for microscopy. Leif Boyens is thanked for his flexibility and his accommodation space. The help of Danny Arndt during fieldwork is gratefully acknowledged. The valuable comments and suggestions of the Editor and two anonymous reviewers helped improving the manuscript a lot.

2.10 References

1. Hofstede JLA. Regional differences in the morphologic behaviour of four German Wadden Sea barriers. Quaternary International. 1999;56(1):99–106.
2. Hofstede J. Process-response analysis for the North Frisian supratidal sands (Germany). Journal of Coastal Research. 1997:1–7.
3. Richter G. Beobachtungen zur Ökologie einiger Foraminiferen des Jade-Gebietes; 1961.
4. Müller-Navarra K, Milker Y, Schmiedl G. Natural and anthropogenic influence on the distribution of salt marsh foraminifera in the Bay of Tümlau, German North Sea. Journal of Foraminiferal Research. 2016;46(1):61–74.
5. Horton BP, Edwards RJ. Quantifying Holocene sea level change using intertidal foraminifera: Lessons from the British Isles. Departmental Papers (EES). 2006:50.
6. Lehmann G. Vorkommen, Populationsentwicklung, Ursache fleckenhafter Besiedlung und Fortpflanzungsbiologie von Foraminiferen in Salzwiesen und Flachwasser der Nord-und Ostseeküste Schleswig-Holsteins; (Dissertation). University of Kiel (218 pp). 2000.
7. Gabel B. Die Foraminiferen der Nordsee. Helgoländer wissenschaftliche Meeresuntersuchungen. 1971;22(1):1–65.

8. Jarke J. Die Beziehungen zwischen hydrographischen Verhältnissen, Faziesentwicklung und Foraminiferenverbreitung in der heutigen Nordsee als Vorbild für die Verhältnisse während der Miocän-Zeit. Meyniana. 1961;10:21–36.
9. Moodley L, Boschker HTS, Middelburg JJ, Pel R, Herman PMJ, de Deckere E, Heip CHR. Ecological significance of benthic foraminifera: ^{13}C labelling experiments. Marine Ecology Progress Series. 2000;202:289−295.
10. van Oevelen D, Moodley L, Soetaert K, Middelburg JJ. The trophic significance of bacterial carbon in a marine intertidal sediment: results of an in situ stable isotope labeling study. Limnology and Oceanography. 2006;51:2349−2359.
11. Lei YL, Stumm K, Wickham SA, Berninger UG. (2014). Distributions and biomass of benthic ciliates, foraminifera and amoeboid protists in marine, brackish and freshwater sediments. Journal of Eukaryote Microbiology. 2014;61:493–508.
12. Nordberg K, Asteman IP, Gallagher TM, Robijn A. Recent oxygen depletion and benthic faunal change in shallow areas of Sannäs Fjord, Swedish west coast. Journal of Sea Research. 2017;127:46–62.
13. Alve E, Korsun S, Schönfeld J, Dijkstra N, Golikova E, Hess S, et al. Foram-AMBI: A sensitivity index based on benthic foraminiferal faunas from North-East Atlantic and Arctic fjords, continental shelves and slopes. Marine Micropaleontology. 2016;122:1–12.
14. Duffield CJ, Hess S, Norling K, Alve E. The response of *Nonionella iridea* and other benthic foraminifera to “fresh” organic matter enrichment and physical disturbance. Marine Micropaleontology. 2015;120:20–30.
15. Asteman IP, Nordberg K. Foraminiferal fauna from a deep basin in Gullmar Fjord: The influence of seasonal hypoxia and North Atlantic Oscillation. Journal of Sea Research. 2013;79:40–9.
16. Dolven JK, Alve E, Rygg B, Magnusson J. Defining past ecological status and in situ reference conditions using benthic foraminifera: A case study from the Oslofjord, Norway. Ecological indicators. 2013;29:219–33.
17. Mendes I, Dias JA, Schönfeld J, Ferreira Ó, Rosa F, Lobo FJ. Living, dead and fossil benthic foraminifera on a river dominated shelf (northern Gulf of Cadiz) and their use for paleoenvironmental reconstruction. Continental Shelf Research. 2013;68:91–111.
18. Bouchet VMP, Alve E, Rygg B, Telford RJ. Benthic foraminifera provide a promising tool for ecological quality assessment of marine waters. Ecological indicators. 2012;23:66–75.
19. Mojtahid M, Jorissen F, Lansard B, Fontanier C, Bombled B, Rabouille C. Spatial distribution of live benthic foraminifera in the Rhône prodelta: Faunal response to a continental–marine organic matter gradient. Marine Micropaleontology. 2009;70(3-4):177–200.
20. Mojtahid M, Jorissen F, Lansard B, Fontanier C. Microhabitat selection of benthic foraminifera in sediments off the Rhône River mouth (NW Mediterranean). Journal of Foraminiferal Research. 2010;40(3):231–46.
21. Schönfeld J, Numberger L. The benthic foraminiferal response to the 2004 spring bloom in the western Baltic Sea. Marine Micropaleontology. 2007;65(1-2):78–95.

22. Lutze G. Foraminiferen der Kieler Bucht (Westliche Ostsee): 1.“ Hausgartengebiet“ des Sonderforschungsbereiches 95 der Universität Kiel. Meyniana. 1974;26:9–22.
23. Bertlich J, Nürnberg D, Hathorne EC, Nooijer LJ de, Mezger EM, Kienast M, et al. Salinity control on Na incorporation into calcite tests of the planktonic foraminifera *Trilobatus sacculifer*–evidence from culture experiments and surface sediments. Biogeosciences. 2018;15(20):5991–6018.
24. Wit JC, Nooijer LJ de, Wolthers M, Reichart G-J. A novel salinity proxy based on Na incorporation into foraminiferal calcite. Biogeosciences. 2013;10:6375–87.
25. Elderfield H, Yu J, Anand P, Kiefer T, Nyland B. Calibrations for benthic foraminiferal Mg/Ca paleothermometry and the carbonate ion hypothesis. Earth and Planetary Science Letters. 2006;250(3-4):633–49.
26. Nürnberg D. Magnesium in tests of *Neogloboquadrina pachyderma* sinistral from high northern and southern latitudes. Journal of Foraminiferal Research. 1995;25(4):350–68.
27. Keul N, Langer G, Thoms S, Nooijer LJ de, Reichart G-J, Bijma J. Exploring foraminiferal Sr/Ca as a new carbonate system proxy. Geochimica et Cosmochimica Acta. 2017;202:374–86.
28. Keul N, Langer G, Nooijer LJ de, Bijma J. Effect of ocean acidification on the benthic foraminifera *Ammonia sp*. is caused by a decrease in carbonate ion concentration. Biogeosciences. 2013;10(10):6185–98.
29. Ni Y, Foster GL, Bailey T, Elliott T, Schmidt DN, Pearson P, et al. A core top assessment of proxies for the ocean carbonate system in surface-dwelling foraminifers. Paleoceanography. 2007;22(3).
30. Bijma J, Spero HJ, Lea DW. Reassessing foraminiferal stable isotope geochemistry: Impact of the oceanic carbonate system (experimental results). Use of proxies in paleoceanography: Springer; 1999:489–512.
31. Alve E, Murray JW, Skei J. Deep-sea benthic foraminifera, carbonate dissolution and species diversity in Hardangerfjord, Norway: An initial assessment. Estuarine, Coastal and Shelf Science. 2011;92(1):90–102.
32. Berkeley A, Perry CT, Smithers SG, Horton BP, Taylor KG. A review of the ecological and taphonomic controls on foraminiferal assemblage development in intertidal environments. Earth-Science Reviews. 2007;83(3-4):205–30.
33. Boltovskoy E., Wright R. Ecology. In Recent Foraminifera Springer Netherlands, Dordrecht.1976;223–274.
34. Murray JW. Ecology and Applications of Benthic Foraminifera. Cambridge University Press; 2006.
35. Schönfeld J. Monitoring benthic foraminiferal dynamics at Bottsand coastal lagoon (western Baltic Sea). Journal of Micropalaeontology. 2018;37(1):383–93.
36. Weinmann AE, Goldstein ST. Changing structure of benthic foraminiferal communities: Implications from experimentally grown assemblages from coastal Georgia and Florida, USA. Marine Ecology. 2016;37(4):891–906.
37. Uthicke S, Momigliano P, Fabricius KE. High risk of extinction of benthic foraminifera in this century due to ocean acidification. Scientific Reports. 2013;3(1):39.

38. Haynert K, Schönfeld J, Riebesell U, Polovodova I. Biometry and dissolution features of the benthic foraminifer *Ammonia aomoriensis* at high pCO_2.Marine Ecology . Prog. Ser. 2011;432:53–67.
39. Milker Y, Horton BP, Nelson AR, Engelhart SE, Witter RC. Variability of intertidal foraminiferal assemblages in a salt marsh, Oregon, USA. Marine Micropaleontology. 2015;118:1–16.
40. Leorri E, Gehrels WR, Horton BP, Fatela F, Cearreta A. Distribution of foraminifera in salt marshes along the Atlantic coast of SW Europe: Tools to reconstruct past sea-level variations. Quaternary International. 2010;221(1-2):104–15.
41. Haslett SK, Strawbridge F, Martin NA, Davies CFC. Vertical saltmarsh accretion and its relationship to sea-level in the Severn Estuary, UK: An investigation using foraminifera as tidal indicators. Estuarine, Coastal and Shelf Science. 2001;52(1):143–53.
42. Edwards RJ, Horton BP. Reconstructing relative sea-level change using UK salt-marsh foraminifera. Marine Geology. 2000;169(1-2):41–56.
43. Hayward BW, Grenfell HR, Scott DB. Tidal range of marsh foraminifera for determining former sea-level heights in New Zealand. New Zealand Journal of Geology and Geophysics. 1999;42(3):395–413.
44. Thomas E, Varekamp JC. Paleo-environmental analyses of marsh sequences (Clinton, Connecticut): Evidence for punctuated rise in relative sealevel during the latest Holocene. Journal of Coastal Research. 1991:125–58.
45. Murray JW, Alve E. Natural dissolution of modern shallow water benthic foraminifera: Taphonomic effects on the palaeoecological record. Palaeogeography, Palaeoclimatology, Palaeoecology. 1999;146(1-4):195–209.
46. Green MA, Aller RC, Aller JY. Carbonate dissolution and temporal abundances of foraminifera in Long Island Sound sediments. Limnology and Oceanography. 1993;38(2):331–45.
47. Murray JW. Syndepositional dissolution of calcareous foraminifera in modern shallow-water sediments. Marine Micropaleontology. 1989;15(1-2):117–21.
48. Douglas RG, Liestman J, Walch C, Blake G, Cotton ML. The transition from live to sediment assemblage in benthic foraminifera from the southern California borderland. Department of Geological Sciences University of Southern California Los Angeles. 1980.
49. Schönfeld J, Alve E, Geslin E, Jorissen F, Korsun S, Spezzaferri S. The FOBIMO (FOraminiferal BIo-MOnitoring) initiative—Towards a standardised protocol for soft-bottom benthic foraminiferal monitoring studies. Marine Micropaleontology. 2012;94:1–13.
50. Polovodova I, Nikulina A, Schönfeld J, Dullo W-C. Recent benthic foraminifera in the Flensburg Fjord (western Baltic Sea). Journal of Micropalaeontology. 2009;28(2):131–42.
51. Nooijer LJ de. Shallow water benthic foraminifera as proxy for natural versus human-induced environmental change: Utrecht University; 2007.
52. Lutze G. Zur Foraminiferen-Fauna der Ostsee. Meyniana. 1965;15:75–142.
53. Lutze G, Altenbach A. Technik und Signifikanz der Lebendfärbung benthischer Foraminiferen mit Bengalrot. Geologisches Jahrbuch. Reihe A, Allgemeine und regionale

Geologie BR Deutschland und Nachbargebiete, Tektonik, Stratigraphie, Paläontologie. 1991(128):251–65.
54. Wefer G. Umwelt, Produktion und Sedimentation benthischer Foraminiferen in der westlichen Ostsee. 1976.
55. Schönfeld J, Golikova E, Korsun S, Spezzaferri S. The Helgoland Experiment–assessing the influence of methodologies on Recent benthic foraminiferal assemblage composition: Geological Society of London; 2013.
56. Lübbers J, Schönfeld J. Recent saltmarsh foraminiferal assemblages from Iceland. Estuarine, Coastal and Shelf Science. 2018;200:380–94.
57. Parent B, Barras C, Jorissen F. An optimised method to concentrate living (Rose Bengal-stained) benthic foraminifera from sandy sediments by high density liquids. Marine Micropaleontology. 2018;144:1–13.
58. Hammer Ø, Harper DAT, Ryan PD. PAST: Paleontological statistics software package for education and data analysis. Palaeontologia Electronica. 2001;4(1):9.
59. Haake F-W. Zum Jahresgang von Populationen einer Foraminiferen-Art in der westlichen Ostsee. Meyniana. 1967;17:13–27.
60. Gooday AJ. A response by benthic foraminifera to the deposition of phytodetritus in the deep sea. Nature. 1988;332(6159):70–3.
61. Bradshaw JS. Preliminary laboratory experiments on ecology of foraminiferal populations. Micropaleontology. 1955;351–8.
62. Murray JW, Alve E. Major aspects of foraminiferal variability (standing crop and biomass) on a monthly scale in an intertidal zone. Journal of Foraminiferal Research. 2000;30(3):177–91.
63. Otto GH. A modified logarithmic probability graph for the interpretation of mechanical analyses of sediments. Journal of Sedimentary Research. 1939;9(2):62–76.
64. Schönfeld J, Voigt T. Sediment geometry, facies analysis and palaeobathymetry of the Schrammstein Formation (upper Turonian–lower Coniacian) in southern Saxony, Germany. Zeitschrift der Deutschen Gesellschaft für Geowissenschaften. 2020;171(2):199–209.
65. Heinz P, Marten RA, Linshy VN, Haap T, Geslin E, Köhler H-R. 70 kD stress protein (Hsp70) analysis in living shallow-water benthic foraminifera. Marine Biology Research. 2012;8(7):677–81.
66. Lutze GF, Wefer G. Habitat and asexual reproduction of *Cyclorbiculina compressa* (ORBIGNY), Soritidae. Journal of Foraminiferal Research. 1980;10(4):251–60.
67. Lutze GF. Siedlungs-Strukturen rezenter Foraminiferen. Meyniana. 1968;18:31–4.
68. Murray JW. Comparative studies of living and dead benthic foraminiferal distributions. Hedley, R. H., and Adams, C. G., eds., Foraminifera. 1976;2:p. 45–109.
69. Alve E, Murray JW. Temporal variability in vertical distributions of live (stained) intertidal foraminifera, southern England. Journal of Foraminiferal Research. 2001;31(1):12–24.
70. Küppers R. Zur Foraminiferenfauna bei Helgoland. (Dissertation) Universität Bonn (303 pp). 1987.
71. Haake F-W. Untersuchungen an der Foraminiferen-Fauna im Wattgebiet zwischen Langeoog und dem Festland. Meyniana. 1962;12:25–64.

72. Rogerson M, Schönfeld J, Leng MJ. Qualitative and quantitative approaches in palaeohydrography: A case study from core-top parameters in the Gulf of Cadiz. Marine Geology. 2011;280(1-4):150–67.
73. Guimerans PV, Currado JC. Distribution of *Planorbulinacea* (benthic foraminifera) assemblages in surface sediments on the northern margin of the Gulf of Cadiz. Boletin-Instituto Espanol de Oceanografia. 1999;15(1/4):181–90.
74. Murray JW. Recent benthic foraminiferids of the Celtic Sea. Journal of Foraminiferal Research. 1979;9(3):193–209.
75. Alve E, Murray JW. Marginal marine environments of the Skagerrak and Kattegat: A baseline study of living (stained) benthic foraminiferal ecology. Palaeogeography, Palaeoclimatology, Palaeoecology. 1999;146(1-4):171–93.
76. Murray JW, Sturrock S, Weston J. Suspended load transport of foraminiferal tests in a tide- and wave-swept sea. Journal of Foraminiferal Research. 1982;12(1):51–65.
77. Hayward BW, Grenfell HR, Sandiford A, Shane PR, Morley MS, Alloway BV. Foraminiferal and molluscan evidence for the Holocene marine history of two breached maar lakes, Auckland, New Zealand. New Zealand Journal of Geology and Geophysics. 2002;45(4):467–79.
78. Grabert B. Zur Eignung von Foraminiferen als Indikatoren für Sandwanderung. Deutsche Hydrografische Zeitschrift. 1971;24(1):1–14.
79. Kitazato H. Ecology of benthic foraminifera in the tidal zone of a rocky shore. Revue de paléobiologie. 1988:815–25.
80. Schönfeld J. Recent benthic foraminiferal assemblages in deep high-energy environments from the Gulf of Cadiz (Spain). Marine Micropaleontology. 2002;44(3-4):141–62.
81. Hansen A, Knudsen KL. Recent foraminiferal distribution in Freemansundet and Early Holocene stratigraphy on Edgeøya, Svalbard. Polar Research. 1995;14(2):215–38.
82. Murray JW. Living and dead Holocene foraminifera of Lyme Bay, southern England. Journal of Foraminiferal Research. 1986;16(4):347–52.
83. Conradsen K. Recent benthic foraminifera in the southern Kattegat, Scandinavia: Distributional pattern and controlling parameters. Boreas. 1993;22(4):367–82.
84. Thomas E, Gapotchenko T, Varekamp JC, Mecray EL, Brink B. Benthic foraminifera and environmental changes in Long Island Sound. Journal of Coastal Research. 2000:641–55.
85. Knudsen KL. Marine interglacial deposits in the Cuxhaven area, NW Germany: A comparison of Holsteinian, Eemian and Holocene foraminiferal faunas. E&G Quaternary Science Journal. 1988;38(1):69–77.
86. Knudsen KL. Foraminiferal stratigraphy of Quaternary deposits in the Roar, Skjold and Dan fields, central North Sea. Boreas. 1985;14(4):311–24.
87. Konradi PB. Foraminifera in Eemian deposits at Stensigmose, southern Jutland. Danmarks Geologiske Undersøgelse. 1976;105:1-57.
88. Bird C, Schweizer M, Roberts A, Austin WEN, Knudsen KL, Evans KM, et al. The genetic diversity, morphology, biogeography, and taxonomic designations of *Ammonia* (Foraminifera) in the Northeast Atlantic. Marine Micropaleontology. 2020;155:101726.

89. Fish PR, Whiteman CA. Chalk micropalaeontology and the provenancing of middle Pleistocene lowestoft formation till in eastern England. Earth Surface Process and Landforms. 2001;26:953–970.
90. Langer M, Hottinger L, Huber B. Functional morphology in low-diverse benthic foraminiferal assemblages from tidal flats of the North Sea. Senckenbergiana Maritima. 1989;20(3-4):81–99.
91. Lopez E. Algal chloroplasts in the protoplasm of three species of benthic foraminifera: Taxonomic affinity, viability and persistence. Marine Biology. 1979;53(3):201–11.
92. Jauffrais T, LeKieffre C, Koho KA, Tsuchiya M, Schweizer M, Bernhard JM, et al. Ultrastructure and distribution of kleptoplasts in benthic foraminifera from shallow-water (photic) habitats, Marine Micropaleontology. 2018;138: 46–62.
93. Goldstein ST, Richardson EA. Fine structure of the foraminifer *Haynesina germanica* (Ehrenberg) and its sequestered chloroplasts. Marine Micropaleontology. 2018;138:63–71.
94. LeKieffre C, Spangenberg JE, Mabilleau G, Escrig S, Meibom A, Geslin E. Surviving anoxia in marine sediments: The metabolic response of ubiquitous benthic foraminifera *(Ammonia tepida*). PloS one. 2017;12(5):e0177604.
95. Debenay J-P, Bénéteau E, Zhang J, Stouff V, Geslin E, Redois F, et al. *Ammonia beccarii* and *Ammonia tepida* (Foraminifera): Morphofunctional arguments for their distinction. Marine Micropaleontology. 1998;34(3-4):235–44.
96. Bouchet VMP, Debenay J-P, Sauriau P-G. First report of *Quinqueloculina carinatastriata* (Foraminifera) along the French Atlantic coast (Marennes-Oléron Bay and Ile de Ré). Journal of Foraminiferal Research. 2007;37(3):204–12.
97. Gollasch S, MacDonald E, Belson S, Botnen H, Christensen JT, Hamer JP, et al. Life in ballast tanks. In: Invasive aquatic species of Europe. Distribution, impacts and management: Springer; 2002;217–31.
98. McGann M, Sloan D, Cohen AN. Invasion by a Japanese marine microorganism in western North America. Hydrobiologia. 2000;421(1):25–30.
99. Guy-Haim T, Hyams-Kaphzan O, Yeruham E, Almogi-Labin A, Carlton JT. A novel marine bioinvasion vector: Ichthyochory, live passage through fish. Limnology and Oceanography Letters. 2017;2(3):81–90.
100. Debenay J-P, Sigura A, Justine J-L. Foraminifera in the diet of coral reef fish from the lagoon of New Caledonia: Predation, digestion, dispersion. Revue de micropaléontologie. 2011;54(2):87–103.
101. Alve E, Goldstein ST. Dispersal, survival and delayed growth of benthic foraminiferal propagules. Journal of Sea Research. 2010;63(1):36–51.

2.11 Appendix

2.11.1 Appendix 1. Foraminiferal reference list and taxonomic notes.

Taxonomy of benthic foraminifera identified in this study. Genera and species are listed in alphabetical order. The type references were retrieved from the Ellis and Messina [1] catalogue. Emphasis was given to publications on North Sea foraminifera for species determination. Papers on genetic-morphological investigations of *Ammonia* and *Elphidium* species were also considered. If possible, at least one reference to a high-quality image in a recent publication is provided for each species.

Ammonia aberdoveyensis Haynes 1973 [2], p. 184, fig. 38, nos. 1-7, pl. 18, fig. 15. "*Ammonia beccarii* var. *aberdoveyensis*" [3], p. 56, fig. 18., nos. A-C. Horton and Edwards [4] (, p. 70, pl. 3, figs. 10a-c. "*Ammonia* sp. T2" Bird et al. [5], p. 19, fig. 2., nos. CK02, CK28, CK69, LK74. Note: most specimens are dull and corroded, and the last chamber is often missing. The spiral side of the biconvex test is shallow conical, the sutures are oblique and slightly raised. The straight sutures on the umbilical side show narrow incisions close to the umbilicus where the chamber extensions are raised and thickened. A small umbilical knob is present in many specimens giving the umbilical area a stellate appearance. Our specimens from Japsand are very similar to the T2b cryptic species of [5], while this genotype has not been recorded in the North Sea to date. The umbilical area of our specimens is similar to *Ammonia catesbyana* [6] reported from the southern North Sea by Langer et al. [7], even though the spiral side of the latter is rather flat than conical, and their outline is lobate rather than as smooth as in *A. aberdoveyensis*.

Ammonia batava (Hofker) = *Streblus batavus* Hofker 1951 [8], p. 498, figs. 335, 340, 341. "*Streblus batavus*" Haake [9], p. 52, pl. 6, figs. 6-12. Langer et al. [7], p. 90, pl. 1, figs. 8-13. Schönfeld et al. [10], fig. 2a, pl. 1, figs. 1-3, 14-17, 31-34. Müller-Navarra et al. [11], p. 74, fig. 3, nos. 15, 16. Note: the species is common in the North Sea. Their test is compressed biconvex. The last chambers are inflated in adult specimens and may be separated by a fissure from the penultimate whorl where the sutures are raised on the spiral side. A distinct umbilical knob is surrounded by thickened and pointed chamber extensions, which is a diagnostic character of this species. The genotype T3S has been assigned to *A. batava* by Bird et al. [5].

Ammonia tepida (Cushman) = *Rotalia beccarii* var. *tepida* Cushman 1926 [12], p. 79, pl. 1. Hayward et al. [13] p. 353, pl. 1, figs. 1-8. Hayward et al. [14], p. 264, pl. 2-4, fig. T. "*Ammonia beccarii*" Polovodova et al. [15], p. 141, pl. 1, figs. 1-4. "Phylotype T6" Richirt et al. [16], fig. 7, no. Ai052. Note: the specimens from Japsand show morphological features of both, T1 and T6 genotypes, in particular raised or flush sutures, a narrow or wide umbilicus. These features are not developed in a consistent manner in that a secure distinction between both varieties would be possible. Therefore, the species name *Ammonia aomoriensis* [17], which has been used for T6 [18], cannot be applied here [5]. The pore size is, however, diagnostic for a morphological distinction of T1 and T6 genotypes [16, p. 85]. This feature cannot be resolved by light microscopy, and not every specimen can be examined under the SEM. As the Japsand specimens are morphologically in reasonable good agreement with *A. tepida* locotypes, we keep with this more generally used species name [e.g., 19, p. 295].

Ammoscalaria runiana (Heron-Allen and Earland) = *Haplophragmium runiana* Heron-Allen and Earland 1916 [20], p. 224, pl. 40, figs. 15-18. Kripner [21], p. 21, pl. 2, figs. 1-15. Lutze [22], p. 91, pl. 11, figs. 1-18, pl. 15, figs. 18-20. Murray and Alve [23], p. 25, fig. 15, nos. 2-5. Nordberg et al. [24], pl. 1, fig. j. Note: the chambers are rather indistinct and they rapidly increase in diameter, leaving the central area depressed. A detachment of the last chambers was only observed in one specimen from Japsand.

Bolivina earlandi Parr 1950 [25], p. 339. Gabel [26], pl. 14, figs. 32, 33. "*Brizalina earlandi*" Küppers [27], p. 129, pl. 5, figs. 13a, b. Note: Despite the findings of Gabel [26] and Küppers [27], *Bolivina earlandi* was not recorded in the North Sea, Channel and adjacent northeastern Atlantic northward of Ria de Vigo, Spain [28]. The species was particularly reported from cold seep sediments and oil production sites [29–31].

Bolivina pseudoplicata Heron-Allen and Earland 1930 [32], p. 81, pl. 3, figs. 36-40. Gabel [26], pl. 14, figs. 38, 39. Küppers [27], p. 125, pl. 5, figs. 8-11. Murray [33], p. 19, fig. 5, no. 17.

Bolivina pseudopunctata Höglund 1947 [34], p. 273, pl. 24, fig. 5, pl. 32, figs. 23, 24. Hofker [35], p. 241, pl. 4, fig. 24. "*Brizalina pseudopunctata*" Küppers [27], p. 130, pl. 5, fig. 14. "*Bolivinella pseudopunctata*" Gustafsson and Nordberg [36], p. 11, pl. 1, fig. 3. Note: the specimens from Helgoland harbour are smaller than those from Gullmar fjord. The twisted, irregular shape and coarse pores at the lower part of the chamber walls discriminate this taxon from other *Bolivina* species [37].

Buccella frigida (Cushman) = *Pulvinulina frigida* Cushman 1922 [38], p. 12, fig. 144. Haake [9], p. 44, pl. 4, figs. 3-6. Feyling-Hansen et al. [39], p. 253, pl. 8, figs. 12-14. Schroeder-Adams et al. [40], p. 24, pl. 8, figs. 10,11.

Buliminella elegantissima (d'Orbigny) = *Bulimina elegantissima* d'Orbigny 1839 [6], p. 51, pl. 7, figs. 13, 14. Haake [9], p. 34, pl. 2, figs 1,2. Murray [3], p. 41, fig. 11, nos. K, L. "*Buliminella borealis*" Müller-Navarra et al. [11], p. 74, fig. 3, no. 10. Note: Haynes [2] recognised a difference between a spruce-cone shaped North Atlantic and a spindle-shaped Pacific morphotype. The latter is resembling d'Orbigny's [6] species concept. *Buliminella borealis* was consequently established as new species confined to the Atlantic realm. However, specimens from the Peruvian Oxygen Minimum Zone [e.g., 41, fig. 12.17], are almost identical in shape to the holotype of *B. borealis* from Caernavon Bay, Wales. Furthermore, Haake [9] recognised both end member morphologies in the same population on tidal flats off Langeoog, southern North Sea. We therefore consider *B. borealis* as junior synonym of *Buliminella elegantissima*.

Cassidulina laevigata d'Orbigny 1826 [42], p. 282, pl. 15, figs. 4, 5. Feyling-Hansen et al. [39], p. 246, pl. 7, figs. 20,21, pl. 18, fig. 12. Schiebel [37], p. 39, pl. 2, fig. 11. Murray [33], p. 21, fig. 6, nos. 8-10.

Cibicides lobatulus (Walker and Jacob) = *Nautilus lobatulus* Walker and Jacob 1798 [43], p. 642, pl. 14, fig. 36. Haynes [2], p. 173, pl. 20, figs. 1-2, fig. 35, nos. 4-10. Horton and Edwards [4], p. 72, pl. 3, figs. 14a-c. Küppers [27], p. 152, pl. 7, figs. 1-3.

Eggerelloides scaber (Williamson) = *Bulimina scabra* Williamson 1858 [44], p. 65, pl. 5, figs. 136, 137. "*Eggerella scabra"* Jarke [45], p. 27, pl. 1, figs. 5a-c. "*Eggerelloides scabrum"* Haynes [2], p. 44, pl. 2, figs. 7, 8, pl. 19, figs. 10, 11, fig. 8, nos.1–4. „"*Eggerella scabra*" de Nooijer [46], pl. 2, fig. B. Note: *Eggerelloides scaber* is common in the southern North Sea [45], at depths below 20 m [cf. 47], and where the salinity is higher than 24 units during most of the year [48].

Elphidium albiumbilicatum (Weiss) = *Nonion pauciloculum* Cushman subsp. *albiumbilicatum* Weiss 1954 [49], p. 157, pl. 32, figs. 1, 2. "*Nonion depressulum* forma *asterotuberculatum*" Haake [9], p. 41, pl. 3, fig. 5. "*Cribrononion asklundi*" Lutze [22], p. 104, pl. 15, fig. 42. Alve and Murray [50], p. 191, pl. 1, figs. 12, 13. Polovodova et al. [15], p. 141, pl. 1, figs. 17-19. Note: a few, faint bundles of pustules forming chamber projections are bridging the sutures between later chambers. The sutures are markedly curved and incised until close to the margin, whereas the sutural depressions of *Haynesina orbicularis* are rather straight and terminate in the middle of the chambers. The similar species *Elphidium magellanicum* Heron-Allen and Earland [51] shows commonly five instead of seven to eight chambers as in *E. albiumbilicatum*. Their tests are more compressed that in the latter species.

Elphidium clavatum Cushman = *Elphidium incertum* var. *clavatum* Cushman 1930 [52], p. 20, pl. 7, fig. 10. "*Cribrononion excavatum clavatum*" Lutze [22], p. 96, pl. 15, figs. 40, 41. "*Elphidium excavatum* forma *clavata*" Miller et al. [53], p. 124, pl. 1, figs. 5, 6, pl. 2, figs. 3-8, pl. 3, figs. 3-8, pl. 4, figs. 1-6, pl. 5, figs. 4-8, pl. 6, figs. 1-5. "*Elphidium excavatum clavatum*" Schönfeld and Numberger [54], p. 57, pl. 1, figs. 7-9. Darling et al. [55], p. 16, fig. 3-F, no. S4. Note: the circular structure of chamber projections and a knob in the umbilicus is diagnostic for this stout *Elphidium*. The higher thickness/diameter ratio of ca. 0.5-0.6 discriminates it from *Elphidium excavatum* [56], which is with ca. 0.4-0.5 slightly more compressed [22]. Both taxa were considered as subspecies based on their different habitats and distribution pattern in the western Baltic Sea [57]. This view has been corroborated by genetic investigations [18]. The dissimilarity to other *Elphidium* genotypes even justifies the consideration of *E. clavatum* as individual species [55], which is followed herein.

Elphidium gerthi van Voorthuysen 1957 [58], p. 32, pl. 23, fig. 12. Haake [9], p. 46, pl. 5, fig. 10. "*Cribrononion* cf. *gerthi*" Kripner [21], p. 17, pl. 1, figs. 21-24. Feyling-Hansen et al. [39], p. 274, pl. 11, fig. 14. Nikulina et al. [59], p. 46, pl. 1, figs. 16, 17. Note: the small size, numerous chambers and dense sutural pits, and an umbilical boss or a depression with glossy calcite are diagnostic for this species.

Elphidium incertum (Williamson) = *Polystomella umbilicatula* var. *incerta* Williamson 1858 [44], p. 44, pl. 3, fig. 82a. "*Cribrononion incertum*" Lutze [22], p. 103, pl. 21, figs. 43-

44. Haynes [2], p. 199, pl. 22, fig. 6, pl. 24, figs 14-16, pl. 28, figs. 8, 9. Horton and Edwards [4], p. 76, pl. 4, figs. 18 a, b. Darling et al. [55], p. 17, fig. 3/B, no. S6. Schönfeld [60], p. 388, pl. 1, figs. 1-3, 6-15. Note: the test is rather compressed and shows narrow sutural furrows that are bridged by a few bundles of pustules commonly recognised as chamber extensions. Thereby, they create elongated, slit-like sutural pits. The chamber projections form a circular, shield-alike structure around the umbilicus. Both features are diagnostic for *E. incertum*.

Elphidium margaritaceum (Cushman) = *Elphidium advenum* (Cushman) var. *margaritaceum* Cushman 1930 [52], p. 25, pl. 10, figs. 3a, 3b. Haake [9], p. 49, pl. 5, fig. 11. van Voorthuysen [61], p. 45, pl. 4, figs 7a, b. Küppers [27], p. 195, pl. 9, figs. 4, 5.

Elphidium oceanensis d'Orbigny = *Polystomella oceanensis* d'Orbigny 1826 [42], p. 285, no. 8. "*Elphidium gunteri*" Haake [9], p. 48, pl. 5, figs. 3, 4. "*Elphidium gunteri*" Richter [62], p. 345, fig. 7. Alve and Murray [50], p. 190, pl. 1, figs. 14, 15. Austin [63], fig. 6.12 no. 5. Camacho et al. [64], p. 27, fig. 5, nos. 19-21. "*Elphidium oceanense*" Darling et al. [55], p. 20, fig. 3/F, no. S3. Note: *Elphidium gunteri* Cole [65] is considered a junior synonym of *E. oceanensis* [3, p. 52].

Elphidium selseyense (Heron-Allen and Earland) = *Polystomella striatopunctata* var. *selseyensis* Heron-Allen and Earland 1911 [66], p. 448. Haake [9], p. 49, pl. 5, fig 15, pl. 6, fig. 1-5 (pars). Hofker [35], p. 257, pl. 8, figs. 8, 9, pl. 9, fig. 1. "*Elphidium excavatum selseyense*" Langer et al. [7], p. 90, pl. 2, figs. 19-21. "*Elphidium excavatum*" Müller Navarra et al. [11], p. 74, fig. 3, nos. 17-19. Darling et al. [55], p. 17, fig. 3/F, no. S5. Note: The test is flat, the outline lobate and the chambers are inflated. The sutures are curved backwards and show a few septal bars on later chambers. The depressed umbilical area is covered with pustules and granules. *Elphidium selseyense* has been considered as one of five ecophenotypes of *Elphidium excavatum* [56], which is linked to the other formae in an intergradational series [53]. None-the-less, distinct distributional patterns provided evidence for a discrimination of these formae on subspecies or species level [e.g., 62, p 352 ff.]. While *E. selseyense* is frequent on near shore sands, the genuine *E. excavatum* is found at greater depths in the North Sea [10, 27]. The latter species shows no granules in the umbilical area but thin, pointed chamber extensions [67].

Elphidium voorthuyseni Haake 1962 [9], p. 50, pl. 5, figs 6, 7. "*Elphidium* sp." Darling et al. [55], p. 18, fig 3/B, no. S14. Note: The test shows 8-10 chambers and is very flat, the outline is almost smooth. The sutures are slightly curved and sharply turning backwards close to the margin. They show 3 – 5 sutural pits that are very small and indistinct. The umbilicus is almost closed and surrounded by cuspid chamber projections. Haynes [2] examined locotypic specimens and did not recognise a distinctive difference to *E. incertum*, even though the latter is characterised by slit-like sutural openings and a shielded umbilicus. The very similar and yet formally undescribed *Elphidium* sp. was only recorded around Scotland and assigned to genotype S14 [55].

Elphidium waddense van Voorthuysen 1951 [68], p. 25, pl. 2, figs. 16a, b. "*Elphidium selseyense*" Haake [9], pl. 5, figs. 12-14 (pars, "Extremform 1"). Haynes [2], p. 206, pl.

24, figs. 4, 10. Hofker [35], p. 259, pl. 9, fig. 6. "*Elphidium excavatum* forma *selseyensis*" Küppers [27], p. 186, pl. 8, figs. 10a, b. Note: This species has been confused with *E. selseyense* in the literature, though the tests are rather discoidal than flat with a depressed umbilicus. They are generally smaller than *E. selseyense*, the sutures are less curved and less depressed, the umbilical area shows either a glassy boss or numerous small granules. The umbilical area and earlier chambers often appear rough or frosty. It has to be noted that SEM images of *Elphidium lidoense* Cushman [69], applied to genotype S13 [55], depict an umbilical structure very similar to *E. waddense* but show no septal bars as the latter.

Elphidium williamsoni Haynes 1973 [2], p. 207, pl. 27, fig. 7, pl. 25, figs. 6, 9, pl. 27, figs. 1-3. "*Elphidium excavatum*" Haake [9], p. 47, pl. 5, fig. 5. "*Elphidium excavatum*" Richter [62], p. 345, figs. 3, 4. "*Cribrononion* cf. *alvarezianum*" Lutze [22], p. 101, pl. 15, fig. 46. Langer et al. [7], p. 90, pl. 2, figs. 22-25. Darling et al. [55], fig. 3/A, no. S1. Müller-Navarra et al. [11], p. 74, fig. 3, nos. 20, 21. Roberts et al. [70], p. 8, fig. 2, nos. A-F. Note: Roberts et al. [70] studied and sequenced type specimens and topotypic material as well as syntype specimens of *Polystomella umbilicatula* Walker and Jacob [43]. Even though the assemblage from the type locality showed a wide morphological variety, a particular combination of morphological characters allowed a secure discernation from the co-occurring *E. clavatum* and *E. selseyense*. Genotype S1 has been assigned to *E. williamsoni* by Darling et al. [55].

Fissurina lucida (Williamson) = *Entosolenia marginata* var. *lucida* Williamson 1848 [71], p. 17, pl. 2, fig. 17. Haake [9], p. 38, pl. 2, figs. 11, 12. Hofker [35], p. 239, pl. 4, fig. 17. Gabel [26], pl. 15, figs. 34, 35. Note: Küppers [27] recognised a continuous range of variability between *F. lucida* and *Fissurina laevigata* Reuss [72] morphotypes and therefore considered the latter as variant of *F. lucida*. Specimens from tidal flats are about half the size as specimens from deeper waters in the North Sea.

Haynesina depressula (Walker & Jacob) = *Nautilus depressulus* Walker and Jacob 1798 [43], p. 641, pl. 14, fig. 33. "*Nonion umbilicatulum*" Haake [9], p. 41, pl. 3, figs. 3, 4. "*Nonion depressulus*" Haynes [2], p. 209, pl. 22, figs. 8-11, pl. 29, fig. 9, fig. 44, nos. 1-3. "*Nonion depressulus*" Horton and Edwards [4], pl. 4, figs. 22a, b. "*Nonion depressulum*" Hofker [35], p. 254, pl. 8, fig. 3. Darling et al. [55], p. 21, fig. 3/G, no. S17. Note: The tests of *H. depressula* are rather compressed, the margin is acute rather than broadly rounded as in *Haynesina germanica* [73], and the depressed umbilical area is covered with small granules. The species has been assigned to *Haynesina* by Banner and Culver [74] due to its possession of short, intercameral lacunae. Genetic data group *H. depressula* specimens to a separate clade G, with a marked difference to another clade C with *H. germanica* [55]. Therefore, the genus *Haynesina* could be polyphyletic.

Haynesina germanica (Ehrenberg) = *Nonionina germanica* Ehrenberg 1840 [75], p. 23. "*Nonionina germanica*" Ehrenberg [73], pl. 2, figs. 1a-g. "*Nonion depressulum*" Haake [9], p. 40, pl. 3, figs. 1, 2. "*Protelphidium anglicum*" Haynes [2], p. 216, pl. 22, figs. 15, 16, pl. 23, figs. 1, 2, pl. 27, figs 6-9. Langer et al. [7], p. 90, pl. 2, figs. 14-18. 12-14. Darling et al. [55], p. 21, fig. 3/C, no. S16. Müller-Navarra et al. [11], p. 74, fig. 3, nos. Note: The shape is highly variable. Most tests are planspiral involute, some are evolute [e.g., 62, fig. 1]. The umbilicus is depressed or shows an umbilical boss on both sides, which is created by earlier chambers [e.g., 11, fig. 3 no. 13] and oblique coiling [e.g., 60, pl.1, fig. 23]. Later chambers may be slightly inflated or flush. Minute pustules cover the umbilicus, extend into the intercameral lacunae [e.g., 11, fig. 3 no. 12], and may cover the apertural face of the final chamber [76].

Haynesina orbicularis (Brady) = *Nonionina orbiculare* Brady 1881 [77], p. 415, pl. 21, fig. 5. "*Protelphidium orbiculare*" Feyling-Hanssen et al. [39], p. 289, pl. 14, figs. 8-11, pl. 24, figs. 6-8. Schröder-Adams et al. [40], p. 32, pl. 8, fig. 9. Pillet et al. [78], p. 13, pl. 1, figs. E-H., Lübbers and Schönfeld [79], pl. 2, figs. 4a-c. Note: the specimens from Japsand are rather small, thin-shelled, and much thicker than *H. germanica* in the same samples. The last whorl shows 4-6 instead of 8-11 chambers as in *H. germanica*. The inflated chambers rapidly increase in size as added [e.g., 79, pl. 2, fig. 4b]. The umbilical area and sutural depressions are covered by small pustules [e.g., 78, pl. 1 fig. F]. This feature, and the low number of chambers is also recognised in *Elphidium magellanicum* Heron-Allen and Earland [51] but their tests are much more compressed than *H. orbicularis*.

Hopkinsina pacifica Cushman 1933 [80], p. 86, pl. 8, fig. 16. "*Spiroloxostoma* sp." – Moodley [81], p. 60, pl. 1, figs. 1-3. Alve and Murray [82], pl. 2, fig. 10. "*Hopkinsina atlantica*" Debenay et al. [55], pl. 4, fig. 14. de Nooijer [46], pl. 1, fig. J. Note: Cushman [83] introduced a new, *atlantica* variety of *Hopkinsina pacifica* by the disjunct distribution of tropical Pacific and Atlantic New England coast, and because the Atlantic specimens showed smaller, twisted and compressed tests with more oblique sutures. In the living assemblage from the North Sea off Helgoland [10], any transitions between twisted and compressed tests with oblique sutures and more cylindrical tests with straight sutures were recognised. The cylindrical tests were even smaller than the compressed tests. We therefore consider the *atlantica* variety of cylindrical specimens with straight sutures as an endmember in the range of morphological variability of *H. pacifica.*

Jadammina macrescens (Brady) = *Trochammina inflata* var. *macrescens* Brady 1870 [84], p. 290, pl. 11, figs. 5a-c. "*Jadammina polystoma*" Haake [9], p. 31, pl. 1, figs. 7-9. Lehmann [85], p. 133, pl. 5, figs. 1, 2. Horton and Edwards [4], p. 66, pl. 1, fig. 4. Müller-Navarra et al. [11], p. 74, fig. 3, nos. 4, 5. Note: The compressed test, supplementary, tubular apertures on the areal face, the smooth test wall, in which planar agglutinated grains flush with the surface, the almost closed umbilicus and comparatively long, later chambers discriminate this species from *Balticammina pseudomacrescens* Brönnimann, Lutze and Whittaker [86] or *Trochamminita irregularis* Cushman and Brönnimann [87].

Labrospira jeffreysii (Williamson) = *Nonionina jeffreysii* Williamson 1858 [44], p. 34, pl. 3, figs. 72, 73. Höglund [34], p.146, pl. 11, fig. 3. "*Cribrostomoides jeffreysi*" Küppers [27], p. 40, pl. 2, fig. 3. "*Cribrostomoides jeffreysii*" Murray [33], p. 11, fig. 2, no. 5.

Morulaeplecta bulbosa Höglund 1947 [34], p. 165, pl. 12, fig. 2, text-figs. 142a, b. Murray [33],

p. 13, fig. 3, nos. 4, 5. Note: The specimens are very small and the test wall is rather fragile. Fragments may easily be mixed with *Textularia earlandi* Parker [88]. Therefore, this species is probably scarcely recorded.

Nonion pauperatus (Balkwill and Wright) = *Nonionina pauperata* Balkwill and Wright 1885 [89], p. 353, pl. 13, figs. 25, 26. *"Nonion pauperatum"* Haake [9], p. 42, pl. 3, figs. 6, 7. *"Nonion pauperatum"* Gabel [26], pl. 12, figs. 14, 15. *"Nonion (Florilus) pauperatum"* Haynes [2], pl. 22, figs. 13, 14, pl. 23, fig. 4, fig. 44, nos. 4-7. Murray [33], p. 24, fig. 9, no. 1.

Nonionella crassesuturalis van Voorthuysen 1958 [90], p. 23. Hofker [35], p. 254, pl. 8, fig. 2. Note: The specimens from Japsand are only half the size as those reported from the Netherlands.

Paratrochammina (Lepidoparatrochammina) haynesi (Atkinson) = *Trochammina haynesi* Atkinson 1969 [91], p. 529, pl. 6, figs. 1a–c. "*Trochammina haynesi*" Haynes [2], p. 35, fig. 6. Murray and Alve [92], p. 26, fig. 15, nos. 13, 14. Dorst and Schönfeld [93], p. 173, fig. 2, no. 1, fig. 9, no. 5, fig. 10, no. 4.

Patellina corrugata Williamson 1858 [44], p. 46, pl. 3, figs. 86-89. Haake [9], p. 43, pl. 3, fig. 9. Küppers [27], p. 83, pl. 4, figs. 5a-c. Murray [33], p. 24, fig. 9, nos. 6, 7.

Planorbulina mediterranensis d'Orbigny 1826 [42], p. 280, pl. 14, figs. 4-6. Jarke [45], pl. 4, figs. 1a-c. Küppers [27], p. 155, pl. 7, fig. 6. Murray [33], p. 24, fig. 9, no. 8. Mendes [94], p. 193, pl. 4, figs. 1a-j. Note: The specimens from Japsand are very small and depict the early ontogenetic phase [e.g., 94, plate 4, figs. 1d-f].

Quinqueloculina seminulum (Linné) = *Serpula seminulum* Linné 1758 [95], p. 786. "*Quinqueloculina seminula*" Jarke [45], p. 27, pl. 1, fig. 6. Hofker [35], p. 234, pl. 3, fig. 3. "*Quinqueloculina* sp." de Nooijer [46], pl. 1, fig. L. Note: This species is abundant in the southern North Sea at salinities of >24 permil [35,45]. The elongated elliptical and triangular shape, and the rounded chambers with thick walls discriminate *Q. seminulum* from other *Quinqueloculina* species.

Stainforthia fusiformis (Williamson) = *Bulimina pupoides* d'Orbigny var. *fusiformis* Williamson 1858 [44], p. 63, pl. 5, figs. 129-130. Gooday and Alve [96], figs. 3, 4, pl. 1, figs. H–L, pl. 3, figs. A-J. Alve [97], fig. 1.

Trochammina inflata (Montagu) = *Nautilus inflatus* Montagu 1808 [98], p. 81, pl. 18, fig. 3. Richter [62], p. 346, fig. 6. Horton and Edwards [4], p. 69, pl. 2, figs. 8a-d. Lehmann [85], p. 141, pl. 4, figs. 10, 11. Müller-Navarra et al. [11], p. 74, fig. 3, nos. 4, 5.

2.11.1.2 References of Appendix 1

1. Ellis BF, Messina AR. Cataloque of foraminifera. Micropaleontology Press, New York (http://www. micropress.org). 1940.
2. Haynes JR. Cardigan Bay recent foraminifera. Bulletin of the British Museum (Natural History) Zoology, Supplement 4: British Museum London; 1973.
3. Murray JW. British nearshore foraminiferids. Academic Press, London; 1979.
4. Horton BP, Edwards RJ. Quantifying Holocene sea level change using intertidal foraminifera: Lessons from the British Isles. Departmental Papers (EES). 2006:50.
5. Bird C, Schweizer M, Roberts A, Austin WEN, Knudsen KL, Evans KM, et al. The genetic diversity, morphology, biogeography, and taxonomic designations of *Ammonia* (Foraminifera) in the Northeast Atlantic. Marine Micropaleontology. 2020;155:101726.
6. d'Orbigny A. Foraminiféres. Voyage dans l'Amerique Méridionale. P. Bertrand, Paris and Strasbourg. 1839;5(5): 1–86.
7. Langer M, Hottinger L, Huber B. Functional morphology in low-diverse benthic foraminiferal assemblages from tidal flats of the North Sea. Senckenbergiana Maritima. 1989;20(3-4):81–99.
8. Hofker J. The foraminifera of the Siboga expedition. Part III. Siboga-Expeditie, Monographie IVa. 1951:1–513.
9. Haake F-W. Untersuchungen an der Foraminiferen-Fauna im Wattgebiet zwischen Langeoog und dem Festland. Meyniana. 1962;12:25–64.
10. Schönfeld J, Golikova E, Korsun S, Spezzaferri S. The Helgoland Experiment–assessing the influence of methodologies on Recent benthic foraminiferal assemblage composition: Geological Society of London; 2013.
11. Müller-Navarra K, Milker Y, Schmiedl G. Natural and anthropogenic influence on the distribution of salt marsh foraminifera in the bay of Tümlau, German North Sea. Journal of Foraminiferal Research. 2016;46(1):61–74.
12. Cushman JA. Recent foraminifera from Porto Rico. Publications of the Carnegie Institution of Washington, 1926;342:73–84.
13. Hayward BW, Buzas MA, Buzas-Stephens P, Holzmann M. The lost types of *Rotalia beccarii var. tepida* Cushman 1926. Journal of Foraminiferal Research. 2003;33(4):352–4.
14. Hayward BW, Holzmann M, Grenfell HR, Pawlowski J, Triggs CM. Morphological distinction of molecular types in *Ammonia*–towards a taxonomic revision of the world's most commonly misidentified foraminifera. Marine Micropaleontology. 2004;50(3-4):237–71.
15. Polovodova I, Nikulina A, Schönfeld J, Dullo W-C. Recent benthic foraminifera in the Flensburg Fjord (western Baltic Sea). Journal of Micropalaeontology. 2009;28(2):131–42.
16. Richirt J, Schweizer M, Bouchet VMP, Mouret A, Quinchard S, Jorissen FJ. Morphological distinction of three *Ammonia* phylotypes occurring along European coasts. Journal of Foraminiferal Research. 2019;49(1):76–93.

17. Asano K. Part 14. Rotaliidae. In: Stach, L.W. (Ed.), Illustrated Catalogue of Japanese Tertiary Smaller Foraminifera. Hosokawa Printing. 1951: 1–21.
18. Schweizer M, Polovodova I, Nikulina A, Schönfeld J. Molecular identification of *Ammonia* and *Elphidium* species (foraminifera, Rotaliida) from the Kiel Fjord (SW Baltic Sea) with rDNA sequences. Helgoland Marine Research. 2011;65(1):1–10.
19. Richter G. Faziesbereiche rezenter und subrezenter Wattensedimente nach ihren Foraminiferen-Gemeinschaften. Senckenbergiana lethaea. 1967;48:291–335.
20. Heron-Allen E, Earland A. The Foraminifera of the West of Scotland. Collected by Prof. WA Herdman, FRS, on the Cruise of the SY 'Runa,'July-Sept. 1913. Being a Contribution to 'Spolia Runiana.'. Transactions of the Linnean Society of London. 2nd Series: Zoology. 1916;11(13):197–299.
21. Kripner J. Zur Foraminiferen-Fauna im Wattenmeer bei Sylt: Christian-Albrechts-Universität; 1965.
22. Lutze G. Zur Foraminiferen-Fauna der Ostsee. Meyniana. 1965;15:75–142.
23. Murray JW, Alve E. The distribution of agglutinated foraminifera in NW European seas: Baseline data for the interpretation of fossil assemblages. Palaeontologia Electronica. 2011;14(2):1–41.
24. Nordberg K, Asteman IP, Gallagher TM, Robijn A. Recent oxygen depletion and benthic faunal change in shallow areas of Sannäs Fjord, Swedish west coast. Journal of Sea Research. 2017;127:46–62.
25. Parr WJ. Foraminifera. Reports of the British, Australian and New Zealand Antarctic Research Expedition 1929-31, Series B. Zoology and Botany. 1950;5:232–392.
26. Gabel B. Die Foraminiferen der Nordsee. Helgoländer wissenschaftliche Meeresuntersuchungen. 1971;22(1):1–65.
27. Küppers R. Zur Foraminiferenfauna bei Helgoland. (Dissertation) Universität Bonn (303 pp). 1987.
28. Diz P, Francés G, Costas S, Souto C, Alejo I. Distribution of benthic foraminifera in coarse sediments, Ría de Vigo, NW Iberian margin. Journal of Foraminiferal Research. 2004;34(4):258–75.
29. Robinson CA, Bernhard JM, Levin LA, Mendoza GF, Blanks JK. Surficial hydrocarbon seep infauna from the Blake Ridge (Atlantic Ocean, 2150 m) and the Gulf of Mexico (690–2240 m). Marine Ecology. 2004;25(4):313–36.
30. Levin LA. Ecology of cold seep sediments: interactions of fauna with flow, chemistry, and microbes. Oceanography and Marine Biology: an annual review. 2005;43:1–46.
31. Jorissen FJ, Bicchi E, Duchemin G, Durrieu J, Galgani F, Cazes L, et al. Impact of oil-based drill mud disposal on benthic foraminiferal assemblages on the continental margin off Angola. Deep Sea Research Part II: Topical Studies in Oceanography. 2009;56(23):2270–91.
32. Heron-Allen E, Earland A. The foraminifera of the Plymouth district. Journal of the Royal Microscopical Society. 1930;50(1):46–84.
33. Murray JW. An illustrated guide to the benthic foraminifera of the Hebridean shelf, west of Scotland, with notes on their mode of life. Palaeontologia Electronica. 2003;5(1):31.

34. Höglund H. Foraminifera in the Gullmar Fjord and the Skagerak. Uppsala University. Zoologiska Bidrag. 1947;26:1–328.
35. Hofker J. The foraminifera of Dutch tidal flats and salt marshes. Netherlands Journal of Sea Research. 1977;11(3-4):223–96.
36. Gustafsson M, Nordberg K. Living (stained) benthic foraminiferal response to primary production and hydrography in the deepest part of the Gullmar Fjord, Swedish West Coast, with comparisons to Hoglund's 1927 material. Journal of Foraminiferal Research. 2001;31(1):2–11.
37. Schiebel R. Rezente benthische Foraminiferen in Sedimenten des Schelfes und oberen Kontinentalhanges im Golf von Guinea (Westafrika). Berichte, Reports, Geologisch-Paläontologisches Institut und Museum Christian-Albrechts-Universität Kiel;51:1–126.
38. Cushman JA. Results of the Hudson Bay expedition, 1920. I. The Foraminifera. Contribution Canadian Biology. 1922;9:135–147.
39. Feyling-Hanssen RW, Jørgensen JA, Knudsen KL, Lykke-Andersen A-L. Late Quaternary Foraminifera from Vendsyssel, Denmark and Sandnes, Norway: Geological Society of Denmark Copenhagen; 1971.
40. Schröder-Adams CJ, Cole FE, Medioli FS, Mudie PJ, Scott DB, Dobbin L. Recent Arctic shelf foraminifera; seasonally ice covered vs. perennially ice covered areas. Journal of Foraminiferal Research. 1990;20(1):8–36.
41. Erdem Z, Schönfeld J. Pleistocene to Holocene benthic foraminiferal assemblages from the Peruvian continental margin. Palaeontologia Electronica. 2017;20(2, Article Nr. 35A).
42. d'Orbigny A. Tableau Methodique de la Classe des Cephalopodes. Annales des Sciences Naturelles. 1826;7:96–314 + 245–314.
43. Walker, G., Jacob, E. Essays on the Microscope. 2nd Edition with considerable additions and improvements by F. Kanmacher. Dillon and Keeting. Adams, E. (Ed.). 1798;712 pp.
44. Williamson WC. On the recent foraminifera of Great Britain: Ray Society, London; 1858.
45. Jarke J. Die Beziehungen zwischen hydrographischen Verhältnissen, Faziesentwicklung und Foraminiferenverbreitung in der heutigen Nordsee als Vorbild für die Verhältnisse während der Miocän-Zeit. Meyniana. 1961;10:21–36.
46. Nooijer LJ de. Shallow water benthic foraminifera as proxy for natural versus human-induced environmental change: Utrecht University; 2007.
47. Wang P. Verbreitung der Benthos-Foraminiferen im Elbe-Aestuar. Meyniana. 1983;35:67–83.
48. Lutze GF. Siedlungs-Strukturen rezenter Foraminiferen. Meyniana. 1968;18:31–4.
49. Weiss L. Foraminifera and origin of the Gardiners Clay (Pleistocene), Eastern Long Island, New York. United States Geological Survey Professional Paper. 1954;254-G:143–63.
50. Alve E, Murray JW. Marginal marine environments of the Skagerrak and Kattegat: A baseline study of living (stained) benthic foraminiferal ecology. Palaeogeography, Palaeoclimatology, Palaeoecology. 1999;146(1-4):171–93.
51. Heron-Allen E, Earland A. Foraminifera: Part 1 The ice free area of the Falkland Islands and adjacent seas. Discovery Reports. 1932;4:291–460.

52. Cushman JA. The Foraminifera of the Atlantic Ocean: Part 7. *Nonionidae, Camerinidae, Peneroplidae* and *Alveolinellidae*. Bulletin of the United States National Museum. 1930;104:1–79.
53. Miller AAL, Scott DB, Medioli FS. *Elphidium excavatum* (Terquem); ecophenotypic versus subspecific variation. Journal of Foraminiferal Research. 1982;12(2):116–44.
54. Schönfeld J, Numberger L. The benthic foraminiferal response to the 2004 spring bloom in the western Baltic Sea. Marine Micropaleontology. 2007;65(1-2):78–95.
55. Darling KF, Schweizer M, Knudsen KL, Evans KM, Bird C, Roberts A, et al. The genetic diversity, phylogeography and morphology of *Elphidiidae* (Foraminifera) in the Northeast Atlantic. Marine Micropaleontology. 2016;129:1–23.
56. Terquem O. Essai sur le classement des animaux qui vivent sur la plage et dans les environs de Dunkerque. Mémoires de la Société Dunkerquoise pour l'Encouragement des Sciences des Lettres et des Arts (1874–1875). 1875;19:405–57.
57. Lutze G. Foraminiferen der Kieler Bucht (Westliche Ostsee): 1." Hausgartengebiet" des Sonderforschungsbereiches 95 der Universität Kiel. Meyniana. 1974;26:9–22.
58. van Voorthuysen JH. Foraminiferen aus dem Eemien (Riss-Würm-Interglazial) in der Bohrung Amersfoort I (Locus typicus). Mededelingen van de Geologische Stichting, Nieuwe Serie. 1957;11:27–39.
59. Nikulina A, Polovodova I, Schönfeld J. Foraminiferal response to environmental changes in Kiel Fjord, SW Baltic Sea. EEarth. 2008;3(1):37–49.
60. Schönfeld J. Monitoring benthic foraminiferal dynamics at Bottsand coastal lagoon (western Baltic Sea). Journal of Micropalaeontology. 2018;37(1):383–93.
61. van Voorthuysen JH. Foraminiferal ecology in the Ria de Arosa, Galicia, Spain. Zoologische Verhandelingen. 1973;123:3–82.
62. Richter G. Zur Ökologie der Foraminiferen. I. Die Foraminiferen-Gesellschaften des Jadegebietes. Natur und Museum. 1964;94(9):343–53.
63. Austin HA. The biology and ecology of benthic foraminifera inhabiting intertidal mudflats. (Ph.D. thesis): University of St Andrews; 2003.
64. Camacho SG, Jesus Moura DM de, Connor S, Scott DB, Boski T. Taxonomy, ecology and biogeographical trends of dominant benthic foraminifera species from an Atlantic-Mediterranean estuary (the Guadiana, southeast Portugal). Palaeontologia Electronica. 2015;18(1):1–27.
65. Cole WS. The Pilocene and Pleistocene foraminifera of Florida, Florida State Geol. Surv. Bull., Tallahassee, Florida. 1931(6):34.
66. Heron-Allen E, Earland A. On the Recent and Fossil Foraminifera of the Shore-sands of Selsey Bill, Sussex.—VII. Supplement (Addenda et Corrigenda). Journal of the Royal Microscopical Society. 1911;31(3):298–343.
67. Lévy A, Mathieu R, Momeni I, Poignant A, Rosset-Moulinier M, Rouvillois A, et al. Les representants de la famille des *Elphidiidae* (foraminifires) dans les sables des plages des environs de Dunkerque. Remarques sur les espices de Polystomella signalees par. 0. Terquem. Revue de Micropaleontologie. 1969;12:92–8.

68. van Voorthuysen JH. Recent (and derived Upper Cretaceous) foraminifera of the Netherlands Wadden Sea (tidal flats). Mededelingen van de Geologische Stichting, Nieuwe Serie. 1951;5:23–32.
69. Cushman JA. Three new foraminifera from the Miocene Bowden Marl of Jamaica. Contributions from the Cushman Foundation for Foraminiferal Research. 1936;12:3–5.
70. Roberts A, Austin W, Evans K, Bird C, Schweizer M, Darling K. A new integrated approach to taxonomy: The fusion of molecular and morphological systematics with type material in benthic foraminifera. PloS one. 2016;11(7):e0158754.
71. Williamson WC. On the recent British species of the genus Lagena. Annals and Magazine of Natural History. 1848;1(1):1–20.
72. Reuss AV. Neues Foraminiferen aus den Schichten des Österreichischen Tertiärbeckens. Denkschriften der Akademie des Wissenschaften Wein. 1850;1:365–90.
73. Ehrenberg CG. Eine weitere Erläuterung des Organismus mehrerer in Berlin lebend beobachterer Polythalamien der Nordsee. Bericht über die zur Bekanntmachung geeigneten Verhandlungen der Königlichen Preussischen Akademie der Wissenschaften zu Berlin. 1840;18–23.
74. Banner FT, Culver SJ. Quaternary *Haynesina n. gen.* and Paleogene *Protelphidium Haynes;* their morphology, affinities and distribution. Journal of Foraminiferal Research. 1978;8(3):177–207.
75. Ehrenberg CG. Über noch jetzt zahlreich lebende Thierarten der Kreidebildung und den Organismus der Polythalamien. Königliche Akademie der Wissenschaften Berlin, Physik-Mathematik II., Abhandlungen. 1841;1839:81–174.
76. Austin HA, Austin WEN, Paterson DM. Extracellular cracking and content removal of the benthic diatom *Pleurosigma angulatum* (Quekett) by the benthic foraminifera *Haynesina germanica* (Ehrenberg). Marine Micropaleontology. 2005;57(3-4):68–73.
77. Brady HB. Notes on some of the reticularian Rhizopoda of the" Challenger" Expedition. Part III. 1. Classification. 2. Further notes on new species. 3. Note on Biloculina mud. Quarterly Journal of Microscopical Science, new series. 1881;21:31–71.
78. Pillet L, Voltski I, Korsun S, Pawlowski J. Molecular phylogeny of *Elphidiidae* (foraminifera). Marine Micropaleontology. 2013;103:1–14.
79. Lübbers J, Schönfeld J. Recent saltmarsh foraminiferal assemblages from Iceland. Estuarine, Coastal and Shelf Science. 2018;200:380–94.
80. Cushman JA. Some new Recent foraminifera from the tropical Pacific. Contributions from the Cushman Laboratory for Foraminiferal Research. 1933;9(4):86.
81. Moodley L. Southern North Sea seafloor and subsurface distribution of living benthic foraminifera. Netherlands Journal of Sea Research. 1990;27(1):57–71.
82. Alve E, Murray JW. Temporal variability in vertical distributions of live (stained) intertidal foraminifera, southern England. Journal of Foraminiferal Research. 2001;31(1):12–24.
83. Cushman JA. Foraminifera from the shallow water of the New England Coast. Cushman Laboratory for Foraminiferal Research, Special Publication. 1944;12:1–37.
84. Brady, GS. Robertson, D. I.—The Ostracoda and Foraminifera of Tidal Rivers. With an analysis and descriptions of the Foraminifera, by Henry B. Brady, FLS. Annals and Magazine of Natural History, 1870,:31(6):1-33.

85. Lehmann G. Vorkommen, Populationsentwicklung, Ursache fleckenhafter Besiedlung und Fortpflanzungsbiologie von Foraminiferen in Salzwiesen und Flachwasser der Nord- und Ostseeküste Schleswig-Holsteins; (Dissertation). University of Kiel (218 pp). 2000.
86. Brönnimann P, Lutze GF, Whittaker JE. *Balticammina pseudomacrescens*, a new brackish water trochamminid from the western Baltic Sea, with remarks on the wall structure. Meyniana. 1989;41:167–77.
87. Cushman JA, Brönnimann P. Some new genera and species of foraminifera from brackish water of Trinidad. Contributions from the Cushman Laboratory for Foraminiferal Research. 1948;24(1):15–21.
88. Parker FL. Foraminiferal distribution in the Long Island Sound-Buzzards Bay area: Bulletin of the Museum of Comparative Zoology. Harvard College. 1952;106(10):428–73.
89. Balkwill FP, Wright J. Report on Some Recent Foraminifera Found off the Coast of Dublin and in the Irish Sea (With Plates XII., XIII., and XIV.). The Transactions of the Royal Irish Academy. 1880;28:317–72.
90. van Voorthuysen JH. Les Foraminiferes mio-pliocènes et quaternaires du Kruisschans. Institut Royal des Sciences Naturelles de Belgique Memoire. 1958;142:1–34.
91. Atkinson K. The association of living foraminifera with algae from the littoral zone, south Cardigan Bay, Wales. Journal of Natural History. 1969;3(4):517–42.
92. Alve E, Murray JW, Skei J. Deep-sea benthic foraminifera, carbonate dissolution and species diversity in Hardangerfjord, Norway: An initial assessment. Estuarine, Coastal and Shelf Science. 2011;92(1):90–102.
93. Dorst S, Schönfeld J. Taxonomic notes on recent benthic foraminiferal species of the family *Trochamminidae* from the Celtic Sea. Journal of Foraminiferal Research. 2015;45(2):167–89.
94. Mendes I. Benthic foraminifera as paleo-environmental indicators in the Northern Gulf of Cadiz. (Tese Doutoramento). Universidade do Algarve, Portugal. 2010;242 pp.
95. Linné C. Systema naturæ per regna tria naturæ, secundum classes, ordines, genera, species, cum characteribus, differentiis, synonymis, locis. Tomus I. Editio decima, reformata. Laurentii Salvii, Holmiæ. 1758;10:824 pp.
96. Gooday AJ, Alve E. Morphological and ecological parallels between sublittoral and abyssal foraminiferal species in the NE Atlantic: A comparison of *Stainforthia fusiformis* and *Stainforthia sp*. Progress in Oceanography. 2001;50(1-4):261–83.
97. Alve E. A common opportunistic foraminiferal species as an indicator of rapidly changing conditions in a range of environments. Estuarine, Coastal and Shelf Science. 2003;57(3):501–14.
98. Montagu G. Testacea Britannica, or Natural History of British Shells, marine, land, and fresh-water, including the most minute. Supplement, S. Woolmer, Exeter. 1808:183 pp.

2.11.2 Appendix 2: Tables.

Table S2.1: Foraminiferal census data of the living fauna, Japsand, German Wadden Sea.

Station	A	A	1	B	B	2
Sample	1	2	1	1	2	1
Sampling date	29.07.19	29.07.19	29.05.19	29.07.19	29.07.19	29.05.19
Latitude	54°34.28.3'N	54°34.28.3'N	54°34.28.8'N	54°34.35.5'N	54°34.35.5'N	54°34.28.3'N
Longitude	8°27.52.0'E	8°27.52.0'E	8°27.54.7'E	8°27.57.1'E	8°27.57.1'E	8°27.56.3'E
Transect Distance (m)	0	0	45	50	50	77.4
Floatate / total residue:	floatate	floatate	total residue	total residue	total residue	floatate
Size fraction (µm):	63-2000	63-2000	63-2000	63-2000	63-2000	63-2000
Species dead/alive	alive	alive	alive	alive	alive	alive
Ammonia batava	11	7	35	452	163	10
Elphidium gerthi						
Elphidium selseyense	23	15	19	40	32	52
Elphidium williamsoni				1		1
Elphidium oceanense	2		1			
Haynesina germanica			5	5	8	
Haynesina depressula						1
Bulliminella elegantissima				1		
Saccammina sp.						1
Eggerelloides scaber						1
Total:	36	22	60	499	203	66
Species no.:	3	2	4	5	3	6
Split (n):	1	1	1	1	1	1
Sample volume (cm^3):	22	24	23	20	22	24
Abundance (tests/10 cm^3):	16	9	27	246	91	27
Fisher alpha diversity index:	1.3	0.5	1.3	0.6	0.5	2.0
Species richness:	3	2	4	5	3	6
Salinity:	34	34	30.3			
Temperature (°C):	21.1	21.1	21.6			

Table S2.1 Continued.

Station	F	F	3	4	5	6
Sample	1	2	1	1	1	1
Sampling date	30.07.19	30.07.19	29.05.19	29.05.19	29.05.19	29.05.19
Latitude	54°35.08.0'N	54°35.08.0'N	54°34.27.5'N	54°34.23.5'N	54°34.20.7'N	54°34.18.9'N
Longitude	8°28.58.0'E	8°28.58.0'E	8°28.02.2'E	8°28.16.0'E	8°28.19.4'E	8°28.22.9'E
Transect Distance (m)	90	90	183.6	441	513	583.2
Floatate / total residue:	floatate	floatate	floatate	floatate	floatate	floatate
Size fraction (µm):	63-2000	63-2000	63-2000	63-2000	63-2000	63-2000
Species dead/alive	alive	alive	alive	alive	alive	alive
Ammonia batava	5		1			
Elphidium gerthi					1	
Elphidium selseyense	12	3			1	26
Elphidium williamsoni						
Elphidium oceanense						
Haynesina germanica						
Haynesina depressula						
Bulliminella elegantissima						

Saccammina sp.						
Eggerelloides scaber						
Total:	17	3	1	0	2	26
Species no.:	2	1	1	0	2	1
Split (n):	1	1	1	1	1	1
Sample volume (cm^3):	22	24	25	24	28	29
Abundance (tests/10 cm^3):	8	1	0.4		1	9
Fisher alpha diversity index:	0.8	0.5	0		0	0.6
Species richness:	2	1	1		2	1
Salinity:	31.6	31.6	31.5			
Temperature (°C):	24.7	24.7	22.8			

Table S2.1 Continued.

Station	7	E	E	C	C	8
Sample	1	1	2	1	2	1
Sampling date	29.05.19	30.07.19	30.07.19	30.07.19	30.07.19	29.05.19
Latitude	54°34.14.9'N	54°34.33.1'N	54°34.33.1'N	54°34.06.5'N	54°34.06.5'N	54°33.56.2'N
Longitude	8°28.40.2'E	8°29.07.9'E	8°29.07.9'E	8°29.10.5'E	8°29.10.5'E	8°29.54.7'E
Transect Distance (m)	990	1330	1330	1490	1490	2320
Floatate / total residue:	floatate	floatate	floatate	floatate	floatate	floatate
Size fraction (µm):	63-2000	63-2000	63-2000	63-2000	63-2000	63-2000
Species dead/alive	alive	alive	alive	alive	alive	alive
Ammonia batava						2
Elphidium gerthi						
Elphidium selseyense			2		1	1
Elphidium williamsoni	11	1		112	88	
Elphidium oceanense						
Haynesina germanica		1				
Haynesina depressula						
Bulliminella elegantissima						
Saccammina sp.						
Eggerelloides scaber						
Total:	11	2	2	112	89	3
Species no.:	1	2	1	1	2	2
Split (n):	1	1	1	1	1	1
Sample volume (cm^3):	29	22	22	23	15	25
Abundance (tests/10 cm^3):	4	1	1	48	58	1
Fisher alpha diversity index:	0.4	0	0.8	0.2	0.4	0
Species richness:	1	2	1	1	2	2
Salinity:		38.1	38.1			40.3
Temperature (°C):		26.3	26.3			19.4

Table S2.1 Continued.

Station	D	D	G	G	Hooge	Total
Sample	1	2	1	2		
Sampling date	30.07.19	30.07.19	30.07.19	30.07.19	29.05.19	

Latitude	54°33.47.4'N	54°33.47.4'N	54°33.56.4'N	54°33.56.4'N	54°34.11.0'N	
Longitude	8°30.27.4'E	8°30.27.4'E	8°30.58.6'E	8°30.58.6'E	8°31.16.3'E	
Transect Distance (m)	2950	2950	3460	3460	3700	
Floatate / total residue:	total residue	total residue	floatate	floatate	floatate	
Size fraction (µm):	63-2000	63-2000	63-2000	63-2000	63-2000	
Species dead/alive	alive	alive	alive	alive	alive	
Ammonia batava	18	22	15	13		754
Elphidium gerthi						1
Elphidium selseyense	40	27	4	5		303
Elphidium williamsoni						214
Elphidium oceanense	2					5
Haynesina germanica	6	2	4	7		38
Haynesina depressula						1
Bulliminella elegantissima	1					2
Saccammina sp.						1
Eggerelloides scaber						1
Total:	67	51	23	25	0	1320
Species no.:	5	3	3	3	0	10
Split (n):	1	1	1	1	1	
Sample volume (cm^3):	25	25	28	28	17	
Abundance (tests/10 cm^3):	27	21	8	9		
Fisher alpha diversity index:	1.7	0.7	1.0	0.9		
Species richness:	5	3	3	3		
Salinity:	32.4	32.4	37.7	37.7		
Temperature (°C):	24.4	24.4	23	23		

Table S2.2: Foraminiferal census data of the dead assemblage, Japsand, German Wadden Sea.

Station	A	1	B	2	3
Sample	1		1		
Sampling date:	29.7.2019	29.5.2019	29.7.2019	29.5.2019	29.5.2019
Latitude (°N)	54° 34.472'N	54° 34.480'N	54° 34.592'N	54° 34.472'N	54° 34.458'N
Longitude (°E)	8° 27.867'E	8° 27.912'E	8° 27.952'E	8° 27.938'E	8° 28.037'E
Transect Distance (m)	0	45	50	77.4	183.6
Floatate / total residue:	floatate	total residue	total residue	floatate	floatate
Size fraction (µm):	63-2000	63-2000	63-2000	63-2000	63-2000
Species dead/alive	dead	dead	dead	dead	dead
Ammonia aberdoveyensis	8		6	27	4
Ammonia batava	88	54	31	115	10
Ammonia tepida	3	3	8	2	
Ammoscalaria runiana	5	1		7	
Buccella frigida					
Buliminella elegantissima		3	1		
Cassidulina laevigata	1				
Cibicides lobatulus					
Elphidium albiumbilicatum					
Elphidium clavatum	6		5	7	
Elphidium gerthi	1		6		
Elphidium incertum	1		4		
Elphidium oceanensis					1
Elphidium selseyense	1		54	26	9
Elphidium voorthuyseni					1
Elphidium waddense	13	2	52	13	11

Elphidium williamsoni	5	17	15	31	1
Fissurina lucida		1	1		
Haynesina depressula	1		14		1
Haynesina germanica	27	96	80	113	15
Haynesina orbicularis		21	5	3	1
Jadammina macrescens		1		1	
Nonionella crassesuturalis					1
Nonion pauperatus					
Planorbulina mediterranensis			1		
Trochammina inflata				1	
others, indet. spp.	2				1
Total:	162	199	283	346	56
Species no.:	15	10	15	12	12
Split (n):	1	0.538	0.2318	0.0685	1
Sample volume (cm^3):	22	22.6	20.3	24.3	24.6
Abundance (tests/10 cm^3):	74	164	601	2079	23
Fisher alpha diversity index:	4.04	2.22	3.38	2.41	4.69
Species richness	14	10	15	12	12

Table S2.2. Continued.

Station	4	5	6	F	7	E
Sample				1		1
Sampling date:	29.5.2019	29.5.2019	29.5.2019	30.7.2019	29.5.2019	30.7.2019
Latitude (°N)	54° 34.392'N	54° 34.345'N	54° 34.315'N	54° 35.133'N	54° 34.248'N	54° 34.552'N
Longitude (°E)	8° 28.267'E	8° 28.323'E	8° 28.382'E	8° 28.967'E	8° 28.670'E	8° 29.132'E
Transect Distance (m)	441	513	583.2	900	990	1330
Floatate / total residue:	floatate	floatate	floatate	floatate	floatate	floatate
Size fraction (µm):	63-2000	63-2000	63-2000	63-2000	63-2000	63-2000
Species dead/alive	dead	dead	dead	dead	dead	dead
Ammonia aberdoveyensis	2	15	2	5	4	
Ammonia batava	4	57	37	39	13	13
Ammonia tepida		1	5			
Ammoscalaria runiana		1		3		
Buccella frigida		1	2			
Buliminella elegantissima			1			
Cassidulina laevigata						
Cibicides lobatulus						
Elphidium albiumbilicatum		1				
Elphidium clavatum		13	9		2	1
Elphidium gerthi		1		1		
Elphidium incertum			4		1	
Elphidium oceanensis					1	
Elphidium selseyense		68	55	4	3	2
Elphidium voorthuyseni						1
Elphidium waddense	1	22	48	4	5	5
Elphidium williamsoni	1	26	20	6	49	3
Fissurina lucida						
Haynesina depressula		6	21	1	3	
Haynesina germanica	1	54	49	23	8	8
Haynesina orbicularis		1	5	4	1	
Jadammina macrescens			1	1		
Nonionella crassesuturalis						
Nonion pauperatus					2	
Planorbulina mediterranensis			1			
Trochammina inflata						
others, indet. spp.		2	1	1		
Total:	9	269	261	92	92	33

Species no.:	5	16	16	12	12	7
Split (n):	1	0.2547	0.4809	1	1	1
Sample volume (cm^3):	15.6	18.3	20	22.3	23.5	22
Abundance (tests/10 cm^3):	6	577	271	41	39	15
Fisher alpha diversity index:	4.63	3.73	3.76	3.68	3.68	2.72
Species richness	5	15	16	12	12	7

Table S2.2. Continued.

Station	C	8	D	G	Hooge	Total
Sample	1		1	1		
Sampling date:	30.7.2019	29.5.2019	30.7.2019	30.7.2019	29.5.2019	
Latitude (°N)	54° 34.108'N	54° 33.937'N	54° 33.790'N	54° 33.940'N	54° 34.183'N	
Longitude (°E)	8° 29.175'E	8° 29.912'E	8° 30.457'E	8° 30.977'E	8° 31.272'E	
Transect Distance (m)	1490	2320	2950	3460	3700	
Floatate / total residue:	floatate	floatate	total residue	floatate	floatate	
Size fraction (µm):	63-2000	63-2000	63-2000	63-2000	63-2000	
Species dead/alive	dead	dead	dead	dead	dead	
Ammonia aberdoveyensis	1	14	4	9	2	103
Ammonia batava	9	46	45	45	7	613
Ammonia tepida			4	2	1	29
Ammoscalaria runiana				1		18
Buccella frigida			1			4
Buliminella elegantissima			2			7
Cassidulina laevigata						1
Cibicides lobatulus		1	1			2
Elphidium albiumbilicatum						1
Elphidium clavatum	1	12	7	4	1	68
Elphidium gerthi			2	1		12
Elphidium incertum		2	2	1		15
Elphidium oceanensis			2			4
Elphidium selseyense		59	48	23	1	353
Elphidium voorthuyseni			7	2		11
Elphidium waddense	8	31	75	39	2	331
Elphidium williamsoni	27	10	15	6	2	234
Fissurina lucida		1				3
Haynesina depressula	1	5	13	1		67
Haynesina germanica	4	23	34	35	4	574
Haynesina orbicularis			32	9		82
Jadammina macrescens						4
Nonionella crassesuturalis			1	1		3
Nonion pauperatus						2
Planorbulina mediterranensis						2
Trochammina inflata						1
others, indet. spp.	1	1	1	1		11
Total:	52	205	296	180	20	2555
Species no.:	8	12	19	16	8	
Split (n):	1	1	0.1227	0.4945	1	
Sample volume (cm^3):	23.3	19.5	24.8	28.3	16.5	
Abundance (tests/10 cm^3):	22	105	973	129	12	
Fisher alpha diversity index:	2.64	2.78	4.53	4.24	4.94	
Species richness	8	12	19	16	8	

Table S2.5. Foraminiferal census data of the living fauna from Helgoland inner port.

Locality:	Helgoland, inner port
Station:	Bunkerpier
Sample:	0-1 cm
Sampling date:	29.03.2011
Latitude:	54° 10.706'N
Longitude:	7° 53.305'E
Height (m NHN):	-3.3
Floatate / total residue:	Residue
Size fraction:	63-2000 µm
Species	living
Ammonia batava	1
Ammonia tepida	1
Bolivina earlandi	1
Bolivina pseudoplicata	4
Bolivina pseudopunctata	8
Buliminella elegantissima	10
Cibicides lobatulus	1
Cribrostomoides jefreysii	2
Eggerelloides scaber	16
Elphidium albiumbilicatum	5
Elphidium margaritaceum	2
Elphidium selseyense	119
Fissurina lucida	1
Haynesina depressula	3
Haynesina germanica	6
Hopkinsina pacifica	4
Morulaeplecta bulbosa	2
Paratrochammina haynesi	3
Patellina corrugata	2
Stainforthia fusiformis	10
others, indet. spp.	3
Total:	204
Species no.:	23
Split (n):	0.1288
Sample volume (cm^3):	11
Abundance (tests/10 cm^3):	1440
Fisher alpha diversity index:	6.66

Table S2.6: Foraminiferal census data of the living fauna from the Bay of Tümlau, near Westerhever [4] (reference list from main chapter) used for the comparison of locations in this study.

Locality:	Bay of Tümlau	Bay of Tümlau	Bay of Tümlau	Bay of Tümlau	Bay of Tümlau		
Station:	D15	E11	E12	F13	F14		
Sample:	0-1 cm	0-1 cm	0-1 cm	0-1 cm	0-1 cm		
Sampling date:	April 2013	April 2013	April 2013	April 2013	April 2013		
Latitude (N)	54° 22,0429'N	54° 22,0659'N	54° 22,0569'N	54° 21,8749'N	54° 21,8699'N		
Longitude (E)	8° 40,5189'E	8° 40,6559'E	8° 40,6569'E	8° 40,5999'E	8° 40,5779'E		
Height (m above MTL)	0.92	0.72	0.84	1.21	0.35		
Floatate / total residue:	Residue	Residue	Residue	Residue	Residue		
Size fraction:	63-500 µm	63-500 µm	63-500 µm	63-500 µm	63-500 µm		
Species	living	living	living	living	living	Total	Percent
Ammonia batava	4	1	3		1	9	5.2
Ammonia cf. *beccarii*	2					2	1.2
Elphidium excavatum	1			1	1	3	1.7
Elphidium williamsoni	1			1	1	3	1.7
Haynesina germanica	20	6	56	6	68	156	90.2
Total	28	7	59	8	71	173	
Species no.:	5	2	2	3	4		
Sample volume (cm^3):	32	42	39	32	30		
Abundance (tests/10 cm^3):	8.8	1.7	15.1	2.5	23.7		
Sand content (%)	49.7	57.2	41	58.5	67.5		

Table S2.7. Foraminiferal census data of the living fauna from Schobüll.

Locality:	Schobüll, tidal flat
Station:	1
Sample:	1
Sampling date:	17.11.2018
Latitude:	54° 30.752'N
Longitude:	8° 59.383'E
Height (m NHN):	0.79
Floatate / total residue:	Residue
Size fraction:	63-2000 µm
Species	living
Ammonia aberdoveyensis	1
Ammonia tepida	19
Elphidium oceanensis	3
Elphidium selseyense	5
Haynesina germanica	83
Quinqueloculina seminulum	3
Total:	114
Species no.:	6
Split (n):	0.063
Sample volume (cm^3):	10
Abundance (tests/10 cm^3):	1810
Fisher alpha diversity index:	1.35

3. Scientific Chapter II. Heavy metal uptake of near-shore benthic foraminifera during multi-metal culturing experiments

Accepted to be published in *Biogeoscience* as: Schmidt, S., Hathorne, E. C., Schönfeld, J., & Garbe-Schönberg, D. (2021). Heavy metal uptake of near-shore benthic foraminifera during multi-metal culturing experiments. *Biogeosciences Discussions*, 1-50.

Abstract.
Heavy metal pollution originating from anthropogenic sources, e.g., mining, industry and extensive land use, is increasing in many parts of the world and influences coastal marine environments even after the source has ceased pollution. The elevated input of heavy metals into the marine system potentially affects the biota because of their toxicity, persistence and bioaccumulation. An emerging tool for environmental applications is the heavy metal incorporation into foraminiferal calcite tests, which facilitates monitoring of anthropogenic footprints on recent and past environmental systems. The aim of this study was to investigate whether the incorporation of heavy metals in foraminifera is a direct function of their concentration in seawater. Culturing experiments with a mixture of dissolved chromium (Cr), manganese (Mn), nickel (Ni), copper (Cu), zinc (Zn), silver (Ag), cadmium (Cd), tin (Sn), mercury (Hg) and lead (Pb) in artificial seawater were carried out over a wide concentration range to assess the uptake of heavy metals by the near-shore foraminiferal species *Ammonia aomoriensis*, *Ammonia batava* and *Elphidium excavatum*. Seawater analyses revealed increasingconcentrations for most metals between culturing phases and high metal concentrations in the beginning of the culturing phases due to the punctual metal addition. Furthermore, a loss of metals during the culturing process was discovered, by an offset between the added and the actual concentrations of the metals in seawater. Laser ablation ICP-MS analysis of the newly formed calcite revealed species-specific differences in the incorporation of heavy metals. The foraminiferal calcite of all three species exhibited Pb and Ag concentrations strongly correlated with concentrations in the seawater culturing medium (partition coefficients and standard deviation for Ag: *Ammonia aomoriensis*=0.50 ±0.02, *Ammonia batava*=0.17 ±0.01, *Elphidium excavatum*=0.47 ±0.04; for Pb: *Ammonia aomoriensis*=0.39 ±0.01, *Ammonia batava*=0.52 ±0.01, *Elphidium excavatum*=0.91 ±0.01). *Ammonia aomoriensis* further showed a correlation with Mn and Cu, *A. batava* with Mn and Hg and *E. excavatum* with Cr and Ni, and partially also with Hg. However, Zn, Sn and Cd showed no clear trend for the species studied, which in case of Sn was maybe caused by the lack of variation of the seawater Sn concentration . The calibrations and the calculated partition coefficients render *A. aomoriensis*, *A. batava* and *E. excavatum* as natural archives that enable the determination of variations of some heavy metal concentrations in seawater in polluted and pristine environments.

3.1 Introduction

Particular heavy metals e.g., zinc (Zn), iron (Fe), molybdenum (Mo), cobalt (Co) and copper (Cu) serve as micronutrients (e.g., Hänsch and Mendel, 2009) for eukaryotic life and play an important role for metabolism, growth, reproduction and enzymatic activity of organisms (e.g., Martín-González et al., 2005; Gallego et al., 2007). Other metals like mercury (Hg), on the other hand, are not known to have any positive effect on the body and are therefore believed to have a higher toxic potential (Jan et al., 2015). All these metals occur naturally in the environment as geogenic traces in soils, water, rocks and, consequently, in plants and animals. However, at higher concentrations, most heavy metals become toxic and have hazardous effects on marine biota (Stankovic et al., 2014). Heavy metals are defined herein as elements with a density >7 g/cm^3 (Venugopal and Luckey, 1975) and an atomic number beyond calcium (Bjerrum, 1936; Thornton, 1995). Furthermore, they are highly persistent in the marine environment and are not easily excreted by organisms after the uptake of these metals into their system and cells (Flora et al., 2012; Kennish, 2019). Coastal environments act as natural catchments for anthropogenic pollutants because these areas are directly affected by industry, agriculture and urban runoff (e.g., Alloway, 2013; Julian, 2015; Tansel and Rafiuddin, 2016).

In marginal seas and coastal areas, benthic foraminifera are common, and the chemical composition of their calcite test can be used as proxies for changing environmental parameters like water temperature (Mg/Ca; e.g., Nürnberg et al., 1995; 1996), salinity (Na/Ca; e.g., Wit et al., 2013, Bertlich et al., 2018) and redox conditions (Mn/Ca; Groeneveld and Filipsson, 2013b; Koho et al., 2015; 2017; Kotthoff et al., 2017; Petersen et al., 2018; Guo et al., 2019). Foraminifera take up heavy metals and incorporate them into their calcium carbonate shells during calcification (e.g., Boyle, 1981; Rosenthal et al., 1997; Dissard et al., 2009; 2010a; 2010b; Munsel et al., 2010; Nardelli et al., 2016; Frontalini et al., 2018a; 2018b; Titelboim et al., 2018; Smith et al., 2020). Moreover, foraminifera have a short life cycle (< 1 year; e.g., Haake, 1967; Boltovskoy and Lena, 1969; Wefer, 1976; Murray, 1992) and thus, react immediately to changing environmental conditions and contamination levels of the surrounding environment. Therefore, foraminifera archive environmental signals and fossil records from sediments can be used to determine parameters of interest throughout space and time.

Species of the foraminiferal genera *Elphidium* and *Ammonia* are among the most abundant foraminiferal taxa in intertidal and shelf environments worldwide. They are found from subtidal water depths to the outer continental shelves (Murray, 1991). Furthermore, their calcite tests are often well preserved in the fossil record (Poignant et al., 2000; McGann, 2008; Xiang et al., 2008) and therefore provide the opportunity to assess past environmental conditions. The combination of all these properties make foraminifera, and especially *Elphidium* and *Ammonia* species, suitable indicators of anthropogenic pollution (e.g., Sen Gupta et al., 1996; Platon et al., 2005). As such, this group of organisms are excellent candidates for monitoring the spatial and temporal distribution of heavy metals in seawater to evaluate, for example, the effectiveness of contemporary measures of reducing emissions caused by anthropogenic inputs.

The majority of culturing studies on heavy metal incorporation into benthic foraminifera were designed to assess the influence and uptake of one particular metal, e.g., manganese (Mn) (Barras et al., 2018), copper (Cu) (De Nooijer et al., 2007), chromium (Cr) (Remmelzwaal et al., 2019), lead (Pb) (Frontalini et al., 2015), zinc (Zn) (e.g., Smith et al., 2020), mercury (Hg) (Frontalini et al., 2018a) or cadmium (Cd) (Linshy et al., 2013). This approach is adequate to detail the effects on shell chemistry, growth or physiology. Only two studies reported culturing experiments with elevated levels of Cu, Mn and Ni (Munsel et al., 2010) and elevated levels of Mn, Ni and Cd (Sagar et al., 2021b) in the same culturing medium. However, in reality there is rarely only one metal polluting environments but instead a combination of several pollutant metals is usually found (e.g., Mutwakil et al., 1997; Cang et al., 2004; Vlahogianni et al., 2007; Huang et al., 2011; Wokhe, 2015; Saha et al., 2017). How foraminifera incorporate and react to heavy metals when they are co-exposed to more than one metal at a time is less constrained to date. A mixture of different metals will lead to interactions, which may result in a more severe damage of tissue than exposure to each of them individually (Tchounwou et al., 2012). For example, a co-exposure to arsenic and cadmium causes more damage of human kidneys than only one of these elements (Nordberg et al., 2005). Furthermore, a chronic low-dose exposure to multiple elements can cause similar synergistic effects (e.g., Wang et al., 2008). It is therefore reasonable to assume that other organisms are likewise harmed more when exposed to several potentially toxic elements simultaneously.

Here we present results from culturing studies with *Ammonia aomoriensis*, *Elphidium excavatum* and *Ammonia batava* assessing the relationship between heavy metal concentrations in seawater and foraminiferal tests. The partitioning factor between the concentration of an element in the ambient seawater and the calcium carbonate of the foraminifers is constrained by determining both the dissolved metal concentrations in water and the metal contents of individual chambers of the foraminiferal shell that have been precipitated in the culturing medium. In particular, foraminifera were grown while exposed to a combination of ten different heavy metals, i.e., cadmium (Cd), copper (Cu), chromium (Cr), lead (Pb), manganese (Mn), mercury (Hg), nickel (Ni), silver (Ag), tin (Sn) and zinc (Zn) over a range of concentrations that prevail in polluted near-shore environments today. These metals are the most common representatives of marine heavy metal pollution (Alve, 1995; Martinez-Colon et al., 2009). Once the carbonate/seawater metal partitioning coefficients are known, investigations of the chemistry of benthic foraminiferal shells offer a reliable method to monitor short-term changes of the concentration of heavy metals in seawater.

3.2 Material and Methods

3.2.1 Field sampling

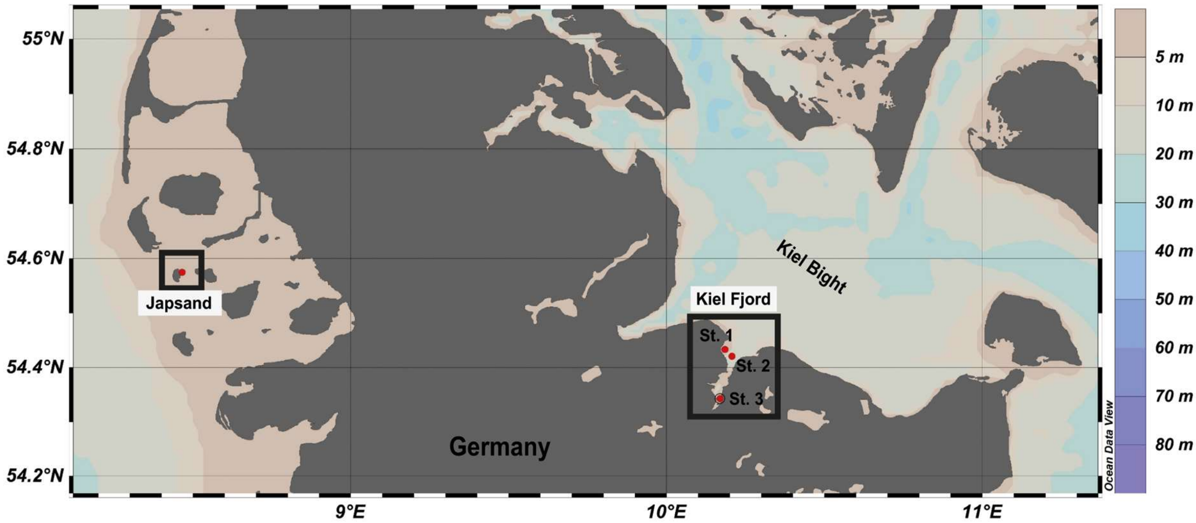

Figure 3.1: Location of the sampling stations in the North Sea (Japsand area) and in the Baltic Sea (Kiel Fjord, St.1 Strander Bucht, St. 2 Laboe, St. 3 Mönkeberg). The map was drawn with Ocean Data View (Schlitzer, 2016) on the basis of bathymetric data. Water depths in m are indicated by the colour scale.

3.2.1.1 North Sea, Japsand

Living specimens of *A. batava* were collected at the barrier sand Japsand near Hallig Hooge in the German Wadden Sea in July 2019 at two stations (St. 1: 54°34.480´N, 8°27.919´E; St. 2: 54°34.491´N, 8°27.895´E) (Fig. 3.1). The sediment was a glacial till or Eemian clay at Station 1 and fine to medium sand at Station 2. Temperature and salinity of seep waters were measured with a WTW 3210 conductivity meter in excavated holes in the vicinity. The temperature at Station 1 was 21.1 ° C and at Station 2 21.6 ° C, respectively. Salinity was 34 PSU at station 1 and 33.6 PSU at station 2. The samples were recovered during low tide by scrapping off the uppermost centimetre of the surface sediment with a spoon made out of stainless steel. Natural seawater (NSW) with a salinity of 30.3 PSU was collected near the sites for further processing of the samples. Once back on the nearby island Hallig Hooge, the sediment was washed with NSW through stacked sieves with a mesh size of 2000 and 63 µm. The 2000 µm sieve was used to remove larger organisms and excess organic material (macroalgae, gastropods, lugworms etc.) that could have induced anoxic conditions in the sediment during transport and storage. The residue was stored in Mucasol soap-washed and acid-cleaned Emsa CLIP and CLOSE® boxes, sparged with air and some algae food was provided. Back in the laboratory at GEOMAR, the residue was stored at 8 °C in a fridge until culturing. These stock cultures were fed twice a week with green-coloured *Nannochloropsis* concentrate (BlueBioTech) and water was partly exchanged with NSW from the sampling site once a week.

3.2.1.2 Baltic Sea, Kiel Bight

Living specimens of *A. aomoriensis* and *E. excavatum* were collected from different stations in Kiel Fjord, western Baltic Sea (St.1, Strander Bucht, 54°26.001´N, 10°11.1078´E; St. 2, Laboe, 54°25.254´N, 10°12.346´E; St. 3, Mönkeberg, 54°20.752´N, 10°10.150´E; water depth: 12.5 m, 12.3 m and 14.3 m, respectively) in September and October 2019 with F.B. Polarfuchs and F.S. Alkor, respectively (Fig. 3.1). A Rumohr corer (inner diameter 55 mm) was used on F.B. Polarfuchs and 9 cores were taken (2 at St. 1 and 7 at St. 3). The sediment from the cores was collected in Mucasol treated and acid-cleaned plastic containers with NSW from the site.

On F.S. Alkor, a Reineck box corer was used (200 x 250 mm) and 3 replicates at each station were taken (St. 1-3). The first 1 to 2 cm of the sediment surface of the box core were scrapped off with a spoon made out of stainless steel and the material was stored in a Mucasol treated and acid-cleaned plastic box with NSW from the location.

Back in the laboratory at GEOMAR, the samples were treated the same way as Japsand samples from the North Sea. Artificial seawater (ASW, Tropic Marin) with a salinity of 30 PSU was used for washing and storage of the surface samples from Kiel Fjord. The use of artificial seawater ensured that no harmful microorganism could invade the cultures.

3.2.2 Culturing setup

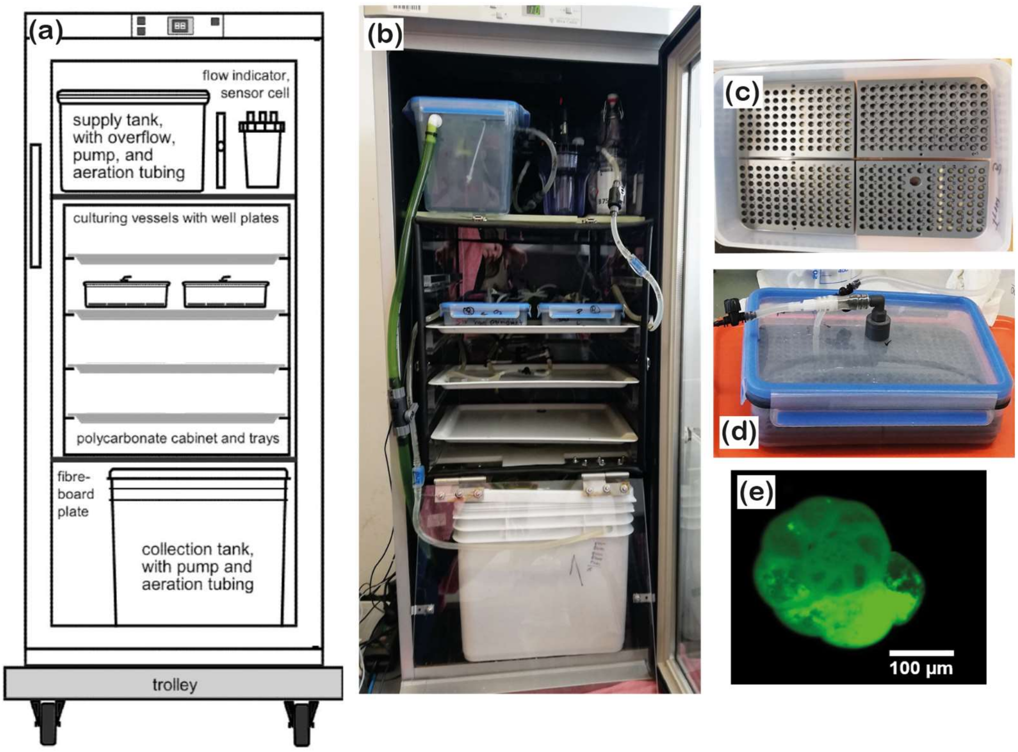

Figure 3.2: Culturing setup. a: conceptual draft and b: assembly of the system. Tubing and hoses were omitted from the draft for clarity. c: a well plate with mounted specimens and sand, d: closed culturing vessel with well plates and conduits. e: with calcein stained foraminifer under a fluorescence microscope. Please note that the last 2 ½ chambers are labelled and fluorescing brightly. The specimen shown in the picture was dead, cleaned and dried, which ensured that the test itself and not the cytoplasm showed the fluorescence.

3.2.2.1 Picking of the samples

The three foraminiferal species that were used in this study have been described in detail in the literature (e.g., Lutze, 1965; Nikulina et al., 2008; Schweizer et al., 2011; Francescangeli et al., 2021; Schmidt and Schönfeld, 2021). For extracting the foraminiferal specimens from the sediment, about 1 cm^3 of the 63 to 2000 µm size fraction was transferred to a petri dish. All living specimens were picked with a paintbrush from this subsample and collected in a small petri dish with ASW. All plastic utensils were treated with Mucasol water and rinsed with 5% HNO_3 prior to use. The paintbrush was cleaned with ethanol to protect the culture from harmful microorganisms. Only specimens with a glossy, transparent and undamaged test were chosen. After picking, a drop of concentrated food (pure culture of *Nannochloropsis*, green coloured algae) was added and the foraminifera were left untouched for a night.

Specimens that met one or more of the following criteria were considered as living and used for further procedures:

- The cytoplasm of the specimens was present in more than two chambers that were connected and including the innermost chambers,
- Specimens showed a structural infill of cytoplasm with a bright green colour, indicating they took up the food over night,
- they developed a film or strings of pseudopodia firmly sticking to sediment particles or food,
- they had covered themselves or gathered a cyst of sediment or food particles.

Specimens were identified and sorted by speciesand stained with calcein (10 mg l^{-1}, Bernhard et al., 2004) (bis[N,N-bis(carboxymethyl)aminomethyl]-fluorescein) (Sigma-Aldrich) directly before each culturing phase to ensure that freshly labelled foraminifera were inserted into the culturing system (Fig. 3.2e). Staining lasted for 14 days. Petri dishes were stored at 8 °C in a fridge, partial water exchanges and feeding of the foraminifera was performed twice a week. After the staining, the foraminifera were transferred to a petri dish with ASW and left for 1 to 2 days to remove excess calcein from seawater vacuoles in their cytoplasm prior to the introduction into the culturing system.

3.2.2.2 Culturing system

We used two closed-circulation incubation systems for foraminifera (Fig. 3.2a, b) provided by the Institute of Microbiology, Kiel University (Woehle et al., 2018, their Fig. S3.4). The systems were further developed based on earlier closed-circulation systems for culturing foraminifera (Hintz et al. 2004; Haynert et al., 2011). They were slightly modified for the requirements of this study, but the basic operational principle is described by Woehle et al., 2018. In detail, the systems consisted of three levels with different functions. They were built into a Bauknecht WLE 885 fridges for temperature control. Each system accommodated two culturing vessels, which were arranged pairwise on a tray in a polycarbonate cabinet (Fig. 3.2a, b). The water was pumped from the collection tank at the lowest level to the top level into the supply tank. From the supply tank, the water was directed to the culturing vessels and the flow was regulated ensuring that the same amount of water was provided to every culturing vessel. After passing the culturing vessels, the water was redirected to the collection tank. The systems were filled with 15 L of ASW with a salinity of 30.5 PSU. The water was aerated in the supply and the collection tank with filtered (0.2 µm) air from outside the system. Monitoring of temperature and salinity were performed with a WTW 3210 conductivity meter. Uncertainty of the conductivity measurements was ± 0.5% and ± 0.1 °C for temperature according to the manufacturer's test certificate. pH was monitored using a pH electrode (GHL) for aquarium purposes with uncertainties of ± 0.06. All parts that were introduced into the system were sterilised before use either by autoclaving, UV-lamp exposure, or by applying DanKlorix®.

3.2.2.3 Preparation for incubation

For the incubation of the foraminifera, well plates with cavities made from PVC were used (Fig. 3.2c). All well plates had been used in previous experiments for culturing foraminifera in seawater, which ensured that potentially toxic substances or additives were already released from the material (Woehle et al., 2018). Before the foraminifera were placed in the cavities, each cavity was filled with sterile quartz sand up to 1.5 mm height. The cavities were subsequently filled with artificial seawater and the specimens were inserted randomly. Prepared well plates were left untouched for one night, to make sure that the foraminifera were able to spread their pseudopodial network before incubation. This ensures that they were stably anchored in the cavities and did not float when the culturing vessels were filled and mounted (Haynert et al., 2011). Four well plates were assembled in each airtight Emsa CLIP and CLOSE® box (Fig. 3.2d).Each culturing vessel had a lid with an inflow and an outflow conduit, for which cleaned food grade Tygon® tubing was used. To guarantee that the foraminiferal specimens were not flushed away by the incoming water, the inflow conduit reached almost the bottom of the culturing vessel and was placed between two well plates. Once all well plates were arranged in the culturing vessel, the lid was equipped with an additional, elastic sealing and closed. Before the culturing vessels were placed in the culturing systems, each chamber was slowly filled with ASW. Thereafter, the culturing vessels were placed on the shelve in the culturing system, and were connected to the supply hoses.

3.2.2.4 Culturing experiment

The culturing experiment had four different phases. The first, phase 0 was dedicated as control phase and no heavy metals were added. This phase allowed both systems to equilibrate in terms of physicochemical and biological processes and made it possible to determine the background values in terms of seawater constituents. This phase lasted 21 days. Afterwards, one system was used as the control system, where no heavy metals were added. In the other system, three phases with elevated heavy metal concentrations were performed. The phases lasted 21 days each. Tropic Marin Pro-Reef salt was mixed with deionized water for adjusting the salinity. This artificial salt contains all elements and nutrients in sufficient amounts required by marine organisms. A stock solution containing all metals of interest was mixed and this solution is called the multi metal stock solution hereafter. It was added to the supply tank of the system (see Fig. 3.2a) (phase 1 = 1 ml, phase 2 = 10 ml, phase 3 = 150 ml) at the beginning of each phase to reach the target concentration (Table 3.1). Additionally, a smaller aliquot of the same multi metal stock solution (Phase 1 = 0.1 ml, Phase 2 = 1 ml, Phase 3 = 10 ml) was introduced twice a week during the three weeks of a phase. This was to counteract the loss of metals during the culturing phase through e.g., uptake of metals by foraminifera or algae or by adsorption to surfaces of the culturing system. The target concentration of the elements at each phase were chosen after earlier culturing experiments with foraminifers (Mn, Cu, Ni: Munsel et al., 2010; Pb: Frontalini et al., 2015 & 2018b; Zn: Nardelli et al., 2016; Cd: Linshy et al., 2013; Cu: De Nooijer et al., 2007; Le Cadre and Debenary et al., 2006; Cr: Remmelzwaal et al., 2019, Hg: Frontalini et al., 2018a) and to resemble conditions observed in threatened environments. Examples for such environments are the San Francisco Bay, California (Thomas et al., 2002), the Black Sea, Turkey (Baltas et al., 2017) or the Gulf of Chabahar, Oman Sea (Bazzi, 2014). Furthermore, the Adriatic Sea (Ag; Barriada et al., 2007), Jakarta Bay (Williams et al., 2000; Putri et al., 2012), and polluted U.S. and European rivers (Byrd and Andreae, 1982; Kannan et al., 1998; Thomas et al., 2002) were considered. Table A3.4 summarizes the heavy metal concentration in seawater in different areas around the world to compare to the experimental values. Additionally, the maximum metal concentration as recommended by the EPA (Environmental Protection Agency, USA) is the lower boundary of the concentration range from this study (Prothro, 1993). This was taken into account to ensure that the foraminifera were not limited in their growth and able to maintain normal physiological functions. A lower concentration than the EPA value is also covered by our study during the control phase or in the control system. The heavy metal concentrations in the culturing media obtained during each phase were monitored by frequent water sampling.

Table 3.1: Heavy metal concentration in the multi metal stock solution, target concentration of these metals in each phase and used salt compounds. All salts used were provided in pro analysi quality and were purchased from Carl Roth ($CrCl_3 \cdot 6\ H_2O$; $SnCl_2 \cdot 2\ H_2O$ and $PbCl_2$), Walter CMP ($CdCl_2$) and Sigma Aldrich ($MnCl_2 \cdot 4\ H_2O$, $NiCl_2 \cdot 6\ H_2O$, $CuCl_2 \cdot 2\ H_2O$, $ZnCl_2$, $AgNO_3$ and $HgCl_2$).

			Target conc. in µg l^{-1}		
	Salt compound	**Conc. in mg l^{-1} Multi metal stock solution**	**Phase 1**	**Phase 2**	**Phase 3**
Chromium (Cr)	$CrCl_3 \cdot 6\ H_2O$	25	0.5	5	50
Manganese (Mn)	$MnCl_2 \cdot 4\ H_2O$	40	40	400	4000
Nickel (Ni)	$NiCl_2 \cdot 6\ H_2O$	5	0.1	1	10
Copper (Cu)	$CuCl_2 \cdot 2\ H_2O$	2	0.05	0.5	5
Zinc (Zn)	$ZnCl_2$	50	0.8	8	80
Cadmium (Cd)	$CdCl_2$	4	0.08	0.8	8
Silver (Ag)	$AgNO_3$	3.5	0.1	1	10
Tin (Sn)	$SnCl_2 \cdot 2\ H_2O$	10	0.1	1	10
Mercury (Hg)	$HgCl_2$	0.04	0.01	0.1	1
Lead (Pb)	$PbCl_2$	10	0.1	1	10

Over the entire culturing period, both systems were exposed to a natural day and night cycle and the flow rate was adjusted to 1.02 ml min^{-1} (one drop per second) within the culturing vessels. The foraminifera were fed with *Nannochloropsis* concentrate twice a week (~ 2000 µg). After 21 days (meaning after each culturing phase) one culturing vessel per system was exchanged. Vessels and specimens were left in the culturing system for the complete culturing phase (21 days) and no exchange took place during a culturing phase.

Temperature and salinity were kept stable at 15.0 ±0.1 °C and 30.2 ±0.3 PSU (heavy metals) and at 14.9 ±0.2 °C and 30.4 ±0.4 PSU (control) over the complete culturing period. As the system was mostly closed, evaporation had a minor effect. Demineralized water was added when necessary to keep the salinity stable. The exchanges of culturing vessels between phases inferred a partial water exchange of approximately 10 % (= 1.5 l) every three weeks, which ensured a repetitive renewal of water with adequate quality.

3.2.3 Water samples

3.2.3.1 Collection of water samples

Water samples for determining the heavy metal concentrations were taken frequently from the supply tanks (see Fig. 3.2a) of both systems using acid cleaned syringes (Norm-Ject® disposable syringe, 20 ml, sterile) and sample bottles (LLG narrow neck bottles, 50 ml, LDPE = Low Density Polyethylene; Hg: GL 45 Laboratory bottle 250 ml with blue cap and ring, boro 3.3). From the beginning of phase 1, sampling was performed once a week. Water samples to be analysed for mercury concentrations had to be treated differently due to analytical constraints as detailed below. The water was filtered through a 0.2 µm PES filter (CHROMAFIL Xtra disposable filters, membrane material: polyether sulfone pore) for heavy metal samples and through a 0.2 µm quartz filter for Hg samples (HPLC syringe filters, 30 mm glass fibre syringe filters/ nylon). Filters were rinsed with the sample water before taking the sample. Every water sample was immediately acidified with concentrated ultrapure HCl to a pH of approximately 2 to avoid changes in the heavy metal concentrations due to adsorption to the sample bottle walls or the formation of precipitates.

3.2.3.2 Preparation of water samples before analysis

For Mn, Zn, Ni, Pb, Cu, and Cd concentration analyses, the water samples were pre-concentrated offline using a SeaFAST system (ESI, USA). Twelve mL of each sample were used to fill a sample loop and preconcentrated by a factor of 25 using the SeaFAST column into 1.5M HNO_3. All samples were spiked with indium as an internal standard for monitoring and the pre-concentration procedure. Both MilliQ water and bottle blanks of acidified MilliQ water (pH ~ 2) stored in the same bottles until the samples were passed through the pre-concentration system. Additionally, procedural blanks which were filtered as the samples were also pre-concentrated and measured. A variety of international (Open Ocean Seawater NASS-6, River Water SLRS-6, Estuarine Seawater SLEW-3, all distributed by NRC-CNRC Canada) and in-house (South Atlantic surface water, South Atlantic Gyre water) reference materials were preconcentrated like the samples. All samples were subsequently analysed by ICP-MS (inductively coupled plasma mass spectrometry).

Other metals (Cr, Ag and Sn) were diluted 1/25 and directly introduced into the ICP-MS as they are not retained on the Nobias resin used by the SeaFAST system. The dilution was performed with indium-spiked nitric acid (2%) and to match the matrix of these samples, blanks and standards with added NaCl were prepared.

All heavy metals except mercury were measured using an Agilent 7500ce quadrupole ICP-MS. Raw intensities were calibrated with mixed standards, which were made from single element solutions covering a wide concentration range. Additionally, a dilution series (dilution factors: 1, 1/10, 1/100 and 1/1000) of SLRS-6 of river water reference material (NRC Canada; Yeghicheyan et al., 2019) was measured for quality control. Mean values and relative standard deviations (RSD) derived from the reference materials are summarised in the appendix (Table A3.2).

Prior to the measurements of Hg concentrations, all samples were treated with BrCl solution at least 24 hours before the analysis to guarantee the oxidation and release of mercury species that were possibly present in a different oxidation states or phases. The BrCl was removed again by adding hydroxylamine hydrochloride at least one hour prior to analysis before the Hg was reduced to the volatile Hg^0 species with acidic $SnCl_2$ (20 % w v^{-1}) during the measuring process. All preparations of the water samples took place in a Clean Lab within a metal clean atmosphere and all vials were acid cleaned prior to use. Mercury concentrations were determined using a Total Mercury Manual System (Brooks Rand Model III). The reduced volatile Hg^0 was nitrogen-purged onto a gold-coated trap and released again by heating before it was measured via cold vapour atomic fluorescence (CVAFS) under a continuous argon carrier stream. Quality control of the Hg measurements was carried out by measuring mixed standards, made from single element solutions and confirmed with replicate measurements throughout each analysis. The measurement uncertainty was smaller than 4.5 % RSD for all analyses.

The calcium concentration of culture seawater was analysed using a VARIAN 720-ES ICP-OES (inductively coupled plasma optical emission spectrometer). Yttrium was added as an internal spike and samples were diluted 1/10. IAPSO seawater standard (ORIL) was measured after every 15 samples for further quality control which revealed a measurement uncertainty < 0.35 (RSD %) for the elements analysed (mean Ca concentration IAPSO this study = 419.6 ± 0.15 mg l^{-1}; reference Ca concentration IAPSO Batch 161 = 423 mg l^{-1}).

3.2.4 Foraminiferal samples

After every culturing phase, the culturing vessels were taken out of the culturing system and foraminiferal specimens were collected from their cavities within one day. The individuals were cleaned with tap water and ethanol before they were mounted in cell slides to mechanically remove salt scale and organic coatings with a paintbrush. Dead specimens could be identified because they lost the colour of their cytoplasm and furthermore, they did not gather food and particles anymore and thus were lacking a detritus cyst by their aperture.

In order to check the growth of foraminifera during the culture experiment, the total number of chambers were counted before and after the experiment for every specimen (Table 3.2). This was performed to double check the growth in cases where calcein staining may have failed. As the foraminifera were stained with calcein before the experiment, it was possible to cross-check the growth with a fluorescent microscope (Zeiss Axio Imager 2) if new chambers without fluorescence were added, and hence whether the specimen had grown or not (Fig. 3.2e). Only individuals clearly showing new chambers were analysed by Laser ablation ICP-MS.

Prior to the laser ablation analyses, the foraminifera were transferred into individual acid-leached, 500 µl micro-centrifuge tubes and thoroughly cleaned, applying a procedure adapted from Martin and Lea (2002). The specimens were rinsed three times with MilliQ water and introduced into the ultrasonic bath for a few seconds at the lowest power setting after each rinse. Afterwards, clay and adhering particles were removed by twice rinsing the sample with ethanol, which was followed by three MilliQ rinses again with minimal ultrasonic treatment. Oxidative cleaning was applied using 250 µl of a 0.1M NaOH and 0.3 % H_2O_2 mixture added to each sample and the vials were kept for 20 min in a 90 °C water bath. Afterwards, the samples were rinsed with MilliQ three times to remove the remaining chemicals. The reductive step of the cleaning procedure was not applied. This step is necessary to remove metal oxides, which of course could also influence the heavy metal concentration within the foraminiferal shell carbonate but these are usually considered to be added during early deposition (e.g., Boyle, 1983) and therefore unlikely to occur during culture experiments. For Laser Ablation Inductively Coupled Plasma Mass Spectroscopy (LA-ICP-MS) measurements, all cleaned specimens were fixed on a double-sided adhesive tape (PLANO).

Micro-analytical analyses with LA-ICP-MS were performed at the Institute of Geosciences, Kiel University, using a 193nm ArF excimer GeoLasPro HD system (Coherent) with a large volume ablation cell (Zurich-type LDHCLAC, Fricker et al., 2011) and helium as the carrier gas with 14 mL min^{-1} H_2 added prior to the ablation cell. For the foraminiferal samples, the pulse rate was adjusted to 4 to 5 Hz with a fluence between 2 and 3.5 J cm^{-2}. The spot size was set to 44 or 60 µm depending on the size of the foraminiferal chamber. All chambers of a foraminifer that were built up in the culturing medium were analysed, starting from the earliest, inner chamber adjacent to the calcein-stained chamber. The laser was manually stopped once it broke through the foraminiferal shell. The ablated material was analysed by a tandem ICP-MS/MS instrument (8900, Agilent Scientific Instruments) in no gas mode. The NIST SRM 612 glass (Jochum et al., 2011) was used for calibration and monitoring of instrument drift while NIST SRM 614 was measured for quality control. The glass was chosen because all elements of interest (except Hg) were reported in the literature, which was not the case for established carbonate reference materials. Glasses were ablated with a pulse rate of 10 pulses per second, an energy density of 10 J cm^{-2} and a crater size of 60 µm. Dueñas-Bohórquez et al. (2009) demonstrated that different energy densities between the foraminiferal calcite and the glass standard does not affect the analyses. Carbonate matrix reference materials coral JCp-1, giant clam JCt-1, limestone ECRM752-1 and synthetic spiked carbonate MACS-3 (Inoue et al., 2004; Jochum et al., 2019) in the form of nano-particle pellets (Garbe-Schönberg and Müller, 2014) were analysed for quality control. Carbonate reference material were ablated with a pulse rate of 5 pulses per second, an energy density of 5 J cm^{-2} and a crater size of 60 µm. MACS-3 was used for calibrating the mercury content in the samples as Hg is not present in the NIST SRM glasses. All results for the reference materials are given in the appendix (Table A3.3). Trace element-to-calcium ratios were quantified using the following isotopes: ^{26}Mg, ^{27}Al, ^{52}Cr, ^{55}Mn, ^{60}Ni, ^{63}Cu, ^{65}Cu, ^{68}Zn, ^{107}Ag, ^{111}Cd, ^{114}Cd, ^{118}Sn, ^{201}Hg, ^{202}Hg and ^{208}Pb normalised to ^{43}Ca. If more than one isotope was measured for an element, the average concentration of these was used after data processing. Analytical uncertainty (in % RSD) was better than 5 % for all TE/Ca ratios. The lowest RSD % based on the NIST SRM 612 glass was 2.1 % for Mn/Ca and the highest 5.0 % for Ag/Ca. Uncertainties of all used standards and reference materials are summarized in Table A3.3. Each acquisition interval lasted for 90 seconds, started and ended with measuring 20 s of gas blank, used as the background baseline to subtract from sample intensities during the data reduction process. Furthermore, the background monitoring ensured that the system was flushed properly after a sample. In cases when foraminiferal test walls were very fragile causing the test to break very quickly and, hence, the length of the sample data acquisition interval was less than 15 seconds, these profiles were excluded from further consideration.

Transient logs of raw intensities given in counts per seconds for all isotopes measured were processed with the software Iolite (Version 4, Paton et al., 2011) producing averages of every time-resolved laser profile. The determination of element/Ca ratios was performed after the method of Rosenthal et al. (1999). High values of ^{25}Mg, ^{27}Al or ^{55}Mn at the beginning of an ablation profile were related to contamination on the surface of the foraminiferal shell or remains of organic matter (e.g., Eggins et al., 2003) and these parts of the profiles were excluded from further data processing. The detection limit was defined by 3.3*SD of the gas blank in counts per seconds for every element in the raw data. Only values above this limit were used for further analyses and no data below the LOQ (limit of quantification = 10*SD) were interpreted.After processing the data with Iolite, an outlier detection of the TE/Ca ratios of the samples was performed. If trace metal values from a spot deviated more than ±2SD from the average of the samples from the corresponding culturing phase, values were defined as outliers and discarded. The number of rejected points is indicated in the supplementary material (Table S3.1).

All statistical tests of the TE/Ca values in the foraminiferal shell and the water were carried out using the statistical program PAST (Hammer, 2001). As the concentration of heavy metals in seawater varied during individual phases in the metal system (Table A3.1 and Fig. B3.1 in the appendix), the mean concentration was calculated by applying an individual curve fit for every phase. The curve was either linear, exponential or a power function depending on the trend the particular metal showed. If the type of trend was not clear, the curve type with the highest p and R^2 values were chosen. Based on these curves, water values were calculated for every day and the weighted average from all days was used for further calculations. This ensured that high concentrations in the beginning of each phase did not influence the mean value disproportionately. The partition coefficients of the different trace metal-to-calcium ratios were calculated using the trace element (TE) and calcium ratios in calcite and seawater. The following equation was used:

$$D_{TE} = (TE/Ca)_{calcite}/(TE/Ca)_{seawater}.$$

When the correlation between the metal concentration in seawater and the metal concentration in the foraminiferal test was positive and significant ($R^2 > 0.4$, $p < 0.05$), the D_{TE}´s are derived from the mean values of all phases and represent the slope of the calculated regression line. In cases where a significant positive correlation between phases could not be identified, the D_{TE} values were calculated from the means of each phase separately and the ranges given. The regression line was forced through the origin, which is a common practice and is applied in many other studies (e.g., Lea and Spero, 1994; Munsel et al., 2010; Remmelzwaal et al., 2019; Sagar et al., 2021a). The reason for this approach is that foraminifers are expected not to incorporate any metals into their shell if the metals concentration is zero in the seawater. In cases where there was clearly a non-zero intercept (Mn of *A. batava* with phase 3 and Hg of *E. excavatum* without phase 3), obvious if the course of the regression line changed significantly or the R^2 value decreased, then the trend line was not forced through the origin.

3.3 Results

3.3.1 Survival Rates/ Growth rates / Reproductions

Table 3.2: Number of inserted and recovered foraminifera from the different systems (C = control system, M = metal system) and phases (0–3). Numbers of living individuals after the experiment and individuals that formed chambers during their individual culturing phase are given in %. Note that the percentage of living foraminifera is based on the number of foraminifera that could be recovered alive and not on the number of inserted individuals. The number of laser spots is indicated as well.

	C0	C1	C2	C3	M0	M1	M2	M3	Total
No. of inserted individuals									
Ammonia aomoriensis	50	24	20	20	19	70	70	72	345
Ammonia batava	22	20	20	20	16	43	72	72	285
Elphidium excavatum	45	24	20	20	19	70	69	70	337
Total	117	68	60	60	54	183	211	214	967
No. of recovered individuals									
Ammonia aomoriensis	43	20	10	19	11	57	58	56	274
Ammonia batava	11	15	16	14	7	29	65	56	213
Elphidium excavatum	36	20	20	14	7	62	58	53	270
Total	90	55	46	47	25	148	181	165	757
Living individuals (end of experiment) in %									
Ammonia aomoriensis	86	100	80	100	90.9	100	81	98.2	92.0
Ammonia batava	81.8	100	100	92.9	100	100	100	100	96.8
Elphidium excavatum	91.7	100	95	92.9	100	88.7	91.4	94.3	94.3
Total	86.5	100	91.7	95.3	97.0	96.2	90.8	97.5	94.4
Ind. that formed chambers (end of the experiment) in %									
Ammonia aomoriensis	62.8	84.2	100	93.8	81.8	100	92.3	90	88.1

Ammonia batava	45.5	85.7	100	100	71.4	100	100	100	87.8
Elphidium excavatum	69.4	65	56.3	38.5	57.1	67.7	75	62.3	61.4
Total	59.2	78.3	85.4	77.4	70.1	89.2	89.1	84.1	79.1
No. of laser spots									
Ammonia aomoriensis	22	18	17	20	9	39	40	36	201
Ammonia batava	14	20	19	19	6	17	52	57	204
Elphidium excavatum	14	13	13	12	1	36	24	31	144
Total	50	51	49	51	16	92	116	124	549

On average 74.5 % of the specimens inserted into the experiment could be recovered after their individual culturing phase of 21 days and 94.4 % of these recovered specimens survived. Approximately 79.1 % of the surviving specimens also formed at least one new chamber. Fewer specimens of *E. excavatum* formed new chambers (61.4 %) than *A. batava* (87.8%) or *A. aomoriensis* (88.1 %) (Table 3.2). On average, *E. excavatum* formed only one or rarely two new chambers, whereas both *Ammonia* species formed usually more than four new chambers. Reproduction happened very sporadically occurring in between 2 and 6 specimens per phase, on average 5 %, for the two *Ammonia* species but not for *E. excavatum*. No malformed chambers were observed in specimens that were recovered from the heavy-metal contaminated system.

3.3.2 Culturing media

Table 3.3: Weighted mean TE/Ca values in the culturing medium of the control and the metal system ± the standard error of the mean (standard deviation σ/√n). Furthermore, the factors between the target concentrations (Table 3.1) and the measured concentrations as well as the factors between individual phases are given. Values given without a standard error originate from only one measurement. Averaged TE/Ca values of a phase were calculated based on single values measured on samples from different days during the culturing phase. These single values can be found in the Appendix (Table A3.1). BDL = below detection limit.

	Cr/Ca	Mn/Ca	Ni/Ca	Cu/Ca	Zn/Ca	Ag/Ca	Cd/Ca	Sn/Ca	Hg/Ca	Pb/Ca
Control System	µmol mol^{-1}	mmol mol^{-1}	µmol mol^{-1}	µmol mol^{-1}	µmol mol^{-1}	µmol mol^{-1}	µmol mol^{-1}	µmol mol^{-1}	nmol mol^{-1}	µmol mol^{-1}
Phase 0	BDL	0.94 ± 0.02	7.0 ± 0.1	9.3 ± 4.3	118.3 ± 4.5	0.43 ± 0.214	0.41 ± 0.001	2.2 ± 0.4	5.8 ± 0.6	0.44 ± 0.06
Phase 1	BDL	0.92 ± 0.00	6.3 ± 0.1	4.4 ± 1.4	91.6 ± 1.1	0.19 ± 0.013	0.41 ± 0.002	2.5 ± 0.1	4.5 ± 1.0	0.39 ± 0.02
Phase 2	1.3 ± 0.3	0.90 ± 0.02	5.7 ± 0.1	2.1 ± 0.2	74.8 ± 2.0	0.19 ± 0.003	0.38 ± 0.006	2.1 ± 0.1	13.2 ± 5.8	0.31 ± 0.02
Phase 3	2.0 ± 0.4	0.89 ± 0.01	6.8 ± 0.3	1.5 ± 0.1	78.3 ± 0.8	0.16 ± 0.009	0.37 ± 0.006	1.8 ± 0.1	5.8 ± 1.8	0.28 ± 0.01
Metal System	µmol mol^{-1}	mmol mol^{-1}	µmol mol^{-1}	µmol mol^{-1}	µmol mol^{-1}	µmol mol^{-1}	µmol mol^{-1}	µmol mol^{-1}	nmol mol^{-1}	µmol mol^{-1}
Phase 0	8.0 ± 1.8	0.84 ± 0.01	7.4 ± 0.1	12.9 ± 4.5	104.8 ± 1.4	0.09 ± 0.02	0.43 ± 0.002	3.0 ± 0.1	5.28	0.50 ± 0.04

Phase 1	8.6 ± 0.5	0.83 ± 0.004	7.3 ± 0.1	2.8 ± 0.3	95.2 ± 0.3	0.10 ± 0.02	1.12 ± 0.01	4.1 ± 0.1	39.7 ± 2.7	0.69 ± 0.03
Phase 2	14.7 ± 0.1	0.81 ± 0.003	9.6 ± 0.1	2.4 ± 0.2	134.8 ±0.5	0.40 ± 0.14	4.86 ± 0.03	5.2 ± 0.03	337.6 ± 52.1	2.63 ± 0.3
Phase 3	36.3 ± 1.9	1.41 ± 0.004	61.3 ± 1.8	4.0 ± 1.0	547.5 ± 20.5	6.1 ± 2.5	78.92 ± 1.9	7.5 ± 1.0	3132.4 ± 323.7	57.84 ± 6.4
Factor between target conc. and measured conc.										
Phase 1	17.2	20.8	73.0	56.0	119.0	1.0	14.0	41.0	4.0	6.9
Phase 2	2.9	2.0	9.6	4.8	16.9	0.4	6.1	5.2	3.4	2.6
Phase 3	0.7	0.4	6.1	0.8	6.8	0.6	9.9	0.8	3.1	5.8
Factor between Phases										
Phase 0-1	1.1	1.0	1.0	0.2	0.9	1.1	2.6	1.4	7.5	1.4
Phase 1-2	1.7	1.0	1.3	0.9	1.4	4.0	4.3	1.3	8.5	3.8
Phase 2-3	2.5	1.7	6.4	1.7	4.1	15.3	16.2	1.4	9.3	22.0

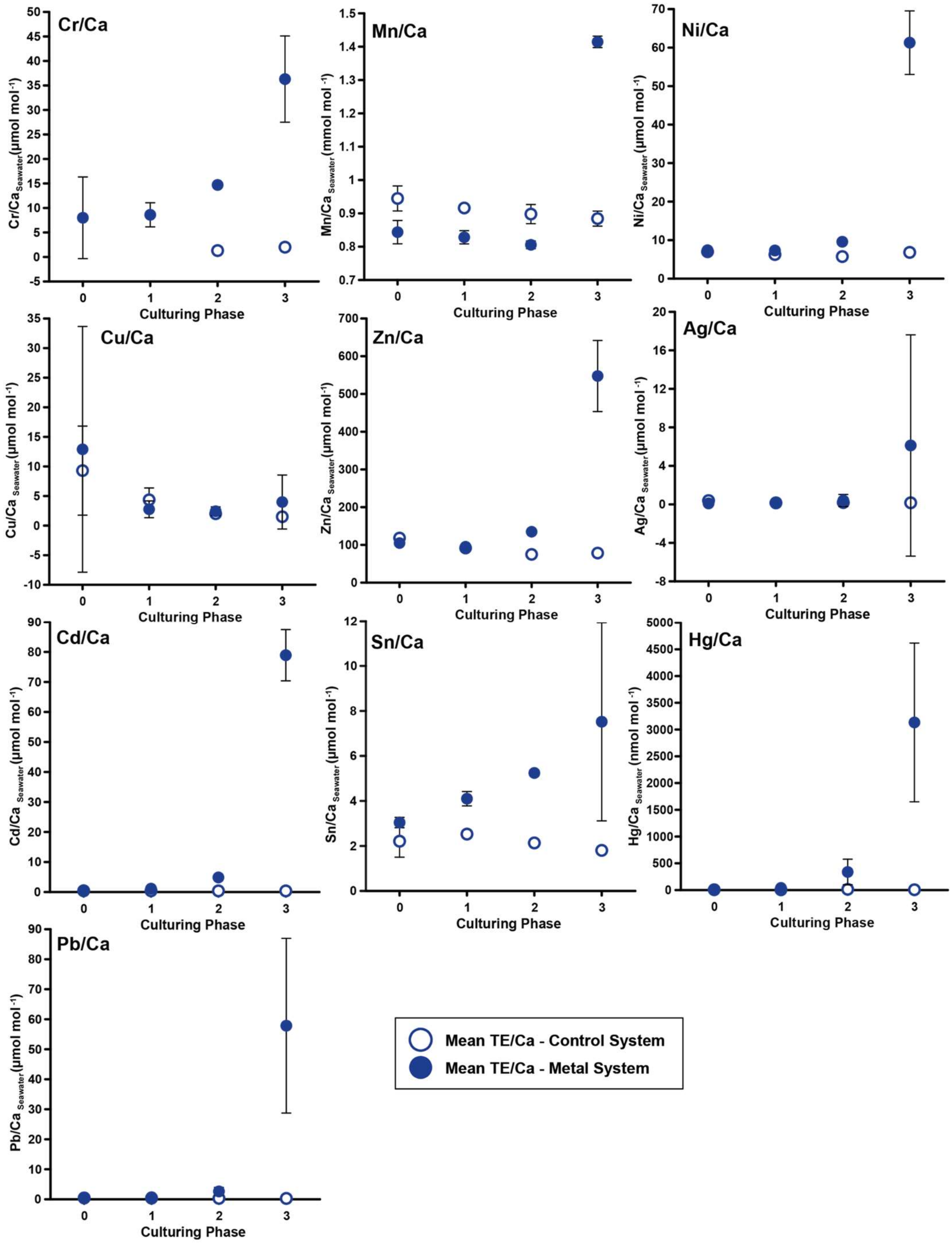

Figure 3.3: Weighted mean TE/Ca values in the culturing medium in µmol mol^{-1}. Error bars display the standard error of the mean (standard deviation σ/√n). Open symbols represent the control system, where no extra metals were added during the complete culturing period (phase 0 to 3) and closed symbols represent the metal system. In this system, phase 0 is the control phase without any extra added metals and for phase 1 to 3, the heavy metal concentration in the culturing medium was elevated. Note that the standard error is comparably high in phase 3 because the heavy metal concentration in this phase varied more strongly, which is shown in the appendix (Table A3.1, Fig. B3.1). Therefore, this error is derived from the real values in the seawater and not from analytical uncertainties. Note that the Cr/Ca values from the control system in phase 0 and 1 are not given as these values were below the detection limit.

In phases 1 and 0 the concentration in both systems were nearly equal for most elements. Only Cr and Sn had slightly elevated concentrations in the metal system. Furthermore, Cu concentration was higher in the metal system in phase 0 and phase 3 (Fig. 3.3). In phase 2, all metals but Mn and Cu showed higher concentrations in the metal system than in the control system. Mn concentrations were higher in the control system during phase 0 to phase 2. In phase 3, the concentration of all heavy metals were elevated in the metal system compared to the control system. The variation of the metal concentration was highest in phase 3, in both systems, for all elements but Cu, which showed highest variation in phase 0 (Fig. 3.3). The control system generally displayed a smaller degree of variation than the metal system.

Even though, the aim was to maintain the target concentrations shown in Table 3.1 during the 21 days of each culturing period by the bi-weekly addition of an aliquot of the multi metal stock solution, the target concentration of the metals was not obtained for most metals in phase 1 and 2, the only exception was Ag in phase 1 (Table 3.3). The difference factors between the target and measured concentration was highest (> 50) for Ni, Cu and Zn in phase 1 and decreased in phase 2 and 3. In phase 3, metals Cr, Mn, Cu, Ag and Sn reached concentrations closer (factor 0.4-0.8) to the target concentration and Ni, Zn, Cd, Hg and Pb concentrations were higher (factor 3.1-9.9) than expected. Furthermore, the change in metal concentration was small for the transition from phase 0 to 1 (factor <1.4) for all elements but Cd (factor 2.6) and Hg (factor 7.5).

3.3.3 Incorporation of heavy metals into the foraminiferal shell

Table 3.4: Mean heavy metal–to–calcium values of *A. aomoriensis*, *A. batava* and *E. excavatum* in the control and the metal system. Errors are standard errors of the mean (standard deviation σ/√n). Values marked with an asterisk were derived from only one laser spot and thus are not considered for further discussion. Furthermore, the calculated D_{TE} values, the slope of the linear regression line (OLS-Ordinary Least Squares) of all means, Pearson's correlation coefficient (R^2) and its significance (p) are given for the calculation with all phases and when removing phase 3 from the calculations. Cases where the regression lines were forced through the origin are indicated.. In cases when a regression did not show significant correlation, the D_{TE} range calculated separately from the individual phases is given. In cases when the

regression was significant, the D_{TE} values represent the slope of the regression line. Ph = Phase, SD = Standard deviation. Values in Table S3.1 are the basis of all calculations.

	Phase	Cr/Ca	Mn/Ca	Ni/Ca	Cu/Ca	Zn/Ca
Control System		µmol mol^{-1}	mmol mol^{-1}	µmol mol^{-1}	µmol mol^{-1}	µmol mol^{-1}
A. aomoriensis	0	18.6 ± 2.5	0.11 ± 0.02	1.3 ± 0.2	5.6 ± 0.9	53.2 ± 8.8
	1	12.6 ± 0.6	0.53 ± 0.12	5.9 ± 0.8	8.6 ± 1.0	34.2 ± 4.7
	2	13.6 ± 0.5	0.27 ± 0.07	2.1 ± 0.2	3.6 ± 0.2	18.6 ± 1.9
	3	10.2 ± 0.6	0.43 ± 0.08	4.3 ± 0.7	8.1 ± 2.0	29.5 ± 6.1
A. batava	0	11.6 ± 0.7	0.04 ± 0.01	1.4 ± 0.2	7.2 ± 1.1	23.9 ± 4.5
	1	10.9 ± 0.5	0.03 ± 0.00	2.6 ± 0.3	5.9 ± 0.6	17.8 ± 1.3
	2	9.0 ± 0.3	0.03 ± 0.00	0.9 ± 0.1	5.0 ± 1.0	12.9 ± 1.4
	3	9.1 ± 0.4	0.03 ± 0.01	1.9 ± 0.2	6.5 ± 1.3	14.9 ± 2.2
E. excavatum	0	22.9 ± 2.9	0.43 ± 0.13	9.4 ± 2.5	22.3 ± 7.9	28.1 ± 4.5
	1	88.9 ± 34.1	2.29 ± 0.56	7.8 ± 1.9	20.3 ± 8.0	48.9 ± 12.1
	2	16.2 ± 1.7	1.55 ± 0.26	5.9 ± 1.0	6.7 ± 1.4	21.9 ± 2.9
	3	26.7 ± 3.3	1.88 ± 0.55	4.4 ± 0.6	4.7 ± 0.7	16.8 ± 2.0
Metal System						
A. aomoriensis	0	16.0 ± 0.5	0.08 ± 0.02	5.5 ± 0.9	15.2 ± 2.6	29.8 ± 5.1
	1	14.0 ± 0.7	0.39 ± 0.08	3.1 ± 0.3	6.7 ± 0.7	30.0 ± 4.0
	2	11.1 ± 0.3	0.20 ± 0.05	5.3 ± 0.5	5.8 ± 0.5	28.3 ± 2.3
	3	14.1 ± 1.0	0.71 ± 0.12	3.8 ± 0.3	6.3 ± 1.5	42.2 ± 6.1
A. batava	0	16.5 ± 0.7	0.07 ± 0.01	1.1 ± 0.1	7.7 ± 1.6	68.0 ± 9.6
	1	15.2 ± 1.2	0.04 ± 0.01	1.8 ± 0.3	2.5 ± 0.6	20.7 ± 2.7
	2	9.7 ± 0.2	0.02 ± 0.00	1.8 ± 0.1	8.3 ± 1.8	12.9 ± 1.2
	3	12.2 ± 0.3	0.17 ± 0.04	2.9 ± 0.2	8.3 ± 1.2	49.8 ± 3.5
E. excavatum	0	17.30*	0.29*	4.30*	12.20*	26.70*
	1	32.9 ± 3.4	0.70 ± 0.12	8.2 ± 1.1	12.8 ± 1.8	18.5 ± 0.9
	2	41.8 ± 5.2	0.77 ± 0.15	8.6 ± 1.1	11.5 ± 1.5	29.8 ± 3.6
	3	54.1 ± 8.2	0.88 ± 0.15	17.0 ± 2.2	22.6 ± 3.6	43.1 ± 3.3
Calculations with Phase 3						
A. aomoriensis						
Slope of regression line ±SD			0.38 ±0.30		1.18 ±0.25	
Correlation coefficient (R^2)			0.83		0.80	
Significance (p)			0.05		0.05	
D_{TE} ±SD		0.4-10.3	0.38 ±0.30	0.06-0.94	1.18 ±0.25	0.08-0.45
Forced through origin		Single points	Yes	Single points	Yes	Single points
A. batava						
Slope of regression line ±SD			0.23 ±0.04			
Correlation coefficient (R^2)			0.84			
Significance (p)			0.001			
D_{TE} ±SD		0.4-6.8	0.23 ±0.04	0.05-0.41	0.60-4.35	0.09-0.65
Forced through origin		Single points	No	Single points	Single points	Single points
E. excavatum						
Slope of regression line ±SD		2.1 ±0.28		0.19 ±0.04		
Correlation coefficient (R^2)		0.82		0.79		
Significance (p)		0.01		0.003		
D_{TE} ±SD		2.1 ±0.28	0.34-2.50	0.19 ±0.04	0.95-5.67	0.08-0.53
Forced through origin		Yes	Single points	No	Single points	Single points
Calculations without Phase 3						
A. aomoriensis						
Slope of regression line ±SD						
Correlation coefficient (R^2)						
Significance (p)						

D_{TE} ±SD	0.74-10.3	0.09-0.53	0.19-0.94	0.61-5.42	0.21-0.45
Forced through origin	Single points	Single points	Single points	Single points	Single points
A. batava					
Slope of regression line ±SD					
Correlation coefficient (R^2)					
Significance (p)					
D_{TE} ±SD	0.65-6.8	0.02-0.08	0.15-0.41	0.60-4.35	0.10-0.65
Forced through origin	Single points	Single points	Single points	Single points	Single points
E. excavatum					
Slope of regression line ±SD					
Correlation coefficient (R^2)					
Significance (p)					
D_{TE} ±SD	2.5-13.4	0.34-2.50	0.64-1.35	0.95-4.73	0.22-0.53
Forced through origin	Single points	Single points	Single points	Single points	Single points

Table 3.4 continued.

	Phase	Ag/Ca	Cd/Ca	Sn/Ca	Hg/Ca	Pb/Ca
Control System		µmol mol^{-1}	µmol mol^{-1}	µmol mol^{-1}	nmol mol^{-1}	µmol mol^{-1}
A. aomoriensis	0	0.27 ± 0.08	7.6 ± 1.0	0.33 ± 0.07	1.54 ± 0.46	1.23 ± 0.22
	1	0.28 ± 0.05	3.8 ± 0.3	1.60 ± 0.30	3.11 ± 0.68	1.14 ± 0.16
	2	0.16 ± 0.04	3.6 ± 0.2	0.21 ± 0.03	1.13 ± 0.31	0.81 ± 0.10
	3	0.31 ± 0.11	2.9 ± 0.2	0.19 ± 0.03	8.02 ± 1.72	1.45 ± 0.42
A. batava	0	0.09 ± 0.03	4.7 ± 0.5	0.27 ± 0.05	1.3 ± 0.4	0.67 ± 0.10
	1	0.07 ± 0.01	2.5 ± 0.2	0.65 ± 0.09	1.2 ± 0.3	0.29 ± 0.03
	2	0.05 ± 0.00	2.7 ± 0.1	0.08 ± 0.02	1.5 ± 0.4	0.39 ± 0.03
	3	0.06 ± 0.01	1.9 ± 0.1	0.10 ± 0.02	4.4 ± 0.6	0.36 ± 0.05
E. excavatum	0	0.22 ± 0.09	3.6 ± 1.1	0.99 ± 0.40	15.0 ± 4.4	1.83 ± 0.59
	1	0.07 ± 0.01	20.1 ± 9.2	8.21 ± 2.63	83.0 ± 33.4	2.22 ± 0.54
	2	0.10 ± 0.03	1.2 ± 0.2	0.45 ± 0.08	16.9 ± 3.8	0.94 ± 0.10
	3	0.04 ± 0.01	2.3 ± 0.4	0.27 ± 0.03	35.8 ± 6.3	0.55 ± 0.11
Metal System						
A. aomoriensis	0	0.08 ± 0.03	4.9 ± 0.3	0.62 ± 0.09	2.6 ± 0.6	1.17 ± 0.24
	1	0.25 ± 0.04	4.0 ± 0.4	0.84 ± 0.10	1.8 ± 0.2	0.90 ± 0.13
	2	0.52 ± 0.08	5.5 ± 0.4	1.70 ± 0.17	9.1 ± 1.7	3.85 ± 0.45
	3	3.03 ± 0.39	5.4 ± 0.4	0.55 ± 0.10	10.3 ± 1.3	22.14 ± 2.37
A. batava	0	0.06 ± 0.03	6.2 ± 0.2	0.19 ± 0.04	1.0 ± 0.2	1.27 ± 0.08
	1	0.04 ± 0.01	3.1 ± 0.3	0.59 ± 0.12	0.2 ± 0.0	0.42 ± 0.07
	2	0.18 ± 0.04	3.1 ± 0.2	0.46 ± 0.06	4.5 ± 1.1	0.52 ± 0.05
	3	1.05 ± 0.17	6.5 ± 0.3	0.21 ± 0.02	7.7 ± 1.0	29.82 ± 3.70
E. excavatum	0	0.40*	5.60*	0.18*	6.80*	1.59*
	1	0.03 ± 0.01	3.0 ± 0.3	2.63 ± 0.32	85.7 ± 19.7	1.36 ± 0.15
	2	0.69 ± 0.18	3.9 ± 0.5	2.89 ± 0.47	120.4 ± 44.7	4.61 ± 0.86
	3	2.84 ± 0.64	4.7 ± 0.5	2.74 ± 0.42	94.9 ± 16.2	52.51 ± 6.17
Calculations with Phase 3						
A. aomoriensis						
Slope of regression line ±SD		0.50 ±0.02				0.39 ±0.01
Correlation coefficient (R^2)		0.97				0.97
Significance (p)		< 0.0001				< 0.0001
D_{TE} ±SD		0.50 ±0.02	0.07-18.49	0.07-0.63	0.003-1.39	0.39 ±0.01
Forced through origin		Yes	Single points	Single points	Single points	Yes
A. batava						

Slope of regression line ±SD	0.17 ±0.01			0.003 ±0.001	0.52 ±0.01
Correlation coefficient (R^2)	0.98			0.63	1
Significance (p)	< 0.0001			0.01	< 0.0001
D_{TE} ±SD	0.17 ±0.01	0.08-14.42	0.03-0.26	0.003 ±0.001	0.52 ±0.01
Forced through origin	Yes	Single points	Single points	Yes	Yes
E. excavatum					
Slope of regression line ±SD	0.47 ±0.04				0.91 ±0.01
Correlation coefficient (R^2)	0.96				1
Significance (p)	< 0.0001				< 0.0001
D_{TE} ±SD	0.47 ±0.04	0.06-49.45	0.06-3.25	0.03-18.51	0.91 ±0.01
Forced through origin	Yes	Single points	Single points	Single points	Yes
Calculations without Phase 3					
A. aomoriensis					
Slope of regression line ±SD					1.6 ±0.17
Correlation coefficient (R^2)					0.91
Significance (p)					< 0.001
D_{TE} ±SD	0.70-2.57	1.14-18.49	0.10-0.63	0.003-1.39	1.60 ±0.17
Forced through origin	Single points	Single points	Single points	Single points	Yes
A. batava					
Slope of regression line ±SD	0.35 ±0.09				
Correlation coefficient (R^2)	0.91				
Significance (p)	0.03				
D_{TE} ±SD	0.35 ±0.09	0.63-14.42	0.04-0.26	0.005-0.76	0.20-5.52
Forced through origin	Yes	Single points	Single points	Single points	Single points
E. excavatum					
Slope of regression line ±SD				0.26 ±0.11	2 ±0.28
Correlation coefficient (R^2)				0.53	0.90
Significance (p)				0.05	0.003
D_{TE} ±SD	0.23-4.25	0.80-49.45	0.06-3.25	0.26 ±0.11	2.0 ±0.28
Forced through origin	Single points	Single points	Single points	No	Yes

Measurable incorporation into the foraminiferal calcite was found for all the heavy metals analysed but the degree of incorporation varied profoundly within and between species (Fig. 3.4 and Table 3.4). In both systems, the heavy metal concentration in *E. excavatum* was higher than in the other species (*A. aomoriensis* and *A. batava*) for Cr, Mn, Ni, Hg and Sn. This trend is also visible but less pronounced in the Cu values of the control system.

Cr, Ni, Cu, Zn, Cd, Pb and Ag values of *A. aomoriensis* displayed the highest standard error of the mean paired with highest concentrations in the water in the metal system. Sn, Mn and Hg did not show any clear pattern. In the control system, all heavy metal concentrations had higher standard errors of the mean when the concentration of these metals in the culturing medium was higher. The trend was also shown in *A. batava* and *E. excavatum* for all heavy metals of the control and the metal system. Note that even though no extra metals were added to the culturing medium of the control system, differences in the heavy metal concentration occurred (Fig. 3.3 and Table 3.3).

Calculations were performed with and without phase 3 of the metal system (Fig. 3.4, Fig. B3.2 and Table 3.4) to address a possible overload effect when it comes to higher metal concentrations in the seawater.

When phase 3 was included, a strong positive correlation ($R^2 > 0.9$, $p \leq 0.05$) between Ag and Pb concentrations in the foraminiferal shell and the culturing medium was found for all three species. Furthermore, *A. batava* also displayed a positive correlation for Hg ($R^2 = 0.63$, $p < 0.01$), *A. aomoriensis* for Cu ($R^2 = 0.80$, $p < 0.05$) and *E. excavatum* for Cr ($R^2 = 0.82$, $p < 0.01$) and Ni ($R^2 = 0.79$, $p < 0.003$). Weaker but still significant positive correlations were recorded for Mn ($R^2 > 0.84$, $p \leq 0.05$) for both *Ammonia* species. An indistinct correlation of the concentration in the seawater and in the foraminiferal test was recognised for Zn in all three species, whereas Cd and Sn showed no covariance (Fig. 3.4 and Table 3.4).

When phase 3 was excluded from the calculations, *A. aomoriensis* and *E. excavatum* showed a positive correlation for Pb ($R^2 > 0.9$, $p \leq 0.003$), *A. batava* for Ag ($R^2 = 0.91$, $p = 0.03$) and in *E. excavatum* Hg correlated weaker positively ($R^2 > 0.53$, $p \leq 0.05$). All other elements show no significant correlation (Fig. 3.4 and Table 3.4).

3.3.4 Partition coefficient (D_{TE})

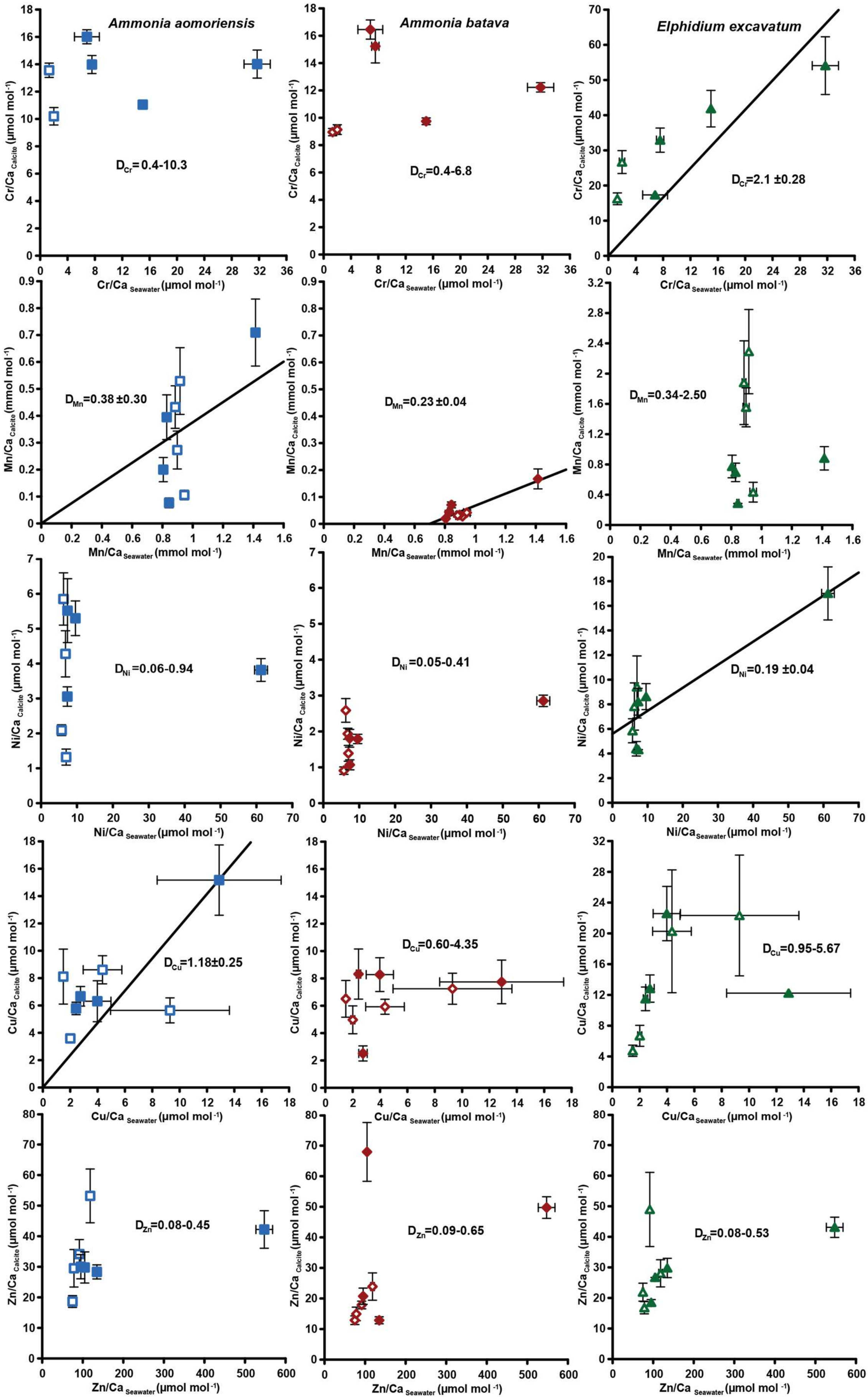

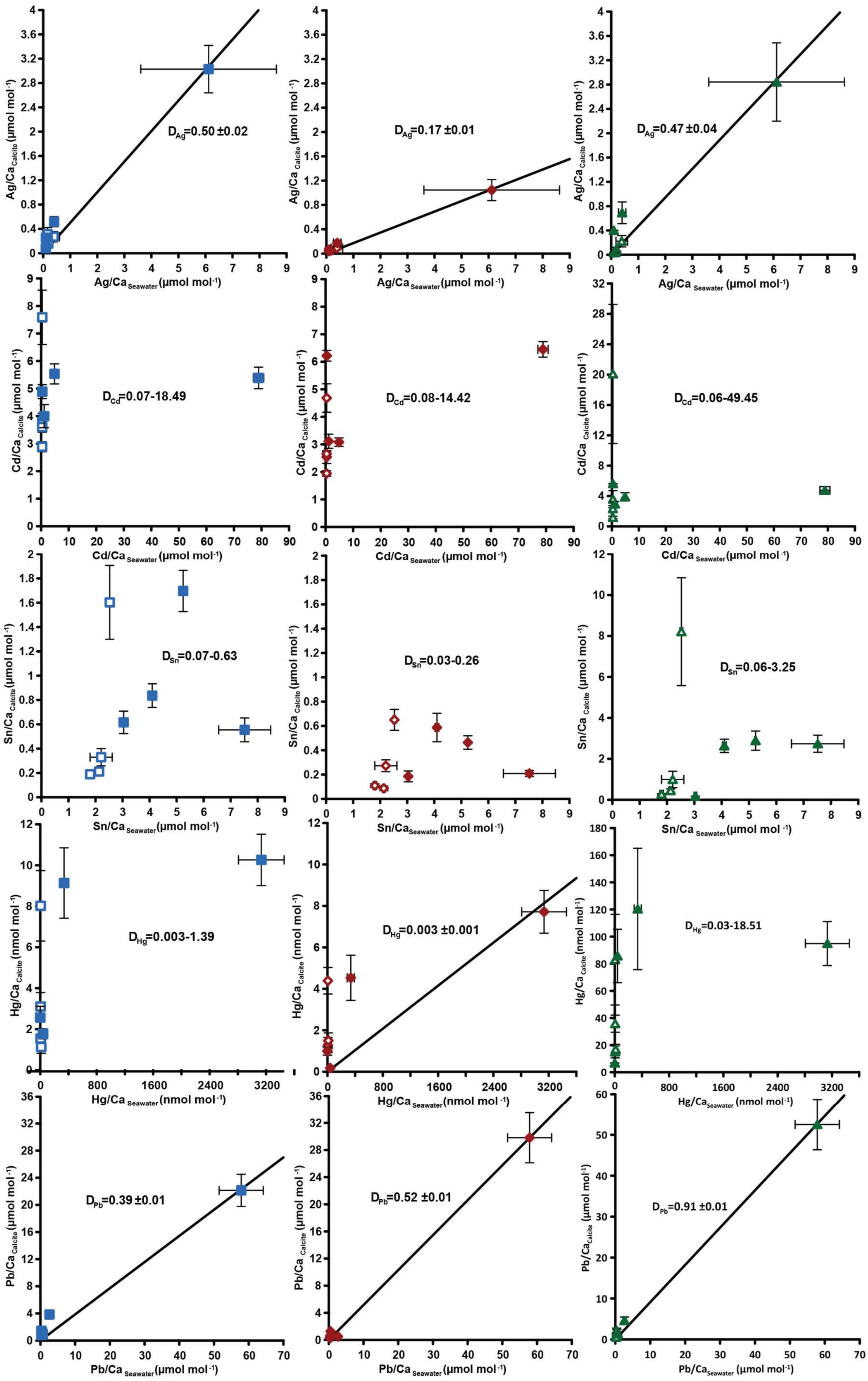
D_Ag=0.50 ±0.02
D_Ag=0.17 ±0.01
D_Ag=0.47 ±0.04
Ag/Ca_Calcite (µmol mol⁻¹)
Ag/Ca_Seawater (µmol mol⁻¹)
D_Cd=0.07-18.49
D_Cd=0.08-14.42
D_Cd=0.06-49.45
Cd/Ca_Calcite (µmol mol⁻¹)
Cd/Ca_Seawater (µmol mol⁻¹)
D_Sn=0.07-0.63
D_Sn=0.03-0.26
D_Sn=0.06-3.25
Sn/Ca_Calcite (µmol mol⁻¹)
Sn/Ca_Seawater (µmol mol⁻¹)
D_Hg=0.003-1.39
D_Hg=0.003 ±0.001
D_Hg=0.03-18.51
Hg/Ca_Calcite (nmol mol⁻¹)
Hg/Ca_Seawater (nmol mol⁻¹)
D_Pb=0.39 ±0.01
D_Pb=0.52 ±0.01
D_Pb=0.91 ±0.01
Pb/Ca_Calcite (µmol mol⁻¹)
Pb/Ca_Seawater (µmol mol⁻¹)

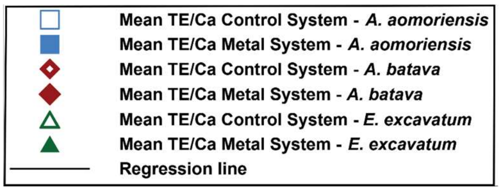

Figure 3.4: Mean TE/Ca values in the foraminiferal calcite versus the mean TE/Ca values in the corresponding culturing medium based on phase 0 to 3. Each data point represents the mean value of all laser ablation ICP-MS measurements on single foraminiferal chambers built up during the individual culturing phase plotted against the mean metal concentrations in the seawater averaged over the culturing phase (Table 3.3). Because calculating p- and R^2 values of the regression lines and the D_{TE}´s with the mean per phase resulted in comparable values to when calculating with the overall dataset, we considered this approach adequate. Error bars symbolize the standard error of the mean. The linear regression line (± standard deviation) is displayed when elements showed a significant correlation between seawater and calcite. D_{TE}'s of *E. excavatum* were considered without values for Phase 0 of the Metal System as only data from one newly formed chamber are available. All values can be found in Table 3.4. An enlarged graph based on the calculations without phase 3 is provided in the appendix (Fig. B3.2).

The majority of D_{TE} were lower than 1 in *A. aomoriensis* (with phase 3 = 61 %, without phase 3 = 57%) and *A. batava* (with phase 3 = 75%, without phase 3 = 73%), i.e., uptake but no enrichment took place. D_{TE} values derived from *E. excavatum* on the other hand showed a smaller proportion < 1 (with phase 3 = 47%, without phase 3 = 42%). For most elements (Cr, Mn, Ni, Cu, Cd, Sn, Pb and Hg) D_{TE} derived from *E. excavatum* were higher than D_{TE} from the two *Ammonia* species (Table 3.4, Fig. 3.4), which showed comparable D_{TE} values for most elements. D_{Zn} built the exception because all values were within a similar range (D_{Zn} ~ 0.08-0.65) independent of the species. For *A. aomoriensis* D_{Cu} was > 1 and D_{Cd} as well as D_{Pb} were also > 1 when phase 3 was excluded from the calculations. *Elphidium excavatum* displayed D_{TE} values > 1 for Cr and Cu for the calculations with phase 3 and also for Pb without phase 3. The highest variation between minimum and maximum D_{TE} for all species was found for Cd and Hg.

3.4 Discussion

3.4.1 Experimental Uncertainties

Calcein was used for staining the foraminiferal test before they were placed into the culturing system. It can be assumed, that a period of 1 or 2 days for removing excess calcein was sufficient because the youngest chambers were not stained. Calcein binds to Ca and is incorporated into the mineralised calcium carbonate (Bernhard et al., 2004). It is conceivable that the heavy metal incorporation could also be affected by calcein. However, no evidence for such effects has been found so far in a variety of studies (e.g., Hintz et al., 2006; De Nooijer et al., 2007; Dissard et al., 2009). Furthermore, calcein was only used prior to the experiment to mark the last chamber that was grown outside the culturing system. Therefore, the incorporation of the metals measured in subsequent chambers was not affected by the calcein application.

The element concentrations within the culturing medium of each culturing phase were comparably stable for most elements in the control system. In the metal system, the variations were higher, which is due to the punctual input of the multi metal stock solution for reaching the next phase concentration (Table A3.1, Fig. B3.1). This sudden addition of metals resulted in a high peak concentration in the beginning of the new phase, which equilibrated after a while. This trend was most pronounced in phase 3 as the added amount of the multi metal stock solution was highest for this phase, which was also why the standard error of this phase was comparably high. Furthermore, the variations of the metal concentrations were in a comparable range than those presented in other culturing studies (e.g., Marechal-Abram et al., 2004; De Nooijer et al., 2007; Munsel et al., 2010; Remmelzwaal et al., 2019). Generally, many other studies (e.g., Remmelzwaal et al., 2019; Sagar et al., 2021a; Titelboim et al., 2021) measured the heavy metal concentration in the seawater less frequently than done in this study. Therefore, the stability of metal concentrations during the culturing phases of those studies are often inferred. Furthermore, pollution events in nature are in most cases not persistent and stable but transient as was mirrored by the concentration changes in our experiments.

The measured metal concentrations in the culturing seawater were smaller than expected (Table 3.3). This in combination with the varying metal concentration within one phase suggested that several processes were affecting the concentration in such a complex culturing system. One possible mechanism was sorption of the metals onto surfaces (e.g., tubing, culturing vessels, plates, organic matter or the foraminiferal test itself), which could have lowered the metal concentration in the culturing medium. Therefore, sorption could have contributed to the overall budget of the metals. On the other hand, Cu appeared to have been released from components of the culturing system even though the system was cleaned before use and was operated with seawater for 14 days before the experiments begun. For instance, the concentration of Cu was high in phase 0, where no metals were added suggesting release from system parts. In phase 1, the Cu concentration decreased meaning the contamination derived from the system was removed by a process similar to that observed for the other metals after additions were made. Similar effects have been reported by De Nooijer et al. (2007) for Cu and Havach et al. (2001) for Cd. Other processes like the uptake of the metals by the foraminifera itself and the growth of algae could further have an influence on the metal concentration in the culturing medium. Germs of algae were introduced accidentally together with the living foraminifera and grew during the experiment. Such processes are difficult to predict and even more challenging to avoid but probably mirror real environments more realistically than sterile petri dish experiments (e.g., Havach et al., 2001; Hintz et al., 2004; Munsel et al., 2010).

Neither the survival rate nor the formation of new chambers was influenced by the elevated metal concentrations during the culturing period. These features were rather constant between the four different phases. Furthermore, no test morphology malformations were recognised. Elevated heavy metal concentrations are thought to induce a higher rate of malformations in benthic foraminifera (e.g., Sharifi et al., 1991; Yanko et al., 1998), whereas recent studies constrained them as a reaction to stressful environments, not necessarily created by high heavy metal concentrations (Frontalini and Coccioni, 2008; Polovodova and Schönfeld, 2008). The lack of malformations in our experiments suggested that the foraminifera were neither poisoned by elevated heavy metal concentrations nor stressed too much by strongly varying environmental parameters, maintaining a normal metabolism and growth. Reproduction was generally very rare, which may indicate that the conditions were not ideal. In field studies foraminiferal reproduction has been linked to short periods of elevated food supply (e.g., Lee et al., 1969; Gooday, 1988; Schönfeld and Numberger, 2007). The regular feeding of foraminifera in our experiment twice a week at constant rates therefore probably did not provide supply levels that trigger reproduction. Nevertheless, it can be assumed that a sufficient amount of food was provided because after the experiments, leftovers covering the sediment surfaces in the cavities were evident. This would have likely been consumed by the foraminifera if they would have needed more. Furthermore, the foraminifera calcified, which would not be the case if any malnourishment occurred (e.g., Lee et al., 1991; Kurtarkar et al., 2019). Therefore, the nutritional status is unlikely to have influenced the metal uptake by the foraminifera.

The calibrations between the heavy metal concentration in seawater and the foraminiferal shell rely on the TE/Ca values from phase 3 because the difference in seawater concentration was highest compared to other phases. Nevertheless, data points from other phases do play a role and forcing through the origin adds a further fixed point. High variability for D_{TE} values like observed here for Cd or Cu is difficult to explain. Such variability suggests there are factors affecting these metals we do not understand and therefore it is also important to show the data for these elements. Furthermore, the experimental design, especially the mixture of metals, was chosen to best simulate metal conditions in real environments, which could naturally enhance the variability of D_{TE}. This knowledge is indispensable for the application of heavy metal concentrations in foraminifera as a proxy for the heavy metal concentration in seawater.

3.4.2 Incorporation of heavy metals in the foraminiferal test

Many heavy metals have been demonstrated to be incorporated into the foraminiferal shell (e.g., Cr: Remmelzwaal et al., 2019; Mn: Koho et al, 2015; 2017; Barras et al., 2018; Cu: De Nooijer et al., 2007; Ni: Munsel et al., 2010; Hg: Frontalini et al., 2018a; Cd: Havach et al., 2001; Pb: Frontalini et al., 2018b; Titelboim et al., 2018; Sagar et al., 2021a; 2021b; Zn: Marchitto et al., 2000; Van Dijk et al., 2017), and the incorporation of all of these metals has been measured here. Additionally, to the best of our knowledge, Sn and Ag were investigated here for the first time. The levels observed were well above control values indicating an elevated incorporation of Ag and Sn into the foraminiferal test calcite with increasing metal concentrations in seawater.

Different factors can influence the incorporation of these metals into the foraminiferal test. First of all, the uptake depends on metabolic pathways during the calcification process. Fundamental biomineralization processes of foraminifera are the subject of an ongoing discussion and several (partly) competing models have been proposed (e.g., Elderfield and Erez, 1996; Erez, 2003; De Nooijer et al., 2009b, 2014; Nehrke et al., 2013). One model proposes that the foraminifera take up ions directly from the surrounding seawater by endocytosis or by building seawater vacuoles, which are transported to the site of calcification (SOC) (Elderfield and Erez, 1996; Erez 2003; De Nooijer et al., 2009b; 2009a; Khalifa et al., 2016). The SOC is located outside the foraminiferal cell and the formation of new calcite takes place in this zone (see De Nooijer et al., 2014 for a summary and illustration). There is evidence that this SOC is separated from the surrounding seawater (e.g., Spindler, 1978; Bé et al., 1979; De Nooijer et al., 2009b; 2014; Glas et al., 2012; Nehrke et al., 2013). The other competing model suggests that the uptake of ions and the transport to the SOC is performed directly from the seawater across the cell membrane by active trans-membrane-transports (TMT) and/ or passive transport via gaps in the pseudopodial network of the foraminifera (Nehrke et al., 2013; De Nooijer et al., 2014). The dependence of heavy metal concentrations in the foraminiferal test on their seawater concentration relies on the prevailing mechanism. Biomineralization based on endocytosis would infer that the metal concentration in the seawater is directly mirrored by their concentration in the foraminiferal shell, which is not generally supported by the results of our study except for Ag and Pb. Several metals showed partition coefficients > 1 or < 1 when the D_{TE}´s were calculated separately for each culturing phase. Only Pb and Cr in *E. excavatum* and Cu and Pb in *A. aomoriensis* consistently displayed mean D_{TE}´s > 1 paired with a positive correlation of the concentration in seawater and in the foraminiferal shell, which could indicate a non-selective uptake of these metals meaning uptake not only driven by the chemical properties of the ion such as the size of the metal ion itself. If this would have been the case, D_{TE} values > than 1 would be expected especially for metals ions that are smaller than Ca (Rimstidt et al., 1998). On the other hand, the D_{TE} values of many elements (Ni, Zn, Cd, Hg, Pb) dramatically decreased with increasing concentration in the seawater in the highest metal treatment in all species (Fig. 3.4). This kind of overload effect has also been noted by Nardelli et al. (2016) for Zn, by Barras et al. (2018) for Mn, by Mewes et al., (2015) for Mg and by Munsel et al. (2010) for Ni. Nardelli et al. (2016) suggested that some biological mechanism expulse or block these metals if the concentration is too high and imminent intoxication is probable, which may be managed by controlling the ion uptake via TMT. Therefore, it may well be possible that the highest concentration of the metals in our study was close to the tipping point of the biological mechanism taking over and protecting the organism.

Besides biologically controlled factors, physicochemical properties also play an important role when it comes to the uptake of ions. One chemical factor is the aqueous speciation and solubility of the metals. Metals with a free ion form with a charge of 2+ are more similar to Ca^{2+}, which makes incorporation more likely (Railsback, 1999). Nearly all metals in this study were added as dissolved chlorides and therefore had a charge of 2+. The only exceptions were Ag, which was added as $AgNO_3$ with a charge of 1+ and Cr, which was added as $CrCl_3$*6 H_20. The charge of the cation as such does not seem to make a major difference as Ag was incorporated into all three species and Cr into *E. excavatum* with a significant positive correlation to concentrations in the culturing medium. Furthermore, it is possible that the oxidative state of the elements changed due to their pH dependency, which will be discussed for every element separately. Furthermore, other ions with a charge of 1+ are also known to be incorporated in calcite. Examples are Li^+ (e.g., Delaney et al., 1985; Hall et al., 2004) and Na^+ (e.g., Wit et al., 2013; Bertlich et al., 2018), which are believed to occupy interstitial positions in calcite where the calcite lattice has defects (Ishikawa and Ichikuni, 1984; Okumura and Kitano, 1986). In addition, rare earth elements with a charge of 3+ are also detected in the foraminiferal calcite (e.g., Haley et al., 2005; Roberts et al., 2012).

The aqueous speciation of many metals is strongly influenced by the pH (e.g., Förstner, 1993; Pagnanelli et al., 2003; Spurgeon et al., 2006; Powell et al., 2015; Huang et al., 2017). As the pH during the experiment was stable around 8.0 ± 0.1 (measured twice a week), speciation changes between phases due to varying pH values can be excluded. However, it is possible that some metals were not available in a form that could be readily incorporated in the calcite such as the free ion or carbonate species. Cr was not available in an optimal speciation to substitute Ca as a pH of 8 would favour Cr^{3+} or Cr^{4+} as well as oxides and hydroxides (Elderfield, 1970; Geisler and Schmidt, 1991). Furthermore, the used Cr-salt may not have dissolved completely, even though the multi metal stock solution was heated and stirred during the process. Both in combination may lead to the small variation in the seawater concentrations between the different phases. Interferences that could possibly have influenced the Cr measurements in the water samples are chlorine oxides or hydroxides (e.g., Tan and Horlick, 1986; McLaren et al., 1987, Reed et al., 1994; Laborda et al., 1994). Measurements of reference materials revealed slightly elevated Cr concentrations compared to those presented in the literature (Table A3.2), which indicates that interferences could be responsible for some of the observed variability for Cr. Similar pH dependant processes could also have affected Cu. Nevertheless, Cu and Cr were taken up by all species and therefore, this factor cannot be decisive when it comes to incorporation of these metals into the foraminiferal shell.

If the incorporation of metals would be straightforward and would only depend on the speciation of the metal and other physicochemical factors, the behaviour of the metals would mostly be influenced by the ionic radius in combination with the charge of the metal ions as described for carbonate minerals by Rimstidt et al. (1998). The endocytotic pathway of seawater into the foraminifer should produce a behaviour of ion incorporation comparable to inorganic calcite precipitation. It was found that cations are incorporated into inorganic calcite by substitution of Ca^{2+} (e.g., Reeder et al., 1999), especially when the effective ionic radius of these ions is comparable to the one of calcium (= 1.0 Å).

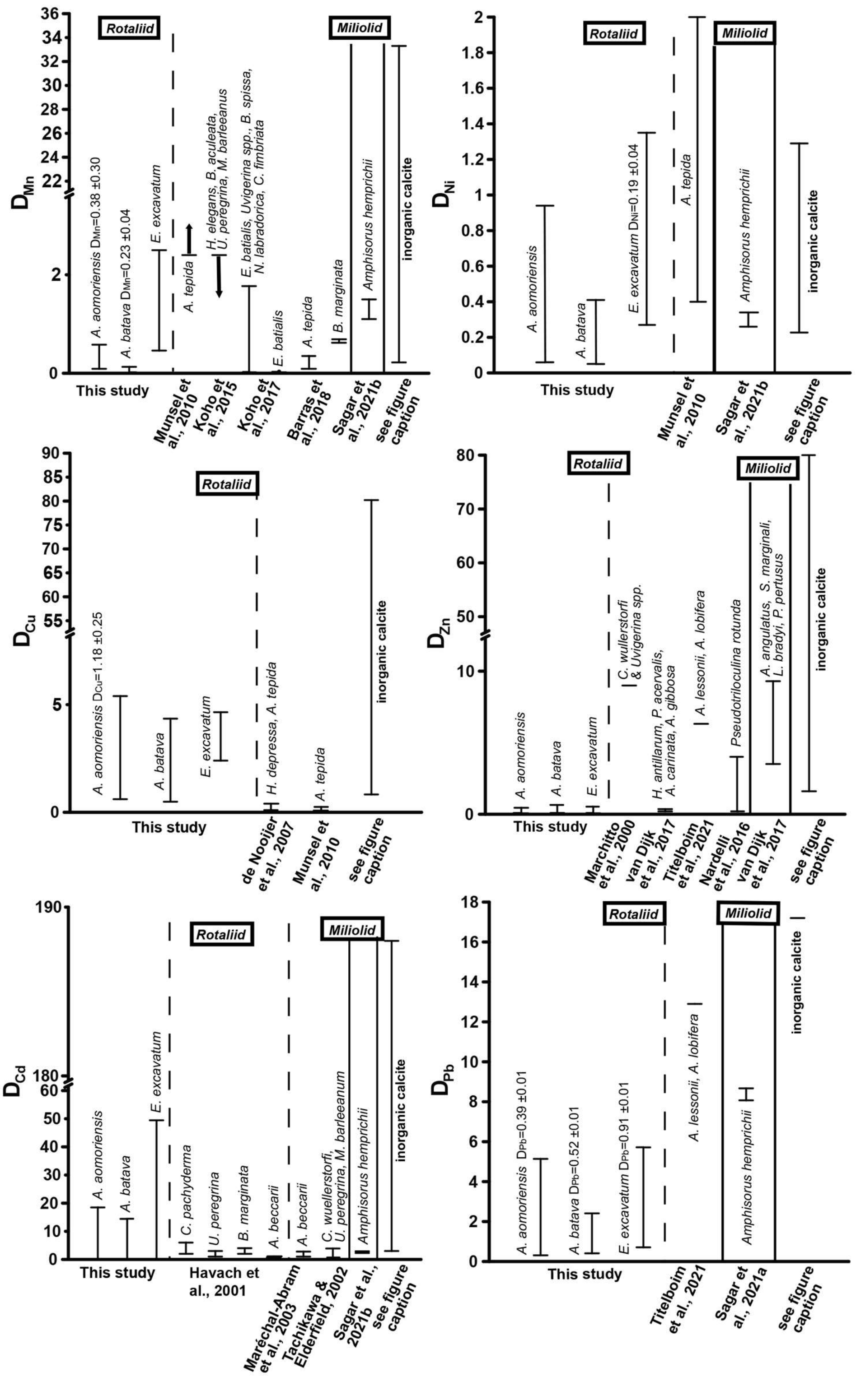

Figure 3.5: Comparison of D_{TE} values of this study with D_{TE} values from literature of different rotaliid and miliolid foraminiferal species. The range of D_{TE} based on the different culturing phases is given and if a correlation between the heavy metal concentration in seawater and the foraminiferal shell was detected, the mean D_{TE} value ±SD (=slope of the regression line) is also indicated. Note that the x-axis was clipped for some elements. (Literature for inorganic calcite D_{TE} values: Ni = Rimstidt et al., 1998; Alvarez et al., 2021; Mn = Lorens, 1981; Dromgoole and Walter, 1990; Wang et al., 2021; Cu =Kitano et al., 1973; 1980; Wang et al, 2021; Zn =

Kitano et al., 1973; 1980; Rimstidt et al., 1998; Wang et al., 2021; Cd = Rimstidt et al., 1998; Day and Henderson, 2013; Pb = Rimstidt et al., 1998.)

Some metals like Mn, Zn and Cu are known to be fundamentally necessary as micro-nutrients to maintain biological and physiological function of a cell (e.g., Mertz, 1981; Tchounwou et al., 2012; Martinez-Colon et al., 2009; Maret, 2016). Therefore, these elements should preferentially be taken up into the foraminiferal cell, where they are used for further processes. This in turn could lead to the consumption of these metals before they can be incorporated into the foraminiferal tests. The artificial sea salt used in this study ensured that these elements were present in a sufficient amount of micronutrients. All of these ions have a similar ionic radius (Cu = 0.73 Å, Mn = 0.67 Å, Zn = 0.74 Å) in six-fold coordination (Rimstidt et al., 1998), which would also suggest, that their behaviour is comparable. The ionic radii are much smaller than that of Ca, but are rather similar to Mg (0.72 Å, Rimstidt et al., 1998).

Mn showed a positive correlation between its concentration in seawater and the foraminiferal test in the two *Ammonia* species when the calculations included phase 3. This indicates that this element serves as a well-behaved proxy influenced mainly by its concentration in seawater. However, *E. excavatum* did not show this positive correlation. D_{Mn} values of this study were comparable with rotaliid and miliolid species and partly with D_{Mn} values from inorganic precipitation (Fig. 3.5). Species-specific partition coefficients of elements like Mg or Na are already reported in the literature (e.g., Toyofuku et al., 2011; Barras et al., 2018; Wit et al., 2013) and could also explain the different D_{TE} values of *E. excavatum* in this study (see below). Furthermore, it is known that the presence of toxic metals such as Cd, Ni or Hg can inhibit the uptake of essential metals like Mn into the cell if these metals are present in low concentrations (e.g., Sunda and Huntsman, 1998a, 1998b). It is possible that this mechanism is more pronounced in *E. excavatum* than in the *Ammonia* species. Zn was clearly incorporated above control levels into all three species, but it´s behaviour was influenced by more factors than the concentration of Zn in the culturing medium (Fig. 3.4, Table 3.4). D_{Zn} values of this study are in good agreement with those calculated by Van Dijk et al. (2017) for four hyaline species and Nardelli et al. (2016) for the miliolid *Pseudotriloculina rotunda* (Fig. 3.5) Other studies reported higher values. It is again possible that the mixture of metals inhibited the uptake of essential metals like Zn similar to Mn. Cu showed a simple well-behaved proxy behaviour with a significant positive correlation in *A. aomoriensis* but not in the other two species. The D_{Cu} presented in the literature for rotaliid species are lower than D_{Cu} from this study. Inorganic values were mostly higher (Fig. 3.5). These differences could arise from the lower concentration of Cu in this study or from the mixture of metals. It is also reported, that the exposure to more than one metal can cause an increased uptake of another metal into the cell (Archibald and Duong, 1984; Martinez-Finley et al., 2012; Bruins et al., 2000; Shafiq et al., 1991). If more Cu is taken up into the cell after the usage of Cu as micronutrient more Cu is left over and could possibly be deposited into the calcite. It is therefore conceivable that one particular metal in our study was effecting a co-uptake of Cu, which lead to an elevated incorporation into the calcite as compared to other studies.

The non-essential elements Hg, Cd and Pb are not used in physiological processes and are therefore believed to have a higher toxic potential (Barbier et al., 2005; Raikwar et al, 2008; Ali and Khan, 2019). This could first of all make the foraminifera prevent the uptake of these metals into their cell. But if the uptake of heavy metals into the cell cannot be prevented, the foraminifera may remove the metals to their shell instead of keeping them in their cell. This is a common mechanism for avoiding intoxication reported for various organisms (benthic foraminifera: Bresler and Yanko, 1995; Yeast: Adle et al., 2007; Bacteria: Shaw and Dussan, 2015; Microalgae: Duque et al., 2019). Furthermore, this would mean thatthe incorporation of these metals into the foraminiferal calcite increases. The ionic radii of Pb^{2+} in calcite-coordination is 1.19 Å, which is remarkably higher than those of Hg^{2+} (1.02 Å) and Cd^{2+} (0.95 Å), which are comparable to Ca.This similarity should also favour the incorporation of Cd and Hg into calcite, which holds only partly true, as Cd showed no trends with complex behaviour, but Hg was linearly incorporated in *A. batava* and in *E. excavatum* if the high concentrations of phase 3 are excluded. Pb emerged as a well-behaved proxy under these experimental conditions with all three species incorporating Pb linearly (Fig. 3.4, Table 3.4). When comparing D_{Pb} values in the literature, our D_{Pb} are slightly lower (Fig. 3.5). For Hg, no partition coefficients were published so far. D_{Cd} values from different studies (Havach et al., 2001; Tachikawa and Elderfield, 2002; Maréchal-Abram et al., 2004, Sagar at al., 2021b) have overall a smaller range of D_{Cd} values than found here (Fig. 3.5). The greater variability in D_{Cd} of our study makes a comparison difficult.

The importance of other metals like Sn, Cr, Ag and Ni is not fully understood yet but some of them are believed to have certain biological functions in the cells of animals or plants (Horovitz, 1988; Mertz, 1993; Lukaski, 1999; Pilon-Smits et al., 2009; Hänsch & Mendel, 2009; Chen et al., 2009). For example, Ni is important for plants and bacteria (Poonkothai and Vijayavathi, 2012; Maret, 2016). The ionic radii of these metals in calcite-coordination is rather different (Sn = 1.18 Å; Ag = 1.15 Å; Cr = 0.62 Å; Ni = 0.69 Å) and deviate from the ionic radius of Ca^{2+}, too.

Ni was incorporated with a positive trend in *E. excavatum,* but with no clear trend in the *Ammonia* species (Fig. 3.4, Table 3.4). D_{Ni} values from rotaliid and miliolid foraminifera and from inorganic calcite are in good agreement with our results (Fig. 3.5). Ag exhibited a strong positive correlation between seawater and foraminiferal shell in all three foraminiferal species. Partition coefficients for Ag (*A. aomoriensis* $D_{Ag} = 0.50 \pm 0.02$, *A. batava* $D_{Ag} = 0.17 \pm 0.01$, *E. excavatum* $D_{Ag} = 0.47 \pm 0.04$) cannot be compared to other studies as no literature data are available.

Cr and Sn, on the other hand, were not incorporated in a higher amount when the concentration of these metals in the culturing medium was raised, except for Cr in *E. excavatum*, which showed a positive correlation. The D_{Cr} values presented in Remmelzwaal et al. (2019) ($D_{Cr} > 107$), based on culturing experiments with the tropical, symbiont bearing foraminifera *Amphistegina spp.,* are at least one order of magnitude higher than D_{Cr} values in this study (*A. aomoriensis* D_{Cr} = 0.74-10.3, *A. batava* D_{Cr} = 0.4-6.8, *E. excavatum* $D_{Cr} = 2.1 \pm 0.28$). One possible reason for dynamics of Cr are the comparable low concentrations in the culturing medium and furthermore, the differences between the phases were also very low (Fig. 3.3, Fig.

B3.1 and Table 3.3). It may be that the concentration of Cr needs to be further elevated and the concentration range needs to be extended before the foraminifera are able to incorporate Cr with significant differences between concentrations. For Sn, no comparative studies are available so we may speculate that the same could apply for Sn. Nevertheless, we recognised a correlation between the concentration of Cr in the culturing medium and in the foraminiferal calcite of *E. excavatum*, but not for both *Ammonia* species.

3.4.3 Interspecies variability

The three different species cultured in this study clearly incorporated the same metal in different ways, which is most visible in the overall higher TE/Ca values of *E. excavatum* compared to species from the genus *Ammonia* (Fig. 3.4 and 3.5, Table 3.4). Koho et al. (2017) suggested that these differences in the incorporation result from different microhabitats used by different foraminiferal species. This might be true in nature. In our experiments, however, the sediment in the cavities was only a few mm thick and no redox horizon was recognised when recovering the foraminifera after the experiment. Therefore, all foraminifera were living in the same microhabitat. Leftover food may have created a microhabitat but this effect would have been the same in all cavities and therefore cannot account for the differences between the species. In our experiment, dead *Nannochloropsis* were fed, which is certainly not the preferred food source for *E. excavatum* (Pillet et al., 2011). This could lead to a slower growth and *E. excavatum* built on average only 1 chamber during the individual culturing period of 21 days while *Ammonia* species built more than four chambers. Furthermore, *E. excavatum* did not reproduce, even though the culturing period is close to the generation time of this species (Haake, 1962). When growth is slower, it could be possible that a higher amount of a metal is incorporated into the shell, which would lead to higher TE/Ca values in this species. It is possible that a more preferred food source would have stimulated enhanced growth and influenced the incorporation of heavy metal into the shells of *E. excavatum*. For instance, the closely related species *E. clavatum* prefers bacillariophycean diatoms (Schönfeld and Numberger, 2007). It may also be possible that *E. excavatum* is simply a slower growing species than *Ammonia*, which seems not to be necessarily connected to a specific food source (e.g., Haynert et al., 2020). One could assume that a slower growth would provide more time to remove potentially toxic metals from the cell to the foraminiferal shell, which could explain why *E. excavatum* incorporated a higher metal concentration than *A. aomoriensis* and *A. batava*.

Another possibility for the higher metal concentration found in *E. excavatum* is the timing of chamber formation. As *E. excavatum* formed on average one new chamber, it is possible that this chamber was formed during the high peak in the metal concentration during the beginning of the culturing phases (Fig. B3.1, Table A3.1). This could in turn lead to a higher uptake of the metals and apparently higher D_{TE} values. Both *Ammonia* species on the other hand, formed more chambers, which makes it most likely that the first high concentrations did not particularly influence the overall D_{TE} value. Unfortunately, it is not possible to constrain exactly when the specimens formed their new chambers. It was checked whether the evolution of the metal concentration in seawater of phase 3 was reflected in the intra-test (chamber to chamber) data for the two *Ammonia* species. Particularly, the initial high concentration of certain heavy metals was found in the first chambers of very few individuals after the staining (i.e. the first chamber built in culture). This is most likely due to the individual timing of calcification. Furthermore, it could also be possible that the foraminifera did not calcify during the first high peak due to an initial intoxication. Therefore, a mean value over the whole culturing phase was considered as most representative.

Comparing *Ammonia* and *Elphidium* species showed that the D_{TE} of the *Ammonia* species of this study are partly comparable to literature data (Fig. 3.5).

D_{TE} values are known to be generally higher in tropical high-Mg calcite taxa like *Amphistegina* (e.g., Titelboim et al., 2021) and also high-Mg miliolid taxa like *Amphisorus* (e.g., Sagar et al., 2021a) incorporate a higher amount of metals compared to rotaliid low-Mg taxa like *Ammonia* or *Elphidium*. Comparing our data with high-Mg species, it is visible that this trend can be partly confirmed (Fig. 3.5). For Mn, both *Ammonia* species of this study show lower values than miliolid species but D_{Mn} of *E. excavatum* is comparable. D_{Ni} values of *A. hemprichii* determined by Sagar et al. (2021b) display the same range as the values for low-Mg species here and furthermore D_{Zn} values of the miliolid *P. rotunda* (Nardelli et al., 2017) overlap with our findings. On the other hand, D_{Zn} values from miliolids in van Dijk et al., (2017) and high-Mg rotaliids from Titelboim et al. (2021) are much higher. The same trend is observed for D_{Pb} (Titelboim et al., 2021; Sagar et al., 2021a). When comparing the Zn/Ca concentration in the foraminiferal shell directly to values from Titelboim et al. (2018), who analysed the Cu, Zn and Pb concentration in rotaliid and miliolid species from a field site, our values show similarities with both groups. Zn/Ca in the foraminiferal calcite of our study was a maximal ~ 68 µmol/mol, which is slightly lower than reported in Titelboim et al. (2018) for the low-Mg species *Pararotalia calcariformata* (195 µmol/mol), but much lower than Zn/Ca reported for the high-Mg species *Lachlanella* (2540 µmol/mol). Differences between the low-Mg species may be due to different concentrations in the seawater the foraminifera grew in. As the seawater metal concentration is not given in Titelboim et al. (2018) this cannot be evaluated. It may also be possible hat high-Mg species have more defects in their tests, which would result in more interstitial space, leading to more space for ions other than Ca. Maximum Cu/Ca values of our study are ~ 23 µmol/mol in *E. excavatum*, which fits the findings of Titelboim et al. (2018) for rotaliid species (*P. calcariformata* ~21 µmol/mol) and is lower than in high-Mg species (*Lachlanella* ~ 186 µmol/mol). Pb/Ca of ~ 12 µmol/mol in *P. calcariformata* described by Titelboim et al. (2018) are lower than found here (max. Pb/Ca in *E. excavatum* of this study ~ 53 µmol/mol), whereas our findings are more comparable to *Lachlanella* (Pb/Ca ~ 125 µmol/mol).

3.5 Conclusion

Culturing experiments with different foraminiferal species (*A. aomoriensis*, *A. batava* and *E. excavatum*) that were exposed to a mixture of ten different metals (Cr, Mn, Ni, Cu, Zn, Ag, Cd, Sn, Hg and Pb) at varying concentrations (Table 3.3, Fig. 3.3, Fig. B3.1) were carried out and laser ablation ICP-MS analysis of the newly formed calcite revealed the following:

1. All metals used in this study were incorporated into the foraminiferal calcite of all three species (Fig. 3.4, Table 3.4).

2. Species-specific differences in the incorporation of heavy metals occurred.
3. The following metals showed a positive correlation between the metal concentration in seawater and the foraminiferal calcite inferring that the uptake of these metals mainly depends on its concentration in seawater:
    a. *Ammonia aomoriensis*: D_{Mn} = 0.38 ±0.3, D_{Cu} = 1.18 ±0.25, D_{Ag} = 0.50 ±0.02, D_{Pb} = 0.39 ±0.01
    b. *Ammonia batava*: D_{Mn} = 0.23 ±0.04, D_{Ag} = 0.17 ±0.01, D_{Hg} = 0.003 ±0.001; D_{Pb} = 0.52 ±0.01
    c. *Elphidium excavatum*: D_{Cr} = 2.1 ±0.28, D_{Ni} = 0.19 ±0.04, D_{Ag} = 0.47 ±0.04, D_{Pb} = 0.91 ±0.01
4. Other metals like Zn, Sn and Cd showed no clear correlation between seawater and calcite, which may be linked to the mixture of metals leading to synergetic effects.
5. D_{TE} values of Ni, Zn, Cd, Hg and Pb decreased with increasing heavy metal concentration in the seawater, which may be evidence for an early protective mechanism, prior to damage, reduced growth or death of the organism.

The results of this study facilitate the determination of variations in the heavy metal concentration in seawater for elements showing a correlation between TE/Ca ratios in calcite and seawater (*A. aomoriensis* = Mn, Cu, Ag, Pb; *A. batava* = Mn, Ag, Hg, Pb; *E. excavatum* = Cr, Ni, Ag, Pb). Such estimates can be based on foraminiferal samples from the fossil sediment record and recent surface sediments. This facilitates monitoring of anthropogenic footprints on the environment today and in the past. Foraminifera offer the opportunity of long- and short-term monitoring of the heavy metal concentration because they are storing environmental signals over a period of time and not only at one point in time.

3.6 Appendix

3.6.1 Appendix A: Additional Tables

Table A3.1: TE/$Ca_{Seawater}$ values from single weeks during the culturing period of the metal system. Measurements were carried out with ICP-MS. These values are the basis for the calculations of the mean TE/Ca values in Table 3.3 and for figure B3.1.

Metal System			Sampling date	Cr/Ca	Mn/Ca	Ni/Ca	Cu/Ca	Zn/Ca	Ag/Ca	Cd/Ca	Sn/Ca	Hg/Ca	Pb/Ca
	Phase	Day		µmol mol^{-1}	µmol mol^{-1}	µmol mol^{-1}	µmol mol^{-1}	µmol mol^{-1}	µmol mol^{-1}	µmol mol^{-1}	µmol mol^{-1}	nmol mol^{-1}	µmol mol^{-1}
FR0 W2	0	10	10.2.20	12.80	818.54	7.60	27.75	100.19	0.16	0.44	3.20		0.63
FR0 W3	0	17	19.2.20	3.16	858.94	7.23	3.74	107.69	0.05	0.43	2.94	5.28	0.43
FR1 W1	1	2	27.2.20	13.59	862.52	7.08	6.25	97.45	0.37	1.00	4.98	43.07	1.03
FR1 W2	1	9	5.3.20	5.86	796.65	6.69	2.23	93.09	0.04	1.06	3.87	19.13	0.69
FR1 W3	1	13	9.3.20	7.03	819.38	6.86	2.14	95.50	0.06	1.08	4.23	27.17	0.62
FR1 W4	1	20	16.3.20	7.75	844.23	7.94	2.77	95.75	0.11	1.19	4.11	60.20	0.68
FR2 W1	2	2	19.3.20	13.68	825.59	10.02	4.15	129.09	1.88	5.20	5.37	933.50	5.70
FR2 W2	2	8	26.3.20	16.49	820.63	9.75	2.78	134.85	0.41	4.96	5.46	494.26	3.07
FR2 W3	2	15	2.4.20	13.31	811.64	9.44	2.23	132.12	0.31	4.89	5.10	287.70	2.50
FR2 W4	2	19	6.4.20	15.47	789.96	9.77	2.23	135.50	0.33	4.75	5.19	210.66	2.20
FR3 W1	3	2	9.4.20	52.74	1558.73	74.72	15.89	772.38	31.53	87.65	18.31	6123.75	125.25
FR3 W2	3	7	14.4.20	39.90	1281.58	46.73	3.67	455.31	7.95	61.37	11.84		70.27
FR3 W3	3	16	23.4.20	26.97	1469.59	66.07	3.55	579.52	4.13	84.82	5.87	2858.26	53.51
FR3 W4	3	20	27.4.20	25.59	1397.18	65.00	3.01	550.78	4.31	84.23	5.02	1640.01	45.72

Table A3.2: Average concentration, RSD (1σ in %), literature values, accuracy in comparison to literature values and number of measurements of the reference materials SLRS-6, SLEW-3, in-house reference materials (South Atlantic surface water and South Atlantic Gyre water) and NASS-6 measured with ICP-MS. Average concentration, RSD and accuracy values displayed here are averaged from single measuring days. Cr values are analysed after dilution of the samples and all other elements were analyses after preconcentration with a SeaFAST system. NRCC – National Research Council Canada. *Values originated from 1:10 dilution of SLRS-6.

Reference Materials	Cr	Mn	Ni	Cu	Zn	Cd	Pb
SLRS-6	**nmol kg^{-1}**	**nmol kg^{-1}**	**nmol kg^{-1}**	**nmol kg^{-1}**	**nmol kg^{-1}**	**nmol kg^{-1}**	**nmol kg^{-1}**
Average conc.	4732	52956	9811	338014*	31391*	62	786
RSD%	3.5	3.9	6.0	1.7*	7.2*	12.8	0.8
Yeghicheyan et al., 2019	4509	38616	10496	376378*	26920*	56	820
Accuracy	0.96	0.74	1.08	1.11*	0.86*	0.90	1.04
Number	4	11	11	13*	13*	7	7
SLEW-3							
Average conc.		40007	17508	22907	4442	343	
RSD%		4.3	3.5	4.2	9.1	4.8	
Leonhard et al., 2002		29326	20958	24409	3074	427	

Accuracy		0.74	1.21	1.07	0.78	1.28
Number		12	12	12	12	12
South Atlantic Gyre water						
Average conc.		1615	2189	2649	5614	
RSD%		6.2	3.7	5.3	13.2	
Number		10	10	10	10	
South Atlantic surface water						
Average conc.		1959	2417	2646	39718	
RSD%		6.8	2.8	5.8	2.2	
Number		6	6	6	6	
NASS-6						
Average conc.	6747	11162	3557	5206	5158	169
RSD%	15.9	5.2	3.2	3.0	25.3	7.0
NRCC	2293	9654	5129	3528	3931	165
Accuracy	0.34	0.87	0.76	0.35	0.81	0.98
Number	9	11	11	11	11	2

Table A3.3: Average concentration, RSD (1 σ in %), literature values, accuracy in comparison to literature values and number of measurements of the reference materials, NIST SRM 614, JCt-1, JCp-1, MACS-3 and ECRM752-1 measured with LA-ICP-MS. Please note that for the ECRM752-1 no reported values for the elements of interest are available, which is also the case for some elements in other reference materials. It is important to note that the Hg/Ca values in the NIST glasses are not reliable as Hg is volatile and most likely volatilized during the glass formation. Average concentration, RSD and accuracy values displayed here are averaged from single measuring days.

Reference materials	Cr/Ca	Mn/Ca	Ni/Ca	Cu/Ca	Zn/Ca	Ag/Ca	Cd/Ca	Sn/Ca	Hg/Ca	Pb/Ca
NIST SRM 614	µmol mol^{-1}	µmol mol^{-1}	µmol mol^{-1}	µmol mol^{-1}	µmol mol^{-1}	µmol mol^{-1}	µmol mol^{-1}	µmol mol^{-1}	nmol mol^{-1}	µmol mol^{-1}
Mean value	19.28	10.31	8.43	15.86	67.58	2.13	15.53	5.97	20.93	5.23
RSD%	10.57	4.47	4.66	3.03	2.44	4.92	5.69	2.98	20.69	1.98
Jochum et al., 2011	10.78	12.18	8.83	10.16	20.11	1.83	2.35	6.67		5.28
Accuracy	0.57	1.19	1.06	0.64	0.30	0.86	0.23	1.12		1.01
Number of spots	35	38	37	39	38	38	38	39	19	39
MACS-3	mmol mol^{-1}	mmol mol^{-1}	mmol mol^{-1}	mmol mol^{-1}	mmol mol^{-1}	mmol mol^{-1}	mmol mol^{-1}	mmol mol^{-1}	µmol mol^{-1}	mmol mol^{-1}
Mean value	0.21	0.97	0.093	0.17	0.13	0.065	0.041	0.042	5.11	0.026
RSD%	1.60	1.36	1.90	1.92	2.19	6.37	2.83	2.68	9.23	2.18
Jochum et al., 2019	0.23	0.99	0.10	0.19	0.20	0.054	0.051	0.049	5.41	0.031
Accuracy	1.13	1.02	1.09	1.11	1.50	0.84	1.24	1.15	1.07	1.16
Number of spots	45	45	44	46	46	42	46	46	44	46
JCt-1NP	µmol mol^{-1}	µmol mol^{-1}	µmol mol^{-1}	µmol mol^{-1}	µmol mol^{-1}	µmol mol^{-1}	µmol mol^{-1}	µmol mol^{-1}	nmol mol^{-1}	µmol mol^{-1}
Mean value	6.16	0.91	0.37	1.14	1.46	0.01	1.60	2.30	8.93	0.063
RSD%	14.25	15.59	9.56	7.44	10.37	6.57	11.75	5.06	23.95	5.86
Jochum et al., 2019	0.93	1.01	1.03	1.48						0.064

Accuracy	0.15	1.19	2.71	1.31						1.04
Number of spots	44	38	45	47	45	11	46	13	26	48
JCp-1NP	µmol mol^{-1}	µmol mol^{-1}	µmol mol^{-1}	µmol mol^{-1}	µmol mol^{-1}	µmol mol^{-1}	µmol mol^{-1}	µmol mol^{-1}	nmol mol^{-1}	µmol mol^{-1}
Mean value	9.61	2.11	0.50	0.84	1.81	0.02	0.98	0.06	8.25	0.13
RSD%	7.91	4.62	6.89	6.36	6.53	11.34	11.08	10.68	20.96	6.15
Jochum et al., 2019	1.27	2.16	1.05	1.29	3.53					0.15
Accuracy	0.15	1.06	2.10	1.25	1.96					1.19
Number of spots	37	41	41	40	41	21	36	30	21	47
ECRM752-1	µmol mol^{-1}	µmol mol^{-1}	µmol mol^{-1}	µmol mol^{-1}	µmol mol^{-1}	µmol mol^{-1}	µmol mol^{-1}	µmol mol^{-1}	nmol mol^{-1}	µmol mol^{-1}
Mean value	14.75	144.44	3.87	2.34	8.40	0.01	1.54	0.04	19.14	0.86
RSD%	7.78	2.54	4.97	6.21	2.37	87.11	7.76	9.22	18.03	3.82
Number of spots	27	31	26	28	27	15	29	24	19	31

Table A3.4: Comparison of the heavy metal concentrations in seawater of different regions of the world to values used for the culturing experiments in this study. It is indicated whether the values of this study are comparable to environmental values or if values from this study are higher or lower. EPA = Environmental Protection Agency, USA, FI = Field Injection, SF-ICP-MS = Sector Field Inductively Coupled Plasma Mass Spectrometry, GF = Graphite Atomic, (F)AAS = (Flame) Graphite Atomic Absorption Spectrometry, APDC-MIBK = Ammonium Pyrrolidine Dithiocarbamat-Methyl Isobutyle Ketone, ASV = Anodic Stripping Voltammetry, AES = Atomic Emission Spectrometry, CVAFS = Cold Vapor Atomic Fluorescence Spectrometry, FPD = Flame Photometric Detector.

Element	Study area	Concentration in µg l^{-1}	Comparable?	Reference	Pretreatment + measurement technique
Ag		0.06-4.61		**This study**	Dilution + ICP-MS
	EPA Recommended Values (acute)	1.9	yes	Prothro, 1993	
	Restronguet Creek, U.K. + Adriatic Sea	0.0025-0.03	yes	Barriada et al., 2007	FI preconc.+ SF-ICP-MS
	Ibaraki coast + Watarase river	0.014-0.03	yes	Shijo et al., 1989	Solvent extraction, Microscale backextraction + GFAAS
Cd		0.14-30.61		**This study**	SeaFAST preconc. + ICP-MS
	EPA Recommended Values (chronic)	7.9	yes	Prothro, 1993	-
	Suva, Fiji	150-250	no, low	Arikibe and Prasad, 2020	FAAS
	Black Sea in Rize, Turkey	1-3	yes	Baltas et al., 2017	ICP-MS
	Gulf of Chabahar, Oman Sea	0.15-0.19	yes	Bazzi, 2014	APDC-MIBK procedure + FAAS
	Gulf of Kutch, Arabian Sea	200-1580	no, low	Chakraborty et al., 2014	AAS
	East London + Port Elizabeth harbours, U.K.	200-72600	no, low	Fatoki and Mathabatha, 2001	APDC-MIBK procedure + AAS

	Yalujiang Estuary, China	0.83-1.33	yes	Li et al., 2017	ICP-MS
	Gulf San Jorge, Argentina	0.01-0.09	yes	Muse et al., 1999	APDC-MIBK procedure + AAS
	Alang–Sosiya ship scrapping yard, Gulf of Cambay, India	34-560	yes	Reddy et al., 2005	APDC-MIBK procedure + FAAS
	Kamal estuary, Jakarta	0.01-0.02	no, high	Putri et al., 2012	AAS
	Jakarta Bay	0.04-0.104	yes	Williams et al., 2000	ASV
	Kepez harbor of Canakkale, Turkey	19-73800	yes	Yılmaz and Sadikoglu, 2011	Sample mineralization + ICP-AES
Cr		0.1-14.0		**This study**	Dilution + ICP-MS
	EPA Recommended Values (chronic)	50	no, low	Prothro, 1993	-
	Gulf of Chabahar, Oman Sea	20.16-21.46	yes	Bazzi, 2014	APDC-MIBK procedure + FAAS
	Gulf of Kutch, Arabian Sea	260-3010	no, low	Chakraborty et al., 2014	AAS
	Yalujiang Estuary, China	0.113-0.14	yes	Li et al., 2017	ICP-MS
	Gulf San Jorge, Argentina	0.04-0.5	yes	Muse et al., 1999	APDC-MIBK procedure + AAS
	Jakarta Bay	0.511-5.25	yes	Williams et al., 2000	ASV
	Alang–Sosiya ship scrapping yard, Gulf of Cambay, India	35-765	no, low	Reddy et al., 2005	APDC-MIBK procedure + FAAS
Cu		0.6-6.2		**This study**	SeaFAST preconc. + ICP-MS
	EPA Recommended Values (chronic)	3.1	yes	Prothro, 1993	-
	Suva, Fiji	880-10290	no, low	Arikibe and Prasad, 2020	FAAS
	Black Sea in Rize, Turkey	30-242	no, low	Baltas et al., 2017	ICP-MS
	Gulf of Chabahar, Oman Sea	3.37-5.74	yes	Bazzi, 2014	APDC-MIBK procedure + FAAS
	Gulf of Kutch, Arabian Sea	1350-1850	no, low	Chakraborty et al., 2014	AAS
	East London + Port Elizabeth harbours, U.K.	500-42600	no, low	Fatoki and Mathabatha, 2001	APDC-MIBK procedure + AAS
	Yalujiang Estuary, China	1.8-4.7	yes	Li et al., 2017	ICP-MS
	Gulf San Jorge, Argentina	0.02-0.65	yes	Muse et al., 1999	APDC-MIBK procedure + AAS
	Jakarta Bay	0.405-4.04	yes	Williams et al., 2000	ASV
	Alang–Sosiya ship scrapping yard, Gulf of Cambay, India	32-3939	yes	Reddy et al., 2005	APDC-MIBK procedure + FAAS
Hg		0.00035-0.273		**This study**	amalgamation + CVAFS
	EPA Recommended Values (chronic)	0.94	yes	Prothro, 1993	-
	South Florida Estuaries	0.0034-0.0074	yes	Kannan et al., 1998	amalgamation + CVAFS
	Guadalupe River and San Francisco Bay, California	0.0017-0.135	yes	Thomas et al., 2002	amalgamation + CVAFS

	Vembanad, India	0.0024-0.206	yes	Ramasamy et al., 2017	amalgamation + CVAFS
	Kamal estuary, Jakarta	0.1-0.2	yes	Putri et al., 2011	GFAAS
	Yalujiang Estuary, China	0.006-0.049	yes	Li et al., 2017	AFS
Mn		320-549		**This study**	SeaFAST preconc. + ICP-MS
	Black Sea in Rize, Turkey	3-14	yes	Baltas et al., 2017	ICP-MS
	Gulf of Chabahar, Oman Sea	15.43-24.76	no, high	Bazzi, 2014	APDC-MIBK procedure + FAAS
	Gulf of Kutch, Arabian Sea	13000-18000	no, low	Chakraborty et al., 2014	AAS
	East London + Port Elizabeth harbours, U.K.	300-23900	yes	Fatoki and Mathabatha, 2001	APDC-MIBK procedure + AAS
	Alang–Sosiya ship scrapping yard, Gulf of Cambay, India	31-4920	yes	Reddy et al., 2005	APDC-MIBK procedure + FAAS
Ni		2.3-24.3		**This study**	SeaFAST preconc. + ICP-MS
	EPA Recommended Values (chronic)	8.2	yes	Prothro, 1993	-
	Suva, Fiji	230-800	no, low	Arikibe and Prasad, 2020	FAAS
	Black Sea in Rize, Turkey	0.006-0.036	yes	Baltas et al., 2017	ICP-MS
	Gulf of Chabahar, Oman Sea	16.42-17.14	yes	Bazzi, 2014	APDC-MIBK procedure + FAAS
	Gulf of Kutch, Arabian Sea	190-330	no, low	Chakraborty et al., 2014	AAS
	Jakarta Bay	0.058-5.25	yes	Williams et al., 2000	ASV
	Alang–Sosiya ship scrapping yard, Gulf of Cambay, India	32-944	yes	Reddy et al., 2005	APDC-MIBK procedure + FAAS
Pb		0.11-28.35		**This study**	SeaFAST preconc. + ICP-MS
	EPA Recommended Values (chronic)	5.6	yes	Prothro, 1993	-
	Suva, Fiji	880-1770	no, low	Arikibe and Prasad, 2020	FAAS
	Black Sea in Rize, Turkey	6-130	yes	Baltas et al., 2017	ICP-MS
	Gulf of Chabahar, Oman Sea	4.24-4.25	yes	Bazzi, 2014	APDC-MIBK procedure + FAAS
	Gulf of Kutch, Arabian Sea	20-120	yes	Chakraborty et al., 2014	AAS
	East London + Port Elizabeth harbours, U.K.	600-16300	no, low	Fatoki and Mathabatha, 2001	APDC-MIBK procedure + AAS
	Yalujiang Estuary, China	0.4-1.8	yes	Li et al., 2017	ICP-MS
	Gulf San Jorge, Argentina	0.1-0.5	yes	Muse et al., 1999	APDC-MIBK procedure + AAS
	Alang–Sosiya ship scrapping yard, Gulf of Cambay, India	30-2036	yes	Reddy et al., 2005	APDC-MIBK procedure + FAAS
	Kamal estuary, Jakarta	1.3-4	yes	Putri et al., 2011	AAS
	Jakarta Bay	0.485-3.62	yes	Williams et al., 2000	ASV

	Kepez harbor of Canakkale, Turkey	49-9390	yes	Yılmaz and Sadikoglu, 2011	sample mineralization + ICP-AES
Sn		0.86-3.95		**This study**	Dilution + ICP-MS
	estuarine seawater, Galicia Coast, Spain	0.53-1.23	yes	Bermejo-Barrera et al., 1999	hydride generation + AAS
	U.S. and European rivers	0.0001-0.1	yes	Byrd and Andreae, 1982	hybride generation + FPD
Zn		30.0-226.9		**This study**	SeaFAST preconc. + ICP-MS
	EPA Recommended Values (chronic)	81	yes	Prothro, 1993	-
	Suva, Fiji	80-1450	yes	Arikibe and Prasad, 2020	FAAS
	Black Sea in Rize, Turkey	38-178	yes	Baltas et al., 2017	ICP-MS
	Gulf of Chabahar, Oman Sea	18.01-22.62	yes	Bazzi, 2014	APDC-MIBK procedure + FAAS
	Gulf of Kutch, Arabian Sea	11000-31000	no, low	Chakraborty et al., 2014	AAS
	East London + Port Elizabeth harbours, U.K.	500-27600	yes	Fatoki and Mathabatha, 2001	APDC-MIBK procedure + AAS
	Yalujiang Estuary, China	9.2-19.6	yes	Li et al., 2017	ICP-MS
	Gulf San Jorge, Argentina	0.01-0.55	no, high	Muse et al., 1999	APDC-MIBK procedure + AAS
	Jakarta Bay	2-30.1	yes	Williams et al., 2000	ASV
	Alang–Sosiya ship scrapping yard, Gulf of Cambay, India	33-5832	yes	Reddy et al., 2005	APDC-MIBK procedure + FAAS

3.6.2 Appendix B: Additional Figures

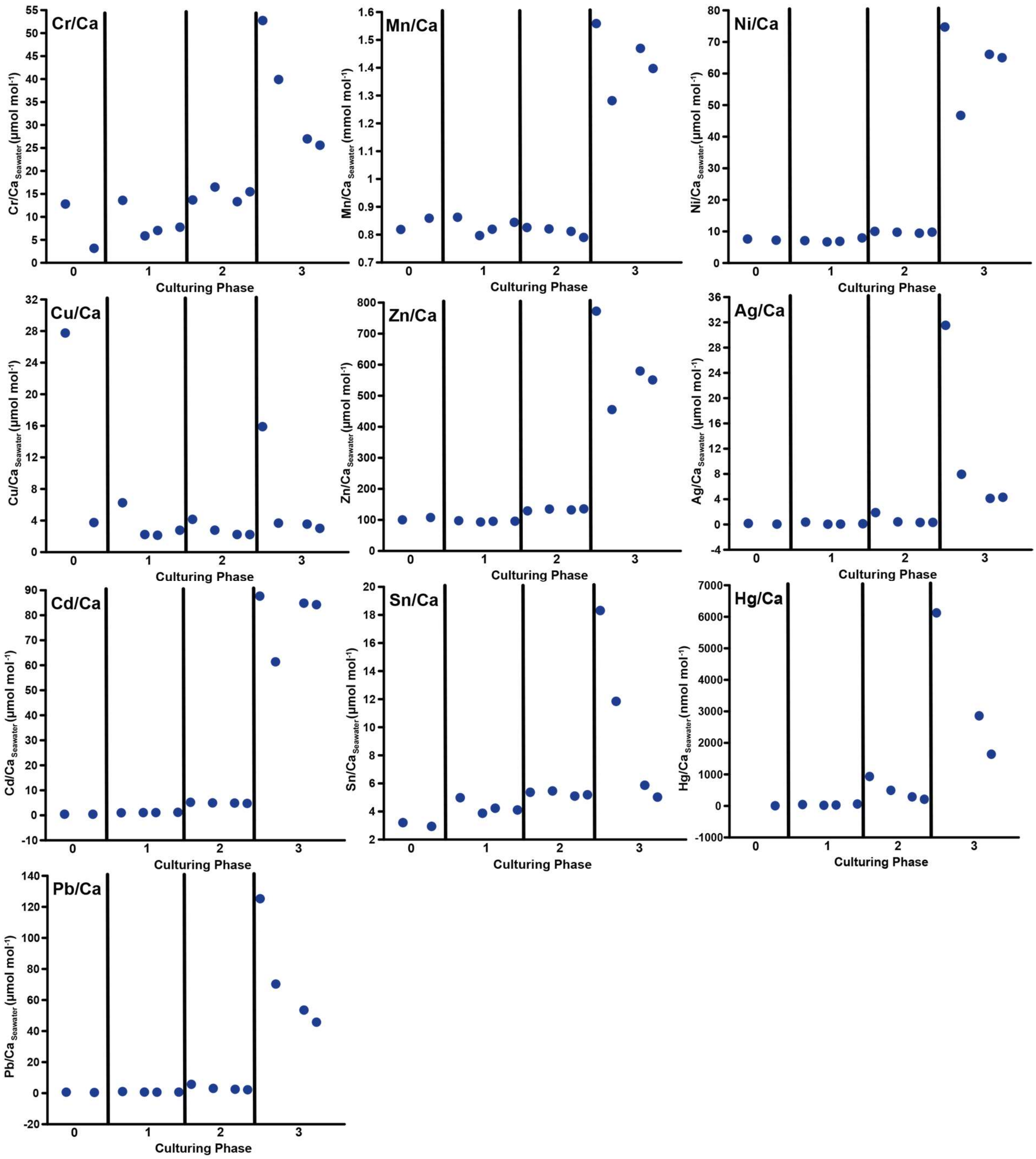

Figure B3.1: TE/Ca values in the culturing medium of the metal system in µmol mol^{-1} or nmol mol^{-1} divided by individual culturing phases. In this system, phase 0 is the control phase without any extra added metals and for phase 1 to 3, the heavy metal concentration in the culturing medium was elevated. The data the figure is based on can be found in Table A3.1.

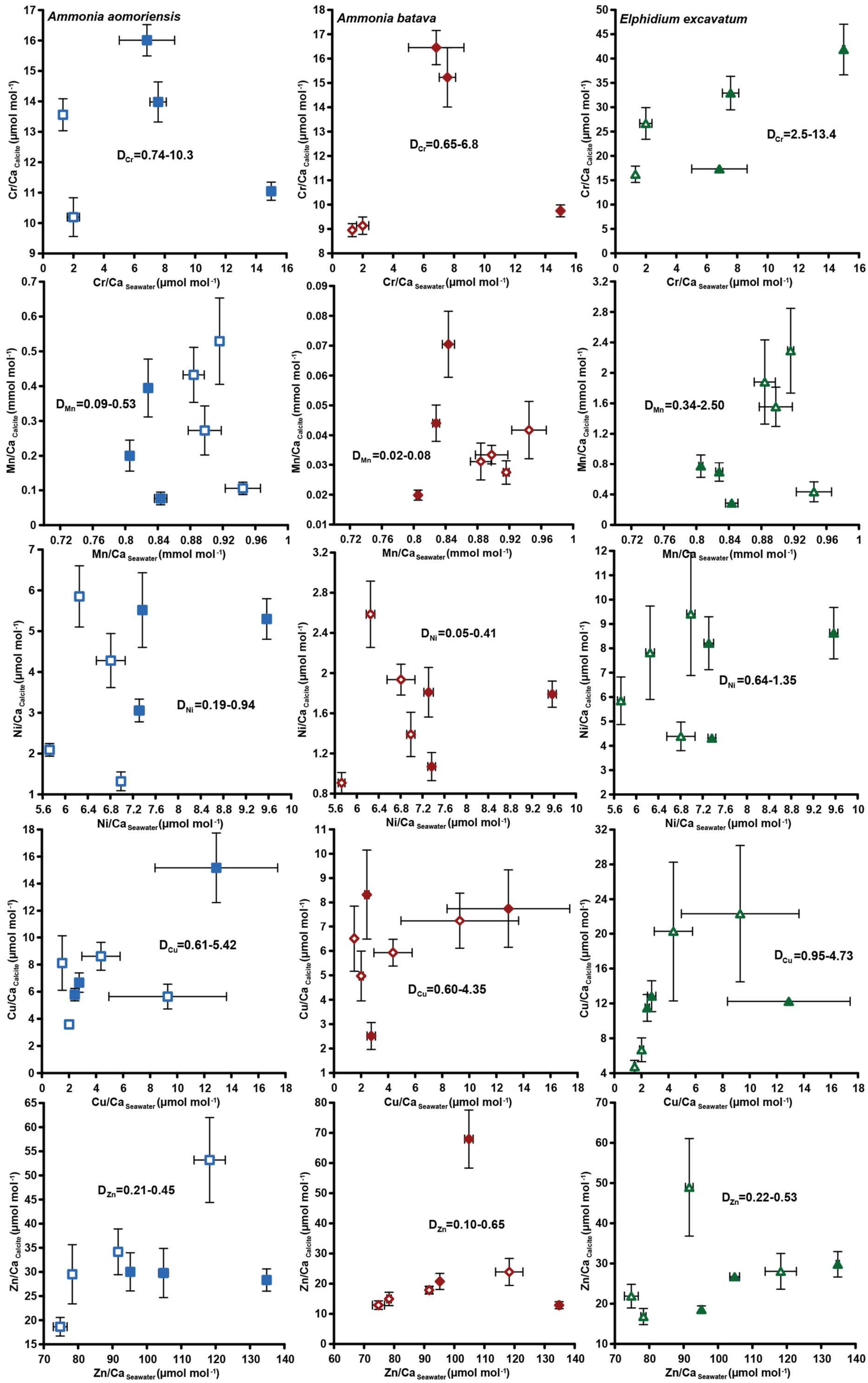
Ammonia aomoriensis
Ammonia batava
Elphidium excavatum
D_Cr=0.74-10.3
D_Cr=0.65-6.8
D_Cr=2.5-13.4
Cr/Ca Calcite (µmol mol-1)
Cr/Ca Seawater (µmol mol-1)
D_Mn=0.09-0.53
D_Mn=0.02-0.08
D_Mn=0.34-2.50
Mn/Ca Calcite (mmol mol-1)
Mn/Ca Seawater (mmol mol-1)
D_Ni=0.19-0.94
D_Ni=0.05-0.41
D_Ni=0.64-1.35
Ni/Ca Calcite (µmol mol-1)
Ni/Ca Seawater (µmol mol-1)
D_Cu=0.61-5.42
D_Cu=0.60-4.35
D_Cu=0.95-4.73
Cu/Ca Calcite (µmol mol-1)
Cu/Ca Seawater (µmol mol-1)
D_Zn=0.21-0.45
D_Zn=0.10-0.65
D_Zn=0.22-0.53
Zn/Ca Calcite (µmol mol-1)
Zn/Ca Seawater (µmol mol-1)

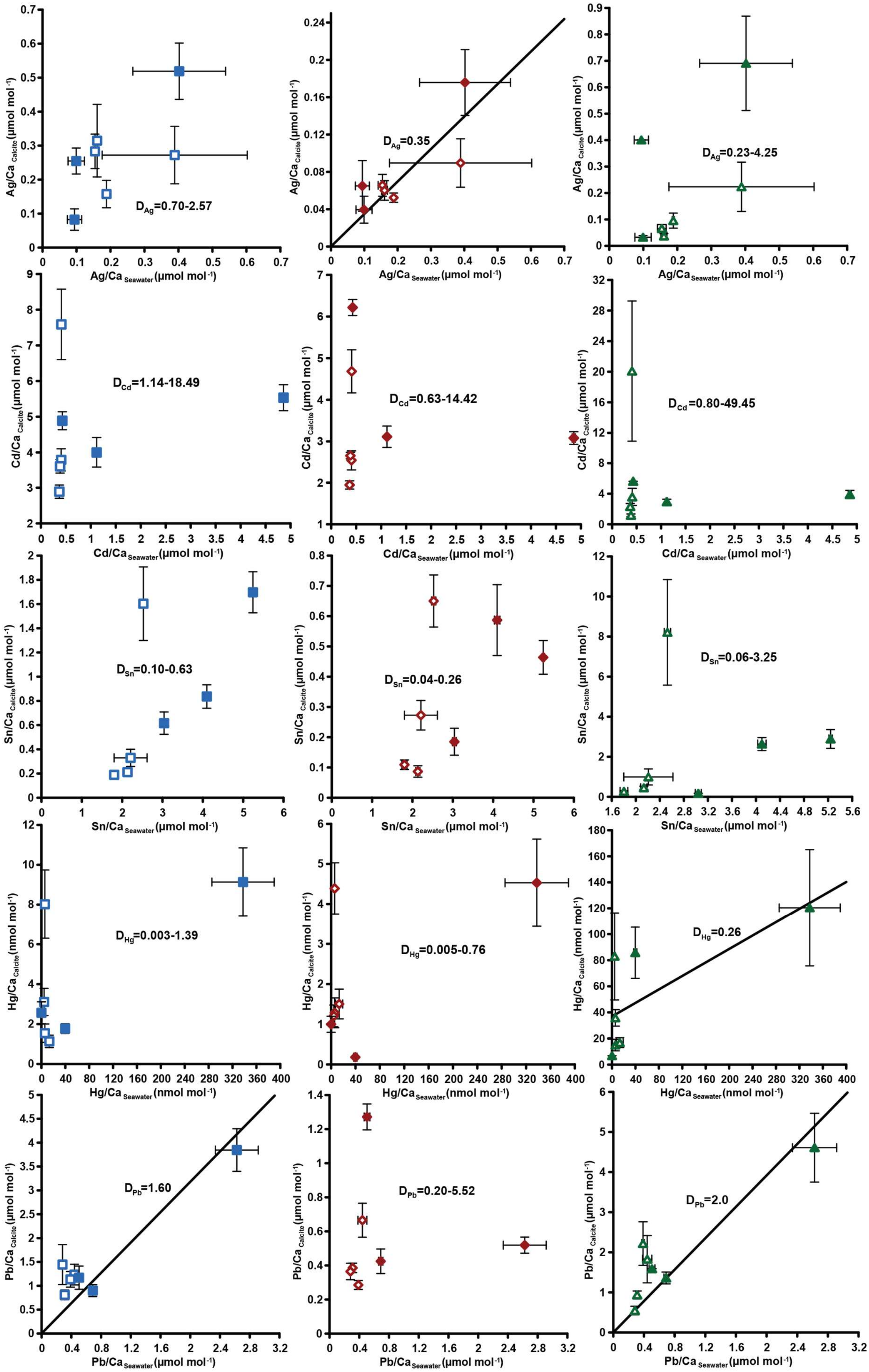

Ag/Ca Calcite (μmol mol-1)
Ag/Ca Seawater (μmol mol-1)
D_Ag=0.70-2.57
D_Ag=0.35
D_Ag=0.23-4.25
Cd/Ca Calcite (μmol mol-1)
Cd/Ca Seawater (μmol mol-1)
D_Cd=1.14-18.49
D_Cd=0.63-14.42
D_Cd=0.80-49.45
Sn/Ca Calcite (μmol mol-1)
Sn/Ca Seawater (μmol mol-1)
D_Sn=0.10-0.63
D_Sn=0.04-0.26
D_Sn=0.06-3.25
Hg/Ca Calcite (nmol mol-1)
Hg/Ca Seawater (nmol mol-1)
D_Hg=0.003-1.39
D_Hg=0.005-0.76
D_Hg=0.26
Pb/Ca Calcite (μmol mol-1)
Pb/Ca Seawater (μmol mol-1)
D_Pb=1.60
D_Pb=0.20-5.52
D_Pb=2.0

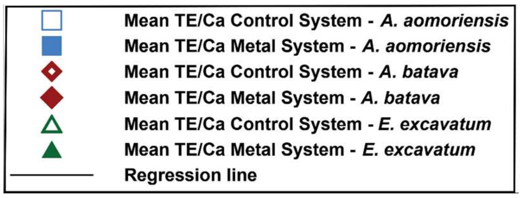

Figure B3.2: Mean TE/Ca values in the foraminiferal calcite versus the mean TE/Ca values in the corresponding culturing medium without phase 3. Each data point represents the mean value of all laser ablation ICP-MS measurements on single foraminiferal chambers built up during the individual culturing phase plotted against the mean metal concentrations in the seawater averaged over the culturing phase (Table 3.3). Error bars symbolize the standard error of the mean. The linear regression line is based on the calculations excluding phase 3 and is only displayed when elements showed a significant correlation between seawater and calcite. D_{TE}'s of *E. excavatum* where considered without values for Phase 0 as only data from one newly formed chamber are available. All values can be found in Table 3.4.

3.6.3 Appendix S: Supplementary material

Table S3.1: TE/$Ca_{Calcite}$ values from *Ammonia aomoriensis*. Values represent single laser ablation spots on foraminiferal chambers that were formed during the individual culturing period in the control and the metal system. Only values above the detection limits of the individual element are presented. Furthermore, outliers are also excluded. These values are the basis for the calculation of the mean TE/Ca values in Table 3.4 and Fig. 3.4. The sample ID indicates the species (AA = *A. aomoriensis*), the culturing phase, the system (R = metal system, L = control system), the individual and the chamber that was ablated, starting from the innermost chamber going to the youngest one.

A. aomoriensis	Phase	Cr/Ca	Mn/Ca	Ni/Ca	Cu/Ca	Zn/Ca	Ag/Ca	Cd/Ca	Sn/Ca	Hg/Ca	Pb/Ca
Metal System		µmol mol^{-1}	mmol mol^{-1}	µmol mol^{-1}	µmol mol^{-1}	µmol mol^{-1}	µmol mol^{-1}	µmol mol^{-1}	µmol mol^{-1}	nmol mol^{-1}	µmol mol^{-1}
AA0R1F1	0	13.91	0.00	1.75	7.58	14.56	0.03	4.28	0.23	1.44	0.13
AA0R2F0	0	16.18	0.08	2.49	8.72	10.89			0.29		0.55
AA0R2F1	0	15.41	0.17	2.53	7.63	14.77	0.01		0.31		0.51
AA0R4F0	0	15.65	0.02	7.38	19.83	25.08	0.02	4.69	0.64		0.83
AA0R4F1	0	15.86	0.02	8.10	19.30	24.47	0.01	4.91	0.53		0.70
AA0R5F1	0	16.21	0.05	6.86	16.71	28.14	0.03		0.89	2.50	2.13
AA0R5F2	0		0.09			48.61	0.18		0.92	3.76	1.69
AA0R5F3	0		0.12	8.35		49.65	0.10	5.67	1.01		2.02
AA0R5F4	0	18.83	0.14	6.68	26.42	51.79	0.27		0.74		1.96
AA1R1F0	1	15.12	0.10	2.18	1.37	14.96		3.12	0.16	1.72	0.35
AA1R1F1	1	20.68	0.03	2.69	1.71	8.46		6.31	0.47	2.08	0.11
AA1R1F2	1	13.38	0.02	1.31	4.31	9.82		3.31	0.35	0.21	0.28
AA1R1F3	1	18.60	0.02	2.58	6.03	18.08		5.07	0.77	0.08	0.47
AA1R1F4	1	20.04	0.02	1.10	2.54	25.29		7.23	0.90	1.72	0.54
AA1R1N-0	1	10.97	0.39	4.65	5.93	10.78	0.04	0.31	0.62		0.47
AA1R1N-1	1	11.33	0.14	3.70	4.71	9.23	0.01	0.41	0.44		0.22
AA1R1N-2	1	20.32	0.26		11.93	13.58	0.06	1.00	1.04		0.47
AA1R2F0	1	10.83	0.49	1.40	4.05	8.41		2.66	0.31	2.64	0.28
AA1R2F1	1	10.27	0.68	2.58	5.14	15.45	0.56	2.83	0.37	4.05	0.70
AA1R2F2	1	13.19	0.30	3.73	7.60	31.71	0.25	3.61	1.06	0.66	1.09
AA1R2F3	1	14.20	0.29	4.49	10.33	43.04	0.20	4.68	1.86	1.37	1.12
AA1R2F4	1	21.21	0.22	6.61	8.97	46.29	0.16	8.04	1.89	2.46	0.77
AA1R2F5	1		0.20	5.21	5.26	33.25		9.34	1.11	3.85	0.67
AA1R3F0	1	9.72	1.51	2.22	2.24	6.17		2.08	0.19	0.99	0.14
AA1R3F1	1	12.85	0.50	2.98	3.30	14.13		3.62	0.21	2.50	0.65
AA1R3F2	1	11.07	1.93	3.04	4.53	20.30	0.10	2.96	0.36	1.37	1.12
AA1R3F3	1	11.82		3.70	6.51	36.10	0.08	3.28	0.48	2.26	1.50
AA1R3F4	1	11.26		2.57	4.30	32.87		3.76	0.41	1.44	1.41
AA1R4F0	1	16.25	0.07	0.46	0.63	14.65		2.93	0.23	1.21	0.41
AA1R4F1	1	15.47	0.39	1.64	4.57	33.93	0.36	3.43	0.83	0.45	1.01
AA1R4F2	1	12.47	0.13	0.87	8.33	26.64	0.33	2.69	0.46		1.13
AA1R4F3	1	14.32	0.06	0.91	6.78	40.98	0.45	4.02	0.40	1.16	1.22
AA1R4F4	1	14.57	0.09	1.89	9.90	72.55	0.48	5.58	1.05	1.24	2.19
AA1R4F5	1	9.42	0.06	1.88	5.68	56.27	0.28	4.06	0.87	1.63	1.66
AA1R4F6	1	7.93	0.09	3.01	5.10	60.92	0.36	4.34	0.91	2.12	1.73
AA1R5F0	1	16.43	0.66	5.28	4.92	10.78		3.29	1.78	0.81	0.64
AA1R5F1	1	15.00	0.74	4.03	4.01	14.91	0.07	3.99	0.86	0.11	0.69
AA1R5F2	1	16.69		4.17			0.37	5.39	1.94		3.22

AA1R5F3	1	17.30		3.50	13.17	39.79	0.55	4.59	0.94	0.56	1.07
AA1R5F4	1		1.64	2.69	9.61	49.85		7.91	1.04		1.50
AA1R6F2	1	12.17	0.07	2.81	13.99	45.94	0.18	2.14	1.31	2.45	
AA1R6F4	1	14.42	0.15	6.00			0.47	6.19		3.98	
AA1R6F5	1	19.21	0.46	5.27	14.29	67.88	0.31	4.73		3.71	
AA1R6F6	1		0.51	5.03	17.67	93.37		9.91		2.63	
AA1R6F7	1		0.47	1.83	3.86	33.37			1.72		1.66
AA1RN2-0	1	10.00	0.03	1.08	2.24	3.30	0.01	0.24	0.27		0.09
AA1RN2-1	1	9.11	0.01	1.26	2.62	6.67	0.01	0.27	0.24		0.19
AA1RN2-2	1	9.81	0.01	2.27	3.33	15.80	0.01	0.28	0.28		0.32
AA2R1F0	2	10.39	0.04	2.37	3.67	8.19	0.08	2.64	1.68		0.31
AA2R1F1	2	9.03	0.02	1.60	2.33	20.25	0.62	3.05	0.50		3.37
AA2R1F2	2	11.09	0.02	2.62	3.41	33.78		4.84	0.78		3.03
AA2R1F3	2	9.89	0.01	2.06	2.87	41.20	2.18	8.02	0.63		3.97
AA2R1F4	2		0.02	3.56	3.34	48.79	1.40	7.83	1.07		4.39
AA2R2F0	2	10.26	0.04	6.17	6.61	16.54	0.21	3.03	1.80		3.95
AA2R2F1	2	11.47		10.59	7.70	22.27	0.34	3.55	2.39	1.37	4.03
AA2R2F2	2	11.60		6.85	5.86	18.33	0.70	4.35	2.21		4.56
AA2R2F3	2	10.41	1.31	3.45	12.07	25.51	1.27	4.24	1.32		3.14
AA2R3F0	2	9.49	0.03	2.59	1.90	3.82	0.08	3.40	0.32	4.24	0.21
AA2R3F1	2	10.29	0.13	2.49	3.14	10.97	0.12	4.66	0.55	5.71	0.71
AA2R3F2	2	11.13	0.25	2.21	6.47	23.84	1.41	4.78	0.57	4.78	1.31
AA2R3F3	2	11.71	0.30	2.20	3.24	24.02	0.67	5.86	0.55	5.23	1.18
AA2R3F4	2	12.94	0.13	2.90	5.02	27.43	0.39	6.79	1.30	2.19	1.36
AA2R3F5	2	13.75	0.17	2.21	3.07	22.73	0.38	6.44	1.00	0.53	1.19
AA2R4F0	2	10.15	0.06	8.05	6.00	34.51	0.46	3.05	3.96		8.61
AA2R4F1	2	12.09	0.09	11.76	8.10	38.32	0.35	7.25			9.51
AA2R4F2	2	10.10	0.18	5.01	4.32	25.45	0.11	3.18	1.52		4.03
AA2R4F22	2	10.60	0.12	5.33	4.35	30.38	0.23	5.92	1.79		4.96
AA2R4F3	2	11.76	0.37	9.04	8.35	48.18	0.22	4.82	2.42		6.86
AA2R4F4	2	12.85	0.48	9.96	10.23	63.47	0.25	6.09	2.65		8.02
AA2R4F5	2	10.60	0.62	10.07	11.13		0.49	5.53	3.28	4.71	9.80
AA2R4F6	2	13.45	0.88		15.16		0.16	4.92		7.22	
AA2R5F4	2		0.64	4.55		55.60		5.25	2.63		9.44
AA2R6F0	2	9.72	0.30	7.16	7.56	36.46	1.34	9.03	1.96	32.84	7.40
AA2R6F1	2	11.26	0.23	7.53	7.21	29.86	0.25	5.52	2.79	11.70	5.43
AA2R6F12	2	10.94	0.59	8.07	10.47	43.39	0.13	6.45		16.55	5.37
AA2R6F2	2	8.81	0.07	6.03	4.64	23.37	0.37	3.91	1.71	5.50	3.41
AA2R6F3	2	16.04	0.06		7.97	25.68	0.48		1.61	19.48	1.58
AA2R6F4	2		0.06	10.77	6.83	30.42	1.24		1.92	22.73	3.07
AA2R6F5	2	14.91		5.80	6.20	40.25	0.20	8.26	1.66	7.94	3.16
AA2R6F6	2	13.74	1.32	7.99	6.48	50.15	0.37	12.46	1.64	9.81	5.06
AA2R7F0	2	8.01	0.03	3.98	3.17	18.63	0.17	3.64	0.95	3.19	1.73
AA2R7F1	2	8.93	0.03	2.64	2.07	10.31	0.06	5.48	0.57	6.87	1.03
AA2R7F2	2	9.50	0.05	5.00	3.72	15.18		7.73	0.83	7.91	1.07
AA2R7F3	2	11.62	0.09	2.82	4.47	15.82		8.31	0.58	14.56	0.76
AA2R7F4	2	12.15	0.15	6.96		57.05	1.12		1.61		4.27
AA2R8F1	2	10.65	0.08	3.66		30.32	0.66	2.81	4.18		3.67
AA2R8F2	2	8.98	0.11	2.30	12.63	17.76	0.54	3.30	3.39		2.15
AA2R8F3	2	11.29	0.08	2.78	7.84	13.98	0.62	6.50	1.98	4.00	2.55
AA3R4F0	3	9.65	0.99	0.92	1.74	7.56	0.21	2.89	0.12	2.92	3.52
AA3R4F1	3	10.07	0.22	1.21	3.66	15.67	1.80	3.86	0.13	11.51	12.18
AA3R4F2	3	9.75	1.27	2.97	18.11	63.03	9.97	5.04	0.40	8.03	24.05
AA3R4F3	3	10.22	2.27	3.12	7.88	54.82	9.85	6.08	0.46	23.34	24.73

AA3R5F0	3	9.30	0.67	1.31	2.05	13.99	1.14	2.58	0.17	2.51	10.33
AA3R5F1	3	10.57	0.72	1.72	2.52	18.61	1.75	3.55	0.26	5.32	13.41
AA3R5F10	3	13.41	1.71	2.50	2.67	32.98	1.60	5.98	0.42	12.69	17.25
AA3R5F2	3	12.74	1.80	2.69	3.92	29.94	4.22	5.52	0.72	5.58	37.55
AA3R5F3	3	13.31	1.64	2.36	2.88	19.02	0.97	6.26	0.53	4.67	18.93
AA3R5F4	3	12.97		3.74	4.92	33.78	5.49	6.14	0.51	7.97	23.53
AA3R5F5	3	14.30		3.44	4.66	39.60	5.39	7.56	0.57	8.21	20.27
AA3R5F6	3	12.57	2.20	3.41	4.35	42.11	6.20	5.71	0.35	7.30	17.47
AA3R5F7	3	13.14	2.06	3.82	4.53	57.61	4.18	5.49	0.54	7.85	26.76
AA3R5F8	3	13.16	1.64	2.83	3.81	44.81	3.02	5.17	0.52	7.32	22.99
AA3R5F9	3	12.10	1.55	1.96	2.58	32.98	1.73	4.85	0.30	8.38	17.45
AA3R6F0	3	9.48	0.03	3.46	2.73	7.56	0.31	2.91	0.15		4.39
AA3R6F1	3	11.82	0.17	4.74	4.11	14.32	1.11	3.12	0.41	2.46	10.12
AA3R6F2	3	10.19	0.87	2.72	4.70	13.78	1.13	2.94	0.22	26.78	6.84
AA3R6F3	3	13.12	0.81	4.54	8.35	43.22	2.31	4.89	0.36	5.86	15.19
AA3R6F4	3	11.02	0.61	3.69	6.01	35.74	2.22	4.69	0.59	8.24	12.51
AA3R7F0	3	13.81	0.11	3.67	4.11	64.83	0.42	5.97	0.29	6.83	
AA3R7F1	3	17.22	0.04	9.01	13.86	52.91	2.65	6.28	0.49	19.07	16.21
AA3R7F2	3		0.18					9.09			
AA3R7F3	3		0.16						2.28		
AA3R7F4	3	30.18	0.29	6.38	46.86	182.23			2.65	19.05	58.74
AA3R7F5	3		0.26	4.91	8.05	91.76	8.76		0.70	6.65	50.92
AA3R7F6	3	22.58	0.30	4.54	6.50	57.02	5.48	10.36	0.43	13.05	29.48
AA3R7F7	3	32.28	0.26	5.02	7.13	59.05	4.54	11.02	0.52		25.08
AA3R7F8	3	14.85	0.60	3.93	5.15	31.80	3.67	5.16	0.31	19.57	17.59
AA3R7F9	3	13.11	0.75	3.91	5.43	35.86	2.83	4.56	0.49	26.43	19.22
AA3R8F0	3	10.89	0.06	4.95	4.23	31.70	2.54	4.25	0.46	4.63	25.75
AA3R8F1	3	11.04	0.16	4.36	4.08	27.86	1.04	4.05	0.41	8.18	23.14
AA3R8F2	3	12.07	0.26	4.48	4.92	41.54	4.51	4.85	0.51	10.01	30.90
AA3R8F3	3	12.39	0.26	6.55	6.07	53.82	4.47	5.51	0.60	10.74	40.06
AA3R8F4	3	13.15	0.61	6.14	10.75	69.07	3.63	5.17	0.58	11.41	19.79
AA3R8F4	3	15.73	0.31	8.58	8.48	74.16	4.71	6.80	0.87	13.19	56.84
Control System											
AA0L1F0	0	12.58	0.07	0.32	1.76	12.32		4.93		0.95	0.41
AA0L1F1	0	12.08	0.10	0.57	2.58	35.50		4.86		1.18	0.83
AA0L1F2	0	10.49	0.27	1.77	11.63	120.41	0.17	5.29	0.38	1.75	2.17
AA0L1F3	0	14.62	0.39	1.87	12.77	146.06	0.27	8.84	0.25	2.41	2.09
AA0L2F2	0	33.18	0.07	0.93	5.99	39.73	0.10	6.92			1.10
AA0L3F0	0	28.18	0.05	0.97	2.81	20.39	0.00	7.99		0.11	0.59
AA0L3F1	0	29.48	0.05	0.90	2.75	14.39		8.18		0.17	0.29
AA0L3F3	0	59.80	0.04	0.79	1.90	83.93	0.08	16.94		0.40	2.35
AA0L4F4	0										
AA0L5F0	0	11.55	0.09	0.38	1.50	17.13	0.01	3.85	0.05	0.90	0.72
AA0L5F1	0	11.84	0.09	0.60	2.54	38.70	0.06	4.32		0.60	0.94
AA0L5F2	0	11.01	0.04	0.41	1.64	9.87	0.01	4.19	0.00	0.37	0.30
AA0L5F3	0	13.05	0.05	0.62	2.77	17.92	0.05	4.98		1.12	0.41
AA0L6F0	0	13.65	0.09	2.22	6.39	42.05	0.14	6.97	0.22	0.70	0.98
AA0L6F1	0	13.14	0.11	3.35	9.03	53.03	0.30	6.88	0.31	1.44	1.95
AA0L6F2	0	15.44	0.12	3.08	11.67	79.97	0.64	10.33	0.31	1.64	2.52
AA0L6F3	0	14.22	0.14	3.87	12.66	131.77	0.53	15.32	0.52	4.48	4.25
AA0L7F1	0	13.28	0.07	0.85	6.71	39.22	0.27	4.02	0.33		0.66
AA0L7F2	0	11.39	0.08	0.62	2.45	36.86	0.17	3.07	0.21		0.48
AA0L7F3	0	13.74	0.07	0.69	3.64	36.06	0.21	4.45	0.34		0.49

AA0L7F4	0	15.95	0.06	0.42	2.43	37.02	0.30	6.60	0.25		0.49
AA0L7F5	0	31.92	0.13	2.47	12.82	104.75	1.57	20.42	1.10		1.91
AA1L1F2	1	12.06	0.24	6.35	8.00	37.16	0.09	3.00	1.15	1.68	1.39
AA1L2F0	1	11.77	0.06	2.40	4.34	17.27		2.43	1.03	2.12	0.41
AA1L2F1	1	11.93	0.04	2.93	6.16	21.73	0.47	2.54	0.89	1.92	1.18
AA1L2F2	1	11.35	0.06	3.65	9.38	34.77	0.34	2.63	1.33	1.48	1.76
AA1L2F3	1	13.21	0.13	6.31	18.03	73.96	0.39	3.79	2.24	3.54	
AA1L3F0	1	18.65		3.80	3.93	20.97			1.30	2.86	0.60
AA1L3F1	1	9.18	1.60	5.48	5.80	15.15		4.05	1.12		0.65
AA1L3F2	1	9.00	1.16	3.30	3.51	11.31		4.30	0.65	0.89	0.46
AA1L3F3	1	9.75	0.73	5.22	4.73	11.81		4.37	0.46	1.54	0.41
AA1L4F1	1	11.34	0.21	3.30	5.14	24.40	0.05	3.02	0.52	3.29	0.52
AA1L4F2	1	12.75	0.22	4.80	10.67	35.72	0.29	3.65	0.80	2.91	1.17
AA1L5F0	1		0.47	9.63	10.88	34.32		5.16	2.46	3.78	0.91
AA1L5F1	1	13.51	1.17	11.96	13.97	66.34	0.12	2.77	3.11	4.24	1.56
AA1L5F2	1	14.82	0.65	13.84	15.51	51.00	0.42	4.31	5.56	9.97	2.04
AA1L5F3	1	16.11	1.51				0.30	8.00			2.84
AA1L6F0	1	10.61	0.07	4.91	5.22	17.12	0.08	2.64	0.50		0.49
AA1L6F1	1	15.40	0.17	4.96	9.21	39.46	0.57	3.94	2.55		1.04
AA1L6F2	1	12.69	0.51	6.62	11.89	68.27		3.77	1.59	0.72	1.86
AA2L1F0	2	11.30	0.03	2.29	5.49	18.69	0.43	2.80	0.42	0.89	1.47
AA2L1F1	2	14.43	0.47	2.37	3.47	9.28		4.45	0.15	2.45	0.29
AA2L1F2	2	14.85	0.40		5.51	16.43	0.22	4.73	0.30	2.39	0.94
AA2L1F3	2	15.18		3.29	4.95	22.24	0.38	5.07	0.30	1.57	1.12
AA2L2F0	2	10.83	0.02	1.69	3.57	28.70	0.05	2.74	0.39	0.14	0.77
AA2L2F1	2	15.92	0.01	2.21	2.84	33.20	0.04	3.30	0.14	0.98	1.48
AA2L2F2	2	17.67	0.01	3.20	3.52	33.96			0.10		1.21
AA2L3F0	2	11.86	0.05	2.55	2.55	7.28		2.50			0.10
AA2L3F1	2	11.07	0.71	2.51	5.32	24.93	0.17	3.09	0.02	0.53	1.27
AA2L3F12	2	10.26	0.15	1.39	2.11	11.32	0.03	2.52	0.06		0.22
AA2L3F2	2	10.30	0.79	2.16	3.20	14.92	0.08	3.39	0.01	0.58	0.58
AA2L4F0	2	13.53	0.43	1.32	3.02	8.93	0.21	3.64	0.37	0.76	0.42
AA2L4F1	2	14.97	0.72	1.57	3.86	14.00	0.06	3.98	0.40	3.04	0.77
AA2L4F2	2	14.99	0.47	1.23	3.56	11.59		4.39	0.20	1.12	0.34
AA2L5F0	2	15.22	0.03	2.45	3.37	19.53		3.76	0.20		0.89
AA2L5F1	2	13.14	0.03	1.46	2.47	19.71		3.32	0.18	0.75	0.98
AA2L5F2	2	15.01	0.05	1.77	3.19	22.17	0.06	3.94	0.14	0.45	0.93
AA3L1F0	3	8.88	0.45	3.27	3.68	13.41	0.15	2.26	0.14		0.41
AA3L1F1	3	10.08	0.35	3.69	5.75	22.99	0.21	3.03	0.22		1.05
AA3L1F2	3	13.63	0.12	5.60	13.77	41.07	1.50	5.44	0.25	0.90	1.71
AA3L2F0	3	8.24		3.24	2.72	7.86	0.08	2.57	0.04		0.25
AA3L2F1	3	9.31	0.48	3.73	2.94	10.11	0.09	2.88	0.07		0.41
AA3L2F2	3	8.08	0.75	3.84	2.61	9.16	0.03	2.36	0.07		0.39
AA3L2F3	3	9.30	0.71	4.73	3.50	12.67	0.04	3.56	0.09		0.43
AA3L2F4	3	8.56	0.45	3.91	6.30	19.62	0.13	3.22	0.08		1.09
AA3L3F0	3	19.74	0.38	10.63	8.07	40.48	0.12		0.25		1.72
AA3L3F1	3	11.88	0.22	6.78	7.76	34.20	0.12	3.01	0.27	3.63	1.97
AA3L3F2	3	8.97	0.40	5.90	5.70	23.20	0.10	2.27	0.26	2.83	2.24
AA3L3F3	3	10.97	0.84	7.56	20.98	92.34	0.85	3.18	0.24	0.72	6.23
AA3L3F4	3	13.25	0.52	10.54	39.89	107.75	0.91	2.95	0.40		6.67
AA3L4F1	3		0.12								
AA3L4F2	3	7.88	0.02	0.66	2.69	17.75		2.05	0.08	7.70	0.34
AA3L4F3	3	9.32	0.01	1.02	3.87	28.69		2.46	0.07	6.91	0.61
AA3L4F4	3	8.48	0.02	1.98	3.15	41.64	0.06	3.43	0.06	12.44	0.94

AA3L5F1	3	7.94	0.13	1.12	3.17	5.80	0.33	1.68	0.30	6.07	0.53
AA3L5F2	3	9.78	0.90	1.18	6.71	11.00		3.01	0.28	12.97	0.23
AA3L5F3	3	9.41	1.34	1.95	10.86	20.98		2.65	0.44	11.13	0.26
Number of rejected points		15	13	10	12	9	45	17	19	63	11

Table S3.2: TE/Ca$_{Calcite}$ values from *Ammonia batava*. Values represent single laser ablation spots on foraminiferal chambers that were formed during the individual culturing period in the control and the metal system. Only values above the detection limits of the individual element are presented. Furthermore, outliers are also excluded. These values are the basis for the calculation of the mean TE/Ca values in Table 3.4 and Fig. 3.4. The sample ID indicates the species (AB = *A. batava*), the culturing phase, the system (R = metal system, L = control system), the individual and the chamber that was ablated, starting from the innermost chamber going to the youngest one.

A. batava	**Phase**	**Cr/Ca**	**Mn/Ca**	**Ni/Ca**	**Cu/Ca**	**Zn/Ca**	**Ag/Ca**	**Cd/Ca**	**Sn/Ca**	**Hg/Ca**	**Pb/Ca**
Metal System		µmol mol^{-1}	mmol mol^{-1}	µmol mol^{-1}	µmol mol^{-1}	µmol mol^{-1}	µmol mol^{-1}	µmol mol^{-1}	µmol mol^{-1}	nmol mol^{-1}	µmol mol^{-1}
AB0R1F3	0	13.3	0.1	0.6	4.2	55.6	0.019	5.7	0.10	1.38	1.2
AB0R1F4	0	16.6	0.1	1.0	7.3	72.3	0.054	5.7	0.15	0.46	1.4
AB0R1F5	0	16.8	0.1	1.1	5.7	92.9		6.6	0.22	0.74	
AB0R1F5.2	0	16.0	0.0	1.1	7.0	60.1	0.028	6.7	0.09	0.74	1.1
AB0R1F6	0	19.1	0.1	1.5	14.5	98.3	0.040		0.36	0.76	1.6
AB0R2F1	0	17.0				28.5	0.184	6.4		1.90	1.1
AB1R1F0	1	10.1	0.0	0.9	1.2	2.1		2.2	0.22		0.1
AB1R1F1	1	11.3	0.0	0.5	0.8	4.2		2.3	0.20	0.18	0.2
AB1R1F2	1	12.9	0.0	1.1	9.9	40.5	0.072	2.7	0.66		1.3
AB1R1F3	1	14.0	0.0	3.1		88.0	0.295	2.3			
AB1R1F4	1	15.7	0.0	1.9	5.5	27.4	0.111	3.8	0.61	1.39	1.1
AB1R2F1	1	12.6	0.1	3.5	2.9	15.0		3.1	1.25		0.3
AB1R2F2	1		0.1	2.0	2.2	25.7			0.31		0.6
AB1R3F0	1	13.4	0.1	1.8	2.1	18.0	0.011	2.4	0.19		0.4
AB1R3F1	1	12.2	0.1	1.5	1.1	22.3		2.4	0.27		0.3
AB1R3F2	1	16.2	0.0	2.8	1.7	18.7		3.6	0.39		0.3
AB1R4F1	1	14.8	0.1	2.6	3.5	33.5		2.8	1.12		0.7
AB1R4F2	1	20.7	0.1	3.2	3.6	29.2		4.1	1.75		0.5
AB1R5F1	1	20.5	0.1	2.9	2.5	20.5		3.5	0.86		0.4
AB1R6F0	1	15.7	0.1	1.0	1.4	15.3		3.9	0.41		0.4
AB1R6F1	1	20.5	0.0	1.8	1.4	28.0			0.32		0.4
AB1R6F12	1	7.9	0.0	0.3	1.5	9.6	0.035	2.1	0.19		0.2
AB1R6F2	1	24.4	0.0	1.4	1.9	28.6		5.4	0.68		0.3
AB2R10F0	2	7.8	0.0	2.2		9.3	0.037	1.9	0.22	1.28	0.4
AB2R10F1	2	11.9	0.0	3.6		12.6		3.5	0.27	2.84	0.6
AB2R10F2	2	9.2	0.0	3.2	41.9	8.1		2.3	0.35	0.32	0.5
AB2R10F3	2	10.2	0.0	3.1	37.2	11.3		2.5	0.27		0.5
AB2R1F0	2	9.7	0.0	0.6	1.0	1.8		2.3	0.22		0.1
AB2R1F1	2	9.9	0.0	0.9	1.6	5.5		2.5	0.33		0.2
AB2R1F2	2	9.4	0.0	1.1	4.8	10.2	0.124	2.8	0.36		0.3
AB2R1F3	2	10.6	0.0	1.3	5.4	14.6	0.136	3.3	0.35		0.4
AB2R1F4	2	10.0	0.0	1.6	3.4	15.3	0.040	3.5	0.38		0.3
AB2R2F0	2	8.4	0.0	1.5	1.9	3.5		2.1	0.48		0.2
AB2R2F1	2	8.5	0.0	1.8	2.1	5.3	0.029	1.9	0.39		0.2
AB2R2F2	2	9.2	0.0	2.2	2.6	11.9	0.177	2.4	0.61		0.3
AB2R2F3	2	9.6	0.0	3.0	6.0	16.9	0.371	3.7	0.90		0.4
AB2R2F4	2	9.9	0.0	2.5	3.1	12.3	0.119	3.8	0.55		0.3
AB2R2F5	2	10.4	0.0	2.1	2.9	12.7	0.051	4.6	0.46		0.2
AB2R2F6	2	12.0	0.0	1.9	2.6	13.5	0.036		0.78		0.3
AB2R3F1	2	9.9	0.0	0.8	1.1	10.7		2.9	0.53	9.13	0.9

AB2R3F2	2	9.8	0.0	0.8	4.1	15.8	0.068	2.8	0.34	9.65	0.8
AB2R3F3	2	9.6	0.0	1.0	5.1	26.4	0.136	2.8	0.73	5.83	1.4
AB2R4F10	2	9.8		2.8	9.1						
AB2R4F11	2	10.4	0.0	1.4	3.3	20.3	0.638	5.8	0.56		1.3
AB2R4F12	2	8.0	0.0	1.1	1.4	8.4	0.253	5.8	0.28		0.4
AB2R4F2	2	6.7	0.0	0.6	1.1	6.0		2.7	0.47		0.8
AB2R4F3	2	7.0	0.0	0.7	2.8	18.4	0.088	2.6	0.48		0.7
AB2R4F4	2	7.1	0.0	1.4	3.1	23.8	0.088	2.9	0.51		0.9
AB2R4F5	2	8.3	0.0	2.7	20.5		0.657	3.9			
AB2R4F6	2	6.1	0.0		8.2	34.7	0.273	5.3	1.91		
AB2R4F7	2	7.2	0.0		6.7	26.1	0.099	3.9			1.2
AB2R4F8	2	9.0	0.0	3.4	5.1	23.5	0.301	2.9	1.74		1.2
AB2R4F9	2	12.2	0.0	2.8	8.3	33.2	0.439	2.6			1.0
AB2R5F1	2	10.5	0.0	2.0	5.5	13.4		2.6	1.03	5.04	0.9
AB2R5F2	2	10.1	0.0	1.3	1.7	5.1	0.139	2.4	0.29	17.58	0.3
AB2R5F3	2	10.8	0.0	1.9	2.9	11.3	0.084	2.9	0.56		0.4
AB2R6F0	2	8.8	0.0	0.7	1.1	3.2		2.2	0.28	1.01	0.2
AB2R6F1	2	9.8	0.0	0.9	1.3	6.6		2.5	0.27	0.50	0.2
AB2R6F2	2	9.6	0.0	0.7	3.3	17.1	0.033	2.9	0.33		0.3
AB2R6F3	2	12.0	0.0	1.2	2.2	22.7	0.024	3.6	0.49		0.4
AB2R6F4	2	13.1	0.0	1.3	1.8	22.4	0.095	4.3	0.56		0.4
AB2R6F5	2	14.0	0.0	1.8	2.2	28.4		4.9	0.47		0.5
AB2R6F6	2	12.6	0.0	1.6	2.3	25.0		4.2	0.54		0.4
AB2R7F0	2	13.7	0.0	2.4	2.6	4.5	0.125	3.5	0.14	7.29	0.4
AB2R7F1	2	9.6	0.0	0.7	1.5	4.5		2.2	0.17	2.04	0.2
AB2R7F2	2	10.5	0.0	0.7	0.9	4.3		2.7	0.11	3.39	0.1
AB2R7F3	2	11.0	0.0	1.6	1.7	10.2		3.1	0.21	4.04	0.3
AB2R7F4	2		0.0	2.1	2.9	16.1	0.047	5.2	0.47	3.91	0.5
AB2R8F1	2	10.4	0.0	1.5	28.4	10.3		2.5	0.27	2.24	0.6
AB2R8F2	2	9.7	0.0	1.4	37.5	16.5		2.6	0.33	2.23	0.8
AB2R8F3	2	11.9	0.0	1.3		21.6		2.8	0.28	3.28	0.9
AB2R9F0	2	11.7	0.0	2.6		11.6		2.3	0.18		0.4
AB2R9F1	2	9.8	0.0	2.3	34.6	6.4		2.2	0.19		0.3
AB2R9F2	2	10.2		2.9	36.7	9.6		2.4	0.28		0.8
AB2R9F3	2			2.4		14.7			0.31		0.9
AB3R1F0	3	13.7	1.0	3.2	3.3	25.1	0.471	7.7	0.14	2.13	13.3
AB3R1F0	3	12.1	0.1	3.4	5.8	68.2	0.380	6.5	0.25	11.25	39.1
AB3R1F1	3	14.6	0.1	3.7	4.5	25.3	0.554	7.0	0.13	1.94	13.1
AB3R1F1	3	12.7	0.1	2.1	6.0	81.8	0.684	6.5	0.10	14.10	28.0
AB3R1F2	3	12.5	0.1	5.0	8.1	41.8	1.763	7.0	0.13	2.81	15.2
AB3R1F2	3	9.9	0.1	0.9	5.8	41.3	0.478	4.0	0.30	9.16	11.4
AB3R1F3	3	11.7	0.4	5.5	7.9	37.2	1.457	6.0	0.25	1.73	14.3
AB3R1F3	3	8.4	0.0	1.6	1.9	17.5	0.131	3.3	0.09	9.04	3.5
AB3R1F4	3	17.2	0.5	3.7	6.0	44.1	1.281	9.6	0.11	2.08	19.8
AB3R1F5	3		1.3		18.3	86.2	2.872		0.69	2.40	21.8
AB3R2F0	3	12.1	0.2	4.9	3.2	15.7	1.554	6.3	0.01	2.29	8.9
AB3R2F0	3	12.0	0.1	2.0	3.3	57.4	0.741	6.6	0.06	0.77	86.4
AB3R2F1	3	10.4	0.2	2.7	5.5	23.4	5.139	5.5	0.13	5.42	9.3
AB3R2F1	3	10.2	0.0	2.6	4.4	38.2	1.313	4.8	0.15	3.32	13.7
AB3R2F2	3	12.8	0.2	3.3	4.7	26.2		8.7	0.16	5.01	14.4
AB3R2F2	3	10.8	0.0	2.2	3.2	36.2	0.795	4.1	0.08	5.66	11.2
AB3R2F3	3	12.9	0.3	4.6	6.3	46.0		7.5	0.30	5.79	22.4
AB3R2F4	3	15.1	0.2	4.8	13.2	70.8		10.7	0.84	9.39	24.9
AB3R3F1	3	8.1	0.7	1.4	5.1	14.3	0.458	4.7	0.05	4.25	9.0

AB3R3F10	3	10.4	0.0	3.8	3.2	40.5	0.485	4.0	0.10	2.80	10.9
AB3R3F2	3	11.3	0.8	2.5	5.2	23.3	0.593	6.4	0.05	1.43	10.9
AB3R3F3	3	9.8	1.3	2.7	7.6	36.8	1.635	6.1	0.08	0.67	13.8
AB3R3F4	3	12.8		3.1	5.7	38.9	2.039	7.1	0.18	0.72	13.0
AB3R3F4	3	12.7	0.0	3.0	5.3	60.8	1.494	6.0	0.20	5.22	14.6
AB3R3F5	3	12.9		3.8	7.3	52.1	2.181	6.5	0.26	1.86	16.4
AB3R3F5	3	15.8	0.0	4.8	5.5	65.3	1.209	6.0	0.65	6.14	26.9
AB3R3F6	3	15.1	0.1		9.7	83.2	1.562	7.5	0.40	4.36	26.3
AB3R3F7	3	13.6	0.1	3.5	3.1	32.6	0.311	7.0	0.03	2.78	17.2
AB3R3F8	3	12.9	0.0	4.8	3.8	34.9	0.368	5.3	0.13	2.02	11.5
AB3R3F9	3	11.6	0.0	3.7	3.3	35.9	0.534	4.4	0.42	2.30	9.7
AB3R4F1	3	12.9	0.1	1.4	4.5	87.1	0.410	7.2	0.36	4.94	91.6
AB3R4F2	3	18.1	0.2	2.6	10.5		1.450		0.66	4.52	
AB3R4F3	3	14.4	0.1	1.8	7.1	67.1	2.318	7.7	0.69		27.2
AB3R4F4	3		0.1	5.2	29.0		6.641	11.8			48.2
AB3R4F5	3	16.2	0.0	2.5	4.3	76.5	1.039	7.8	0.18	9.15	32.4
AB3R4F6	3	9.8	0.0	1.9	2.8	35.1	0.653	3.9	0.13	16.15	11.3
AB3R4F7	3	9.0	0.0	2.6	2.1	36.8	0.435	3.6	0.12	30.82	17.1
AB3R5F1	3	8.7	0.0	1.0	3.9	12.4	0.620	3.0	0.06	3.22	4.0
AB3R5F2	3	9.1	0.1	2.0	2.9	15.0	0.560	3.7	0.06	5.97	5.4
AB3R6F0	3	12.5	0.1	1.5	2.0	39.1	0.315	5.4	0.38	4.21	62.8
AB3R6F1	3	17.7	0.1	2.6	4.9	86.8	1.145	10.2		1.85	96.8
AB3R6F2	3	11.6	0.1	1.3	4.0	83.2	0.479	8.3	0.18	7.95	57.3
AB3R6F3	3	14.5	0.1	2.5	6.8	96.1	0.823	11.3	0.25	4.05	45.7
AB3R6F4	3	12.5	0.1	3.5	6.0	122.0	0.890	8.3	0.55	14.42	58.1
AB3R6F5	3	18.7	0.1	4.6	10.9	140.1	2.174		0.36	16.37	32.4
AB3R6F6	3	15.3	0.0	4.7	5.7	91.3	1.271	8.1	0.25	10.72	38.0
AB3R7F0	3	11.1	0.0	1.7	7.7	36.3	0.128	5.4	0.10	21.60	34.3
AB3R7F1	3	14.6	0.0	3.1	8.7	43.3		7.5	0.12	22.85	21.6
AB3R7F2	3	15.3	0.0	3.1	10.0	63.6		9.1	0.19	20.00	30.9
AB3R7F3	3	13.8	0.0	3.2	14.1	36.0		7.0	0.07	8.24	18.8
AB3R8F1	3	8.7	0.1	1.7	16.5	74.7	0.075	4.9	0.12	22.28	64.8
AB3R8F2	3	10.5	0.1	2.2	15.7	52.6	0.088	3.8	0.69	18.61	37.3
AB3R8F3	3	10.1	0.1	2.8	11.0	48.8	0.068	4.0	0.10	15.96	30.2
AB3R9F0	3	8.1	0.1	2.4	24.1	49.8	0.111	5.7	0.09		
AB3R9F1	3	13.1	0.1	2.0	33.5	89.2	0.065	8.7	0.10	16.47	112.2
AB3R9F2	3	10.3	0.1	2.3	53.6	91.9	1.202	8.8	0.30		78.9
AB3R9F3	3	18.2	0.1					9.2			67.2
Control System											
AB0L2F0	0	9.7	0.1	1.0	13.1	17.3	0.076	2.3		1.01	0.7
AB0L2F1	0	11.4	0.0	1.0	11.1	33.9	0.228	2.3		0.98	0.9
AB0L2F2	0	13.6	0.0	2.2		29.8		3.8		1.41	1.0
AB0L3F1	0	15.6	0.1	0.4	3.9	34.5	0.056	4.4		2.75	0.9
AB0L3F2	0		0.1	2.0	8.8	21.7	0.067	6.2	0.27		0.8
AB0L4F2	0	11.5	0.0	0.8	5.6	14.4	0.033	4.8		0.27	0.5
Ab0L5F1	0	10.3	0.0	2.4	6.5	6.5		5.8			0.2
AB0L5F2	0	10.8	0.0	1.6	5.6	7.4		6.8			0.2
AB0L6F3	0	9.8	0.0	1.1	3.5	49.5	0.078	5.8			1.0
AB1L1F3	1	10.4		1.2	3.0		0.085	2.5	1.47	2.31	0.6
AB1L1F5	1	10.0	0.1	0.9	2.9	30.1	0.057	3.2		0.10	0.3
AB1L2F1	1	7.6	0.1	1.0	5.8	17.6	0.059	1.6		0.50	
AB1L2F2	1	7.9	0.0	0.7	2.8	15.0	0.040	1.7	0.68	1.25	0.4
AB1L3F1	1	9.8	0.0	1.3	3.3	19.4	0.123	1.7	1.53	0.93	0.4

AB1L3F2	1	8.7	0.0	1.1	2.5	18.4	0.085	1.7	0.60	1.25	0.4
AB1L3F3	1	6.9	0.0	1.4	2.5	19.4	0.046	1.7	0.40	1.72	0.5
Ab1L4F1	1	10.1	0.0	1.5	4.6	11.4	0.126	1.7	0.67	0.59	0.2
AB1L4F2	1	10.7	0.0	2.3	4.0	14.9	0.026	1.7	0.57	0.39	0.3
AB1L5F0	1	13.8	0.1	2.0	7.4	12.7		4.2	0.11		0.3
AB1L5F1	1	14.7	0.0	5.5	8.4	13.2		3.0	0.97	1.01	0.2
AB1L5F2	1	11.5	0.0	5.1	9.3	15.0		2.1	0.98	0.46	0.2
AB1L5F3	1	13.6	0.0	4.7	8.2	15.4		2.7	0.32	1.68	0.2
AB1L5F4	1	11.3	0.0	4.6	8.6	24.4		2.0	0.61	0.09	0.3
AB1L6F1	1	12.0	0.0	3.3	7.0	12.8	0.009	3.1	0.61	0.64	0.2
AB1L6F2	1	13.8	0.0	2.5	5.6	12.5		3.7	0.52		0.1
AB1L6F3	1		0.0	3.0	8.6	17.9			0.33	3.84	0.2
AB1L6F42	1	15.4	0.0	3.2	7.1	22.7		5.4	0.35	1.91	0.2
AB1L6F5	1	9.2	0.0	2.7	7.7	28.7		1.7	0.50	0.59	0.2
AB1L6F6	1	11.2	0.0	3.6	9.2			2.7	0.47	1.80	0.3
AB2L1F0	2	8.6		0.6	0.8	9.7		2.5			0.2
AB2L1F1	2	8.7	0.0	0.6	1.5	6.3	0.043	2.2	0.04		0.2
AB2L1F2	2	8.7	0.0	0.5	3.9	13.1	0.049	2.5	0.04	0.78	0.3
AB2L1F4	2		0.1	0.9	3.1			3.2		3.75	0.5
AB2L2F0	2	10.7	0.0	0.7	1.2	3.7		2.6		1.06	
AB2L2F1	2	9.7	0.0	0.5	7.6	10.9		2.5	0.03		0.4
AB2L2F2	2	9.8	0.0	0.8	3.4	9.6	0.040	2.9	0.02		0.4
AB2L2F3	2	9.6	0.0	0.6	2.2	12.7		3.1	0.03		0.5
AB2L3F1	2	9.3	0.0	1.5		14.8		2.5	0.02		0.4
AB2L3F2	2	11.0	0.0	1.6	14.0	27.0		2.9	0.11	1.48	0.5
AB2L3F3	2	11.1	0.0		16.6	23.2		3.0	0.04	2.07	0.4
AB2L4F0	2	8.2	0.0	1.2	1.2	3.5		2.4	0.06		
AB2L4F1	2	8.0	0.0	0.4	1.1	9.0		2.2	0.05		0.2
AB2L4F2	2	7.4	0.0	0.6	5.7	14.8	0.044	2.6	0.07		0.4
AB2L4F3	2	8.7	0.0	0.4	7.1	16.2	0.053	3.3	0.04		0.4
AB2L5F0	2	7.9	0.1	1.9	7.2	12.9		2.4	0.28		0.5
AB2L5F1	2	7.7	0.1	0.9	7.3	20.1	0.054	2.2	0.20		0.6
AB2L5F2	2	7.2	0.0	1.1	2.9	9.0		2.3	0.19		0.3
AB2L5F3	2	8.8	0.0	1.5	2.6	15.5	0.082	3.2	0.16		0.4
AB3L1F3	3	9.8	0.1	2.1	4.0	28.0	0.080	2.4	0.36	5.99	0.7
AB3L1F4	3	9.0	0.1	2.8	4.6	30.8	0.082	2.8	0.15	4.10	0.7
AB3L1F5	3		0.1							3.88	
AB3L1F6	3	9.1	0.0	3.6	3.5	33.1	0.019	2.7	0.16		0.5
AB3L2F0	3	8.0	0.0	1.4	1.8	4.5	0.017	1.7	0.09		0.1
AB3L2F1	3	7.7	0.0	0.6	5.5	14.1	0.119	1.7	0.07		0.4
AB3L2F2	3	7.5	0.0	1.7	4.5	23.2	0.131	1.6	0.07		0.6
AB3L3F0	3	11.5	0.0	1.8	3.6	5.0		1.7	0.11		0.1
AB3L3F1	3	11.1	0.0	2.5	1.7	3.2		1.6	0.07		0.1
AB3L3F2	3	11.0	0.0	1.9	2.3	6.6	0.039	1.6	0.06	0.63	0.2
AB3L3F3	3	10.6	0.0	1.5	2.1	12.1	0.057	1.8	0.08	0.32	0.4
AB3L3F4	3	11.0	0.0	2.0	2.5	14.9	0.058	1.9	0.08	2.45	0.5
AB3L3F5	3	11.1	0.0	1.9	3.2	15.1	0.054	2.8	0.09	5.20	0.2
AB3L4F1	3	7.6	0.0	1.7	17.0	9.2		1.6	0.12	5.08	0.4
AB3L4F2	3	7.7	0.0	1.3	14.3	6.0		1.6	0.06	4.70	0.2
AB3L4F3	3	8.9	0.0	2.1	22.6	9.6		2.1	0.11	5.90	0.2
AB3L5F1	3	7.2	0.1	2.7	6.3	22.3	0.023	1.7	0.13	6.14	0.5
AB3L5F2	3	7.5	0.1	2.1	8.2	24.1	0.042	1.7	0.07	6.30	0.5
AB3L5F3	3	8.0	0.0	1.2	9.3	7.1		1.9	0.09	7.17	0.2

Number of rejected points	9	8	8	11	9	76	11	23	80	11

Table S3.3: TE/Ca$_{Calcite}$ values from *Elphidium excavatum*. Values represent single laser ablation spots on foraminiferal chambers that were formed during the individual culturing period in the control and the metal system. Only values above the detection limits of the individual element are presented. Furthermore, outliers are also excluded. These values are the basis for the calculation of the mean TE/Ca values in Table 3.4 and Fig. 3.4. The sample ID indicates the species (E = *E. excavatum*), the culturing phase, the system (R = metal system, L = control system), the individual and the chamber that was ablated, starting from the innermost chamber going to the youngest one.

E. excavatum	**Phase**	**Cr/Ca**	**Mn/Ca**	**Ni/Ca**	**Cu/Ca**	**Zn/Ca**	**Ag/Ca**	**Cd/Ca**	**Sn/Ca**	**Hg/Ca**	**Pb/Ca**
Metal System		µmol mol^{-1}	mmol mol^{-1}	µmol mol^{-1}	µmol mol^{-1}	µmol mol^{-1}	µmol mol^{-1}	µmol mol^{-1}	µmol mol^{-1}	nmol mol^{-1}	µmol mol^{-1}
E0R5F2	0	17.3	0.3	4.3	12.2	26.7	0.4	5.6	0.2	6.79	1.6
E1R1-0	1	69.8	1.4		24.7	26.0			7.1	131.13	3.5
E1R1-1	1	7.2			18.7		0.1		5.4	123.50	
E1R2-0	1	29.8	0.2	6.4	6.5	20.0	0.0	3.6	0.7	38.71	0.5
E1R2-1	1	44.4	0.4	12.5	7.8	24.3	0.0	6.9	2.5	66.60	2.7
E1R3-0	1	90.7	0.3	8.9	3.4	21.2	0.1		0.3	132.46	0.5
E1R3-01	1	18.7	0.2	6.1	4.3	20.2		2.2	0.7	9.77	0.4
E1R3-1	1	47.0	0.3	2.8	2.5	14.2	0.0	6.5	0.6	83.77	0.7
E1R3-11	1	53.6	0.4	5.1	2.3	23.6	0.0	7.1	0.2	76.82	0.6
E1R3-2	1	18.9	0.2	2.7	1.5	12.0	0.1	2.2	0.2	6.63	0.7
E1R4-0	1	26.5	0.3	26.0	19.0	28.9	0.1	2.8	5.9	32.90	1.7
E1R4-1	1	23.5	0.7	14.0	10.5	22.9	0.0	2.4	3.4	30.52	1.9
E1R5-0	1	31.3	0.1	18.8	11.4	23.0	0.0	3.6	7.0	40.78	3.3
E1R5-1	1	28.0	0.1	15.5	9.2	15.6		3.3	3.8	44.15	2.0
E1R6-1	1	22.3	0.6	12.1	9.1	26.7		2.7	3.6	49.02	0.9
E1R7-0	1	18.4	0.0	3.0	2.3	14.6		2.0	1.5	16.93	0.6
E1R7-1	1	22.5	2.0	2.6	3.3	25.3	0.1	1.8	2.9	19.31	2.2
E1R7-2	1	28.3	3.0	4.6	6.0			2.9	6.5	42.92	3.3
E1R8-0	1	18.0	1.9	4.2	3.0	13.8	0.0	2.0	0.8	7.69	0.5
E1R8-1	1	16.6	2.1	5.2	4.7	13.9	0.0	1.6	1.7	9.36	1.3
E1R8-2	1	36.2	1.2	4.8	4.1	13.0		4.5	1.2	35.66	0.7
E1RN1-0	1		1.1	23.1	39.2	21.4		3.8	2.3		1.2
E1RN10-0	1	76.2	0.1	15.0	33.3	15.8	0.0	7.7	2.7	81.07	1.3
E1RN11-0	1	25.5	0.4	8.3	27.1	23.9		1.4	2.1	16.73	1.4
E1RN12-0	1	12.9	0.1	2.8	10.8	11.1		0.7	0.9	7.77	0.3
E1RN13-ß	1	13.1	1.0	3.3	11.4	10.8	0.0	0.7	2.2	5.21	1.0
E1RN2-0	1	34.5	1.2	2.8	23.6	18.9	0.0	2.5	4.5		2.3
E1RN2-0	1	13.1	0.0	3.1	4.8	9.6	0.0	0.3	0.6	474.19	0.4
E1RN3-0	1	30.9	0.3	5.6	37.1	12.8	0.0	2.0	2.7	54.72	1.5
E1RN3-0	1	17.8	0.1	2.6	7.7	11.5		0.5	0.8	21.43	0.5
E1RN4-0	1		1.6	9.1	19.7	25.2		3.2	3.8	35.98	1.9
E1RN5-0	1	42.3	0.4	7.2	19.6	15.3	0.0	3.9	2.6	300.41	1.5
E1RN5-0	1	17.6	1.1	1.7	4.2	14.9	0.0	0.4	0.7	270.91	0.7
E1RN6-0	1	29.4	0.1	5.9	26.9	15.0		1.7	4.2	438.99	2.1
E1RN6-0	1		0.7	3.5	9.6	25.1		3.2	4.2	26.18	1.2
E1RN8-0	1	64.5	1.0	20.1		21.0	0.0	4.0	2.3	142.17	1.4
E1RN9-0	1	56.6	0.1	9.6	19.7	18.8	0.1	3.2	2.1	40.81	0.9
E2R2-0	2	44.8	0.4	6.4	6.3	25.3	0.3	5.5		2.24	10.1
E2R3-0	2	39.2	0.2	8.1	6.1	26.2	0.8	4.8	5.4	31.13	5.5
E2R3-1	2	36.8	0.7	6.8	6.5	35.2	0.6	3.6	4.2	12.96	7.9

E2R4-1	2	48.6	1.2	14.3	9.5	35.0	0.0	5.4		57.60	15.5
E2R5-0	2	53.7	0.6	23.3	20.7		1.0	8.0		65.98	
E2R6-0	2	43.8	1.2		20.5	67.6	0.6	5.9	2.9	38.39	3.3
E2R7-0	2	13.8	1.3	1.9	2.1	11.4	0.1	1.4	0.6	7.85	1.0
E2R7-1	2	25.0	1.2	14.8	11.5	32.5	1.3	2.4	6.8	19.14	7.5
E2R8-0	2	18.5	0.0	2.4	1.8	9.6	0.0	1.5	0.6	6.77	0.5
E2R8-1	2	29.6	0.1	7.4	2.6	15.9	0.1	3.2	1.3	19.51	2.1
E2R9-0	2	18.0	0.0	5.0	5.8	26.3	0.2	1.6	0.9	6.21	0.7
E2R9-1	2	66.5	0.5	9.7	5.1	26.8	0.3	8.5	1.6	29.96	4.1
E2RN1-0	2	64.0	0.7	13.9	26.9	37.3		5.2	3.1	242.63	2.6
E2RN10-0	2	50.9	2.0	11.0	18.7	33.8	0.7	3.2	4.3	21.84	5.1
E2RN11-0	2	27.3	2.2	6.2	20.0	39.3	0.3	1.9	5.2	98.30	4.0
E2RN12-0	2	127.8	0.3	9.1	21.6	40.3	0.3	10.3	6.7	33.04	4.8
E2RN12-1	2	54.1	0.1	6.4	11.4	25.4	0.2	3.7	3.2	5.88	4.3
E2RN13-0	2	18.1	1.5	2.2	4.6	10.5	0.1	0.9	0.9	47.56	0.8
E2RN2-0	2	71.4	0.4	11.4	19.7	42.2	3.4	6.5	5.5	625.94	5.3
E2RN3-0	2		2.4			68.0	2.5			828.07	15.0
E2RN5-0	2	46.1		12.0	15.8	25.5	1.5	3.1	1.5		2.5
E2RN6-0	2	17.4	0.2	9.2	14.6	16.6	1.6	0.7	1.6	471.33	1.5
E2RN7-0	2	29.0	0.0	5.3	7.9	19.1	0.1	1.5	0.8	87.26	1.0
E2RN8-0	2	18.0	0.4	3.0	4.7	15.4	0.1	1.0	0.5	9.14	1.0
E3R1-0	3	19.8		7.0	9.9	68.1	0.7	3.9	7.1	33.84	21.9
E3R2-0	3	26.8	0.1	27.5	13.0	46.8	0.3	2.5	5.1	27.55	26.2
E3R2-1	3	33.5	2.4	12.4	11.0	58.3	1.4	4.2	3.5	80.27	70.0
E3R3-0	3	11.5	2.2	17.9	18.7	43.4	3.1	1.4	1.2	4.96	91.1
E3R3-1	3	24.8	2.9	23.8	11.2	49.7	8.1	2.4	1.5	20.45	68.8
E3R3-2	3	30.7	0.6	22.6	11.3	38.8	12.1	3.6	2.0	44.04	70.6
E3R4-0	3	27.3	0.7	21.4	14.1	41.2	3.3	4.5	1.2		117.5
E3R4-1	3	19.2	1.9	10.7	5.6	15.6	1.4	1.6	0.5	4.04	23.3
E3R5-0	3	51.3	0.8	20.1	16.8	69.5	9.9	8.1	2.2		102.3
E3R5-1	3	25.0	0.3	7.3	11.4	58.9	5.4	4.2	1.6		84.9
E3R6-0	3	13.8	0.1	4.0	2.9	13.4	0.1	1.4	0.5	6.61	13.2
E3R6-1	3	25.6	0.7	11.7	7.0	39.0	0.7	2.8	2.1		71.7
E3R7-0	3	38.1	0.0	9.7	5.6	36.9	0.8	5.3	0.8		35.9
E3R7-1	3	20.8	0.7	6.7	7.0	49.0	3.4	2.8	0.8		68.7
E3R8-0	3	29.3	1.0	5.5	3.2	26.5	0.9	2.6	1.2	37.22	22.9
E3R9-0	3	82.5	0.2	7.4	35.0	35.7	0.0	5.5		146.20	39.2
E3RN1-0	3		0.0	18.5	24.5	86.0	4.3	10.1	7.7	165.60	22.9
E3RN10-0	3	81.3	0.2	48.6	78.5	59.8	0.2	7.3	6.6	95.42	
E3RN11-0	3	45.2	0.1	12.1	32.8	34.8	5.0	3.3	1.4	92.49	39.1
E3RN11-1	3	52.9	1.2	8.9	18.2	25.2	1.4	3.9	0.9	312.47	20.5
E3RN12-0	3	160.0	0.0	24.1	36.5	35.7	1.0	8.6	4.7	105.58	27.1
E3RN12-1	3	63.2	0.9	12.0	19.7	27.5	0.3	3.5	2.4	139.07	35.5
E3RN13-0	3	68.3	1.3	9.2	26.6	29.0	0.5	3.9	1.8	61.57	15.6
E3RN14-0	3	28.1	0.9	9.8	17.2	22.5	0.7	2.9	1.1	44.50	27.6
E3RN2-0	3	168.2	0.9	49.0	63.1	82.5	2.6	10.4	7.8		85.6
E3RN3-0	3		2.7				12.1		3.9		120.9
E3RN4-0	3	37.0	0.3	17.6	34.3	46.7	1.7	3.0	0.5		36.9
E3RN6-0	3	25.0	0.0	11.1	22.4	28.2	0.7	1.7	0.8	193.70	12.7
E3RN7-0	3	142.3	1.7	44.8	76.6			9.5	4.3	134.40	122.2
E3RN8-0	3	75.4		16.1	29.7	36.5		9.4	1.4	173.07	54.2
E3RN9-0	3	141.7	0.7	12.8	13.4	44.9	0.0	7.8	5.7	163.93	26.3
Control System											

E0L2F0	0	47.6	1.1	36.8				11.8		22.61	8.9
E0L2F1	0	27.7	1.7	6.9	30.9	70.7	1.3		3.6	29.90	2.7
E0L3F1	0	12.7	0.6	1.6	6.0	33.0	0.2	4.3	0.2	5.25	1.2
E0L4F0	0	10.6	0.0	7.9	2.4	7.8	0.0	3.8	0.0	5.82	0.7
E0L4F1	0	13.3	0.2	1.9	7.4	32.5	0.1	5.5	0.4	6.42	2.5
E0LN1-0	0	29.4	0.5	7.4	13.0	23.4	0.1	1.0	0.5	61.10	1.2
E0LN2-0	0				116.1		0.4	12.9	4.8	19.74	
E0LN3-0	0	31.1	0.0	7.7	21.6	36.1	0.2	1.5	1.7		0.9
E0LN4-0	0	36.5	0.1	19.1	27.5	30.4	0.3	1.6	0.4	11.47	1.0
E0LN5-0	0	15.8	0.4	4.3	7.5	14.4	0.0	0.7	0.2	15.90	0.5
E0LN6-0	0	13.6	0.1	5.5	9.8	14.4	0.0	0.4	0.2	6.32	0.9
E0LN6-1	0	18.4	0.2	13.0	21.3	27.9	0.1	1.1	0.4	4.22	1.4
E0LN7-0	0	22.4	0.7	6.3	15.4	28.4	0.0	1.2	0.4	4.08	0.8
E0LN8-0	0	18.9	0.0	3.9	11.3	17.5	0.0	0.6	0.2	1.95	1.1
E1L1F0	1	15.4	0.7	1.1	2.8	10.6		1.8	0.7	3.28	0.3
E1L2-0	1	381.6	0.8					106.0	32.5	631.40	7.7
E1L2-1	1	15.0	0.8	6.7	20.8	30.0	0.1	1.0	2.1	19.74	1.0
E1L2-2	1	313.4	4.4	26.0	75.5	169.4		71.3	20.8	514.98	3.0
E1L3-0	1		0.4		122.9						
E1L3-01	1	43.5	0.7	5.7	9.0	31.6		8.1	2.4	69.91	1.1
E1L3-02	1	43.9	0.5	8.3	11.6	35.9	0.0	9.7	2.3	81.62	1.3
E1L4-0	1	72.2	4.2	9.8	11.7	63.4		16.7	7.3	73.63	2.0
E1L4-01	1	41.6	3.7	5.2	6.8	50.4		7.0	3.3	35.07	1.0
E1L4-1	1	16.1	5.6	2.9	4.1	36.3	0.0	1.9	4.6	14.74	1.7
E1L4-11	1	13.0	5.6	2.7	4.8	43.9	0.0	1.7	3.1	6.87	1.4
E1L5-0	1	65.5	1.9	9.7	15.8	41.1	0.1	8.5	12.9	44.47	3.4
E1L5-1	1	45.8	0.5	7.7	11.1	25.7	0.1	7.2	6.5	36.33	2.9
E2L1-0	2	12.5	3.1	15.0		47.7	0.1	1.2	1.0	12.53	1.0
E2L1-1	2	18.6	2.9	4.0	3.7	19.3	0.1	1.6	0.4	29.90	0.8
E2L2-0	2	19.6	1.1	4.2	3.1	12.7	0.1	2.6	0.3	44.05	1.3
E2L3-0	2	12.5	2.1	6.2	4.9	16.5	0.0	1.2	0.4	22.05	1.4
E2L4-0	2	14.1	1.4	10.0	20.4		0.0	0.9		14.40	
E2L5-0	2	30.8	2.1		10.2	34.0			0.4		0.9
E2L5-1	2	11.6	1.9	6.0	4.0	23.0	0.3	1.2	0.2	15.56	0.8
E2L6-0	2	9.3	0.0	2.8	1.9	10.3	0.0	1.3	0.1	2.83	0.3
E2LN1-0	2		0.8	5.7	9.0	29.7	0.1	1.7	1.0	35.01	1.4
E2LN2-0	2	22.4	0.0	6.1	4.8	17.8	0.0	0.7	0.2	8.70	0.4
E2LN3-0	2	10.3	1.1	2.0	5.7	13.0	0.0	0.3	0.4	2.51	0.8
E2LN3-1	2	16.3	1.4	4.4	6.4	18.1	0.1	0.7	0.5	6.21	1.0
E2LN3-2	2	16.7	2.4	3.8	6.2	20.3	0.2	0.6	0.6	8.58	1.2
E3L1-0	3	25.0	0.1	5.0	10.5	15.1		1.7	0.5	41.00	0.4
E3L2-0	3	35.3	1.1	7.4	4.8	11.2	0.0	2.9	0.1	46.82	0.2
E3L2-1	3	44.0	0.9	5.0	3.4	15.3		4.3	0.3	70.10	0.4
E3L3-0	3	29.2	0.5	8.1	8.6	20.4	0.0	3.8	0.4	36.00	1.5
E3L3-01	3	22.5	0.9		8.6	17.0	0.0	3.9		29.28	
E3L4-0	3	12.5	0.2	3.2	6.1	16.7	0.1	0.7	0.2	10.05	0.6
E3L4-2	3	9.0	0.6	2.0	2.6	14.4	0.0	0.5	0.2	5.64	0.8
E3L5-0	3	18.6	6.6	2.9	2.4	10.5		1.1	0.2	18.06	0.3
E3L5-1	3	14.8	0.0	2.3	2.6	17.7	0.0	0.6	0.2	12.94	0.4
E3L5-2	3	27.6	2.8	2.6	2.4	15.1		1.9	0.2	29.56	0.3
E3L5-3	3	42.2	3.8	5.6	4.1		0.0	3.4	0.3	60.75	0.6
E3L5-4	3	39.3	3.2	4.2	3.7	31.7	0.1	3.2	0.4	69.33	0.6

Number of rejected points	9	5	10	6	11	30	8	9	15	7

3.7 Data availability

All data generated or analysed during this study are included in this chapter and its appendices.

3.8 Acknowledgements

We are indebted to Tal Dagan and Alexandra-Sophie Roy, Kiel University, for providing the basic compounds of the culturing setup and for helping us with setting up the systems. Claas Hiebenthal, KIMOCC, had previously helped with the system design. Furthermore, Regina Surberg carried out the ICP-OES measurements, Kathleen Gosnell performed the Hg measurements in the water samples and Ulrike Westernströer set up and helped with the laser ablation measurements, which was vitally important for this manuscript. The fieldwork was supported by "Schutzstation Wattenmeer" on Hallig Hooge, in particular by a guided tour to the Japsand and by providing laboratory facilities at their station. Leif Boyens is thanked for his flexibility and his accommodation space on Hooge. The help of Danny Arndt during fieldwork is gratefully acknowledged. The paper benefited from the suggestions of two anonymous reviewers and the Associate Editor Hiroshi Kitazato.

3.9 References

Adle, D. J., Sinani, D., Kim, H., and Lee, J.: A cadmium-transporting P1B-type ATPase in yeast *Saccharomyces cerevisiae*, Journal of Biological Chemistry, 282, 947–955, doi:10.1074/jbc.M609535200, 2007.

Ali, H. and Khan, E.: Trophic transfer, bioaccumulation, and biomagnification of non-essential hazardous heavy metals and metalloids in food chains/webs—Concepts and implications for wildlife and human health, Human and Ecological Risk Assessment: An International Journal, 25, 1353–1376, doi:10.1080/10807039.2018.1469398, 2019.

Alvarez, C. C., Quitté, G., Schott, J., & Oelkers, E. H.: Nickel isotope fractionation as a function of carbonate growth rate during Ni coprecipitation with calcite. Geochimica et Cosmochimica Acta, 299, 184-198, doi: 10.1016/j.gca.2021.02.019, 2021.

Alloway, B. J.: Sources of heavy metals and metalloids in soils: In: Alloway B. (eds) Heavy Metals in Soils. Environmental Pollution, Springer, Dordrecht., vol. 22, 11–50, doi:10.1007/978-94-007-4470-7_2, 2013.

Alve, E.: Benthic foraminiferal responses to estuarine pollution: A review, Journal of Foraminiferal Research, 25, 190–203, doi:10.2113/gsjfr.25.3.190, 1995.

Archibald, F. S. and Duong, M.-N.: Manganese acquisition by *Lactobacillus plantarum*, Journal of bacteriology, 158, 1–8, doi:10.1128/jb.158.1.1-8.1984, 1984.

Arikibe, J. E. and Prasad, S.: Determination and comparison of selected heavy metal concentrations in seawater and sediment samples in the coastal area of Suva, Fiji, Marine Pollution Bulletin, 157, 111157, doi:10.1016/j.marpolbul.2020.111157, 2020.

Baltas, H., Kiris, E., and Sirin, M.: Determination of radioactivity levels and heavy metal concentrations in seawater, sediment and anchovy (*Engraulis encrasicolus*) from the Black Sea in Rize, Turkey, Marine Pollution Bulletin, 116, 528–533, doi:10.1016/j.marpolbul.2017.01.016, 2017.

Barbier, O., Jacquillet, G., Tauc, M., Cougnon, M., and Poujeol, P.: Effect of heavy metals on, and handling by, the kidney, Nephron Physiology, 99, p105-p110, doi:10.1159/000083981, 2005.

Barras, C., Mouret, A., Nardelli, M. P., Metzger, E., Petersen, J., La, C., Filipsson, H. L., and Jorissen, F.: Experimental calibration of manganese incorporation in foraminiferal calcite, Geochimica et Cosmochimica Acta, 237, 49–64, doi:10.1016/j.gca.2018.06.009, 2018.

Barriada, J. L., Tappin, A. D., Evans, E. H., and Achterberg, E. P.: Dissolved silver measurements in seawater, TrAC Trends in Analytical Chemistry, 26, 809–817, doi:10.1016/j.trac.2007.06.004, 2007.

Bazzi, A. O.: Heavy metals in seawater, sediments and marine organisms in the Gulf of Chabahar, Oman Sea, Journal of Oceanography and Marine Science, 5, 20–29, doi:10.5897/JOMS2014.0110, 2014.

Bé, A. W. H., Hemleben, C., Anderson, O. R., and Spindler, M.: Chamber formation in planktonic foraminifera, Micropaleontology, 25, 294–307, doi:10.2307/1485304, 1979.

Bermejo-Barrera, P., Ferrón-Novais, M., González-Campos, G., and Bermejo-Barrera, A.: Tin determination in seawater by flow injection hydride generation atomic absorption spectroscopy, Atomic Spectroscopy, 120, doi:10.46770/AS.1999.03.007, 1999.

Bernhard, J. M., Blanks, J. K., Hintz, C. J., and Chandler, G. T.: Use of the fluorescent calcite marker calcein to label foraminiferal tests, Journal of Foraminiferal Research, 34, 96–101, doi:10.2113/0340096, 2004.

Bertlich, J., Nürnberg, D., Hathorne, E. C., de Nooijer, L. J., Mezger, E. M., Kienast, M., Nordhausen, S., Reichart, G.-J., Schönfeld, J., and Bijma, J.: Salinity control on Na incorporation into calcite tests of the planktonic foraminifera *Trilobatus sacculifer*–evidence from culture experiments and surface sediments., Biogeosciences, 15(20), 5991–6018, doi:10.5194/bg-2018-164, 2018.

Bjerrum, N.: Bjerrum's Inorganic Chemistry, 3rd Danish ed. In: Heinemann, London, 1936.

Boltovskoy, E. and Lena, H.: Seasonal occurrences, standing crop and production in benthic Foraminifera of Puerto Deseado., Contributions from the Cushman Foundation for Foraminiferal Research, 20, 87–95, 1969.

Boyle, E. A.: Cadmium, zinc, copper, and barium in foraminifera tests, Earth and Planetary Science Letters, 53, 11–35, doi:10.1016/0012-821X(81)90022-4, 1981.

Boyle, E. A.: Chemical accumulation variations under the Peru Current during the past 130,000 years, Journal of Geophysical Research: Oceans, 88, 7667–7680, doi:10.1029/JC088iC12p07667, 1983.

Bresler, V. and Yanko, V.: Chemical ecology; a new approach to the study of living benthic epiphytic Foraminifera, Journal of Foraminiferal Research, 25, 267–279, doi:10.2113/gsjfr.25.3.267, 1995.

Bruins, M. R., Kapil, S., and Oehme, F. W.: Microbial resistance to metals in the environment, Ecotoxicology and Environmental safety, 45, 198–207, doi:10.1006/eesa.1999.1860, 2000.

Byrd, J. T. and Andreae, M. O.: Tin and methyltin species in seawater: Concentrations and fluxes, Science, 218, 565–569, doi:10.1126/science.218.4572.565, 1982.

Cang, L., Wang, Y.-j., Zhou, D.-m., and Dong, Y.-h.: Heavy metals pollution in poultry and livestock feeds and manures under intensive farming in Jiangsu Province, China, Journal of Environmental Sciences, 16, 371–374, 2004.

Chakraborty, S., Bhattacharya, T., Singh, G., and Maity, J. P.: Benthic macroalgae as biological indicators of heavy metal pollution in the marine environments: A biomonitoring approach for pollution assessment, Ecotoxicology and Environmental safety, 100, 61–68, doi:10.1016/j.ecoenv.2013.12.003, 2014.

Chen, C., Huang, D., and Liu, J.: Functions and toxicity of nickel in plants: Recent advances and future prospects, Clean–soil, air, water, 37, 304–313, doi:10.1002/clen.200800199, 2009.

Day, C. C., & Henderson, G. M.: Controls on trace-element partitioning in cave-analogue calcite. Geochimica et Cosmochimica Acta, 120, 612-627, doi: 10.1016/j.gca.2013.05.044, 2013.

Delaney, M. L., Bé, A. W. H., and Boyle, E. A.: Li, Sr, Mg, and Na in foraminiferal calcite shells from laboratory culture, sediment traps, and sediment cores, Geochimica et Cosmochimica Acta, 49, 1327–1341, doi:10.1016/0016-7037(85)90284-4, 1985.

Dissard, D., Nehrke, G., Reichart, G. J., and Bijma, J.: The impact of salinity on the Mg/Ca and Sr/Ca ratio in the benthic foraminifera *Ammonia tepida*: Results from culture experiments, Geochimica et Cosmochimica Acta, 74, 928–940, doi:10.1016/j.gca.2009.10.040, 2010a.

Dissard, D., Nehrke, G., Reichart, G. J., Nouet, J., and Bijma, J.: Effect of the fluorescent indicator calcein on Mg and Sr incorporation into foraminiferal calcite, Geochemistry, Geophysics, Geosystems, 10, doi:10.1029/2009GC002417, 2009.

Dissard, D., Nehrke, G., Reichart, G.-J., and Bijma, J.: Impact of seawater pCO_2 on calcification and Mg/Ca and Sr/Ca ratios in benthic foraminifera calcite: Results from culturing experiments with *Ammonia tepida*, Biogeosciences, 7, 81–93, doi:10.5194/bg-7-81-2010, 2010b.

Dromgoole, E. L., & Walter, L. M.: Iron and manganese incorporation into calcite: Effects of growth kinetics, temperature and solution chemistry. Chemical Geology, 81(4), 311-336, doi: 10.1016/0009-2541(90)90053-A, 1990.

Dueñas-Bohórquez, A., da Rocha, R. E., Kuroyanagi, A., Bijma, J., and Reichart, G. J.: Effect of salinity and seawater calcite saturation state on Mg and Sr incorporation in cultured planktonic foraminifera. Marine Micropaleontology, 73(3-4), 178-189, doi: 10.1016/j.marmicro.2009.09.002, 2009.

Duffus, J. H.: " Heavy metals" a meaningless term? (IUPAC Technical Report). Pure and applied chemistry, 74(5), 793-807, doi: 10.1351/pac200274050793, 2002.

Duque, D., Montoya, C., and Botero, L. R.: Cadmium (Cd) tolerance evaluation of three strains of microalgae of the genus *Ankistrodesmus*, *Chlorella* and *Scenedesmus*, Revista Facultad de Ingeniería Universidad de Antioquia, 88–95, doi:10.17533/udea.redin.20190523, 2019.

Eggins, S., Deckker, P. de, and Marshall, J.: Mg/Ca variation in planktonic foraminifera tests: Implications for reconstructing palaeo-seawater temperature and habitat migration, Earth and Planetary Science Letters, 212, 291–306, doi:10.1016/S0012-821X(03)00283-8, 2003.

Elderfield, H.: Chromium speciation in sea water, Earth and Planetary Science Letters, 9, 10–16, doi:10.1016/0012-821X(70)90017-8, 1970.

Elderfield, H., Bertram, C. J., and Erez, J.: A biomineralization model for the incorporation of trace elements into foraminiferal calcium carbonate, Earth and Planetary Science Letters, 142, 409–423, doi:10.1016/0012-821X(96)00105-7, 1996.

Erez, J.: The source of ions for biomineralization in foraminifera and their implications for paleoceanographic proxies, Reviews in mineralogy and geochemistry, 54, 115–149, doi:10.2113/0540115, 2003.

Escudero, C., Gabaldón, C., Marzal, P., and Villaescusa, I.: Effect of EDTA on divalent metal adsorption onto grape stalk and exhausted coffee wastes, Journal of Hazardouz Materials, 152, 476–485, doi:10.1016/j.jhazmat.2007.07.013, 2008.

Fatoki, O. S. and Mathabatha, S.: An assessment of heavy metal pollution in the East London and Port Elizabeth harbours, Water SA, 27, 233–240, doi:10.4314/wsa.v27i2.4997, 2001.

Flora, G., Gupta, D., and Tiwari, A.: Toxicity of lead: A review with recent updates, Interdisciplinary toxicology, 5, 47–58, doi:10.2478/v10102-012-0009-2, 2012.

Förstner, U.: Metal speciation-general concepts and applications, International Journal of Environmental Analytical Chemistry, 51, 5–23, doi:10.1080/03067319308027608, 1993.

Francescangeli, F., Milker, Y., Bunzel, D., Thomas, H., Norbisrath, M., Schönfeld, J., and Schmiedl, G.: Recent benthic foraminiferal distribution in the Elbe Estuary (North Sea, Germany): A response to environmental stressors. Estuarine, Coastal and Shelf Science, 251, 107198, doi: 10.1016/j.ecss.2021.107198, 2021.

Fricker, M. B., Kutscher, D., Aeschlimann, B., Frommer, J., Dietiker, R., Bettmer, J., and Günther, D.: High spatial resolution trace element analysis by LA-ICP-MS using a novel ablation cell for multiple or large samples, International Journal of Mass Spectrometry, 307, 39–45, doi:10.1016/j.ijms.2011.01.008, 2011.

Frontalini, F. and Coccioni, R.: Benthic foraminifera for heavy metal pollution monitoring: A case study from the central Adriatic Sea coast of Italy, Estuarine, Coastal and Shelf Science, 76, 404–417, doi:10.1016/j.ecss.2007.07.024, 2008.

Frontalini, F., Curzi, D., Giordano, F. M., Bernhard, J. M., Falcieri, E., and Coccioni, R.: Effects of lead pollution on *Ammonia parkinsoniana* (foraminifera): Ultrastructural and microanalytical approaches, European Journal of Histochemistry, 59, doi:10.4081/ejh.2015.2460, 2015.

Frontalini, F., Greco, M., Di Bella, L., Lejzerowicz, F., Reo, E., Caruso, A., Cosentino, C., Maccotta, A., Scopelliti, G., and Nardelli, M. P.: Assessing the effect of mercury pollution on cultured benthic foraminifera community using morphological and eDNA metabarcoding approaches, Marine Pollution Bulletin, 129, 512–524, doi:10.1016/j.marpolbul.2017.10.022, 2018a.

Frontalini, F., Nardelli, M. P., Curzi, D., Martín-González, A., Sabbatini, A., Negri, A., Losada, M. T., Gobbi, P., Coccioni, R., and Bernhard, J. M.: Benthic foraminiferal ultrastructural alteration induced by heavy metals, Marine Micropaleontology, 138, 83–89, doi:10.1016/j.marmicro.2017.10.009, 2018b.

Gallego, A., Martín-González, A., Ortega, R., and Gutiérrez, J. C.: Flow cytometry assessment of cytotoxicity and reactive oxygen species generation by single and binary mixtures of cadmium, zinc and copper on populations of the ciliated protozoan *Tetrahymena thermophila*, Chemosphere, 68, 647–661, doi:10.1016/j.chemosphere.2007.02.031, 2007.

Garbe-Schönberg, D. and Müller, S.: Nano-particulate pressed powder tablets for LA-ICP-MS, Journal of Analytical Atomic Spectrometry, 29, 990–1000, doi:10.1039/C4JA00007B, 2014.

Geisler, C.-D. and Schmidt, D.: An overview of chromium in the marine environment, Deutsche Hydrografische Zeitschrift, 44, 185–196, doi:10.15835/BUASVMCN-VM:63:1-2:2516, 1991.

Glas, M. S., Langer, G., and Keul, N.: Calcification acidifies the microenvironment of a benthic foraminifer (*Ammonia sp.*), Journal of Experimental Marine Biology and Ecology, 424, 53–58, doi:10.1016/j.jembe.2012.05.006, 2012.

Gooday, A. J.: A response by benthic foraminifera to the deposition of phytodetritus in the deep sea, Nature, 332, 70–73, doi:10.1038/332070a0, 1988.

Groeneveld, J. and Filipsson, H. L.: Mg/Ca and Mn/Ca ratios in benthic foraminifera: The potential to reconstruct past variations in temperature and hypoxia in shelf regions, Biogeosciences, 10, 5125–5138, doi:10.5194/bg-10-5125-2013, 2013.

Guo, X., Xu, B., Burnett, W. C., Yu, Z., Yang, S., Huang, X., Wang, F., Nan, H., Yao, P., and Sun, F.: A potential proxy for seasonal hypoxia: LA-ICP-MS Mn/Ca ratios in benthic foraminifera from the Yangtze River Estuary. Geochimica et Cosmochimica Acta, 245, 290-303, doi.org/10.1016/j.gca.2018.11.007, 2019.Haake, F. W.: Zum Jahresgang von Populationen einer Foraminiferen-Art in der westlichen Ostsee, Meyniana, 17, 13–27, 1967.

Haake, F.-W.: Untersuchungen an der Foraminiferen-Fauna im Wattgebiet zwischen Langeoog und dem Festland, Meyniana, 12, 25–64, 1962.

Haley, B. A., Klinkhammer, G. P., and Mix, A. C.: Revisiting the rare earth elements in foraminiferal tests, Earth and Planetary Science Letters, 239, 79–97, doi:10.1016/j.epsl.2005.08.014, 2005.

Hall, J. M. and Chan, L.-H.: Li/Ca in multiple species of benthic and planktonic foraminifera: Thermocline, latitudinal, and glacial-interglacial variation, Geochimica et Cosmochimica Acta, 68, 529–545, doi:10.1016/S0016-7037(03)00451-4, 2004.

Hammer, Ø., Harper, D. A. T., and Ryan, P. D.: PAST: Paleontological statistics software package for education and data analysis, Palaeontologia Electronica, 4, 9, 2001.

Hänsch, R. and Mendel, R. R.: Physiological functions of mineral micronutrients (Cu, Zn, Mn, Fe, Ni, Mo, B, cl), Current Opinion in Plant Biology, 12, 259–266, doi:10.1016/j.pbi.2009.05.006, 2009.

Havach, S. M., Chandler, G. T., Wilson-Finelli, A., and Shaw, T. J.: Experimental determination of trace element partition coefficients in cultured benthic foraminifera, Geochimica et Cosmochimica Acta, 65, 1277–1283, doi:10.1016/S0016-7037(00)00563-9, 2001.

Haynert, K., Schönfeld, J., Riebesell, U., and Polovodova, I.: Biometry and dissolution features of the benthic foraminifer *Ammonia aomoriensis* at high pCO_2, Marine Ecology Progress Series, 432, 53–67, doi:10.3354/meps09138, 2011.

Haynert, K., Gluderer, F., Pollierer, M. M., Scheu, S., and Wehrmann, A.: Food spectrum and habitat-specific diets of benthic Foraminifera from the Wadden Sea–A fatty acid biomarker approach. Frontiers in Marine Science, 7, 815, doi: 10.3389/fmars.2020.510288, 2020.

Hintz, C. J., Chandler, G. T., Bernhard, J. M., McCorkle, D. C., Havach, S. M., Blanks, J. K., and Shaw, T. J.: A physicochemically constrained seawater culturing system for production of benthic foraminifera, Limnology and Oceanography: Methods, 2, 160–170, doi:10.4319/lom.2004.2.160, 2004.

Horovitz, C. T.: Is the major part of the periodic system really inessential for life?, Journal of Trace Elements and Electrolytes in Health and Disease, 2, 135–144, 1988.

Huang, H., Yuan, X., Zeng, G., Zhu, H., Li, H., Liu, Z., Jiang, H., Leng, L., and Bi, W.: Quantitative evaluation of heavy metals' pollution hazards in liquefaction residues of sewage sludge, Bioresource Technology, 102, 10346–10351, doi:10.1016/j.biortech.2011.08.117, 2011.

Huang, J., Yuan, F., Zeng, G., Li, X., Gu, Y., Shi, L., Liu, W., and Shi, Y.: Influence of pH on heavy metal speciation and removal from wastewater using micellar-enhanced ultrafiltration, Chemosphere, 173, 199–206, doi:10.1016/j.chemosphere.2016.12.137, 2017.

Inoue, M., Nohara, M., Okai, T., Suzuki, A., and Kawahata, H.: Concentrations of trace elements in carbonate reference materials coral JCp-1 and giant clam JCt-1 by inductively coupled plasma-mass spectrometry, Geostandards and Geoanalytical Research, 28, 411–416, doi:10.1111/j.1751-908X.2004.tb00759.x, 2004.

Ishikawa, M. and Ichikuni, M.: Uptake of sodium and potassium by calcite, Chemical Geology, 42, 137–146, doi:10.1016/0009-2541(84)90010-X, 1984.

Jan, A. T., Azam, M., Siddiqui, K., Ali, A., Choi, I., and Haq, Q. M.: Heavy metals and human health: Mechanistic insight into toxicity and counter defense system of antioxidants, International Journal of Molecular Sciences, 16, 29592–29630, doi:10.3390/ijms161226183, 2015.

Jochum, K. P., Garbe-Schönberg, D., Veter, M., Stoll, B., Weis, U., Weber, M., Lugli, F., Jentzen, A., Schiebel, R., and Wassenburg, J. A.: Nano-powdered calcium carbonate reference materials: Significant progress for microanalysis?, Geostandards and Geoanalytical Research, 43, 595–609, doi:10.1111/ggr.12292, 2019.

Jochum, K. P., Weis, U., Stoll, B., Kuzmin, D., Yang, Q., Raczek, I., Jacob, D. E., Stracke, A., Birbaum, K., and Frick, D. A.: Determination of reference values for NIST SRM 610–617 glasses following ISO guidelines, Geostandards and Geoanalytical Research, 35, 397–429, doi:10.1111/j.1751-908X.2011.00120.x, 2011.

Julian, P.: South Florida Coastal Sediment Ecological Risk Assessment, Bulletin of Environmental Contamination and Toxicology, 95, 188–193, doi:10.1007/s00128-015-1583-8, 2015.

Kannan, K., Smith Jr, R. G., Lee, R. F., Windom, H. L., Heitmuller, P. T., Macauley, J. M., and Summers, J. K.: Distribution of total mercury and methyl mercury in water, sediment, and fish from south Florida estuaries, Archives of Environmental Contamination and Toxicology, 34, 109–118, doi:10.1007/s002449900294, 1998.

Kennish, M. J.: Ecology of estuaries: Anthropogenic effects, CRC press, Vol. 1, doi:10.2307/1351438, 2019.

Khalifa, G. M., Kirchenbuechler, D., Koifman, N., Kleinerman, O., Talmon, Y., Elbaum, M., Addadi, L., Weiner, S., and Erez, J.: Biomineralization pathways in a foraminifer revealed using a novel correlative cryo-fluorescence–SEM–EDS technique, Journal of Structural Biology, 196, 155–163, doi:10.1016/j.jsb.2016.01.015, 2016.

Kitano, Y., Kanamori, N., & Fujiyoshi, R.: Distribution of cadmium between calcium carbonate and solution (part 1) Ca $(HCO_3)^{2+}$ Cd^{2+} + bipyridine → carbonate system. Geochemical Journal, 12(3), 137-145, doi: 10.2343/geochemj.12.137, 1978.

Kitano, Y., Okumura, M., & Idogaki, M.: Abnormal behaviors of copper (II) and zinc ions in parent solution at the early stage of calcite formation. Geochemical Journal, 14(4), 167-175, doi: 10.2343/geochemj.14.167, 1980.

Koho, K. A., Nooijer, L. J. de, Fontanier, C., Toyofuku, T., Oguri, K., Kitazato, H., and Reichart, G.-J.: Benthic foraminiferal Mn/Ca ratios reflect microhabitat preferences, Biogeosciences, 14, 3067–3082, doi:10.5194/bg-14-3067-2017, 2017.

Koho, K. A., Nooijer, L. J. de, and Reichart, G. J.: Combining benthic foraminiferal ecology and shell Mn/Ca to deconvolve past bottom water oxygenation and paleoproductivity, Geochimica et Cosmochimica Acta, 165, 294–306, doi:10.1016/j.gca.2015.06.003, 2015.

Kotthoff, U., Groeneveld, J., Ash, J. L., Fanget, A.-S., Krupinski, N. Q., Peyron, O., Stepanova, A., Warnock, J., van Helmond, N. A., and Passey, B. H.: Reconstructing Holocene temperature and salinity variations in the western Baltic Sea region: A multi-proxy comparison from the Little Belt (IODP Expedition 347, Site M0059), Biogeosciences, 14, 5607–5632, doi:10.5194/bg-14-5607-2017, 2017.

Kurtarkar, R. S., Saraswat, R., Kaithwar, A., and Nigam, R.: How will benthic foraminifera respond to warming and changes in productivity?: A Laboratory Culture Study on *Cymbaloporetta plana*. Acta Geologica Sinica-English Edition, 93(1), 175-182, doi: 10.1111/1755-6724.13776, 2019.

Le Cadre, V. and Debenay, J.-P.: Morphological and cytological responses of *Ammonia* (foraminifera) to copper contamination: Implication for the use of foraminifera as bioindicators of pollution, Environmental Pollution, 143, 304–317, doi:10.1016/j.envpol.2005.11.033, 2006.

Lea, D. W., and Spero, H. J.: Assessing the reliability of paleochemical tracers: Barium uptake in the shells of planktonic foraminifera. Paleoceanography, 9(3), 445-452, doi: 10.1029/94PA00151, 1994.

Lee, J. J., Muller, W. A., Stone, R. J., McEnery, M. E., and Zucker, W.: Standing crop of foraminifera in sublittoral epiphytic communities of a Long Island salt marsh, Marine Biology, 4, 44–61, doi:10.1007/BF00372165, 1969.

Lee, J. J., Sang, K., Ter Kuile, B., Strauss, E., Lee, P. J., and Faber, W. W.: Nutritional and related experiments on laboratory maintenance of three species of symbiont-bearing, large foraminifera. Marine Biology, 109(3), 417-425, doi: 10.1007/BF01313507, 1991.

Leonhard, P., Pepelnik, R., Prange, A., Yamada, N., and Yamada, T.: Analysis of diluted sea-water at the ng L^{-1} level using an ICP-MS with an octopole reaction cell, Journal of Analytical Atomic Spectrometry, 17, 189–196, doi:10.1039/B110180N, 2002.

Li, H., Lin, L., Ye, S., Li, H., and Fan, J.: Assessment of nutrient and heavy metal contamination in the seawater and sediment of Yalujiang Estuary, Marine Pollution Bulletin, 117, 499–506, doi:10.1016/j.marpolbul.2017.01.069, 2017.

Linshy, V. N., Saraswat, R., Kurtarkar, S. R., and Nigam, R.: Experiment to decipher the effect of heavy metal cadmium on coastal benthic foraminifer *Pararotalia nipponica* (Asano), Journal of the Palaeontological Society of India, 205–211, 2013.

Lorens, R. B.: Strontium, cadmium, manganese, and cobalt distribution in calcite as a function of calcite precipitation rate. Geochim. Cosmochim. Acta, 45, 553-561, 1981.Losada Ros, M. T., Al-Enezi, E., Cesarini, E., Canonico, B., Bucci, C., Alves Martins, M. V., Papa, S., and Frontalini, F.: Assessing the Cadmium Effects on the Benthic Foraminifer *Ammonia cf. parkinsoniana*: An Acute Toxicity Test, Water, 12, 1018, doi:10.3390/w12041018, 2020.

Lukaski, H. C.: Chromium as a supplement, Annual Review of Nutrition, 19, 279–302, doi:10.1146/annurev.nutr.19.1.279, 1999.

Lutze, G.: Zur Foraminiferen-Fauna der Ostsee. Meyniana, 15, 75-142, 1965.Marchitto Jr, T. M., Curry, W. B., and Oppo, D. W.: Zinc concentrations in benthic foraminifera reflect seawater chemistry, Paleoceanography, 15, 299–306, doi:10.1029/1999PA000420, 2000.

Maréchal-Abram, N., Debenay, J.-P., Kitazato, H., and Wada, H.: Cadmium partition coefficients of cultured benthic foraminifera *Ammonia beccarii*, Geochemical Journal, 38, 271–283, doi:10.2343/geochemj.38.271, 2004.

Maret, W.: The metals in the biological periodic system of the elements: Concepts and conjectures, International Journal of Molecular Sciences, 17, 66, doi:10.3390/ijms17010066, 2016.

Martelli, A., Rousselet, E., Dycke, C., Bouron, A., and Moulis, J.-M.: Cadmium toxicity in animal cells by interference with essential metals, Biochimie, 88, 1807–1814, doi:10.1016/j.biochi.2006.05.013, 2006.

Martin, P. A. and Lea, D. W.: A simple evaluation of cleaning procedures on fossil benthic foraminiferal Mg/Ca, Geochemistry, Geophysics, Geosystems, 3, 1–8, doi:10.1029/2001GC000280, 2002.

Martinez-Colon, M., Hallock, P., and Green-Ruíz, C.: Strategies for using shallow-water benthic foraminifers as bioindicators of potentially toxic elements: A review, Journal of Foraminiferal Research, 39, 278–299, doi:10.2113/gsjfr.39.4.278, 2009.

Martinez-Finley, E. J., Chakraborty, S., Fretham, S. J. B., and Aschner, M.: Cellular transport and homeostasis of essential and nonessential metals, Metallomics, 4, 593–605, doi:10.1039/c2mt00185c, 2012.

Martín-González, A., Borniquel, S., Díaz, S., Ortega, R., and Gutiérrez, J. C.: Ultrastructural alterations in ciliated protozoa under heavy metal exposure, Cell Biology International, 29, 119–126, doi:10.1016/j.cellbi.2004.09.010, 2005.

McCorkle, D. C., Martin, P. A., Lea, D. W., and Klinkhammer, G. P.: Evidence of a dissolution effect on benthic foraminiferal shell chemistry: $\delta^{13}C$, Cd/Ca, Ba/Ca, and Sr/Ca results from the Ontong Java Plateau, Paleoceanography, 10, 699–714, doi:10.1029/95PA01427, 1995.

McGann, M.: High-resolution foraminiferal, isotopic, and trace element records from Holocene estuarine deposits of San Francisco Bay, California, Journal of Coastal Research, 24, 1092–1109, doi:10.2112/08A-0003.1, 2008.

Mertz, W.: The essential trace elements, Science, 213, 1332–1338, doi:10.1126/science.7022654, 1981.

Mertz, W.: Chromium in human nutrition: A review, The Journal of Nutrition, 123, 626–633, doi:10.1093/jn/123.4.626, 1993.

Mewes, A., Langer, G., Thoms, S., Nehrke, G., Reichart, G. J., De Nooijer, L. J., and Bijma, J.: Impact of seawater [Ca 2+] on the calcification and calciteMg/Ca of *Amphistegina lessonii*. Biogeosciences, 12(7), 2153-2162, doi: 10.5194/bg-12-2153-2015, 2015.Millero, F. J., Woosley, R., Ditrolio, B., and Waters Jason: Effect of ocean acidification on the speciation of metals in seawater, Oceanography, 22, 72–85, doi:10.5670/oceanog.2009.98, 2009.

Munsel, D., Kramar, U., Dissard, D., Nehrke, G., Berner, Z., Bijma, J., Reichart, G.-J., and Neumann, T.: Heavy metal uptake in foraminiferal calcite: Results of multi-element culture experiments, Biogeosciences Discussions, 7, doi:10.5194/bg-7-2339-2010, 2010.

Murray, J. W.: Ecology and palaeoecology of benthic foraminifera: Longman Scientific and Technical, Harlow, Essex, UK, doi:10.4324/9781315846101, 1991.

Murray, J. W.: Distribution and population dynamics of benthic foraminifera from the southern North Sea, Journal of Foraminiferal Research, 22, 114–128, doi:10.2113/gsjfr.22.2.114, 1992.

Muse, J. O., Stripeikis, J. D., Fernandez, F. M., d'Huicque, L., Tudino, M. B., Carducci, C. N., and Troccoli, O. E.: Seaweeds in the assessment of heavy metal pollution in the Gulf San Jorge, Argentina, Environmental Pollution, 104, 315–322, doi:10.1016/S0269-7491(98)00096-7, 1999.

Mutwakil, M., Reader, J. P., Holdich, D. M., Smithurst, P. R., Candido, E. P.M., Jones, D., Stringham, E. G., and de Di Pomerai: Use of stress-inducible transgenic nematodes as biomarkers of heavy metal pollution in water samples from an English river system, Archives of Environmental Contamination and Toxicology, 32, 146–153, doi:10.1007/s002449900167, 1997.

Nardelli, M. P., Malferrari, D., Ferretti, A., Bartolini, A., Sabbatini, A., and Negri, A.: Zinc incorporation in the miliolid foraminifer *Pseudotriloculina rotunda* under laboratory conditions, Marine Micropaleontology, 126, 42–49, doi:10.1016/j.marmicro.2016.06.001, 2016.

Nehrke, G., Keul, N., Langer, G., Nooijer, L. J. de, Bijma, J., and Meibom, A.: A new model for biomineralization and trace-element signatures of Foraminifera tests, Biogeosciences, 10, 6759–6767, doi:10.5194/bg-10-6759-2013, 2013.

Nikulina, A., Polovodova, I., and Schönfeld, J.: Environmental response of living benthic foraminifera in Kiel Fjord, SW Baltic Sea. eEarth, 3, 37-49, doi:10.5194/ee-3-37-2008, 2008.

Nooijer, L. J. de, Langer, G., Nehrke, G., and Bijma, J.: Physiological controls on seawater uptake and calcification in the benthic foraminifer *Ammonia tepida*, Biogeosciences, 6, 2669–2675, doi:10.5194/bg-6-2669-2009, 2009a.

Nooijer, L. J. de, Reichart, G.-J., Dueñas Bohórquez, A. D.B., Wolthers, M., Ernst, SR, Mason, P. R.D., and van der Zwaan, G. J.: Copper incorporation in foraminiferal calcite: Results from culturing experiments, Biogeosciences Discussions, 4, 961–991, doi:10.5194/bg-4-493-2007, 2007.

Nooijer, L. J. de, Spero, H. J., Erez, J., Bijma, J., and Reichart, G.-J.: Biomineralization in perforate foraminifera, Earth-Science Reviews, 135, 48–58, doi:10.1016/j.earscirev.2014.03.013, 2014.

Nooijer, L. J. de, Toyofuku, T., and Kitazato, H.: Foraminifera promote calcification by elevating their intracellular pH, Proceedings of the National Academy of Sciences, 106, 15374–15378, doi:10.1073/pnas.0904306106, 2009b.

Nordberg, G. F., Jin, T., Hong, F., Zhang, A., Buchet, J.-P., and Bernard, A.: Biomarkers of cadmium and arsenic interactions, Toxicology and Applied Pharmacology, 206, 191–197, doi:10.1016/j.taap.2004.11.028, 2005.

Nürnberg, D.: Magnesium in tests of *Neogloboquadrina pachyderma sinistral* from high northern and southern latitudes, Journal of Foraminiferal Research, 25, 350–368, doi:10.2113/gsjfr.25.4.350, 1995.

Nürnberg, D., Bijma, J., and Hemleben, C.: Assessing the reliability of magnesium in foraminiferal calcite as a proxy for water mass temperatures, Geochimica et Cosmochimica Acta, 60, 803–814, doi:10.1016/0016-7037(95)00446-7, 1996.

Okumura, M. and Kitano, Y.: Coprecipitation of alkali metal ions with calcium carbonate, Geochimica et Cosmochimica Acta, 50, 49–58, doi:10.1016/0016-7037(86)90047-5, 1986.

Pagnanelli, F., Esposito, A., Toro, L., and Veglio, F.: Metal speciation and pH effect on Pb, Cu, Zn and Cd biosorption onto *Sphaerotilus natans*: Langmuir-type empirical model, Water Research, 37, 627–633, doi:10.1016/S0043-1354(02)00358-5, 2003.

Paton, C., Hellstrom, J., Paul, B., Woodhead, J., and Hergt, J.: Iolite: Freeware for the visualisation and processing of mass spectrometric data, Journal of Analytical Atomic Spectrometry, 26, 2508–2518, doi:10.1039/C1JA10172B, 2011.

Petersen, J., Barras, C., Bézos, A., La, C., Nooijer, L. J. de, Meysman, F., JR, Mouret, A., Slomp, C. P., and Jorissen, F. J.: Mn⁄ Ca intra-and inter-test variability in the benthic foraminifer *Ammonia tepida*, Biogeosciences, 15, 331–348, doi:10.5194/bg-15-331-2018, 2018.

Pillet, L., Vargas, C. de, and Pawlowski, J.: Molecular identification of sequestered diatom chloroplasts and kleptoplastidy in foraminifera, Protist, 162, 394–404, doi:10.1016/j.protis.2010.10.001, 2011.

Pilon-Smits, E. A. H., Quinn, C. F., Tapken, W., Malagoli, M., and Schiavon, M.: Physiological functions of beneficial elements, Current Opinion in Plant Biology, 12, 267–274, doi:10.1016/j.pbi.2009.04.009, 2009.

Platon, E., Gupta, B. K. S., Rabalais, N. N., and Turner, R. E.: Effect of seasonal hypoxia on the benthic foraminiferal community of the Louisiana inner continental shelf: The 20th century record, Marine Micropaleontology, 54, 263–283, doi:10.1016/j.marmicro.2004.12.004, 2005.

Poignant, A., Mathieu, R., Levy, A., and Cahuzac, B.: *Haynesina germanica* (Ehrenberg), *Elphidium excavatum* (Terquem) ls et Porosononion granosum (d'Orbigny), espèces margino-littorales de foraminiféres d'Aquitaine centrale (SO France) au Miocène Moyen (Langhien). Le problème d'*Elphidium* lidoense Cushman, Revue de Micropaléontologie, 43, 393–405, doi:10.1016/S0035-1598(00)90200-9, 2000.

Polovodova, I. and Schönfeld, J.: Foraminiferal test abnormalities in the western Baltic Sea, Journal of Foraminiferal Research, 38, 318–336, doi:10.2113/gsjfr.38.4.318, 2008.

Poonkothai, M. and Vijayavathi, B. S.: Nickel as an essential element and a toxicant, International Journal of Environmental Sciences, 1, 285–288, 2012.

Powell, K. J., Brown, P. L., Byrne, R. H., Gajda, T., Hefter, G., Leuz, A.-K., Sjöberg, S., and Wanner, H.: Chemical Speciation of Environmentally Significant Metals: An IUPAC contribution to reliable and rigorous computer modelling, Chemistry International, 37, 15–19, doi:10.1515/ci-2015-0105, 2015.

Prothro, M. G.: Office of Water policy and technical guidance on interpretation and implementation of aquatic life metals criteria, United States Environmental Protection Agency., 1993.

Putri, L. S. E., Prasetyo, A. D., and Arifin, Z.: Green mussel (*Perna viridis L.*) as bioindicator of heavy metals pollution at Kamal estuary, Jakarta Bay, Indonesia, Journal of Environmental Research and Development, 6, 389–396, 2012.

Raikwar, M. K., Kumar, P., Singh, M., and Singh, A.: Toxic effect of heavy metals in livestock health, Veterinary World, 1, 28, doi:10.5455/vetworld.2008.28-30, 2008.

Railsback, L. B.: Patterns in the compositions, properties, and geochemistry of carbonate minerals, Carbonates and Evaporites, 14, 1, doi:10.1007/BF03176144, 1999.

Ramasamy, E. V., Jayasooryan, K. K., Chandran, M. S., and Mohan, M.: Total and methyl mercury in the water, sediment, and fishes of Vembanad, a tropical backwater system in India, Environmental Monitoring and Assessment, 189, 130, doi:10.1007/s10661-017-5845-2, 2017.

Reddy, M. S., Basha, S., Joshi, H. V., and Ramachandraiah, G.: Seasonal distribution and contamination levels of total PHCs, PAHs and heavy metals in coastal waters of the Alang–Sosiya ship scrapping yard, Gulf of Cambay, India, Chemosphere, 61, 1587–1593, doi:10.1016/j.chemosphere.2005.04.093, 2005.

Reeder, R. J., Lamble, G. M., and Northrup, P. A.: XAFS study of the coordination and local relaxation around Co^{2} Zn^{2+}, Pb^{2+}, and Ba^{2+} trace elements in calcite, American Mineralogist, 84, 1049–1060, doi:10.2138/am-1999-7-807, 1999.

Remmelzwaal, S. R. C., Sadekov, A. Y., Parkinson, I. J., Schmidt, D. N., Titelboim, D., Abramovich, S., Roepert, A., Kienhuis, M., Polerecky, L., and Goring-Harford, H.: Post-depositional overprinting of chromium in foraminifera, Earth and Planetary Science Letters, 515, 100–111, doi:10.1016/j.epsl.2019.03.001, 2019.

Rimstidt, J. D., Balog, A., and Webb, J.: Distribution of trace elements between carbonate minerals and aqueous solutions, Geochimica et Cosmochimica Acta, 62, 1851–1863, doi:10.1016/S0016-7037(98)00125-2, 1998.

Roberts, N. L., Piotrowski, A. M., Elderfield, H., Eglinton, T. I., and Lomas, M. W.: Rare earth element association with foraminifera, Geochimica et Cosmochimica Acta, 94, 57–71, doi:10.1016/j.gca.2012.07.009, 2012.

Rosenthal, Y., Boyle, E. A., and Slowey, N.: Temperature control on the incorporation of magnesium, strontium, fluorine, and cadmium into benthic foraminiferal shells from Little Bahama Bank: Prospects for thermocline paleoceanography, Geochimica et Cosmochimica Acta, 61, 3633–3643, doi:10.1016/S0016-7037(97)00181-6, 1997.

Rosenthal, Y., Field, M. P., and Sherrell, R. M.: Precise determination of element/calcium ratios in calcareous samples using sector field inductively coupled plasma mass spectrometry, Analytical Chemistry, 71, 3248–3253, doi:10.1021/ac981410x, 1999.

Sagar, N., Sadekov, A., Scott, P., Jenner, T., Vadiveloo, A., Moheimani, N. R., and McCulloch, M.: Geochemistry of large benthic foraminifera *Amphisorus hemprichii* as a high-resolution proxy for lead pollution in coastal environments, Marine Pollution Bulletin, 162, 111918, doi:10.1016/j.marpolbul.2020.111918, 2021a.

Sagar, N., Sadekov, A., Jenner, T., Chapuis, L., Scott, P., Choudhary, M., and McCulloch, M.: Heavy metal incorporation in foraminiferal calcite under variable environmental and acute level seawater pollution: multi-element culture experiments for *Amphisorus hemprichii*. Environmental Science and Pollution Research, 1-14, doi.org/10.1007/s11356-021-15913-z, 2021b.

Saha, N., Rahman, M. S., Ahmed, M. B., Zhou, J. L., Ngo, H. H., and Guo, W.: Industrial metal pollution in water and probabilistic assessment of human health risk, Journal of Environmental Management, 185, 70–78, doi:10.1016/j.jenvman.2016.10.023, 2017.

Schlitzer, R.: Ocean Data View, http://odv.awi.de, 2016.

Schmidt, S., and Schönfeld, J.: Living and dead foraminiferal assemblage from the supratidal sand Japsand, North Frisian Wadden Sea: distributional patterns and controlling factors. Helgoland Marine Research, 75(1), 1-22, doi: 10.1186/s10152-021-00551-2, 2021.

Schönfeld, J. and Numberger, L.: The benthic foraminiferal response to the 2004 spring bloom in the western Baltic Sea, Marine Micropaleontology, 65, 78–95, doi:10.1016/j.marmicro.2007.06.003, 2007.

Schweizer, M., Polovodova, I., Nikulina, A., and Schönfeld, J.: Molecular identification of *Ammonia* and *Elphidium* species (foraminifera, Rotaliida) from the Kiel Fjord (SW Baltic Sea) with rDNA sequences. Helgoland Marine Research, 65(1), 1-10, doi: 10.1007/s10152-010-0194-3, 2011.

Sen Gupta, B. K., Eugene Turner, R., and Rabalais, N. N.: Seasonal oxygen depletion in continental-shelf waters of Louisiana: Historical record of benthic foraminifers, Geology, 24, 227–230, doi:10.1130/0091-7613(1996)024<0227:SODICS>2.3.CO;2, 1996.

Shannon, R. T. D. and Prewitt, C. T.: Effective ionic radii in oxides and fluorides, Acta Crystallographica Section B: Structural Crystallography and Crystal Chemistry, 25, 925–946, doi:10.1107/S0567740869003220, 1969.

Sharifi, A. R., Croudace, I. W., and Austin, R. L.: Benthic foraminiferids as pollution indicators in Southampton Water, southern England, UK, Journal of Micropalaeontology, 10, 109–113, doi:10.1144/jm.10.1.109, 1991.

Shaw, D. R. and Dussan, J.: Mathematical modelling of toxic metal uptake and efflux pump in metal-resistant bacterium *Bacillus cereus* isolated from heavy crude oil, Water, Air, & Soil Pollution, 226, 1–14, doi:10.1007/s11270-015-2385-7, 2015.

Shijo, Y., Shimizu, T., and Tsunoda, T.: Determination of silver in seawater by graphite furnace atomic absorption spectrometry after solvent extraction and microscale back-extraction, Analytical Sciences, 5, 65–68, doi:10.2116/analsci.5.65, 1989.

Smith, C. W., Fehrenbacher, J. S., and Goldstein, S. T.: Incorporation of heavy metals in experimentally grown foraminifera from SAPELO island, Georgia and little duck key, Florida, USA, Marine Micropaleontology, 101854, doi:10.1016/j.marmicro.2020.101854, 2020.

Spindler, M.: The development of the organic lining in *Heterostegina depressa* (Nummulitidae; Foraminifera), Journal of Foraminiferal Research, 8, 258–261, doi:10.2113/gsjfr.8.3.258, 1978.

Spurgeon, D. J., Lofts, S., Hankard, P. K., Toal, M., McLellan, D., Fishwick, S., and Svendsen, C.: Effect of pH on metal speciation and resulting metal uptake and toxicity for earthworms, Environmental Toxicology and Chemistry: An International Journal, 25, 788–796, doi:10.1897/05-045R1.1, 2006.

Stankovic, S., Kalaba, P., and Stankovic, A. R.: Biota as toxic metal indicators, Environmental Chemistry Letters, 12, 63–84, doi:10.1007/s10311-013-0430-6, 2014.

Sunda, W. G. and Huntsman, S. A.: Interactions among Cu^{2+}, Zn^{2+}, and Mn^{2+} in controlling cellular Mn, Zn, and growth rate in the coastal alga *Chlamydomonas*, Limnology and Oceanography, 43, 1055–1064, doi:10.4319/lo.1998.43.6.1055, 1998a.

Sunda, W. G. and Huntsman, S. A.: Processes regulating cellular metal accumulation and physiological effects: Phytoplankton as model systems, Science of the Total Environment, 219, 165–181, doi:10.1016/S0048-9697(98)00226-5, 1998b.

Tachikawa, K. and Elderfield, H.: Microhabitat effects on Cd/Ca and $\delta^{13}C$ of benthic foraminifera, Earth and Planetary Science Letters, 202, 607–624, doi:10.1016/S0012-821X(02)00796-3, 2002.

Tansel, B. and Rafiuddin, S.: Heavy metal content in relation to particle size and organic content of surficial sediments in Miami River and transport potential, International Journal of Sediment Research, 31, 324–329, doi:10.1016/j.ijsrc.2016.05.004, 2016.

Tchounwou, P. B., Yedjou, C. G., Patlolla, A. K., and Sutton, D. J.: Heavy metal toxicity and the environment, Molecular, clinical and environmental toxicology, 133–164, doi:10.1007/978-3-7643-8340-4_6, 2012.

Thomas, M. A., Conaway, C. H., Steding, D. J., Marvin-DiPasquale, M., Abu-Saba, K. E., and Flegal, A. R.: Mercury contamination from historic mining in water and sediment, Guadalupe River and San Francisco Bay, California, Geochemistry: Exploration, Environment, Analysis, 2, 211–217, doi:10.1144/1467-787302-024, 2002.

Thornton, I.: Metals in the global environment. Facts and misconceptions: International Council on Metals and the Environment, 1995.

Titelboim, D., Sadekov, A., Hyams-Kaphzan, O., Almogi-Labin, A., Herut, B., Kucera, M., and Abramovich, S.: Foraminiferal single chamber analyses of heavy metals as a tool for monitoring permanent and short term anthropogenic footprints, Marine Pollution Bulletin, 128, 65–71, doi:10.1016/j.marpolbul.2018.01.002, 2018.

Titelboim, D., Sadekov, A., Blumenfeld, M., Almogi-Labin, A., Herut, B., Halicz, L., Benaltabet, T., Torfstein, A., Kucera, M., & Abramovich, S.: Monitoring of heavy metals in seawater using single chamber foraminiferal sclerochronology. Ecological Indicators, 120, 106931, doi: 10.1016/j.ecolind.2020.106931, 2021.Toyofuku, T., Suzuki, M., Suga, H., Sakai, S., Suzuki, A., Ishikawa, T., Nooijer, L. J. de, Schiebel, R., Kawahata, H., and Kitazato, H.: Mg/Ca and $\delta^{18}O$ in the brackish shallow-water benthic foraminifer *Ammonia 'beccarii'*, Marine Micropaleontology, 78, 113–120, doi:10.1016/j.marmicro.2010.11.003, 2011.

Urani, C., Melchioretto, P., Bruschi, M., Fabbri, M., Sacco, M. G., and Gribaldo, L.: Impact of cadmium on intracellular zinc levels in HepG2 cells: Quantitative evaluations and molecular effects, BioMed Research International, 2015, doi:10.1155/2015/949514, 2015.

van Dijk, I., Nooijer, L. J. de, and Reichart, G.-J.: Trends in element incorporation in hyaline and porcelaneous foraminifera as a function of pCO_2, Biogeosciences, 14, 497–510, doi:10.5194/bg-14-497-2017, 2017.

Venugopal, B. and Luckey, T. D.: "Toxicology of nonradio-active heavy metals and their salts", in Heavy Metal Toxicity, Safety and Hormology, T. D. Luckey, B. Venugopal, D. Hutcheson (Eds.). In: George Thieme, Stuttgart, 1975.

Vlahogianni, T., Dassenakis, M., Scoullos, M. J., and Valavanidis, A.: Integrated use of biomarkers (superoxide dismutase, catalase and lipid peroxidation) in mussels *Mytilus galloprovincialis* for assessing heavy metals' pollution in coastal areas from the Saronikos Gulf of Greece, Marine Pollution Bulletin, 54, 1361–1371, doi:10.1016/j.marpolbul.2007.05.018, 2007.

Wang, G. and Fowler, B. A.: Roles of biomarkers in evaluating interactions among mixtures of lead, cadmium and arsenic, Toxicology and Applied Pharmacology, 233, 92–99, doi:10.1016/j.taap.2008.01.017, 2008.

Wang, Z., Chen, J., Cai, H., Yuan, W., & Yuan, S.: Coprecipitation of metal ions into calcite: an estimation of partition coefficients based on field investigation. Acta Geochimica, 40(1), 67-77, doi: 10.1007/s11631-020-00443-1, 2021.

Wefer, G.: Umwelt, Produktion und Sedimentation benthischer Foraminiferen in der westlichen Ostsee, Reports Sonderforschungsbereich 95 Wechselwirkung Meer - Meeresboden, 14, 1–103, 1976.

Williams, T. M., Rees, J. G., and Setiapermana, D.: Metals and trace organic compounds in sediments and waters of Jakarta Bay and the Pulau Seribu Complex, Indonesia, Marine Pollution Bulletin, 40, 277–285, doi:10.1016/S0025-326X(99)00226-X, 2000.

Wit, J. C., Nooijer, L. J. de, Wolthers, M., and Reichart, G.-J.: A novel salinity proxy based on Na incorporation into foraminiferal calcite, Biogeosciences, 10, 6375–6387, doi:10.5194/bg-10-6375-2013, 2013.

Woehle, C., Roy, A.-S., Glock, N., Wein, T., Weissenbach, J., Rosenstiel, P., Hiebenthal, C., Michels, J., Schönfeld, J., and Dagan, T.: A novel eukaryotic denitrification pathway in foraminifera, Current Biology, 28, 2536-2543. e5, doi:10.1016/j.cub.2018.06.027, 2018.

Wokhe, T. B.: Heavy metals pollution of water and sediment in Mada River, Nigeria, Journal of Scientific Research and Reports, 157–164, doi:10.9734/JSRR/2015/14803, 2015.

Xiang, R., Yang, Z., Saito, Y., Fan, D., Chen, M., Guo, Z., and Chen, Z.: Paleoenvironmental changes during the last 8400 years in the southern Yellow Sea: Benthic foraminiferal and stable isotopic evidence, Marine Micropaleontology, 67, 104–119, doi:10.1016/j.marmicro.2007.11.002, 2008.

Yanko, V., Ahmad, M., and Kaminski, M.: Morphological deformities of benthic foraminiferal tests in response to pollution by heavy metals; implications for pollution monitoring, Journal of Foraminiferal Research, 28, 177–200, 1998.

Yeghicheyan, D., Aubert, D., Bouhnik-le Coz, M., Chmeleff, J., Delpoux, S., Djouraev, I., Granier, G., Lacan, F., Piro, J.-L., and Rousseau, T.: A New Interlaboratory Characterisation of Silicon, Rare Earth Elements and Twenty-Two Other Trace Element Concentrations in the Natural River Water Certified Reference Material SLRS-6 (NRC-CNRC), Geostandards and Geoanalytical Research, 43, 475–496, doi:10.1111/ggr.12268, 2019.

Yılmaz, S. and Sadikoglu, M.: Study of heavy metal pollution in seawater of Kepez harbor of Canakkale (Turkey), Environmental Monitoring and Assessment, 173, 899–904, doi:10.1007/s10661-010-1432-5, 2011.

4. Scientific Chapter III. Incorporation of dissolved heavy metals into the skeleton of the scleractinian corals *Porites lobata* and *Porites lichen* based on multi-element culturing experiments

In preparation for submission to a peer-reviewed journal as: Schmidt, S., Hathorne, E. C., Schönfeld, J., Kathleen Gosnell & Garbe-Schönberg, D.: Incorporation of dissolved heavy metals into the skeleton of the scleractinian corals *Porites lobata* and *Porites lichen* based on multi-element culturing experiments.

Abstract.
Coral reefs house an extraordinary biodiversity and provides fish, a tourist attraction and natural shoreline protection and are therefore vitally important for humans. Anthropogenic influences like ship traffic, agriculture, urban runoff or mining increased the level of dissolved heavy metals in some tropical near-shore environments threatening reef ecosystems. Monitoring of the ecosystem status by using chemical tracers in sessile organisms becomes increasingly important for reef risk assessment and environmental management. The skeleton of stony corals like *Porites* species provide a high-resolution geochemical archive for the recent and past heavy metal concentration in the ambient seawater, yet they are not sufficiently calibrated. To address this, culturing experiments exposing *Porites lobata* and *Porites lichen* to a mixture of dissolved chromium (Cr), manganese (Mn), nickel (Ni), copper (Cu), zinc (Zn), silver (Ag), cadmium (Cd), tin (Sn), mercury (Hg) and lead (Pb) over a wide concentration range have been performed. Water samples were taken frequently to monitor expected changes in the heavy metal concentration due to adsorption. The concentrations of some metals declined as anticipated but stabilised a few days after the input of the high metal stock solution. Laser ablation ICP-MS measurements of the coral aragonite revealed metal concentrations that were positively correlated with Cr, Mn, Ni, Zn, Ag, Cd and Pb concentrations in the culturing medium. Cu and Sn showed no variance as the variation in the concentration of these metals in the experimental seawater was minimal. Hg did not exhibit any clear trend, even though the Hg concentration in seawater varied by a factor > 5 between phases. The calibrations and calculated partition coefficients (D_{TE}) values for some metals enable a reconstruction of the heavy metal concentration in seawater for ecosystem monitoring and potentially century long records revealing baseline values before large-scale human disturbance.

4.1 Introduction

Modern tropical reefs are undergoing increasing degradation by natural and man-made factors such as global warming, extreme weather conditions, natural diseases, invasive coral predators, urban and agricultural runoff, ship anchoring, over-tourism and plastic pollution (e.g., Mieremet, 1997; Dar et al., 2018). These impacts impose stress on the corals and other organisms (e.g., Anthony, 1999; Correge, 2006), and also introduce heavy metals to the oceans. Heavy metals occur naturally in the Earth´s crust in generally low concentrations and geogenic sources include the chemical and physical weathering of rocks, leaching of soils and volcanic eruptions (Mansour et al., 2013). Heavy metals are defined here as elements with a density >7 g/cm^3 (Venugopal and Luckey, 1975) and an atomic number beyond calcium (Bjerrum, 1936; Thornton, 1995). They can reach toxic levels if the ambiental concentration exceeds a certain threshold, which can be caused by anthropogenic activities, e.g., through emissions of industrial by-products (e.g., Weis, 2015; Nour, 2019). Heavy metals are highly persistent, not readily biodegradable and are thus concentrated in the food chain of aquatic organisms (Diagomanolin et al., 2004; Santhanam, 2011; Zhang and Gao, 2015; Bosch et al., 2016; Liu et al., 2018; Sonone et al., 2020). The metals occur as dissolved ions, molecular complexes, or bound to colloids and (suspended) sediments (Larocque, and Rasmussen, 1998). Their individual toxicity depends on factors like concentration, synergistic-antagonist effects and physico-chemical properties. They can enter the tissue of organisms through the respiratory tract, digestion or penetration through the skin (Darmono, 2001).

Various marine organisms have been investigated as environmental indicators of heavy metal pollution. For example, plants like seaweed are able to accumulating heavy metals (Davis et al., 2000; Besada et al., 2009; Arumugam et al., 2020), foraminifera can be used as bioindicators for heavy metal pollution in temperate and tropical seas (Frontalini and Coccioni, 2008; Munsel et al., 2010; Titelboim et al., 2021; Oron et al., 2021; Li et al., 2021), and marine sponges are also reported to bioaccumulate heavy metals (Cebrian and Turon, 2007; Batista et al., 2014; Rodríguez and Morales, 2020). Moreover, corals are used as a tool for pollution monitoring because their skeletons are excellent environmental archives and accurately record long- and short-term changes (Al-Rousan et al., 2007; Chen et al., 2010; Abdo et al., 2017; Nour and Nouh, 2020). They are highly sensitive to physical and chemical changes in their environment (Shen, 1996; David, 2003). Nonetheless, they can survive the exposure to high heavy metal concentrations (Readman et al., 1996; El-Sorogy at al., 2012). Metal-to-calcium ratios in coral skeletons are used to investigate historic human activities and long term impacts of these activities on water quality throughout shallow water regions (e.g., Alibert et al., 2003; McCulloch et al., 2003; Fleitmann et al., 2007; Carriquiry and Horta-Puga, 2010; Prouty et al., 2010; Lewis et al., 2012; Nguyen et al., 2013; Sowa et al., 2014; Saha et al., 2016; Jiang et al., 2020). These studies demonstrated changing water quality due to land-use changes, industrialization, mining and deforestation. Guzmán and García (2002), for example, investigated the mercury content in coral skeletons along the Caribbean coast and found elevated values from various sources like erosion, mining or industrial waste. They concluded based on their investigations that Hg is transported over long distances and is therefore also affecting formerly pristine reefs far from the pollution source itself.

The scleractinian coral *Porites* is globally distributed and has a simple growth structure. Different species are found in the tropical Indo-Pacific Ocean (Reyes-Bonilla, 1992;

Kaczmarsky and Richardson, 2007; Tortolero-Langarica et al., 2017), the Great Barrier Reef off eastern Australia (Lough and Barnes, 1996; Wu et al., 2021) and in the Caribbean (Green et al., 2008; Lord et al., 2021). The high growth rate of these massive stony corals allows measurements at sub-annual resolution as well as assembling continuous environmental archives covering hundreds of years (Schneider and Smith, 1982; Kefu et al., 2001; Clark et al., 2012; Leonard et al., 2019).

Most environmental pollution studies based on the analysis of coral skeletons were carried out by using coral samples from field sites and investigated the heavy metal concentration in naturally grown specimens to reconstruct the metal pollution during the past (Barakat et al., 2015; Nour and Nouh, 2020; and reference therein). To date, no culturing studies addressed the extent that changing seawater metal concentrations are incorporated into the coral skeleton. Therefore, the main objective of the present study was to investigate the heavy metal incorporation into the skeleton of the stony corals *Porites lobate* and *Porites lichen*. Culturing experiments with a mixture of metals, i.e., chromium (Cr), manganese (Mn), nickel (Ni), copper (Cu), zinc (Zn), silver (Ag), cadmium (Cd), tin (Sn), mercury (Hg) and lead (Pb), were carried out over a concentration range that covers the situation in polluted and unpolluted near-shore environments today. The partitioning factor (D_{TE}) between the seawater and the aragonite of the corals was constrained by relating the analytical data of weekly to biweekly water samples to laser ablation (LA) ICP-MS measurements of the skeleton grown during culturing. The results refine the use of stony corals as a reliable monitoring tool to track anthropogenic footprints in presumably pristine tropical environments as well as in areas of high human impact.

4.2 Methods

4.2.1 Experimental Concept

Culturing experiments were configured with two experimental aquaria of the same dimensions and design in an air-conditioned room. In addition, one large host aquarium was used for acclimation and nursery of commercially purchased corals. The host aquarium was described by Taubner et al. (2017). Four different coral colonies were acquired and species determined by genotyping. All colonies were divided into subcolonies and maintained in the host tank until the tissue has overgrown the cutting planes. Afterwards, one subcolony was placed in each experimental tank and one was left in the host aquarium. The control aquarium remained unmodified while the trace metal concentration in the metal aquarium was elevated stepwise. The trace metal concentration in both tanks was monitored during the culturing period. Therefore, a direct comparison of a coral from the same colony growing in the same settings with only the heavy metal concentration of the ambient seawater differing was possible. Growth control was performed by Alizarin Red S staining prior and during the experiment. More than 15 months later after the experiment, specimens were cut again and the growth was estimated from the stained bands and the trace metal concentration in the coral skeleton measured by Laser ablation ICP-MS.

4.2.1.1 Culturing System

The two identically aquarium systems were built by Whitecorals, Korntal-Münchingen, Germany (Figure 4.1a). The design was adapted from earlier culturing facilities and professional aquaria (Allison et al., 2014; Taubner et al., 2017). Initial seawater was taken from the host aquarium. This system, which was in operation since 2013 thus provided a complete ecosystem with adequate microbiological ingredients. The host water was mixed with North Sea water of 28 units and the salinity was adjusted to 35 units by adding synthetic sea salt (Tropic Marin Pro-Reef ®). Water exchanges with artificial seawater of approximately 10 vol% were carried out every three to four weeks during the complete culturing period. In addition, one litre of water from the host tank was added to the experimental systems three times a week. Aquaillumination Hydra FiftyTwo HD LED lamps were used for illumination. The down-welling irradiation was set to 220-280 µmol photos m^{-2} s^{-1} and a photoperiod of 10 h dark-14 h light with a dimming period of one hour before transition from dark to light in the morning and from light to dark in the evening was applied. The colour spectrum and intensity of the light was tuned to the values of the illumination of the host tank, because the coral colonies grew in this setting and were of good health before.

The main tank of each experimental aquarium had a water volume of 50 l and was equipped with a Tunze Turbelle nanostream 6045 streaming pump and an EHEIM aquaball 130 filter. Furthermore, an adjustable plastic grid made especially for the tank was installed, which made it possible to guarantee an optimal distance from the lamps to the coral colonies. The water from the main tank flowed via a solid PVC tubing downwards into a filter tank with three different chambers. Larger particles settled in the first chamber. An Aqua Medic Evo 1000 protein skimmer removed hydrophilic proteins by mixing air and water in the second chamber. The protein molecules or particles stacked to the air bubbles and rose until they reached an overflow collection cup where they were removed. The protein skimmer not only removed possible hydrophilic contaminants but also added air to the system, which ensured oxygen saturation of the water. The processed water was pumped back from chamber three into the main tank by an EHEIM compact ON 300 pump with a flow rate of approximately 200 l per hour for the whole system. Water loss through evaporation was compensated by adding deionized water, which was automatically pumped into chamber three of the filter tank when an optical water level sensor (GHL Level Sensor, Optolevel) registered a drop of the water level. For maintaining the temperature at 25 °C, a JBL Cooler 100 chiller, placed on top of the main tank, or an EHEIM thermocontrol 150 Watt heater was placed in the filter tank. Heater and chiller were automatically controlled by the GHL Profilux computer.

Live rocks with a high porosity were placed in the main tank to ensure a functional denitrification process, which is vitally important for the water quality of the aquaria. Soft corals *Capnella* sp. and stony corals *Pocillopora* sp., *Seriatopora* sp. and *Montipora* sp. were the first coral inhabitants. Furthermore, snails and hermit crabs were inserted, which cleaned the aquarium from excessive algae and other leftover particles. The hermit crabs were fed 3 times a week with 1.5 pieces of NovoCrab food from JBL.

During coral growth, calcium and bicarbonate were consumed from the seawater to form coral skeleton. These constituents were replenished by adding an adequate amount of two different stock solutions following the Balling Light method. Stock solution 1 consisted mainly of $CaCl_2$ * 2 H_2O and the Balling solutions 1 (high-purity water, $BaCl_2$ * 2 H_2O, $SrCl_2$ * 6 H_2O) and 2 (high-purity water, $CoCl_2 * 6 H_2O$, $MnSO_4 * H_2O$, $CuSO_4 * 5 H_2O$, $ZnSO_4 * 7 H_2O$, $NiSO_4 * 6 H_2O$, $FeSO_4 * 7 H_2O$, $KCr(SO_4)_2 * 12 H_2O$). The main ingredient of stock solution 2 was $NaHCO_3$ mixed with Balling solution 3 (ultra-purity water, KI, NaF, $Na_2B_4O_7 * 10 H_2O$). Both stock solutions were added four times a day by using a Dupla Marin Dosing Pump P4 Smart. The total amount of the stock solution per day varied due to changes in calcification rates of the corals between 16 and 24 ml.

For measuring salinity, temperature and pH, GHL sensors connected to a GHL Profilux 4 computer were placed in the main tank recording all parameters two times an hour.

Other water parameters like calcium, magnesium, nitrate and phosphate concentration and the carbonate hardness, which approximated the alkalinity in seawater, were monitored once a week. Phosphate and nitrate concentrations were measured with a custom Wasserpantcher photometer. All other tests were performed with JBL quick test stripes. These quick tests were adequate for frequent measurements, which is vitally important because it enables to react to changes in the water quality immediately.

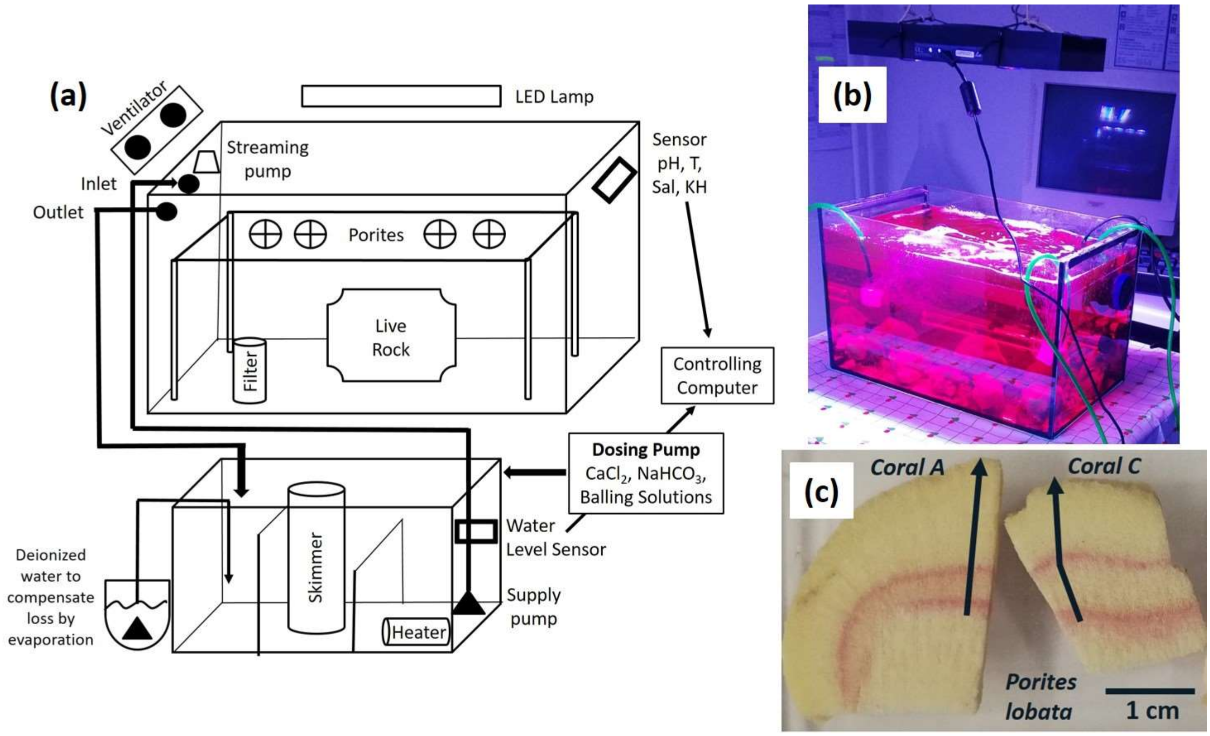

Figure 4.1: Schematic drawing of the culturing system (a), staining procedure with Alizarin Red S (b) and coral slices after culturing (c). Part c shows corals A and C. Furthermore, the course of the laser ablation line is indicated, and the reddish staining lines are visible. Staining took place before phase 0 and before phase 1.

4.2.1.2 Preparation for culturing

Coral culturing was performed at GEOMAR Helmholtz Centre for Ocean Research Kiel from February 2019 to September 2020. Three colonies of *Porites* were purchased from different hobby aquarium zoological retailer companies in Germany. After arrival, samples for DNA analyses of the coral tissue were taken to determine the species of the colonies. Genetic analyses and genotyping were performed by omics2view.consulting, Kiel, Germany. Sanger sequencing of cytochrome c oxidase subunit I mitochondrial genes (COI) and the nuclear ribosomal internal transcribed spacer region (ITS) was applied. The sequences were compared to GenBank data for species determination. Reference sequences of COI and the ITS from Forsman et al. (2009) were retrieved from NCBI (Sayers et al., 2009) and the program BLAST+ v2.9.0 (Altschul et al., 1990) was used to find close relatives for the sequences. Maximum likelihood phylogenetic trees were calculated from multiple sequence alignments (produced with MAFFT v7.427, Katoh et al., 2002; Katoh and Standley, 2013) with IQ-TREE v1.6.10 (Nguyen et al., 2015).

Before the colonies were inserted into the culture aquaria, they were kept in the host tank for several weeks to monitor their health and give them time to acclimate to the new environments. These colonies were divided into three equal subcolonies using a disinfected handsaw. Subcolonies, which were not able to stand on their own, were glued with AQUA SCAPE FIX, Fauna Marin GmbH coral glue to a breed disc holder. The size of the different subcolonies varied according to the size of the mother colony between 5 and 10 cm in diameter. All colonies were maintained in the host tank again for at least 2 months to ensure an adequate recovery after cutting. All colonies grew during that time, showed polyp activity and a bright colour.

The culturing aquaria underwent an initial warm-up period lasting approximately 4 months. During this period, the biological parameters equilibrated (e.g., denitrification processes) and accompanying corals were inserted stepwise. When these corals grew and showed a good vitality, the subcolonies of *Porites* were inserted into the experimental tanks. Prior to this, the growth stage was marked. The subcolonies were set into a smaller aquarium containing water with Alizarin Red S (~16 mg/l; (3,4-Dihydroxy-9,10-dioxo-2-anthracenesulfonic acid sodium salt, Sigma Aldrich; Figure 4.1) and left in there for approximately 8 hours for staining. In the presence of calcium, Alizarin Red S, adsorbs to calcium and forms a pigment that is orange to red in colour. Afterwards, the corals were put back into the host tank for recovery for approximately 1 week until they were inserted into the culturing aquaria.

4.2.1.3 Experimental Setup

The culturing period was divided into different phases. Phase 0 lasted for 19 weeks, phase 1 to 3 took 10 weeks each and phase 4 covered 13 weeks. One aquarium was used as control, where the water was never poisoned and the other tank was used for the heavy metal treatments.

Subcolonies from corals A through D were inserted into the metal and the control system. Phase 0 was an initial control phase without any extra-added metals in both systems. A second staining with Alizarin Red S was carried out after phase 0 to mark the onset of the metal addition and to estimate the growth rate of the colonies (Figure 4.1). Beginning with phase 1, the heavy metal concentration in the metal system was elevated stepwise by adding a certain amount of the stock solution (phase 1=8.2 ml; phase 2=82 ml, phase 3=410 ml; phase 4=2050 ml; Table 4.1). For maintaining the heavy metal concentration during each culturing period as stable as possible, an aliquot (phase 1=0.1 ml; phase 2=1 ml, phase 3=10 ml; phase 4=100 ml) of the stock solution was added daily to counteract the uptake of heavy metals by the corals and other organisms or removal by adsorption on surfaces of the system, protein skimmer and filters. On every water exchange, a higher amount of the stock solution was added to ensure that the metal concentration was not dropping due to the renewal of seawater.

The target concentrations of individual heavy metals (see Table 4.1) were selected to cover a wide range of concentrations resembling conditions as observed in polluted tropical areas, e.g., Jakarta Bay (e.g., Williams et al., 2000). The concentrations were aimed at not to reduce their growth and normal metabolism. Therefore, recommended threshold values provided by the Environmental Protection Agency, USA (EPA) were included. Additionally, values from Reichelt-Brushett and Harrison (2005) addressing the effect of heavy metals on coral fertilization were taken into account. Baudouin and Scoppa (1974) further investigated the toxicity of heavy metals to zooplankton, which was also considered. The heavy metal concentrations in the seawater during each phase were monitored by frequent water sampling. Temperature, pH and salinity were kept stable at 25.1 (±0.2) °C, 8.3 (±0.1) and 34.9 (±0.3) units in the metal system, and at 25.1 (±0.2) °C, 8.2 (±0.1) and 34.8 (±0.2) units in the control system respectively over the entire culturing period.

Table 4.1: Heavy metal concentration in the stock solution, target concentration of these metals in each phase in the metal system and salt compounds. All salts used were p.a. (pro analysi) purity.

			Target conc. in µg/l			
	Salt compound (pro analysi quality)	**Conc. in mg/l Stock solution**	**Phase 1**	**Phase 2**	**Phase 3**	**Phase 4**
Chromium (Cr)	$CrCl_3$ * 6 H_2O	25	0.25	2.5	12.5	62.5
Manganese (Mn)	$MnCl_2$ * 4 H_2O	40	0.4	4	20	100
Nickel (Ni)	$NiCl_2$ * 6 H_2O	5	0.05	0.5	2.5	12.5
Copper (Cu)	$CuCl_2$ * 2 H_2O	2	0.02	0.2	1	5
Zinc (Zn)	$ZnCl_2$	50	0.5	5	25	125
Cadmium (Cd)	$CdCl_2$	4	0.1	1	5	25
Silver (Ag)	$AgNO_3$	3.5	0.04	0.4	2	10
Tin (Sn)	$SnCl_2$ * 2 H_2O	10	0.1	1	5	25
Mercury (Hg)	$HgCl_2$	0.04	0.004	0.04	0.2	1
Lead (Pb)	$PbCl_2$	10	0.1	1	5	25

4.2.2 Water Samples

To constrain the heavy metal concentration in the culturing medium, water samples were frequently taken from the metal and the control system (Table 4.2).

The samples were taken with 25 ml syringes, filtered through a 0.2 µm filter and stored in HDPE bottles until analysis. Filters were flushed with the sample water before the sample was taken. Immediately after collection, the samples were acidified using distilled, concentrated HCl (0.1 vol % of the sample volume). Hg samples were further treated with BrCl to ensure the release of mercury species that are possibly present in a different oxidation state. All water samples were preconcentrated offline with a SeaFAST system (ESI, USA). For metals that cannot be preconcentrated by the SeaFAST system (Cr, Ag and Sn) samples were diluted and analysed directly (Schmidt et al., 2021).

The element concentration in the seawater was determined by different techniques at GEOMAR (Table 4.2). For major elements like Ca, inductively coupled plasma optical emission spectrometry (ICP-OES, Model VARIAN 720-ES) was used. Frequent measurements of an IAPSO standard seawater revealed an internal precision expressed as the relative standard deviation (RSD %) of less than ±0.35 % (mean Ca concentration IAPSO standard = 419.6 ± 0.15 mg/l; reference Ca concentration of IAPSO Batch 161 = 423 mg/l). Cr, Mn, Ni, Cu, Zn, Ag, Cd, Sn and Pb concentrations were measured using an Agilent 7500ce quadrupole ICP-

MS. The accuracy and precision derived from measurements of reference materials are given in Table B4.1. A Total Mercury Manual System (Brooks Rand Model III) was used for analysing the Hg content of the samples. Quality control of the Hg measurements revealed uncertainties smaller than 4.5 % RSD for all analyses.

4.2.3 Coral Samples

After the culturing period, the corals were taken out of the experimental tanks and slices were cut from each individual colony (see Figure 4.1c). These slices were subsequently treated with sodium hypochlorite solution (NaClO, 13% Cl_2) for at least 24 hours to remove organic compounds. Afterwards, the coral slices were rinsed with pure, $CaCO_3$ equilibrated MilliQ water, which was used to avoid leaching of elements from the aragonite surface and dried in an oven over night (T<40 °C).

Micro-analytical analyses with LA-ICP-MS were performed at the Institute of Geosciences, Kiel University, to analyse the heavy metal concentration in the coral skeleton. A 193 nm ArF excimer GeoLasPro HD system (Coherent) with a large volume ablation cell (Zurich-type LDHCLAC, Fricker et al., 2011) and helium as the carrier gas was used. An amount of 14 ml min^{-1} H_2 was added to the helium prior to passing the ablation cell. Line scans were performed orthogonally to the growth direction of the coral from the periphery to the inner parts until below the first staining line that marked the onset of the experiment (see Figure 4.1). Replicate lines were drawn on different parts of the colonies. The energy density of the laser was set to 10 J/cm^3, the laser spot size was 120 µm diameter and the stage moved 50 µm/s. Prior to every scan, a preablation pass with a spot size of 160 µm diameter was carried out to clean the cut surface of the coral skeleton. Before and after each line scan, the gas blank was measured for at least 30 s. These values are considered as the background intensities of the different isotopes. The background signals were subtracted from each ablation profile during the data reducing process. The isotope ^{43}Ca was used as an internal standard and the trace metal concentration of the samples was calibrated using the reference material NIST SRM 612 glass (Jochum et al., 2011). Glasses were ablated with a pulse rate of 10 pulses per second, an energy density of 10 J/cm and a spot size of 60 µm. Since the NIST glass does not contain any mercury, the synthetic spiked carbonate MACS-3 (Inoue et al., 2004; Jochum et al., 2019) was used for the calibration of Hg. Furthermore, carbonate matrix reference materials (coral JCp-1, giant clam JCt-1, limestone ECRM752-1; Inoue et al., 2004; Jochum et al., 2019) were analysed in the form of nano-particle pellets (Garbe-Schönberg and Müller, 2014) for additional quality control. The trace-element-to-calcium ratios were calculated using the following isotopes: ^{26}Mg, ^{27}Al, ^{52}Cr, ^{55}Mn, ^{60}Ni, ^{63}Cu, ^{65}Cu, ^{68}Zn, ^{107}Ag, ^{111}Cd, ^{114}Cd, ^{118}Sn, ^{201}Hg, ^{202}Hg and ^{208}Pb. Once more than one isotope was analysed, the average value of these isotope was used for further analysis. External relative precision, expressed as the relative standard deviation in % (RSD% = standard deviation/average×100), of all TE/Ca measurements was less than 5.5 %. TE/Ca values and uncertainties of all reference materials are provided in the appendix (Table B4.2). Internal relative precision, measured through repeated line scans on the reference materials JCp-1 and MACS-3, were less than 10 % and 5 %, respectively. Time resolves raw intensities (in counts per seconds) for all isotopes measured were processed with the software Iolite (Version 4). Statistical analysis of the data was performed with the program PAST (Hammer, 2001; Schmidt et al., 2021).

The partition coefficients (D_{TE}) of the different trace metal-to-calcium ratios were calculated by using the corresponding concentrations in aragonite and seawater:

$$D_{TE} = (TE/Ca)_{aragonite}/(TE/Ca)_{seawater}.$$

The calculation of growth rates for each subcolony was primarily based on the stained lines that marked the onset of phase 0 and 1. The division between the following culturing phases was based on sudden and persistent elevations of metal concentrations in the coral skeleton as displayed in the LA-ICP-MS records. These markers were available only in the metal system. The surface of the corals after termination of the experiment provided a third age control point available for all subcolonies that survived the experiment.
A composite line was calculated individually for all colonies consisting of the laser ablation measurements along the main growth axis of the coral (coral A line 1-3, coral B line 1-3, coral C line 2 + 3, coral D line 1). Laser ablation measurements along lines that deviated from the main growth axis of the coral were not included in the composite line. Calculations were performed with QAnalyseries (Kotov and Paelike, 2018).

4.3 Results

4.3.1 Species identification

The placement of the samples in the COI tree suggested that samples from coral A, B and C were almost identical, while sample D differed from the others. Combined with information from the ITS phylogeny, the species identification revealed that coral A, B and C belong to the species *Porites lobata* and coral D was identified as *Porites lichen*. *Porites lobata* is a common, cosmopolitan species. Both species co-occure in the tropical parts of the Indian Ocean (e.g., Cacciapaglia and van Woesikand, 2018; Séré et al., 2012) and in the Pacific Ocean (e.g., D'Croz et al., 2001; Tisthammer and Richmond, 2018).

4.3.2 Metals in water

Table 4.2: TE/Ca values in the culturing medium of the control and the metal system. Furthermore, the mean values ± the standard error of the mean (standard deviation σ/√n) are given for both systems at the bottom of the table. Note that no Hg values are available for phase 0 of both systems. CL=Metal system, CR=Control system, W=week, D=Day, SE=Standard Error, Ph=Phase.

Sample ID	Ph	Sampling Date	Cr/Ca	Mn/Ca	Ni/Ca	Cu/Ca	Zn/Ca
Metal System			**µmol/mol**	**mmol/mol**	**µmol/mol**	**µmol/mol**	**µmol/mol**
CL0 W2	0	16.8.19	17.2	0.36	2.22	3.97	1.88
CL0 W3	0	25.8.19	15.2	0.28	2.01	5.28	1.68
CL0 W4	0	29.8.19	18.6	0.59	2.23	4.71	1.69
CL0 W5	0	4.9.19	16.5	0.30	2.02	4.00	1.27
CL0 W6	0	9.9.19	17.5	0.29	1.89	3.47	0.87
CL0 W7	0	16.9.19	16.4	0.53	2.00	3.45	1.06
CL0 W8	0	23.9.19	7.4	0.34	1.87	3.18	0.84
CL0 W9	0	2.10.19	5.2	1.65	2.16	3.11	1.19

CL0 W10	0	7.10.19	1.0	0.38	1.94	2.81	1.01
CL0 W11	0	15.10.19	3.3	0.42	2.76	4.56	1.80
CL0 W12	0	21.10.19	5.2	0.99	2.77	4.19	1.60
CL0 W13	0	28.10.19	22.1	0.41	2.36	3.39	1.07
CL0 W14	0	4.11.19	4.8	15.46	2.42	3.47	1.67
CL0 W15	0	11.11.19	4.7	1.10	2.29	3.75	1.56
CL0 W16	0	21.11.19	3.0	0.48	2.14	3.07	0.89
CL0 W17	0	28.11.19	9.0	54.42	2.35	3.78	1.85
CL0 W18	0	5.12.19	5.9	0.58	2.26	3.51	1.21
CL0 W19	0	10.12.19	8.2	0.42	1.96	2.86	1.19
CL1 W1 D1	1	16.12.19	16.2	42.66	1.91	3.22	4.28
CL1 W1 D2	1	17.12.19	6.1	4.08	1.66	2.71	1.96
CL1 W1 D3	1	18.12.19		1.46	1.61	2.58	1.71
CL1 W1 D4	1	19.12.19	4.8	0.98	1.59	2.45	1.40
CL1 W1 D5	1	20.12.19	3.4	0.72	1.58	2.44	1.38
CL1 W4	1	6.1.20	12.6	0.47	1.52	2.02	1.07
CL1 W5	1	16.1.20	16.6	0.33	1.48	1.87	0.85
CL1 W6	1	23.1.20	17.2	0.32	1.50	1.84	0.97
CL1 W6 D2	1	24.1.20	6.5	53.75	1.77	2.53	4.60
CL1 W7	1	28.1.20	6.6	0.71	1.57	2.14	1.49
CL1 W8	1	6.2.20	11.8	0.38	1.62	2.01	1.25
CL1 W9	1	10.2.20	9.7	0.40	1.68	2.01	2.00
CL1 W10	1	18.2.20	9.9	0.35	1.70	1.90	1.38
CL2 W1 D1	2	24.2.20	21.3	65.72	4.12	3.04	24.45
CL2 W1 D2	2	25.2.20	10.1	13.68	4.44	3.43	24.06
CL2 W1 D3	2	26.2.20	11.4	4.71	4.23	3.25	19.02
CL2 W1 D4	2	27.2.20	10.0	2.11	3.89	3.11	13.61
CL2 W2	2	2.3.20	15.2	0.81	2.50	2.29	5.65
CL2 W3	2	9.3.20	15.6	0.39	2.35	2.12	3.00
CL2 W4	2	16.3.20	23.5	0.74	2.46	2.38	4.25
CL2 W5	2	26.3.20	23.4	0.40	2.38	2.04	4.69
CL2 W6	2	31.3.20	23.7	36.35	3.42	3.10	11.70
CL2 W7	2	7.4.20	12.9	0.94	3.16	2.69	7.83
CL2 W8	2	14.4.20	14.4	0.77	3.23	2.60	6.48
CL2 W9	2	23.4.20	16.4	0.90	3.51	2.52	6.70
CL2 W10	2	30.4.20	19.2	0.78	3.41	2.43	5.35
CL3 W1 D1	3	4.5.20	25.3	471.60	35.74	7.32	231.38
CL3 W1 D2	3	5.5.20	21.5	28.64	25.53	6.23	147.40
CL3 W1 D3	3	6.5.20	21.6	7.93	24.20	6.22	125.60
CL3 W1 D4	3	7.5.20	23.2	4.46	21.68	6.08	97.91
CL3 W1 D5	3	8.5.20	21.1	4.83	21.26	6.06	95.07
CL3 W2	3	12.5.20	28.4	3.97	20.98	6.90	74.34
CL3 W3	3	19.5.20	29.0	1.09	18.50	6.47	54.85
CL3 W4	3	26.5.20	36.6	9.62	23.01	7.61	96.69
CL3 W5	3	4.6.20	33.6	1.49	18.18	7.10	51.46
CL3 W6	3	11.6.20	43.8	1.14	18.00	6.64	49.56
CL3 W7	3	18.6.20	35.7	1.57	19.52	7.27	66.41
CL3 W8	3	25.6.20	35.1	1.48	18.95	6.91	64.78
CL3 W9	3	2.7.20	34.3	2.04	21.37	7.18	80.55
CL3 W10	3	9.7.20	40.8	3.41	22.40	7.33	82.62
CL4 W1 D1	4	15.7.20	45.6	1481.77	115.78	13.96	838.40
CL4 W1 D2	4	16.7.20	43.6	500.63	102.15	13.06	558.04
CL4 W1 D3	4	16.7.20	43.6	169.29	93.66	12.82	474.13

CL4 W1 D4	4	17.7.20	42.7	27.98	85.11	12.02	383.54
CL4 W2	4	22.7.20	43.4	6.02	78.73	10.70	295.59
CL4 W3	4	27.7.20	48.5	6.37	66.31	9.42	239.15
CL4 W4	4	6.8.20	50.4	4.33	26.81	4.42	80.54
CL4 W5	4	13.8.20	52.5	3.89	54.85	9.76	196.20
CL4 W6	4	20.8.20	52.4	3.06	22.87	4.76	67.26
CL4 W7	4	25.8.20	62.6	1.38	24.44	4.58	71.32
CL4 W7 D2	4	27.8.20	41.6	2.04	49.85	8.75	154.53
CL4 W8	4	31.8.20	38.1	1.49	43.09	7.64	112.10
CL4 W8 D2	4	1.9.20	37.7	1.44	43.34	7.46	111.72
CL4 W8 D3	4	2.9.20	35.4	1.48	42.32	7.52	113.40
CL4 W8 D4	4	3.9.20	35.3	1.30	40.38	6.98	105.46
CL4 W9	4	7.9.20	34.3	1.25	37.74	6.69	91.56
CL4 W9 D2	4	8.9.20	37.1	1.19	36.33	6.22	84.47
CL4 W10	4	14.9.20	39.7	131.52	37.21	7.40	152.20
CL4 W10 D2	4	15.9.20	42.5	9.96	32.45	5.96	125.73
CL4 W10 D3	4	17.9.20	38.5	2.97	29.70	5.22	101.48
CL4 W10 D6	4	21.9.20	33.8	1.36	27.61	4.18	63.49
CL4 W11 D1	4	22.9.20	37.8	3.83	27.67	4.28	65.48
CL4 W11 D2	4	24.9.20	30.4	1.08	25.39	3.94	46.74
CL4 W12	4	28.9.20	33.1	1.33	22.83	3.60	37.77
CL4 W12 D2	4	1.10.20	29.3	1.06	22.09	3.51	33.00
CL4 W13 D1	4	5.10.20	31.5	0.13	2.56	0.30	3.18
CL4 W13 D2	4	6.10.20	28.6	0.09	2.66	0.32	3.09
Metal Mean ± SE	0		10.1 ± 1.5	4.4 ± 3.0	2.2 ± 0.1	3.7 ± 0.2	1.4 ± 0.1
Metal Mean ± SE	1		9.7 ± 1.3	8.2 ± 4.8	1.6 ± 0.03	2.3 ± 0.1	1.9 ± 0.3
Metal Mean ± SE	2		16.7 ± 1.3	9.9 ± 5.2	3.3 ± 0.2	2.7 ± 0.1	10.5 ± 2.0
Metal Mean ± SE	3		30.7 ± 1.9	38.8 ± 32.1	22.1 ± 1.2	6.8 ± 0.1	94.2 ± 12.4
Metal Mean ± SE	4		40.4 ± 1.5	87.7 ± 56.0	44.2 ± 5.4	6.9 ± 0.7	170.7 ± 36.1
Control System							
CR0 W2	0	16.8.19	19.7	0.28	1.92	3.22	2.37
CR0 W3	0	25.8.19	23.1	0.24	1.70	5.31	1.22
CR0 W4	0	29.8.19	22.0	0.82	3.14	6.79	3.06
CR0 W5	0	4.9.19	22.0	0.95	2.98	5.63	1.72
CR0 W6	0	9.9.19	21.7	1.98	2.81	5.68	1.50
CR0 W7	0	16.9.19	20.9	0.80	2.90	5.21	1.64
CR0 W8	0	23.9.19	0.2	0.53	2.64	4.37	1.28
CR0 W9	0	2.10.19	2.4	1.72	2.21	3.35	1.31
CR0 W10	0	7.10.19	0.6	0.38	2.16	3.10	0.81
CR0 W11	0	15.10.19		0.36	2.50	3.84	0.98
CR0 W12	0	21.10.19	2.5	0.77	2.67	3.68	1.34
CR0 W13	0	28.10.19	0.8	0.34	2.49	7.22	1.78
CR0 W14	0	4.11.19	2.8	11.71	2.49	3.08	1.39
CR0 W15	0	11.11.19	2.9	1.25	2.33	3.47	1.66
CR0 W16	0	21.11.19	3.4	0.42	2.23	3.09	1.41
CR0 W17	0	28.11.19	4.7	51.13	2.47	4.18	2.72
CR0 W18	0	5.12.19	6.6	0.68	2.26	3.88	34.48
CR0 W19	0	10.12.19	1.4	0.42	2.08	3.01	1.66
CR1 W1 D1	1	16.12.19	19.6	54.02	1.82	4.14	2.63
CR1 W4	1	6.1.20	19.0	0.37	1.80	2.38	1.28
CR1 W5	1	16.1.20	7.0	0.35	1.49	2.25	1.37
CR1 W7	1	28.1.20	8.2	0.29	1.59	2.55	1.24
CR1 W10	1	18.2.20	6.0	58.22	1.89	2.90	1.84

CR2 W3	2	9.3.20	23.1	0.32	1.65	2.30	0.96
CR2 W6	2	30.3.20	23.5	26.87	1.80	3.16	2.06
CR2 W8	2	14.4.20	22.9	0.43	1.73	2.46	1.27
CR2 W10	2	30.4.20	14.6	0.43	2.82	3.28	1.78
CR3 W2	3	12.5.20	20.7	0.37	2.25	2.40	1.05
CR3 W5	3	4.6.20	21.9	0.34	2.37	2.60	1.00
CR3 W8	3	25.6.20	12.7	0.49	3.51	2.92	1.71
CR3 W10	3	9.7.20	16.2	0.44	3.37	2.85	1.70
CR4 W4	4	6.8.20	23.7	0.31	2.21	1.91	0.82
CR4 W7	4	27.8.20	22.4	0.34	2.03	1.85	0.77
CR4 W11	4	22.9.20	12.9	0.50	2.73	2.25	1.24
CR4 W12 D2	4	1.10.20	15.7	4.62	26.32	21.97	11.41
CR4 W13	4	5.10.20	15.6	0.62	6.88	2.08	1.29
Control Mean ± SE	0		8.7 ± 2.2	4.2 ± 2.8	2.4 ± 0.1	4.3 ± 0.3	3.5 ± 1.8
Control Mean ± SE	1		12.0 ± 2.7	22.7 ± 12.2	1.7 ± 0.1	2.8 ± 0.3	1.7 ± 0.2
Control Mean ± SE	2		21.0 ± 1.9	7.0 ± 5.7	2.0 ± 0.2	2.8 ± 0.2	1.5 ± 0.2
Control Mean ± SE	3		17.9 ± 1.8	0.41 ± 0.03	2.9 ± 0.3	2.7 ± 0.1	1.4 ± 0.2
Control Mean ± SE	4		18.1 ± 1.9	1.3 ± 0.7	8.0 ± 4.2	6.0 ± 3.6	3.1 ± 1.9

Table 4.2 continued.

Sample ID	Ph	Sampling Date	Ag/Ca	Cd/Ca	Sn/Ca	Hg/Ca	Pb/Ca
Metal System			**nmol/mol**	**µmol/mol**	**µmol/mol**	**nmol/mol**	**µmol/mol**
CL0 W2	0	16.8.19	14.8	0.041	10.27		0.061
CL0 W3	0	25.8.19	20.4	0.033	10.97		0.054
CL0 W4	0	29.8.19	11.8	0.052	9.23		0.058
CL0 W5	0	4.9.19		0.034	9.10		0.045
CL0 W6	0	9.9.19	2.4	0.030	9.20		0.040
CL0 W7	0	16.9.19	22.6	0.041	8.37		0.047
CL0 W8	0	23.9.19		0.027	9.65		0.042
CL0 W9	0	2.10.19		0.057	7.60		0.071
CL0 W10	0	7.10.19		0.031	7.22		0.037
CL0 W11	0	15.10.19		0.035	7.75		0.051
CL0 W12	0	21.10.19		0.051	7.06		0.053
CL0 W13	0	28.10.19	16.1	0.033	7.45		0.035
CL0 W14	0	4.11.19	2.0	0.033	7.09		0.045
CL0 W15	0	11.11.19		0.047	6.74		0.046
CL0 W16	0	21.11.19		0.030	6.72		0.031
CL0 W17	0	28.11.19	7.5	0.069	6.30		0.138
CL0 W18	0	5.12.19		0.039	6.39		0.036
CL0 W19	0	10.12.19	0.2	0.030	6.68		0.027
CL1 W1 D1	1	16.12.19	247.9	0.349	6.05	7.93	0.451
CL1 W1 D2	1	17.12.19	18.9	0.235	5.83		0.117
CL1 W1 D3	1	18.12.19	11.4	0.187	5.63		0.084
CL1 W1 D4	1	19.12.19		0.143	5.57		0.072
CL1 W1 D5	1	20.12.19	5.1	0.125	5.64		0.063
CL1 W4	1	6.1.20	26.2	0.062	6.90	2.50	0.070
CL1 W5	1	16.1.20	14.0	0.043	7.10	1.14	0.050
CL1 W6	1	23.1.20	17.4	0.045	7.34	6.41	0.054
CL1 W6 D2	1	24.1.20	27.8	0.123	6.20	0.90	0.302
CL1 W7	1	28.1.20		0.080	6.58	1.02	0.067
CL1 W8	1	6.2.20		0.063	6.94	0.96	0.067

CL1 W9	1	10.2.20	19.1	0.101	7.04	2.03	0.088
CL1 W10	1	18.2.20		0.067	7.05		0.085
CL2 W1 D1	2	24.2.20	641.0	3.772	6.48	66.51	4.038
CL2 W1 D2	2	25.2.20	46.4	4.191	5.98		1.695
CL2 W1 D3	2	26.2.20	25.9	3.785	6.01		1.115
CL2 W1 D4	2	27.2.20	35.2	3.203	5.99	4.68	0.805
CL2 W2	2	2.3.20	33.9	1.518	6.28	10.58	0.407
CL2 W3	2	9.3.20	27.5	0.805	6.51	4.04	0.309
CL2 W4	2	16.3.20	37.2	0.995	5.95	9.03	0.346
CL2 W5	2	26.3.20	43.4	1.042	6.37	6.69	0.372
CL2 W6	2	31.3.20	193.8	1.607	5.99	31.78	1.052
CL2 W7	2	7.4.20	90.7	1.704	6.35	9.23	0.574
CL2 W8	2	14.4.20	60.7	1.582	6.58	7.05	0.631
CL2 W9	2	23.4.20	47.6	1.733	6.27	7.47	0.574
CL2 W10	2	30.4.20	48.6	1.461	6.82		0.606
CL3 W1 D1	3	4.5.20	16850.5	43.472	6.66	1021.90	54.957
CL3 W1 D2	3	5.5.20	801.3	36.611	6.58	191.13	9.399
CL3 W1 D3	3	6.5.20	270.5	34.488	6.21	152.03	5.997
CL3 W1 D4	3	7.5.20	167.7	30.639	6.31	78.45	4.688
CL3 W1 D5	3	8.5.20	214.1	29.142	6.08	79.88	4.473
CL3 W2	3	12.5.20	235.8	26.277	6.55	49.18	4.054
CL3 W3	3	19.5.20	132.4	20.974	6.81	12.66	2.514
CL3 W4	3	26.5.20	202.7	26.664	6.38	29.20	4.625
CL3 W5	3	4.6.20	136.5	18.387	6.46	18.59	3.027
CL3 W6	3	11.6.20	122.8	17.833	7.90	15.25	3.372
CL3 W7	3	18.6.20	255.4	20.500	6.43	24.98	3.482
CL3 W8	3	25.6.20	272.4	19.904	6.74	24.07	3.483
CL3 W9	3	2.7.20	245.5	23.377	6.12	27.19	3.531
CL3 W10	3	9.7.20	424.1	24.621	7.22	7.56	4.118
CL4 W1 D1	4	15.7.20	52629.0	176.034	5.36	2307.70	145.848
CL4 W1 D2	4	16.7.20	15954.7	154.304	5.27	787.39	37.910
CL4 W1 D3	4	16.7.20	5865.4	147.473	6.30	807.65	26.514
CL4 W1 D4	4	17.7.20	1750.2	139.322	5.96	574.19	16.860
CL4 W2	4	22.7.20	706.4	127.810	6.80	405.30	11.794
CL4 W3	4	27.7.20	494.0	104.438	7.56	430.77	9.299
CL4 W4	4	6.8.20	1578.3	41.647	7.43	658.99	5.238
CL4 W5	4	13.8.20	2367.2	75.609	8.40	944.75	8.508
CL4 W6	4	20.8.20	3789.6	30.389	8.10	678.67	4.882
CL4 W7	4	25.8.20	4071.6	32.304	8.98	800.37	4.548
CL4 W7 D2	4	27.8.20	2838.9	58.698	6.76		7.278
CL4 W8	4	31.8.20	2040.1	47.816	5.83	299.57	5.952
CL4 W8 D2	4	1.9.20	1926.4	45.766	5.72		5.474
CL4 W8 D3	4	2.9.20	1792.1	44.499	5.84		5.758
CL4 W8 D4	4	3.9.20	1518.5	40.283	5.71		5.481
CL4 W9	4	7.9.20	872.6	33.733	5.52	151.21	5.523
CL4 W9 D2	4	8.9.20	828.0	30.321	5.74	0.00	5.111
CL4 W10	4	14.9.20	1097.4	31.508	6.31	42.27	14.818
CL4 W10 D2	4	15.9.20	917.3	28.635	6.44		6.434
CL4 W10 D3	4	17.9.20	397.4	20.320	5.68		5.146
CL4 W10 D6	4	21.9.20	149.7	4.693	4.98		3.914
CL4 W11 D1	4	22.9.20	148.2	4.997	5.14	12.75	3.876
CL4 W11 D2	4	24.9.20	154.2	3.862	4.86		3.477
CL4 W12	4	28.9.20	142.7	3.108	5.04		3.039

CL4 W12 D2	4	1.10.20	130.6	2.995	5.06		2.899
CL4 W13 D1	4	5.10.20	137.4	0.366	4.82		0.258
CL4 W13 D2	4	6.10.20	150.9	0.386	4.92		0.259
Metal Mean ± SE	0		0.1 ± 2.9	0.04 ± 0.003	8.0 ± 0.3		0.05 ± 0.01
Metal Mean ± SE	1		28.5 ± 17.8	0.1 ± 0.02	6.5 ± 0.2	2.9 ± 0.9	0.12 ± 0.03
Metal Mean ± SE	2		102.4 ± 44.7	2.1 ± 0.3	6.3 ± 0.1	15.7 ± 5.9	1.0 ± 0.3
Metal Mean ± SE	3		1452.3 ± 1142.3	26.6 ± 1.9	6.6 ± 0.1	123.7 ± 68.1	8.0 ± 3.5
Metal Mean ± SE	4		3868.5 ± 1932.6	53.0 ± 10.0	6.1 ± 0.2	635.8 ± 145.7	13.2 ± 5.2
Control System							
CR0 W2	0	16.8.19	46.2	0.039	9.40		0.047
CR0 W3	0	25.8.19	74.8	0.036	10.65		0.036
CR0 W4	0	29.8.19	30.6	0.083	8.96		0.071
CR0 W5	0	4.9.19	6.9	0.057	8.71		0.076
CR0 W6	0	9.9.19	34.0	0.049	9.21		0.056
CR0 W7	0	16.9.19	12.0	0.068	8.27		0.059
CR0 W8	0	23.9.19	77.8	0.051	8.29		0.045
CR0 W9	0	2.10.19	2.4	0.064	7.30		0.097
CR0 W10	0	7.10.19		0.031	6.97		0.048
CR0 W11	0	15.10.19		0.042	7.83		0.053
CR0 W12	0	21.10.19	2.3	0.061	6.87		0.067
CR0 W13	0	28.10.19		0.038	6.56		0.182
CR0 W14	0	4.11.19	1.1	0.037	6.80		0.061
CR0 W15	0	11.11.19		0.050	5.46		0.069
CR0 W16	0	21.11.19		0.032	6.04		0.053
CR0 W17	0	28.11.19	6.3	0.093	5.48		0.205
CR0 W18	0	5.12.19		0.037	5.13		0.039
CR0 W19	0	10.12.19	70.8	0.033	5.18		0.050
CR1 W1 D1	1	16.12.19	11.4	0.061	5.37		0.263
CR1 W4	1	6.1.20	13.7	0.026	6.07	0.75	0.051
CR1 W5	1	16.1.20	6.5	0.025	6.54	1.03	0.040
CR1 W7	1	28.1.20	7.9	0.031	5.35	1.56	0.044
CR1 W10	1	18.2.20	22.7	0.056	5.44	1.48	0.241
CR2 W3	2	9.3.20	15.1	0.022	5.51	0.68	0.056
CR2 W6	2	30.3.20	194.0	0.055	4.31	0.34	0.183
CR2 W8	2	14.4.20	27.9	0.026	4.39	2.40	0.051
CR2 W10	2	30.4.20	6.8	0.038	4.37	1.14	0.053
CR3 W2	3	12.5.20	31.7	0.028	3.66	4.42	0.034
CR3 W5	3	4.6.20	22.8	0.027	3.68	0.87	0.033
CR3 W8	3	25.6.20	13.5	0.038	8.92	1.60	0.037
CR3 W10	3	9.7.20	8.8	0.039	4.75	0.91	0.042
CR4 W4	4	6.8.20	28.0	0.026	3.75	0.72	0.054
CR4 W7	4	27.8.20	20.8	0.027	4.59	2.21	0.090
CR4 W11	4	22.9.20	35.8	0.045	3.77	0.40	0.053
CR4 W12 D2	4	1.10.20	22.0	0.327	3.45		0.304
CR4 W13	4	5.10.20	33.0	0.044	3.38		0.032
Control Mean ± SE	0		16.8 ± 7.2	0.05 ± 0.004	7.4 ± 0.4		0.07 ± 0.01
Control Mean ± SE	1		12.5 ± 2.6	0.04 ± 0.01	5.8 ± 0.2	1.2 ± 0.2	0.13 ± 0.05
Control Mean ± SE	2		61.0 ± 38.6	0.04 ± 0.01	4.6 ± 0.3	1.1 ± 0.4	0.09 ± 0.03
Control Mean ± SE	3		19.2 ± 4.4	0.03 ± 0.003	5.3 ± 1.1	1.9 ± 0.7	0.04 ± 0.002
Control Mean ± SE	4		27.9 ± 2.6	0.09 ± 0.05	3.8 ± 0.2	1.1 ± 0.5	0.11 ± 0.04

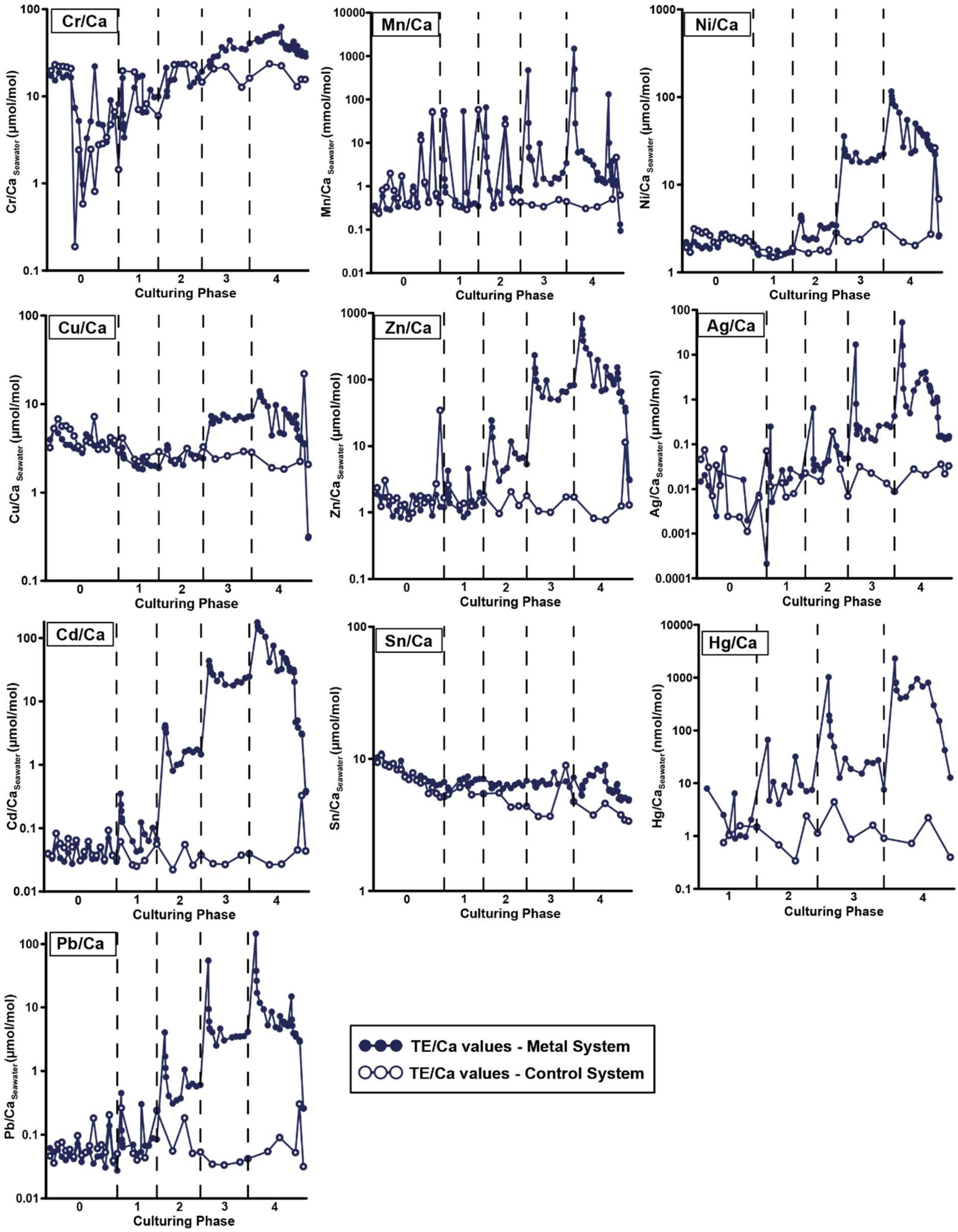

Figure 4.2: TE/Ca values in the culturing medium in µmol mol^{-1} during phases 0 through 4 on a logarithmic scale. Note that the Hg/Ca values from phase 0 of both systems are not given because no Hg samples were taken during this period.

The concentration of all metals used in this study was overall lower in the control system than in the metal system (Figure 4.2, Table 4.2). The concentrations of Cr, Cu and Sn were similar in both systems and no clear elevation was visible in the course of the onset of subsequent culturing phases in the metal system. In the first phases 0 and 1, for Mn and Ag also in phase 2, the metal concentrations in the control system was nearly the same as in the metal system, but in phases 2, 3 and 4, the metal system showed elevated concentrations as expected. The differences between culturing phases in the metal system were clearly visible for Ni, Zn, Ag, Cd, Hg and Pb, and also for Mn even though the elevation between phases was less pronounced. In the beginning of each phase, most elements (Mn, Ni, Cu, Zn, Ag, Cd, Hg and Pb) showed a high peak, which declined after one week. This feature was caused by the sudden addition of the stock solution to reach the next concentration level. Furthermore, some smaller peaks within one culturing phase were linked to water exchange, when stock solution was added to balance the dilution of metals due to the addition of fresh seawater. The concentrations in the control system were comparatively stable over the entire culturing period. A higher scatter was found for Cr and Mn. In the end of the culturing experiment after phase 4, the trace metal concentrations in the metal system overall decreased drastically, which was attributed to the fact that the stock solution was out.

4.3.3 Metals in skeleton

4.3.3.1 Growth rates

Table 4.3: Growth rates of the different coral colonies A, B, C and D in mm/ year. Calculations are based on the staining lines and the outer surface of the colonies after the experimental period. Staining took place before phase 0 (control phase) and before phase 1 (first metal phase). The system, the elemental scan line number and the growth rate in phase 0 and during phases 1 through 4 are indicated. (1) = polluted sites.

Coral	System	Line No.	Growth Rate Phase 0 (mm/yr)	Growth Rate Phase 1-4 (mm/yr)
A	Metal	1	2.7	4.8
A	Metal	2	4.1	4.8
A	Metal	3	2.7	4.8
A	Control	1	9.6	7.3
A	Control	2	9.6	7.3
A	Control	3	5.5	6.7
A*	Control	4	6.8	4.2
B	Metal	1	8.2	12.1
B	Metal	2	8.2	12.1
B	Metal	3	5.5	12.1
B*	Metal	4	6.8	9.1
B	Control	1	6.8	10.9
B	Control	2	6.8	10.3
C*	Metal	1	12.3	7.9
C	Metal	2	16.4	7.3
C	Metal	3	16.4	6.7
C	Control	1	12.3	10.3
C	Control	2	13.7	9.7
C1	Control	1		6.0
C1	Control	2		5.4
C1	Control	3		6.0
D	Metal	1	9.6	8.8
D*	Metal	2	8.2	9.6
D*	Metal	3	4.1	4.0

D*	Metal	4	2.7	2.4
D*	Metal	5	2.7	2.4
D	Control	1	8.2	4.8
D*	Control	2		3.0
D*	Control	3		3.6
D*	Control	4		3.6
D*	Control	5		3.0
Mean ± SD				
A	Metal		3.2 ±0.6	4.8 ±0.0
A	Control		7.9 ±1.8	6.3 ±1.2
B	Metal		7.2 ±1.1	11.3 ±1.3
B	Control		6.8 ±0.0	10.6 ±0.3
C	Metal		15.1 ±1.9	7.3 ±0.5
C	Control		13.0 ±0.7	7.5 ±2.0
D	Metal		5.5 ±2.9	5.4 ±3.1
D	Control		8.2 ±0.0	3.6 ±0.7
Mean ± SD without lines on the side of the colonies				
A	Control		8.2 ±1.9	7.1 ±0.3
B	Metal		7.3 ±1.3	12.1 ±0.1
D	Metal		9.6	8.8
Growth rates from literature				
Reference		**Species**	**Growth rate (mm/yr)**	**Location**
Edinger et al., 2000		*Porites lobata*	13.5-16.0	Ambon (1)
Edinger et al., 2000		*Porites lobata*	14.0-16.2	Sulawesi
Edinger et al., 2000		*Porites lobata*	11.7-16.3	Java
Fallon et al., 1999		*Porites lobata*	5.3 ±1.2	Japan
Guzman and Cortes, 1989		*Porites lobata*	6.5-19.3	Costa Rica
Klein and Loya, 1991		*Porites lobata*	4.8-9.4	Red Sea
Smith et al., 2007		*Porites lobata*	1.2-9.8	American Samoa
Al-Rousan et al., 2007		*Porites sp.*	8.8-10	Red Sea (1)
Cooper et al., 2008		*Porites sp.*	12.8-15.2	Great Barrier Reef (1)
Lough et al., 1999		*Porites lobata*	13.9	Great Barrier Reef
Tortolero-Langarica et al., 2016		*Porites lobata*	3.3-6.5	Central Mexican Pacific

*** line at the side of a coral colony**

Growth rates of the corals varied between subcolonies and within an individual coral specimen (Table 4.3). Furthermore, variations of the growth rate during different culturing phases and between the metal and the control system were identified. It should be noted that coral D died 2.5 weeks after the exposure to the highest metal concentration in phase 4.

Coral colony A in the metal system showed the overall lowest growth rates between 2.3 to 4.8 mm/year. Coral C on the other hand was the fastest growing coral during the control phase 0 in both systems (Mean=7.3 ±0.5-15.1 ±1.9 mm/year). For coral A, the growth rates were generally higher in the control system, which was not the case for the other colonies. Corals A, B and D in the metal system had increased or stable growth rates in phases 1 to 4 compared to the control phase without any added metals. The growth of coral C decreased as soon as the metal concentration in the culturing medium was increased. Within a colony, the growth rates were lower at the sides of the corals. This can for example be seen in coral D in the metal system (line 2 to 5) and in coral B in the metal system (line 4).

The growth rates of this study were overall variable, which was also found by other authors (Table 4.3) in different regions of the world in polluted (Erdinger et al., 2000; Cooper et al.,

2008; Al-Rousan et al., 2007) and less- or unpolluted areas (e.g., Klein and Loya, 1991; Fallon et al., 1999; Tortolero-Langarica et al., 2016). Corals A, B and D from this study showed values that were more comparable to the medium and lower literature values like described by Fallon et al. (1999), Tortolero-Langarica et al. (2016) and Smith et al. (2007), while coral C compared also to higher growth rates like those reported by Guzman and Cortes (1989), Edinger et al. (2000) or Cooper et al. (2008).
Overall, changing growth rates in this study did not follow any clear trends with reference to the culturing system or the heavy metal concentration. Furthermore, the growth rates of the corals compared well to growth rates observed in nature.

4.3.3.2 Metal incorporation into coral aragonite

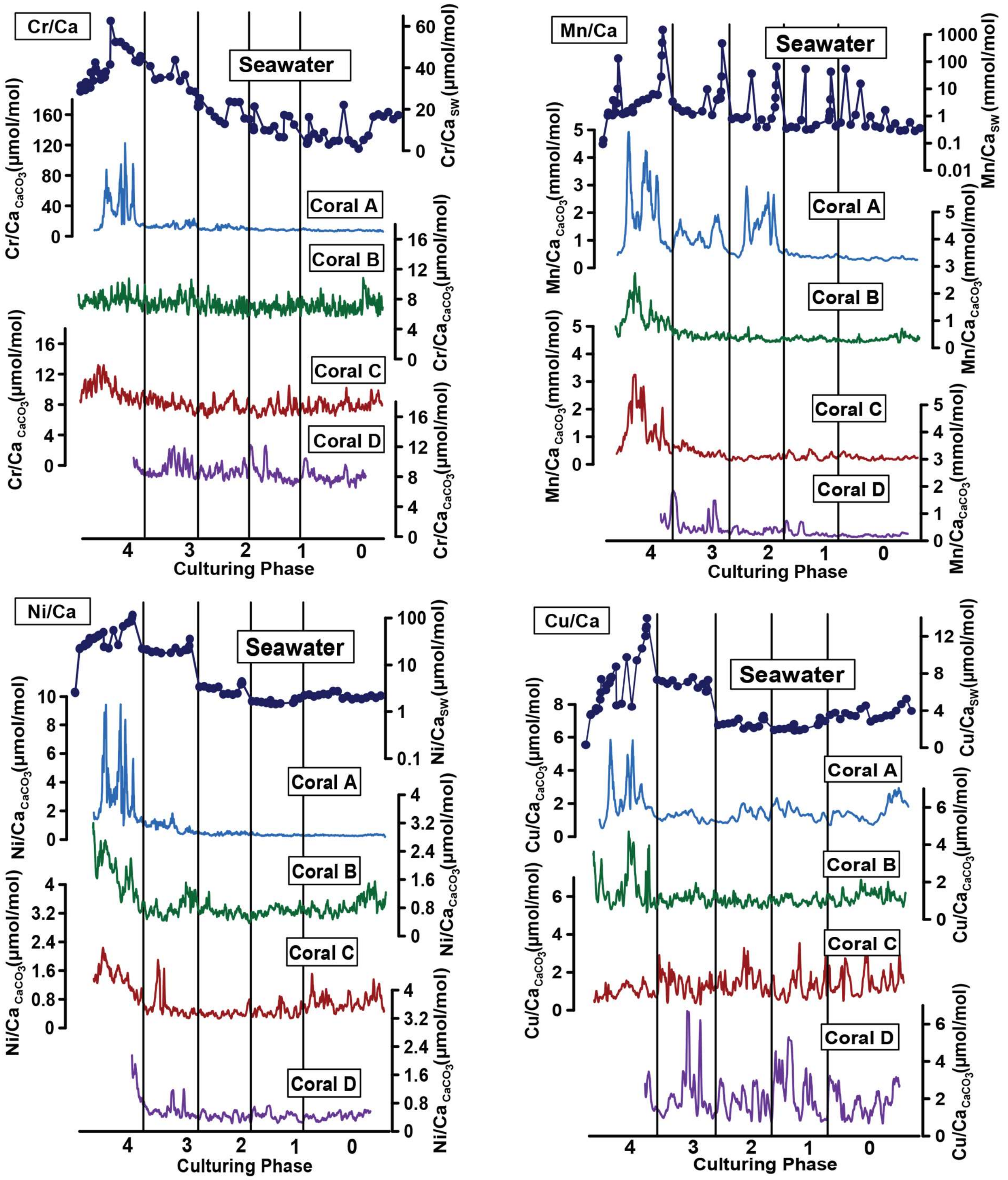

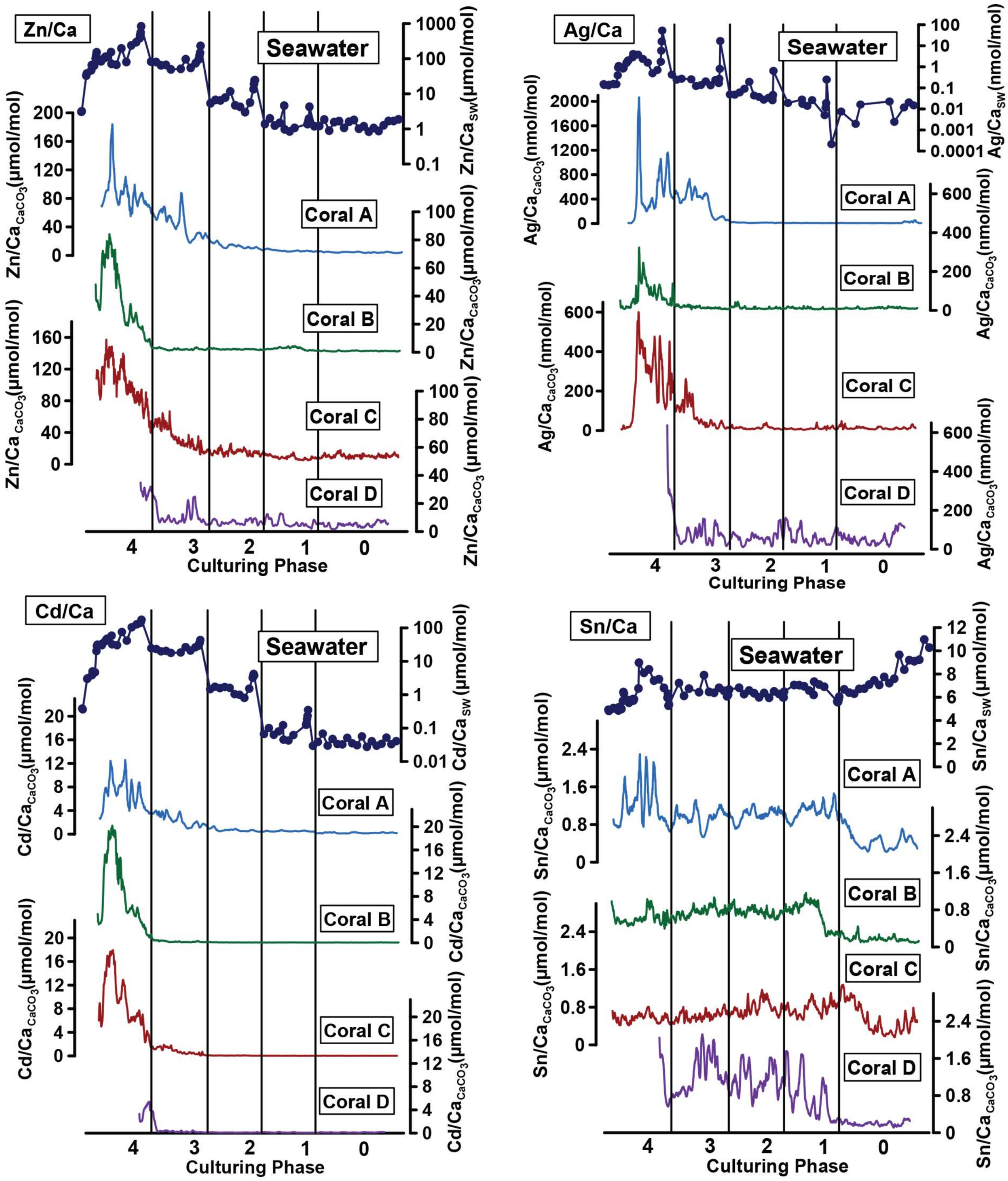
Zn/Ca
Seawater
Coral A
Coral B
Coral C
Coral D
Zn/Ca CaCO3 (µmol/mol)
Zn/Ca SW (µmol/mol)
Culturing Phase
4 3 2 1 0
Ag/Ca
Ag/Ca CaCO3 (nmol/mol)
Ag/Ca SW (nmol/mol)
Cd/Ca
Cd/Ca CaCO3 (µmol/mol)
Cd/Ca SW (µmol/mol)
Sn/Ca
Sn/Ca CaCO3 (µmol/mol)
Sn/Ca SW (µmol/mol)

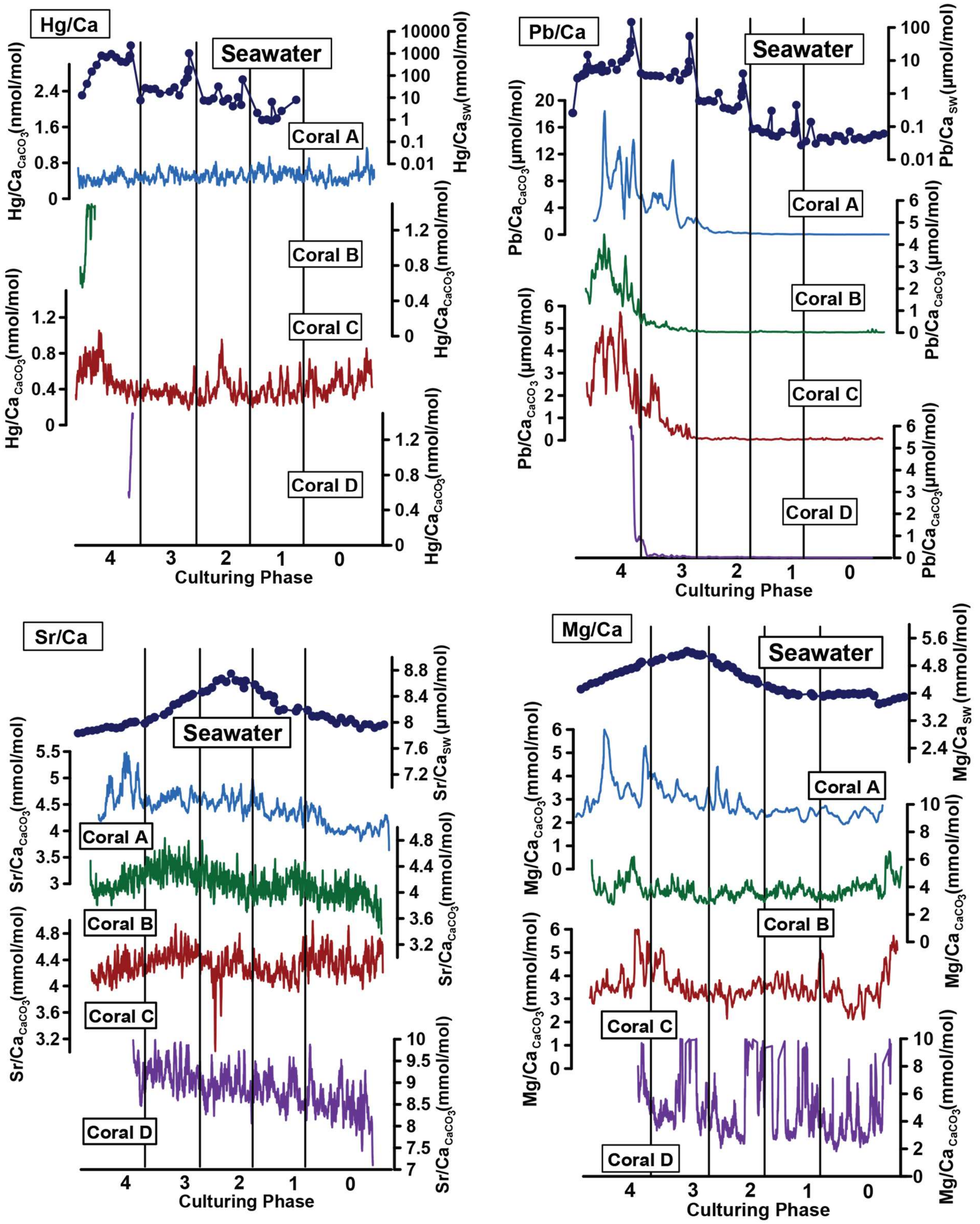

Figure 4.3: Composite line along the maximum growth axis profiles of TE/Ca values of corals A, B, C and D in the metal system measured by laser ablation ICP-MS (lower graphs) and corresponding TE/Ca values in the culturing seawater medium (topmost graph). To facilitate a comparison, all coral and water lines were transformed to the same Y-scale and therefore, differences in growth rates cannot be seen in this figure (see Table 4.3 for growth rates). The lines represent a running average over 5 points. The composite line of all laser scans along the maximum growth axis per colony was calculated with QAnalyserie (Kotov and Paelike, 2018). Note that coral D died at the beginning of phase 4 after approximately 2.5 weeks. All elements

but Cr, Cu, Sn, Sr and Mg are displayed with a logarithmic scale for the water measurements. All values can be found in Table 4.2, Table B4.3 and Tables S4.1-S4.4.

Measurable (> 3 times limit of detection (LOD)) amounts of all metals investigated in this study were detected in the skeleton of all four coral colonies from all phases, but the degree of incorporation varied (Figure 4.3, Table B4.4). Differences between culturing phases occurred and in some lines, not all elements were detectable. Sn was not detectable in Coral D line 5 (Figure A4.8) and Hg in line 3 of coral A and B (Figure A4.2, Figure A4.4). Hg was only detectable in phase 4 in line 2 of coral D (Figure A4.8).

The heavy metal concentration in the coral skeleton partly followed the concentration changes in the culturing medium. No element showed a covariance between the metal concentration in the coral aragonite and the seawater in phase 0, 1 and 2, but several elements showed a covariance in phases 3 and 4, when the heavy metal concentration in seawater was higher. Hg and Sn concentration in the coral skeleton of all colonies in all phases did not follow the concentration changes in the culturing medium.

The seawater Cr concentration was mirrored in coral A in phase 4. Coral C also showed slightly elevated Cr/Ca values when the Cr/Ca concentration in the seawater is highest in phase 4. Corals B and D did not show any covariance. The elevated Mn concentration in the seawater was mapped by all colonies in phase 4 and in coral A and D also partly during phase 2 and 3. During phase 4 and partly in phase 3, all coral colonies had higher concentrations of Ni, Zn, Ag and Pb in their skeleton. Increased Cu concentrations in the coral skeleton was found in coral colonies A and B in phase 4. Coral colony D did not show any clear patterns for Cu. Cd concentrations in the coral skeletons of all colonies were higher in phase 4 compared to the other phases.

4.3.4 Partition Coefficient D_{TE}

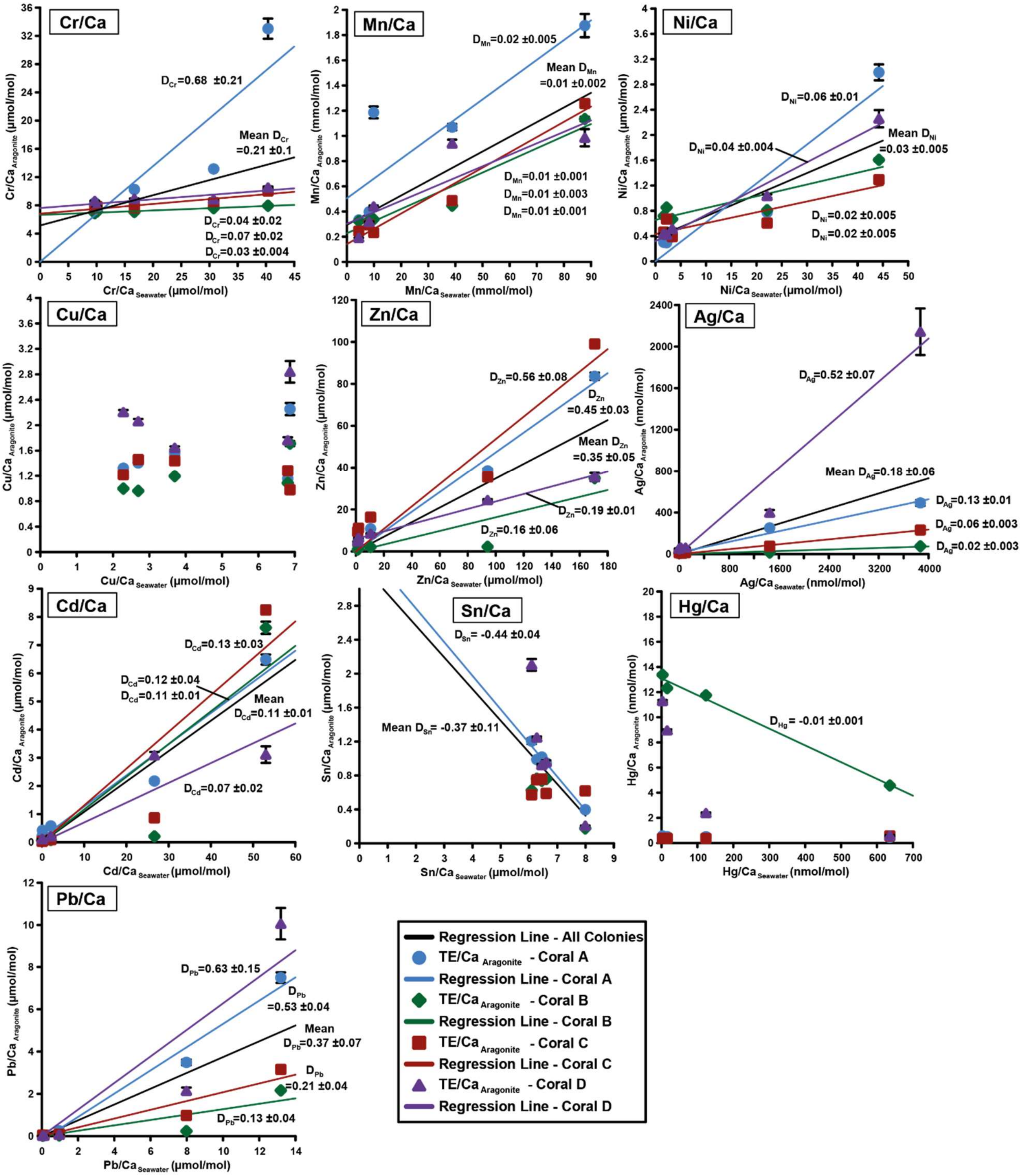

Figure 4.4: TE/Ca values of all coral colonies in the metal system derived from the composite line per colony. TE/Ca in the coral aragonite versus the TE/Ca values in the corresponding culturing medium based on phase 0 to 4 is shown. Each data point represents the averaged phase value plotted against the mean metal concentrations in the seawater averaged over the culturing phase (Table 4.2). Error bars symbolize the standard error of the mean (standard deviation σ/√n). Note that error bars are only given for the TE/Ca values of the coral aragonite as the metal concentration in the culturing medium was strongly varying (see Figure 4.2) due to the punctual input of the stock solution. This results in a disproportional high standard error, which in turn would make it impossible to see distinct features in the plot if it would be displayed. The

linear regression line is given, when elements showed a significant correlation between seawater and aragonite. D_{TE} (±SE) values represent the slope of the regression line, which is forced through the origin in all cases but Sn and Hg. All values can be found in Table B4.4.

Partition coefficients for the different trace elements were deduced from molar coral aragonite TE/Ca and the values of the culturing medium from the corresponding culturing phase. Note that the D_{TE} values represented the slope of the regression line when a positive correlation between seawater TE/Ca and coral aragonite TE/Ca was detected ($p < 0.05$, $R^2 \geq 0.45$). If no correlation was found, no D_{TE} values were given in the figure but in Table B4.4, where all values can be found. D_{TE} values calculated separately for every individual phase are also given. When looking at the values derived from all coral composite lines and all colonies together, significant positive correlations between the TE/Ca was found for Cr, Mn, Ni, Zn, Ag, Cd and Pb. Cu, Sn and Hg overall showed no or negative correlation between seawater and skeleton. Mean D_{TE} derived from the composite lines of all coral colonies was highest for Cr (D_{Cr}=0.21 ±0.1), Zn (D_{Zn}=0.35 ±0.05) and Pb (D_{Pb}=0.37 ±0.07) and lowest for Mn (D_{Mn}=0.01 ±0.002). Values derived from calculations based on single phases only showed that higher heavy metal concentrations in the seawater did not reveal lower D_{TE} values (Table B4.4).

4.3.5 Comparison between species and colonies and between laser ablation lines within a colony – Inter- and intraspecies variability

4.3.5.1 Interspecies variability

When considering every coral colony from the metal system individually, significant positive correlations between seawater and aragonite was visible in all colonies for Cr, Mn, Ni, Zn, Ag, Cd and Pb (Figure 4.4, Table B4.4). No correlation was found for Cu in all colonies and for Sn in all but colony A (negative correlation p=0.002, R^2=0.97). Colonies B showed a negative correlation for Hg. The Hg concentration was overall very low in the coral skeleton, which makes any interpretation of the data difficult.
Comparison between different colonies revealed no clear trends between colonies of the same species or between species. Coral A displayed generally higher TE/Ca values than all other colonies for Cr, Mn, and Ni as well as a steeper regression line. Coral D (*P. lichen*) showed higher TE/Ca values for Ag and Pb. The colonies C and D were generally at the lower boundary of the range of values and coral colony B represented the lowest TE/Ca values for Cr, Mn, Zn, Ag, and Pb. The range of D_{Mn}, D_{Ni}, D_{Zn} and D_{Cd} between the different colonies was within one order of magnitude. D_{Cr}, D_{Ag} and D_{Pb} displayed a wider range.

4.3.5.2 Intraspecies variability

On coral colony A and C grown in the metal system, three lines were measured and clear differences between line 3 and 1, respectively, and the other lines were visible (Figure A4.1, A4.2, Figure A4.5, A4.6). TE/Ca values were remarkably higher for Cr, Ni, Zn, Ag, Cd and Pb compared to the other lines, which showed similar TE/Ca values. These lead in turn to higher D_{TE} values, which were up to ten times higher than those of the other lines (see Table B4.4). Four lines were measured on coral colony B of the metal system and overall all showed the same trends for all elements used in this study (Figure A4.3, A4.4). When looking at one specific metal, differences between individual laser lines showed up but no general patterns were found. D_{TE} values were also variable, but these differences were lower than that found in coral colony A. All five lines measured on coral colony D did not show clear trends or offsets, but when looking at one specific heavy metal, smaller variations were found (Figure A4.7, A4.8). These variations could not be traced to one specific line. For example, line 4 indicated the highest TE/Ca values for Cr, line 3 for Ni, Zn and Cd and line 5 for Ag.

4.4 Discussion

4.4.1 Experimental uncertainties

The TE/Ca concentrations in the culturing medium of the metal system varied at the beginning of each new phase due to the sudden input of the stock solution for rising the concentration of the next phase. Furthermore, variations within a phase occurred due to regular water exchanges. Overall, the measured concentrations during periods of stability were lower than expected (see Table 4.1 and Table 4.2). Ag, Hg and Pb concentrations were 20 to 50 percent lower than the target concentrations in all phases. In phase 1 the concentration was approximately 10 to 20 times higher for Cr, Mn, Cu and Sn. In all other phases, the measured concentration was lower than the target concentration by a factor of 5 to 10 for all elements. The recognized loss of metals could have several different reasons. One possibility was the uptake by the accompanying organisms living in the culturing system, or by algae growth. The protein skimmer, which ensured the oxygenation and skimmed proteins or exopolymers from the system, could also have removed metals adsorbed to these substances. Indeed, metal ions are surface reactive, and it is therefore imaginable, that a certain amount adhered to the inner surface areas of system components, which included the glass panes, tubings, hoses and the fibre filter for larger particles. As the surface space for adhesion was limited, it appears plausible that the concentration of the metals was decreasing until all adhesion spaces were taken. Afterwards, the concentration would be expected to stabilize, and this was observed approximately five days after the input of the stock solution for Ni, Zn, Ag, Cd, Hg and Pb (Figure 4.2). Having foreseen this possibility, it was attempted to counteract adsorptive loss of metals by a regular addition of a certain amount of the stock solution to the metal system. However, this measure was not fully sufficient for maintaining a stable metal concentration. Nevertheless, the short-term concentration changes were mirrored in the aragonite of the corals. This coherent data pattern justified the inclusion of the first, high concentrations at the beginning of a phase for the calculation of average values for each phase.

The growth rates of the corals indicated that the elevated heavy metal concentrations as applied in this experiment did not inhibit or decrease growth. It was therefore expected that coral metabolism maintained at normal levels, also during higher heavy metal concentrations (Table 4.3). Furthermore, D_{TE} values did also not decrease in higher metal phases (Table B4.4). If this would have been the case, an overload effect would be indicated, which was also described for other organisms, e.g., foraminifera (Munsel et al., 2010; Nardelli et al., 2016). It has been suggested that this effect comes into action as soon as the metal concentration exceeds a threshold above which an imminent intoxication is probable. Biological mechanisms expelling metals or blocking the metal uptake take over to protect the organism. There was no evidence for such a response in this study, which corroborated that the metal concentration was within levels at which the corals remain healthy. Generally, all coral colonies were found thriving well over the entire culturing period by visual inspections. A loss of vitality was therefore not recognised as a biasing factor for the heavy metal incorporation into the coral skeleton. One clear exception was coral D, which died after 2.5 weeks in the highest metal phase 4 but showed elevated TE/Ca values prior to death. Coral D belonged to the species *Porites lichen*. We therefore may speculate that this species could have a lower tolerance for heavy metal input. Prior to phase 4, coral D did not show a reduced fitness. As such, a biological effect or disease cannot be excluded. It is possible that the symbionts of coral D were less fit or the amount of symbionts was lower than for the other colonies. The elevation of the heavy metal concentration in phase 4 could therefore have caused the symbionts to disappear within a short period causing the decease of the coral. The other coral colonies may have had the chance to recover from the first high metal concentration peak in the beginning of phase 4 because they had more or fitter symbionts.

Measurements at different positions within the coral colony revealed that line 3 at coral A (Figure A4.1, A4.2) and line 1 at coral C (Figure A4.5, A4.6) showed systematically higher values for Cr, Ni, Zn, Ag, Cd and Pb. Lines on coral colonies B (Figure A4.3, A4.4) and D (Figure A4.7, A4.8) did not show any systematic offset. Sr/Ca and Mg/Ca profiles from coral A line 3 were more variable and had elevated values in phase 4. The same trend was found in coral C line 1 for Mg/Ca. Both other lines on the respective corals did not show strong variations for Sr/Ca, but smaller variations for Mg/Ca. These variations could be connected to higher metal incorporation. Line 3 of coral A was at the side of the colony, while line 1 of coral C was at the top-middle of the colony. If the position in the colony itself would cause a systematic offset, it would be expected that this also influenced the growth rates. This was not the case for coral A, because the growth rates were similar for all lines in phase 1 to 4 (4.8 mm/year). Line 1 of coral C on the other hand, showed slightly higher growth rates of 7.9 mm/year as compared to line 2 and 3 (6.7-7.3 mm/year). If this higher growth rate of line 1 at coral C influenced the incorporation, a higher uptake of the heavy metals from the seawater resulting in the observed higher TE/Ca values in the coral skeleton seems plausible.

Line 1 of coral D showed higher Sr/Ca values than the other lines (Figure A4.7, A4.8). Furthermore, line 3 to 5 showed slightly oscillating features, which point towards a deviation from the main growth axis, which was also indicated by the growth rates and therefore, these lines were not considered for the D_{TE} calculation.

4.4.2 Incorporation of heavy metals into the coral skeleton

Corals have a long history as environmental archives based on the incorporation of different trace elements and metals into their skeleton (e.g., Sr, Na, Mg, K, Zn in Amiel et al., 1973; Cd, Pb, V, Mn, Zn, Ba in Shen and Boyle, 1988; Hg, Cu, Zn, Pb, Mn, Fe, Ni, Cd, V, AI, Cr, Mg, B, Ca, Cd in Hanna and Muir, 1990; Pb, Cu, Zn, Ni, Cr in Esslemont, 2000; Fe, Mn, Ni, Cu, Pb, Zn in Mohammed and Dar, 2010; Mn, Zn, Cu, Cr, Co, Ni, V, As, Cd, Hg, Pb in Jafarabadi et al., 2018; Mg, Cr, Mn, Ni, Cu, Zn, Sr, Cd, Ba, Pb, U, Fe, Co, V in Kourandeh et al., 2021). Saha et al. (2016) provided a comprehensive review on this issue. Nevertheless, to reconstruct past ocean environmental signals like heavy metal concentration in seawater, it is crucial to understand the fundamental biomineralization processes of these animals to gain insights about the way ions are taken up from the ambient seawater. Furthermore, sample preparation and measurement techniques should be reconsidered to be aware of what part of the coral or what kind of incorporation is measured exactly.

Corals precipitate carbonate with the help of their extracellular calicoblastic epithelium. This tissue contains calcifying cells that control the composition of the extracellular calcifying medium (ECM) located between the calicoblastic ectoderm and pre-existing skeleton (e.g., Allemand et al., 2004 & 2011; Tambutté et al., 2011). Different mechanisms are hypothesised to be involved into the transport of ions relevant for calcification from the seawater to this area. One mechanism is the transcellular calcium transport, i.e., describes the transport of calcium ions through the cell membrane of the calicoblastic epithelium via specific biomolecules building ion channels or ion exchangers (Allemand et al., 2004; Capasso et al., 2021). However, many cations other than Ca are also present in the ECM and subsequently in the coral skeleton, which lead to the assumption that Ca transporters may also transport other ions similar to Ca in size and charge. Alternative concepts explain the occurrence of ions other than calcium by direct seawater transport via paracellular pathways or via vacuoles (Gagnon et al., 2012; Mass et al., 2017; Sun et al., 2020). Erez and Braun (2007) also found evidence for paracellular pathways by adding the fluorescent dyes Calcein and FITC-Dextran to seawater and let different coral species grow in this mixture. This means that the composition of the coral skeleton is directly depending on the seawater chemistry, which enables corals to monitor the seawater composition. This theory would also explain the incorporation of ions that have a different size or charge compared to calcium.

In this study, it was found that Cr, Mn, Ni, Zn, Ag, Cd and Pb were incorporated into the coral aragonite following a linear relationship with the seawater concentration (Figure 4.4, Table B4.4). This suggests a paracellular pathway is the major route for the uptake of these metals into the ECM or to a very unspecific uptake via transcellular proteins. Nevertheless, the seawater concentration was not mirrored one by one, which indicates that biological processes indeed affect the metal uptake.

From a crystallographic point of view, Cr, Ni, Mn, Zn and Ag have a smaller effective ionic radius than Ca=1.12 Å, Pb has a slightly bigger one and only Cd shares a similar size (Cr=0.80 Å, Ni=0.69 Å, Ag=0.94 Å, Mn=0.96 Å, Zn=0.90 Å, Cd=1.10 Å, Pb=1.29 Å, Shannon, 1976). It is known that ions with a smaller radius than Ca^{2+} tend to form rhombohedral carbonates while octahedral forms like in aragonite are favoured by bigger ions (Shannon, 1976; Terakado and Masuda, 1988). Nevertheless, Ca^{2+} substitution is reported for Mn^{2+}, Ni^{2+}, Zn^{2+}, Cd^{2+} and Pb^{2+} (e.g., Amiel et al., 1973; Shen and Boyle, 1987; 1988; Pingitore et al., 2002; Anu et al., 2007) even though the ionic radii and the preferred crystal structure deviated from that of Ca^{2+}. Adsorption onto the skeletal surface was found in earlier studies to play a role during times of temporal tissue retraction during stressful situations (St John, 1974; Amiel et al., 1973; Brown et al., 1991). In our experiments, no tissue retraction was observed. One exception was the sudden death of coral D. Afterwards the tissue retracted but previously no reduced fitness was detected and furthermore, coral D showed elevated heavy metal concentrations in the skeleton before death. We therefore consider this process as unlikely to have contributed to the metal concentration in the coral skeleton. Furthermore, massive colonies would adsorb more metals than branching specimens would, because their skeletal-surface-to-tissue ratio is bigger (Anu et al., 2007). This would mean that the branching coral D should show systematically lower

TE/Ca values than the massive corals A, B and C, which was not the case (see Figure 4.4, Table B4.4). Our cleaning procedure should additionally guarantee that as much contamination on the coral surface as possible was removed prior to analysis.
Metals can bind to organic matter in the coral lattice, which was indicated in previous studies (e.g., Bilings and Ragland, 1968; Shen et al., 1991; Allison and Finch, 2004). Cuif et al. (1999) found that coral fasciculi consist of aragonite crystal bundles that are formed from repeated superimposition of few microns thick growth layers. Organic compounds and trace metals like Mg are concentrated at these boundaries (Cuif et al., 2003). The organic matter represents 1 to 2.5 wt% of the coral skeleton (Cuif et al., 2004) and it was found that trace elements concentrate up to 3.5 % in this organic matter (Finch and Allison, 2008, Allison and Finch, 2004). It is possible that this mechanism was contributing to the TE/Ca values of this study, which can be neither proven nor rejected from our dataset. Mg profiles of the composite lines revealed elevated values during phase 4 in the corals A to C, which could hint towards an elevated amount of organic matter that could also have caused an elevated incorporation of heavy metals into this organic matter. Sr profiles did not show or only very barely show any variation in the corals B to D (Figure 4.4, Figure A4.4, A4.8). Only Sr/Ca in coral A was slightly elevated in phase 4, which could point towards deviating calcification.
As mechanism other than Ca^{2+} substitution and binding to organic matter were excluded or considered to play a minor role, most of the metals were thus expected to be incorporated into the coral aragonite lattice or organic matter. Extra-lattice elements could, however, depend on the metal concentration in seawater. If this was the case, an appropriate estimate of past environmental concentrations would likewise have been possible and could not be resolved.
No correlation between the TE/Ca values in seawater and those in the coral aragonite was found for Cu, Sn and Hg (Figure 4.4, Table B4.4). In the cases of Cu and Sn, this pattern was evidentially due to the small variations of these elements in the culturing medium (Figure 4.2, Table 4.2). An assignment of a relationship between these elements in the water and in the coral skeleton was therefore impossible. On the other hand, the dissolved Hg concentration in the seawater covered an appropriate range (Figure 4.2, Table 4.2) but the Hg/Ca values in the coral skeleton were very low making any interpretation speculative.
In summary, the metals showing a linear correlation between seawater and aragonite can be used for the reconstruction of past seawater conditions based on coral skeletons. Their incorporation into the aragonite skeleton of the coral was most likely by Ca^{2+} substitution or by binding to organics and mirrored the seawater concentration without any major counteracting effects.

4.4.3 Partition coefficient D_{TE}

Table 4.4: Comparison of D_{TE} values of the present study to other studies and other coral species. D_{TE} values are derived from the composite line of all coral colonies. Sample preparation: 1 = NaClO+preablation, 2 = H_2O_2 + HNO_3, 3 = acid leaching/ oxidative/ reductive cleaning procedure after Shen and Boyle (1988), 4 = procedure Boyle et al., (1988) deionized water rinse, 5 = destilled water, HNO_3, H_2O_2 + NaOH, H_2NNH_2 + NH_4OH + $C_6H_8O_7$, coprecipitation with APDC + HNO_3, 6 = dilution HCl, $AgNO_3$ carrier for precipitating AgCl, HNO_3, NH_4OH, scavenging with ferric chloride, re-precipitation of silver with nitric acid, drying, dissolving in NH_4OH.

Element	Species	D_{TE}	Comparable? y/n	Reference	Location	Sample preparation	Measurement techniques
Cr	***Porites lobata, Porites lichen* (Mean)**	**0.21 ±0.1**		**This study**	**Laboratory culture**	**1**	**LA-ICP-MS**
	***Porites lobata, Porites lichen* (Range of colonies)**	**0.03-0.68**					
	Porites lutea	0.5	Yes	Jiang et al., 2020	Galapagos island	2	ICP-MS
	Favia palauensis	0.6	Yes				
	Pavona decussata	0.5	Yes				
	Montastrea faveolata	0.3	Yes	Prouty et al., 2008	Meso-american Caribbean Reef System	3	HR-SF-ICP-MS
Mn	***Porites lobata, Porites lichen* (Mean)**	**0.01 ±0.002**		**This study**	**Laboratory culture**	**1**	**LA-ICP-MS**
	***Porites lobata, Porites lichen* (Range of colonies)**	**0.01-0.02**					
	Pavona clavus	1	No, lower	Linn et al., 1990	Galapagos island	3	GFAAS
	Porites panamensis	0.1-0.6	No, lower	Shen et al, 1991			
	Porites panamensis	0.13 ±0.10	No, lower	Carriquiry and Villaescusa, 2010	southern Gulf of California		
	Pavona clivosa	0.10 ±0.10	No, lower				
	Pavona gigantea	0.03 ±0.02	Yes				
Ni	***Porites lobata, Porites lichen* (Mean)**	**0.03 ±0.005**		**This study**	**Laboratory culture**	**1**	**LA-ICP-MS**
	***Porites lobata, Porites lichen* (Range of colonies)**	**0.02-0.06**					
	Porites lobata	0.59	No, lower	Mokhtar et al., 2012	Sabah, Borneo	3	FAAS
Zn	***Porites lobata, Porites lichen* (Mean)**	**0.35 ±0.05**		**This study**	**Laboratory culture**	**1**	**LA-ICP-MS**
	***Porites lobata, Porites lichen* (Range of colonies)**	**0.16-0.54**					
	Porites lutea	1.4	Yes	Jiang et al., 2020	Galapagos island	2	ICP-MS
	Favia palauensis	1.8	Yes				
	Pavona decussata	1.2	Yes				
	Montastrea annularis	11	No, lower	Shen and Boyle, 1988	Florida strait	5	GFAAS
	Porites lutea	0.4	Yes	Livingston and Thompson, 1971	Florida keys	4	neutron activation + γ-spectrometry, ICP-OES
	Diploria strigosa	1	Yes	Shen, 1986	Bermuda	3	GFAAS
Ag	***Porites lobata, Porites lichen* (Mean)**	**0.18 ±0.06**		**This Study**	**Laboratory culture**	**1**	**LA-ICP-MS**
	***Porites lobata, Porites lichen* (Range of colonies)**	**0.02-0.52**					
	Central pacific corals average	0.13	Yes	Veeh and Turekian, 1968	Cetral pacific	6	neutron activation + γ-spectrometry
	Pocillopora	0.09	Yes		Hawaii		
	Leptastrea	0.27	Yes		Hawaii		
	Leptoria	0.15	Yes		Samoa		
	Acropora	0.04	Yes		Samoa		

	Pocillopora	0.05	Yes		Tahiti		
	Acropora	0.06	Yes		Tahiti		
	Favia	0.06	Yes		Tuamotu		
	Fungia (septa)	0.18	Yes		Tuamotu		
	Fungia (base)	0.06	Yes		Tuamotu		
Cd	***Porites lobata, Porites lichen* (Mean)**	**0.11 ±0.01**		**This study**	**Laboratory culture**	**1**	**LA-ICP-MS**
	***Porites lobata, Porites lichen* (Range of colonies)**	**0.07-0.13**					
	Porites lutea	1	No, lower	Jiang et al., 2020	Galapagos island	2	ICP-MS
	Favia palauensis	0.6	Yes				
	Pavona decussata	1.2	No, lower				
	Pavona clavus	0.7-1.3	Partly	Shen and Sanford, 1990	eastern tropical Pacific	3	GFAAS
	Pavona clavus	0.7	Yes	Linn et al., 1990	Galapagos island		
	Pavona clavus	1	No, lower	Shen et al., 1988	Galapagos Islands	5	GFAAS
	Porites panamensis	0.9-2.0	No, lower	Shen, 1991	various in the tropical Pacific		GFAAS
	Pavona clavus	1.3-1.7	No, lower	Grottoli et al., 2013	Gulf of Panama	3	LA-ICP-MS
	Porites panamensis	0.83 ±0.53	Yes	Carriquiry and Villaescusa, 2010	southern Gulf of California		GFAAS
	Pavona clivosa	0.32 ±0.17	Yes				
	Pavona gigantea	0.15 ±0.08	Yes				
Pb	***Porites lobata, Porites lichen* (Mean)**	**0.37 ±0.07**		**This study**	**Laboratory culture**	**1**	**LA-ICP-MS**
	***Porites lobata, Porites lichen* (Range of colonies)**	**0.13-0.63**					
	Porites lutea	1.1	Yes	Jiang et al., 2020	Galapagos island	2	ICP-MS
	Favia palauensis	1.1	Yes				
	Pavona decussata	1.9	Yes				
	Pavona clavus	1.8	Yes	Linn et al., 1990	Galapagos island	3	GFAAS
	Diploria strigose	2.1-2.3	Yes	Shen and Boyle, 1988	North Rock, Bermuda	5	GFAAS

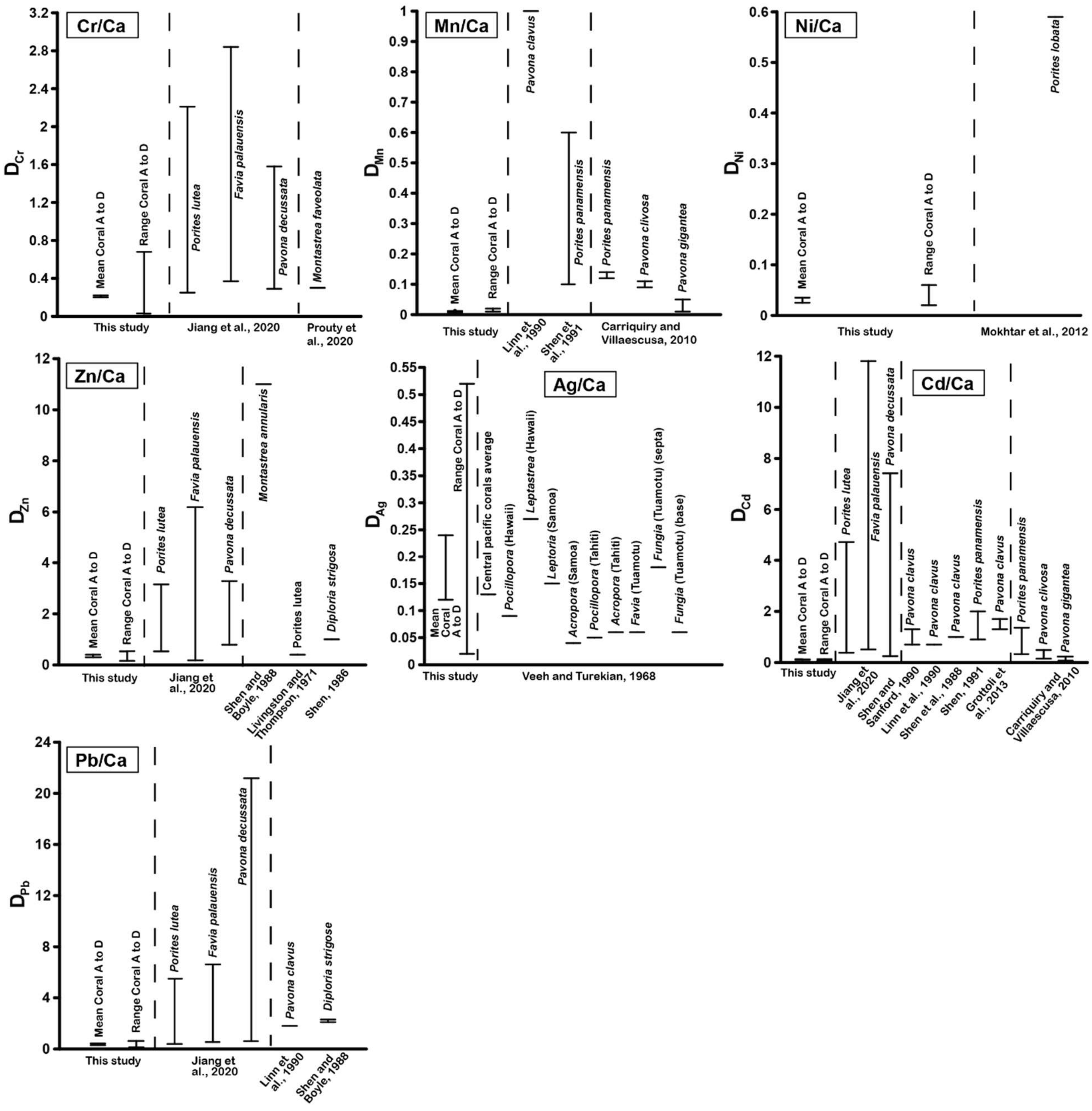

Figure 4.5: Comparison of D_{TE} values of this study with D_{TE} values from literature of different coral species. The range of D_{TE} from the different coral colonies and the mean D_{TE} from all colonies is given. D_{TE} values are based on the correlation between TE/Ca in seawater and the coral skeleton.

Biological processes are believed to have had an influence on the ion uptake of corals. It is imaginable, that essential elements like Mn, Ni or Zn were introduced into the coral or the symbiont cells and were consumed there, which would have eliminated at least a certain amount of them for incorporation into the coral skeleton. Non-essential elements like Cr, Cd and Pb on the other hand could have been actively pumped out of the cell to prevent from intoxication and lethal effects, which would have also prevented a certain amount of the metals to be incorporated. These residual metals were potentially immobilized in the coral skeleton, but this would rather result in a $D_{TE}>1$, which was not found in this study. Furthermore, transcellular

proteins could introduce elements other than Ca to a smaller amount and discriminated against them before they even got the chance to be incorporated.
D_{TE} values of this study did partly agree with literature values derived from field studies (see Table 4.4, Figure 4.5). Some values derived from literature were higher than values reported in this study. D_{Cr} values of this study compared to the lower values of Jiang et al. (2020) and Prouty et al. (2008). D_{Mn} was in the same range than values from Carriquiry and Villaescusa (2010) for *Pavona gigantean*, but lower than other literature values, which also held true for D_{Ni}. D_{Zn} was in the same range than values from Jiang et al. (2020), Livingston and Thompson (1971) and Shen (1986). Calculated D_{Ag} values of this study compared to D_{Ag} from Veeh and Turekian (1968), but it has to be noted that the D_{Ag} range of this study was much higher. The D_{Cd} values of this study were partly in agreement with the lower D_{Cd} values of studies like Jiang et al. (2020), Shen and Sanford (1990) and Carriquiry and Villaescusa (2010) for *Pavona gigantean*, but were generally lower than literature reported. D_{Pb} displayed a similar pattern. D_{Cu}, D_{Sn} and D_{Hg} values were not compared to literature as no correlation between the metal concentration in seawater and in the coral skeleton was found for these elements.
Arising disagreements could possibly be explained by the different species that were used, which is not always likely as in some cases, e.g., for Ni, a *Porites* species was compared (Mokhtar et al., 2012), which should display comparable values but did not. On the other hand, different species compared very well, e.g., Cd in *Pavona gigantean* from Carriquiry and Villaescusa (2010). Therefore, it is unlikely that only the species differences caused disagreements. Another factor that could cause deviation from the literature are different sample preparation and measurement techniques. In earlier studies, more intensive cleaning procedures involving various oxidative and reductive chemical treatments prior to analysis were applied (Table 4.4). An extensive cleaning procedure could lead to the removal of metals from the coral skeleton, which would lead to lower TE/Ca values and therefore lower D_{TE} values. This cannot be proven as the majority of our D_{TE} values were lower and not higher than in the literature. On the other hand, softer cleaning procedures like applied by Jiang et al. (2020), Livingston and Thompson (1971) or Veeh and Turekian (1968) did generally lead to more comparable D_{TE} values indicating that cleaning does make a difference. Measurements techniques were hard to compare because only Grottoli et al. (2013) used LA-ICP-MS for analysis and D_{Cd} of their study was higher than values of this study. Besides the presented differences in species, cleaning and analytics, the exposure to a mixture of metals may lead to synergetic effects between the metals. We cannot clearly entitle one reason for the variation of our values compared to literature, but nevertheless, the presented D_{TE} values did compare to the literature and can possibly enable a reconstruction of the heavy metal concentration in paleo-seawater based on analysing coral skeletons.

4.5 Conclusion

Many environmental studies based on the heavy metal content in the coral skeleton demonstrated that coral aragonite can be used as indicator for heavy metal pollution (e.g., Guzmán and Jiménez, 1992; Esslemont, 2000; Jupiter, 2008; Ali et al., 2011; Nour and Nouh, 2020). In this study, culturing experiments exposed *Porites lobata* and *Porites lichen* to a mixture of ten different metals (Cr, Mn, Ni, Cu, Zn, Ag, Cd, Sn, Hg and Pb) at varying concentrations (Figure 4.2, Table 4.2). Laser ablation ICP-MS measurements of the newly formed aragonite exhibited the following findings:

1. All metals but Hg were detectable above the LOD in all coral colonies (Figure 4.3).
2. Interspecies differences in TE/Ca values occurred but did not follow any systematic patterns.
3. Intraspecies variations could be linked to deviating growth rates (Figure 4.4, Figure A4.1, A4.3, A4.5, A4.7, Table B4.4).
4. Cr, Mn, Ni, Zn, Ag, Cd and Pb showed a positive linear relationship between the heavy metal concentration in the coral skeleton and the culturing medium (Figure 4.4) suggesting that the uptake of these metals mainly depended on their concentration in seawater.
5. The incorporation of heavy metals into the corals aragonite was most likely performed by Ca^{2+} substitution or by adsorption to organic matter.
6. Cu, Sn and Hg did not reveal a correlation between seawater and aragonite (Figure 4.4, Table B4.4). In cases of Cu and Sn, the low variability of these metals in the culturing medium made any correlation unlikely (Figure 4.2, Table 4.2). Hg showed an appropriate concentration range in seawater (Figure 4.2, Table 4.2), but Hg/Ca values in the coral skeleton were too low to interpret (Figure 4.4).
7. D_{TE} values partly compared to a variety of other studies (Table 4.4, Figure 4.5) even though our D_{TE} values were lower than some reported ones.

Generally, the results of this study show new insights into the uptake of heavy metals by corals, provide well-constrained TE/Ca values, and therefore facilitate the use of coral skeletons for paleo-reconstructions. The D_{TE} values presented herein permit an approximation of heavy metal concentrations in seawater, which provides a promising tool for ecosystem status assessments in the future.

4.6 Appendix

4.6.1 Appendix A: Additional Figures

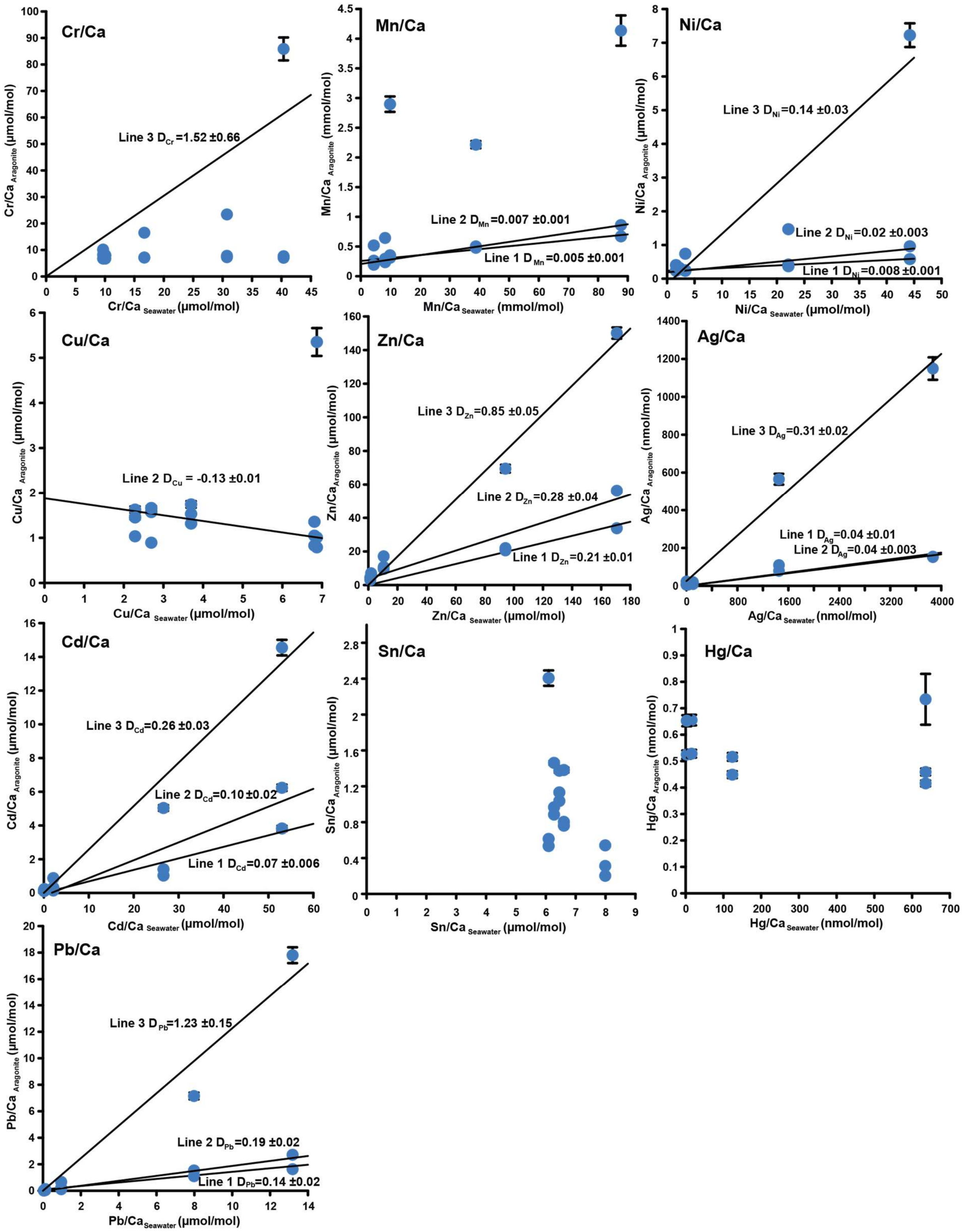

Figure A4.1: Comparison of TE/Ca values of different laser ablation lines of coral colony A. Mean TE/Ca in the coral aragonite versus the mean TE/Ca values in the corresponding culturing medium based on phase 0 to 4 of the metal system is shown. Each data point represents the mean value of laser ablation ICP-MS measurements calculated from the individual culturing phase plotted against the mean metal concentrations in the seawater averaged over the culturing phase (Table 4.2). Error bars symbolize the standard error of the mean (standard deviation $\sigma/\sqrt{n}$). Note that error bars are only given for the TE/Ca values of the coral aragonite as the metal concentration in the culturing medium was strongly varying (see Figure 4.2) due to the punctual input of the stock solution. This results in a disproportional high standard error, which in turn would make it impossible to see distinct features in the plot if it would be displayed. The linear regression line is given, when elements showed a significant correlation between seawater and aragonite. D_{TE} (±SE) values represent the slope of the regression line, which is partly forced through the origin. All values can be found in Table B4.4.

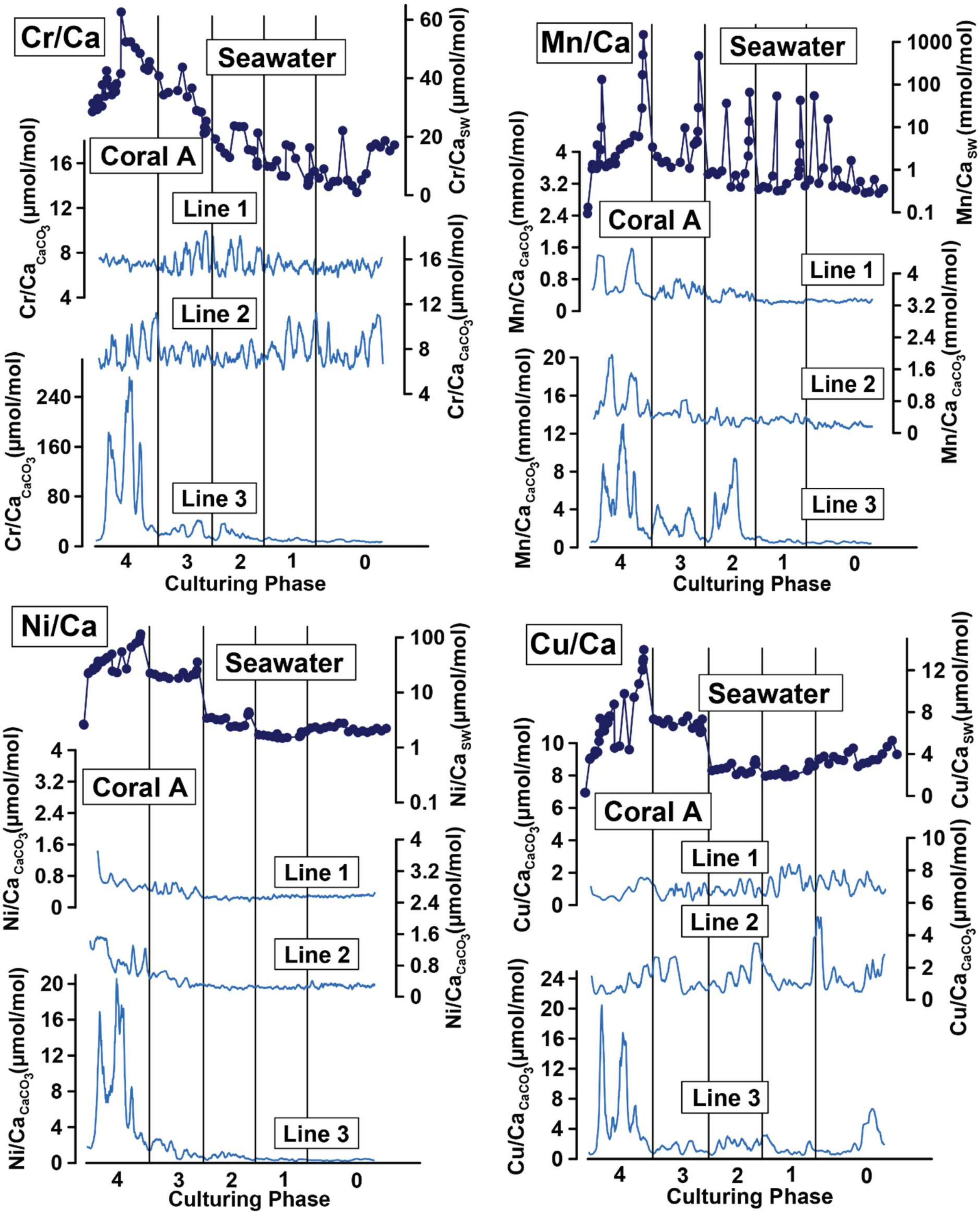
Cr/Ca
Seawater
Coral A
Line 1
Line 2
Line 3
Cr/Ca$_{SW}$(µmol/mol)
Cr/Ca$_{CaCO_3}$(µmol/mol)
Culturing Phase
Mn/Ca
Mn/Ca$_{SW}$(mmol/mol)
Mn/Ca$_{CaCO_3}$(mmol/mol)
Ni/Ca
Ni/Ca$_{SW}$(µmol/mol)
Ni/Ca$_{CaCO_3}$(µmol/mol)
Cu/Ca
Cu/Ca$_{SW}$(µmol/mol)
Cu/Ca$_{CaCO_3}$(µmol/mol)

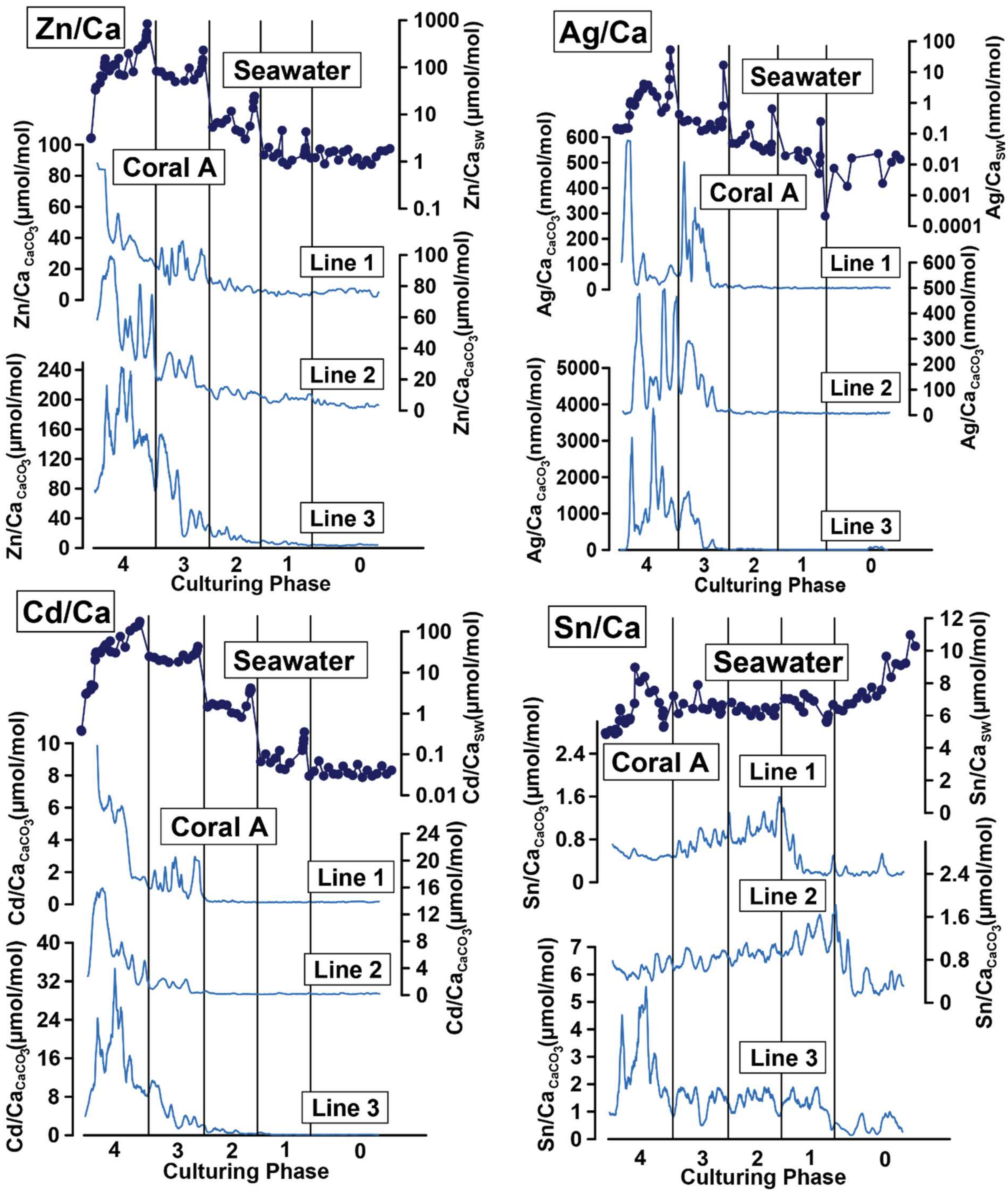
Zn/Ca
Seawater
Coral A
Line 1
Line 2
Line 3
Zn/Ca CaCO3(µmol/mol)
Zn/CaSW(µmol/mol)
Culturing Phase
Ag/Ca
Seawater
Coral A
Line 1
Line 2
Line 3
Ag/Ca CaCO3(nmol/mol)
Ag/CaSW(nmol/mol)
Culturing Phase
Cd/Ca
Seawater
Coral A
Line 1
Line 2
Line 3
Cd/Ca CaCO3(µmol/mol)
Cd/CaSW(µmol/mol)
Culturing Phase
Sn/Ca
Seawater
Coral A
Line 1
Line 2
Line 3
Sn/Ca CaCO3(µmol/mol)
Sn/CaSW(µmol/mol)
Culturing Phase

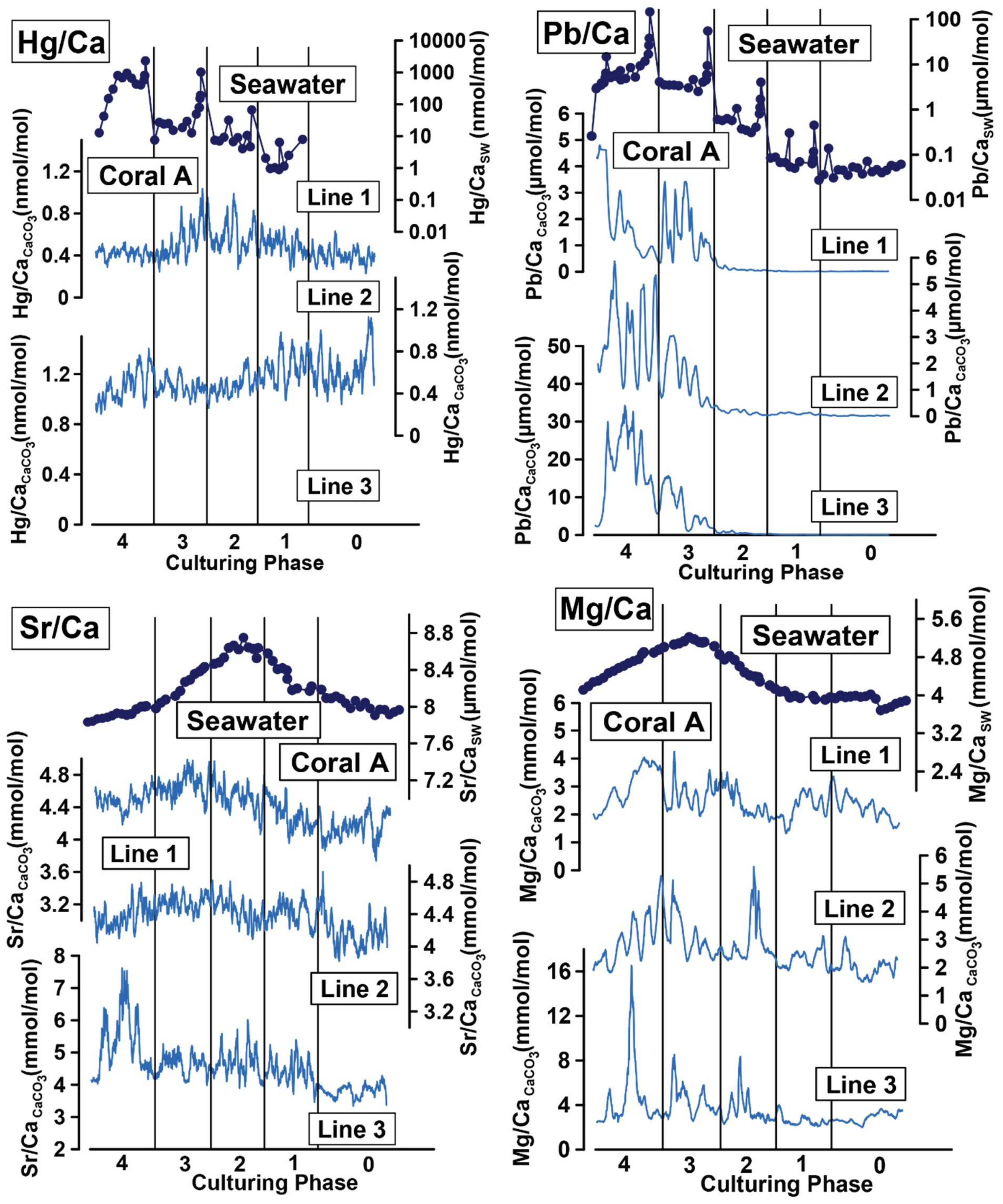

Figure A4.2: TE/Ca values of single lines on coral A cultured in the metal system measured by laser ablation ICP-MS (lower graphs) and corresponding TE/Ca values in the culturing medium (topmost graph). To facilitate a comparison, all coral and water lines were transformed to the same Y-scale and therefore, differences in growth rates cannot be seen in this figure (see Table 4.3 for growth rates). Hg were not detectable in line 3. All elements but Cr, Cu, Sn, Sr and Mg are displayed with a logarithmic scale for the water measurements. All values can be found in Table 4.2 and Tables S4.1-S4.4 (available at PANGAEA = https://doi.pangaea.de/10.1594/PANGAEA.938748).

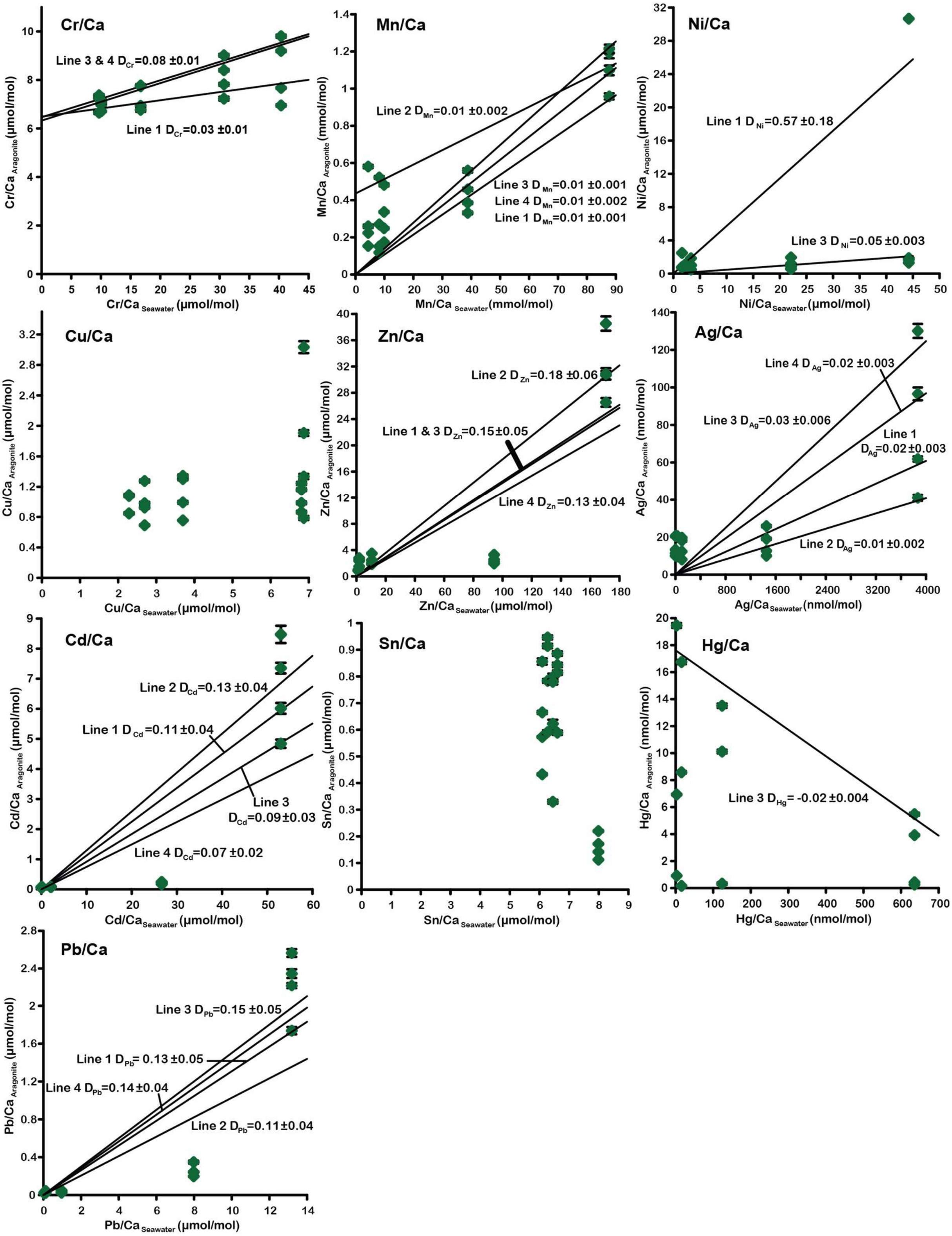

Figure A4.3: Comparison of TE/Ca values of different laser ablation lines of coral colony B. Mean TE/Ca in the coral aragonite versus the mean TE/Ca values in the corresponding culturing medium based on phase 0 to 4 of the metal system is shown. Each data point represents the mean value of laser ablation ICP-MS measurements calculated from the individual culturing phase plotted against the mean metal concentrations in the seawater averaged over the culturing phase (Table 4.2). Error bars symbolize the standard error of the mean (standard deviation $\sigma/\sqrt{n}$). Note that error bars are only given for the TE/Ca values of the coral aragonite as the metal concentration in the culturing medium was strongly varying (see Figure 4.2) due to the punctual input of the stock solution. This results in a disproportional high standard error, which in turn would make it impossible to see distinct features in the plot if it would be displayed. The linear regression line is given, when elements showed a significant correlation between seawater and aragonite. D_{TE} (±SE) values represent the slope of the regression line, which is partly forced through the origin. All values can be found in Table B4.4.

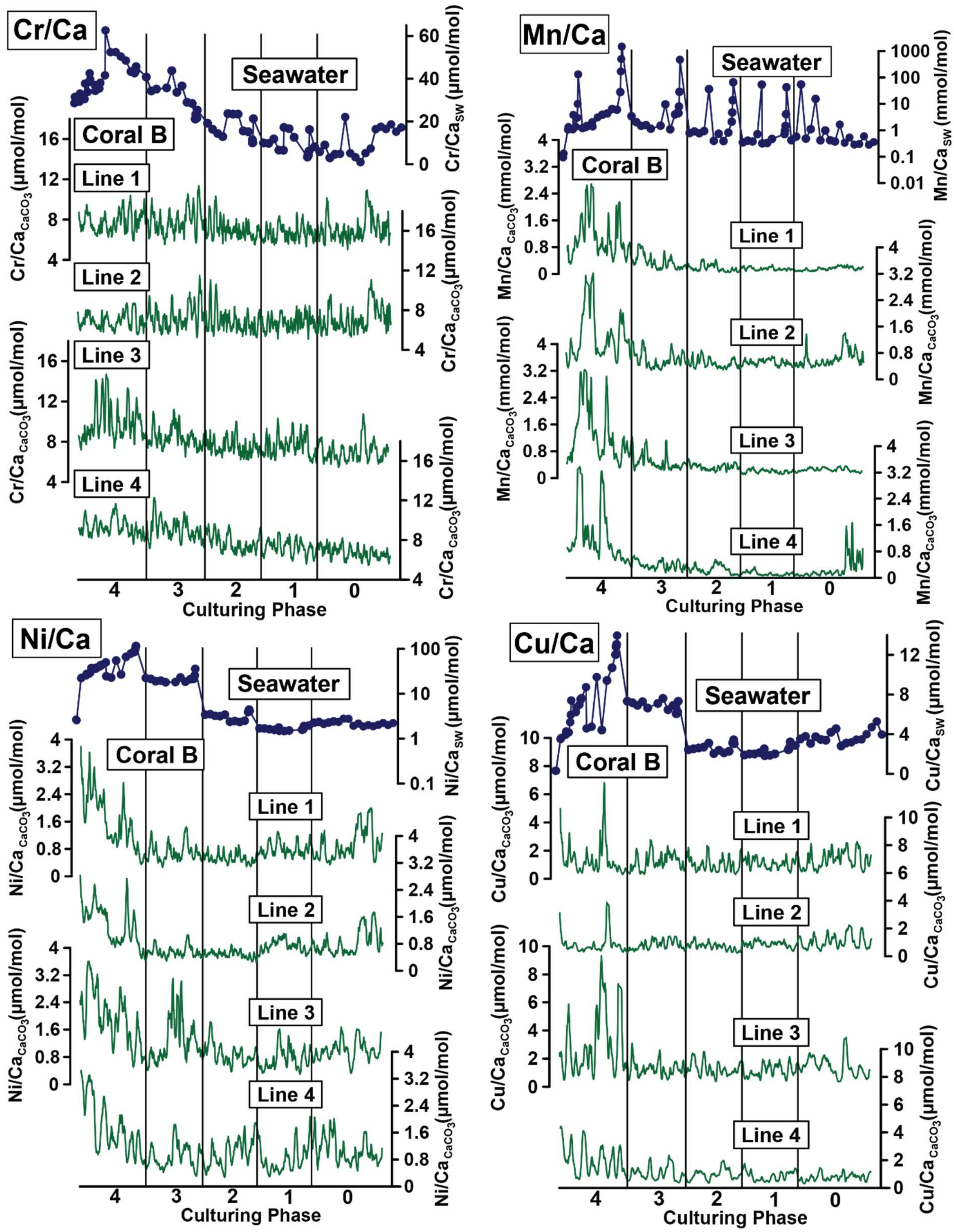
Cr/Ca
Seawater
Coral B
Line 1
Line 2
Line 3
Line 4
Cr/Ca_SW (µmol/mol)
Cr/Ca_CaCO3 (µmol/mol)
Culturing Phase
Mn/Ca
Mn/Ca_SW (mmol/mol)
Mn/Ca_CaCO3 (mmol/mol)
Ni/Ca
Ni/Ca_SW (µmol/mol)
Ni/Ca_CaCO3 (µmol/mol)
Cu/Ca
Cu/Ca_SW (µmol/mol)
Cu/Ca_CaCO3 (µmol/mol)

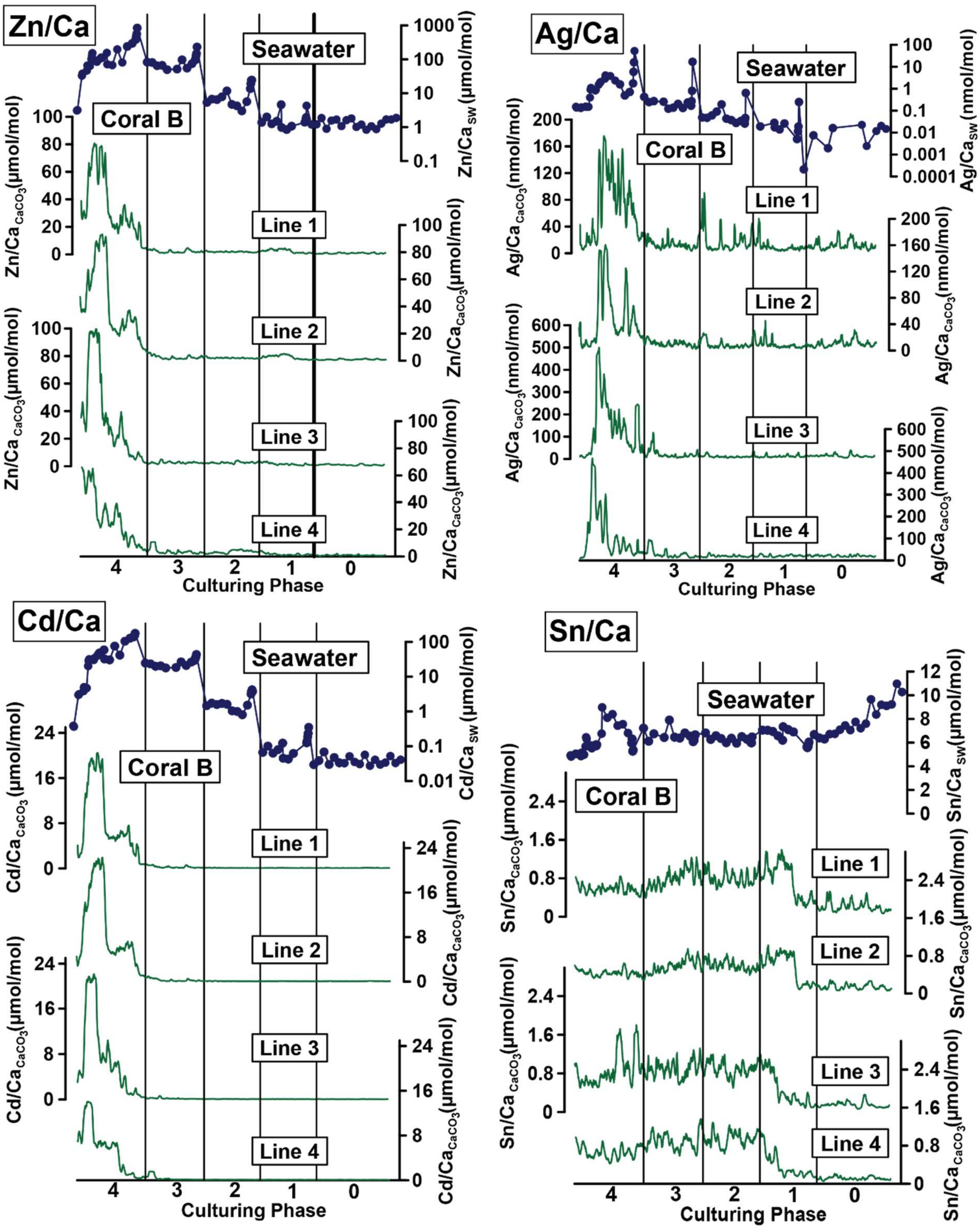
Zn/Ca
Seawater
Coral B
Line 1
Line 2
Line 3
Line 4
Culturing Phase
Ag/Ca
Cd/Ca
Sn/Ca

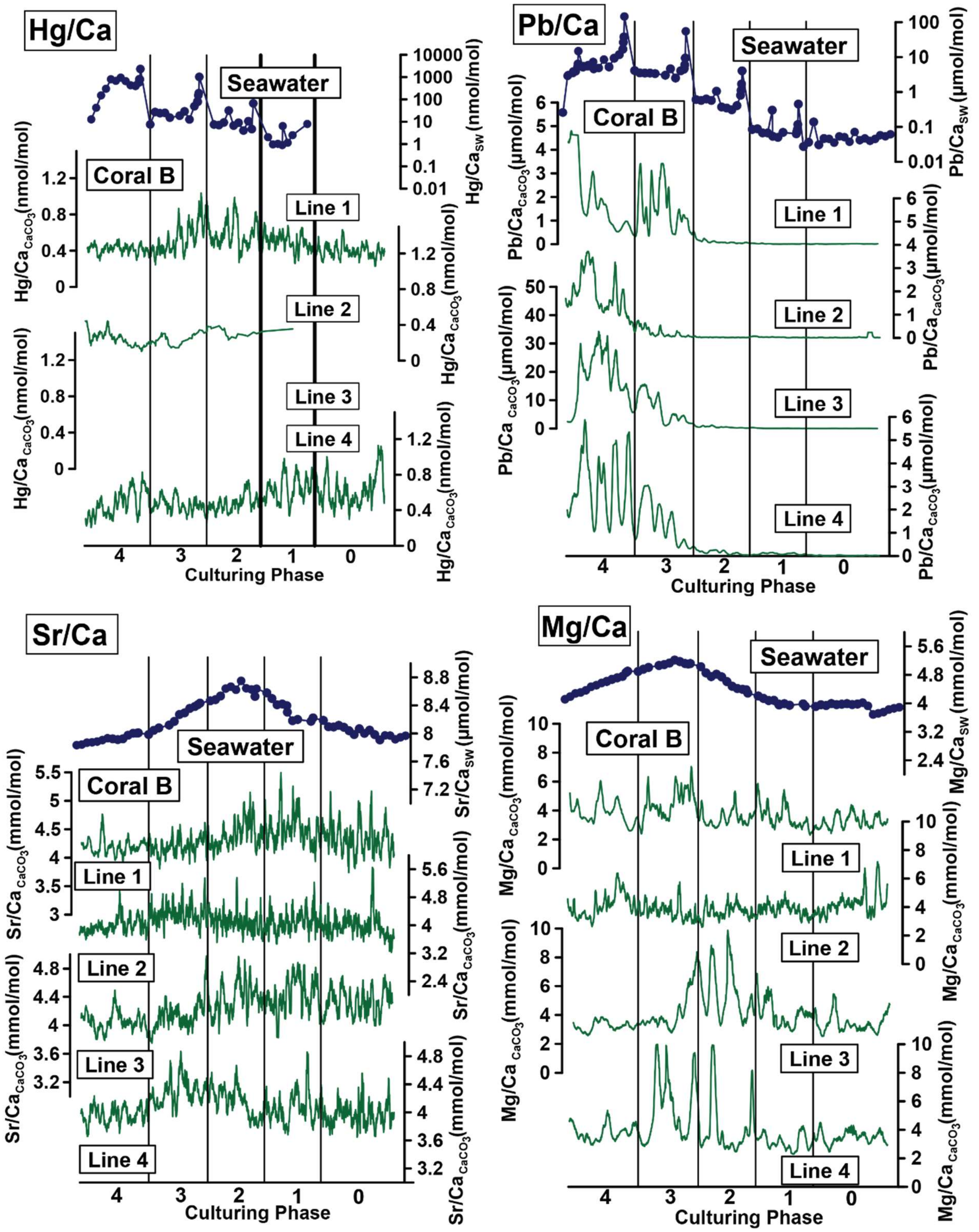

Figure A4.4: TE/Ca values of single lines on coral B cultured in the metal system measured by laser ablation ICP-MS (lower graphs) and corresponding TE/Ca values in the culturing medium (topmost graph). To facilitate a comparison, all coral and water lines were transformed to the same Y-scale and therefore, differences in growth rates cannot be seen in this figure (see Table 4.3 for growth rates). Hg were not detectable in line 3. All elements but Cr, Cu, Sn, Sr and Mg are displayed with a logarithmic scale for the water measurements. All values can be found in Table 4.2 and Tables S4.1-S4.4 (available at PANGAEA = https://doi.pangaea.de/10.1594/PANGAEA.938748).

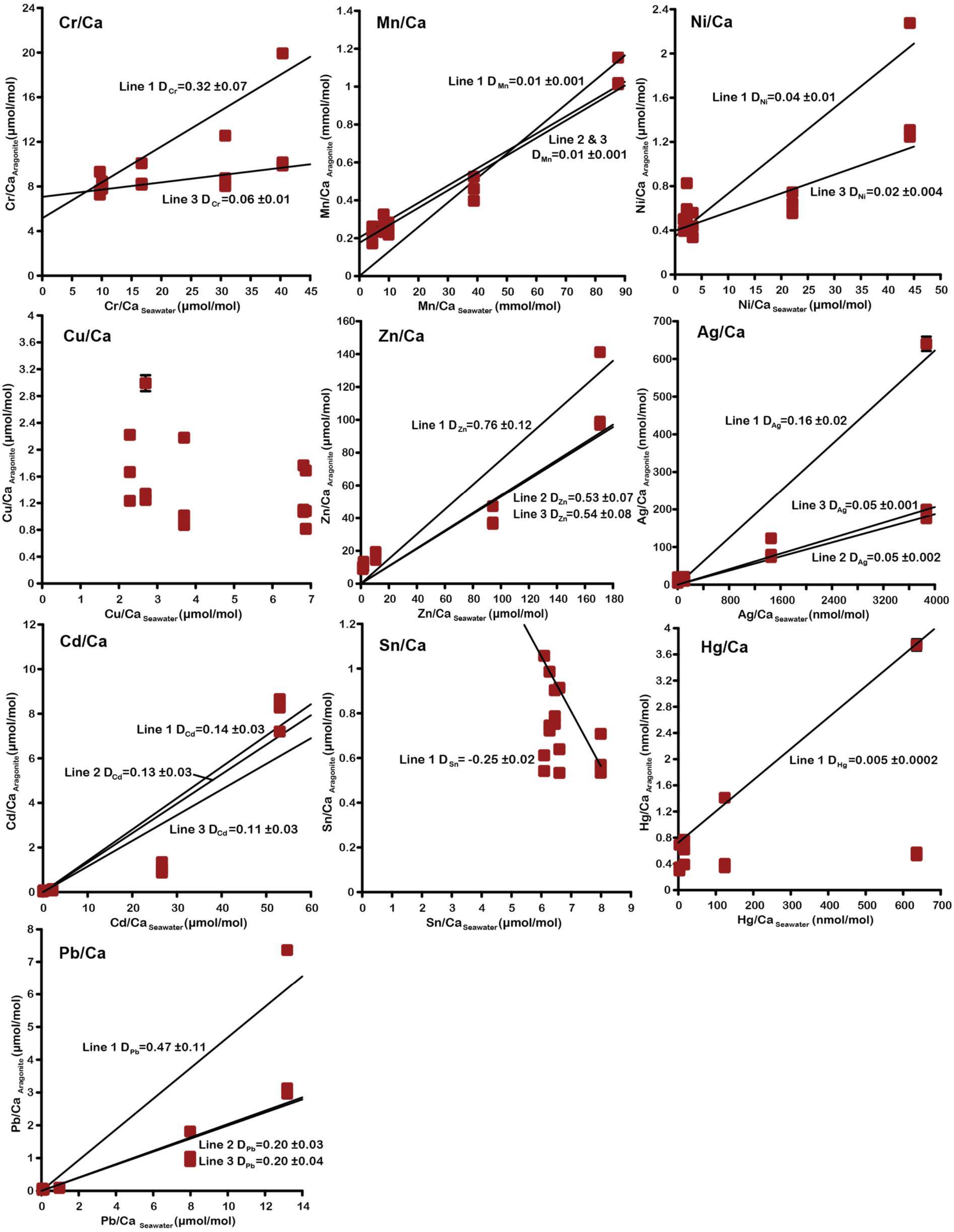

Figure A4.5: Comparison of TE/Ca values of different laser ablation lines of coral colony C. Mean TE/Ca in the coral aragonite versus the mean TE/Ca values in the corresponding culturing medium based on phase 0 to 4 of the metal system is shown. Each data point represents the mean value of laser ablation ICP-MS measurements calculated from the individual culturing phase plotted against the mean metal concentrations in the seawater averaged over the culturing phase (Table 4.2). Error bars symbolize the standard error of the mean (standard deviation $\sigma/\sqrt{n}$). Note that error bars are only given for the TE/Ca values of the coral aragonite as the metal concentration in the culturing medium was strongly varying (see Figure 4.2) due to the punctual input of the stock solution. This results in a disproportional high standard error, which in turn would make it impossible to see distinct features in the plot if it would be displayed. The linear regression line is given, when elements showed a significant correlation between seawater and aragonite. D_{TE} (±SE) values represent the slope of the regression line, which is partly forced through the origin. All values can be found in Table B4.4.

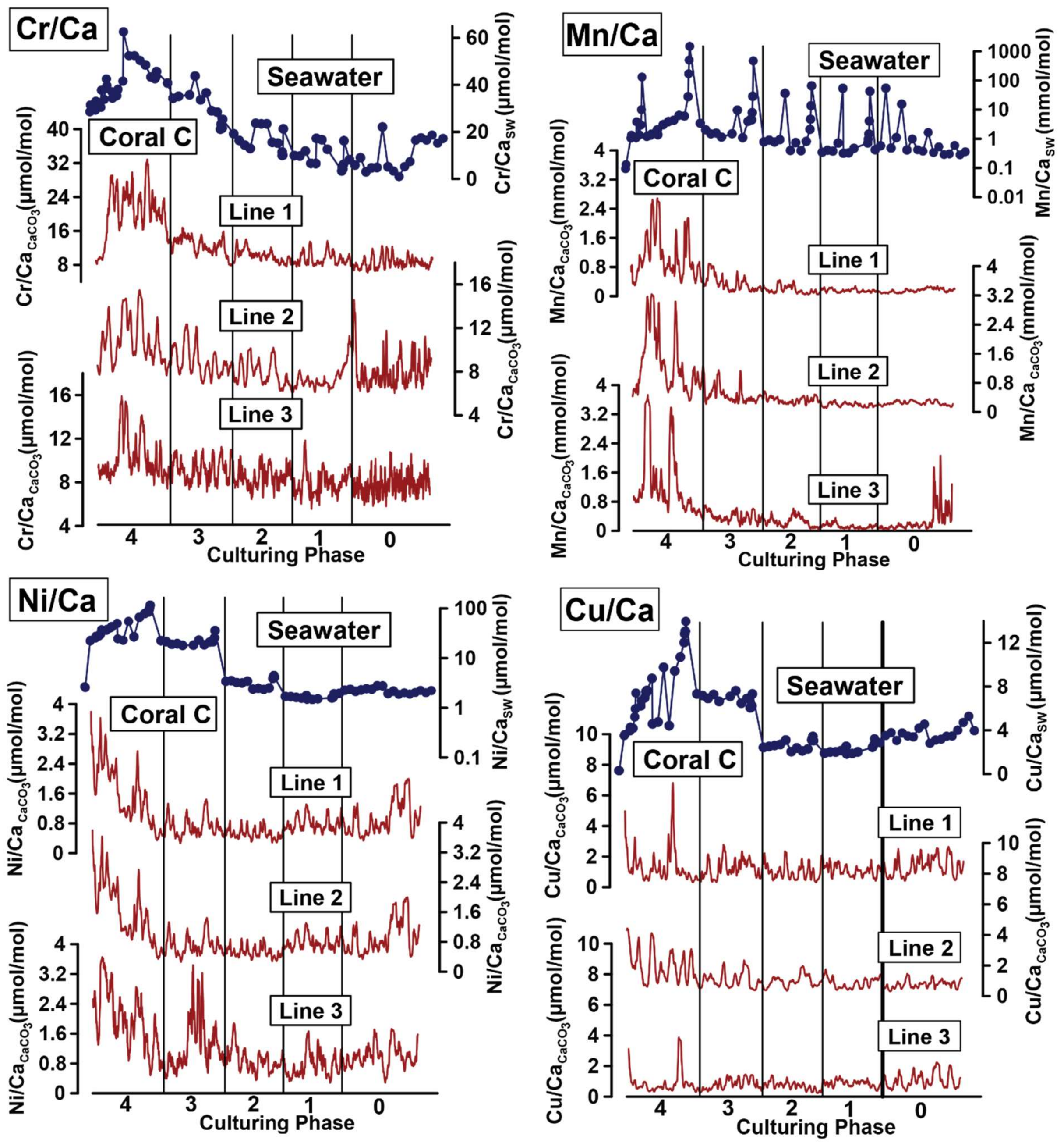
Cr/Ca
Seawater
Coral C
Line 1
Line 2
Line 3
Culturing Phase
Mn/Ca
Seawater
Coral C
Line 1
Line 2
Line 3
Culturing Phase
Ni/Ca
Seawater
Coral C
Line 1
Line 2
Line 3
Culturing Phase
Cu/Ca
Seawater
Coral C
Line 1
Line 2
Line 3
Culturing Phase

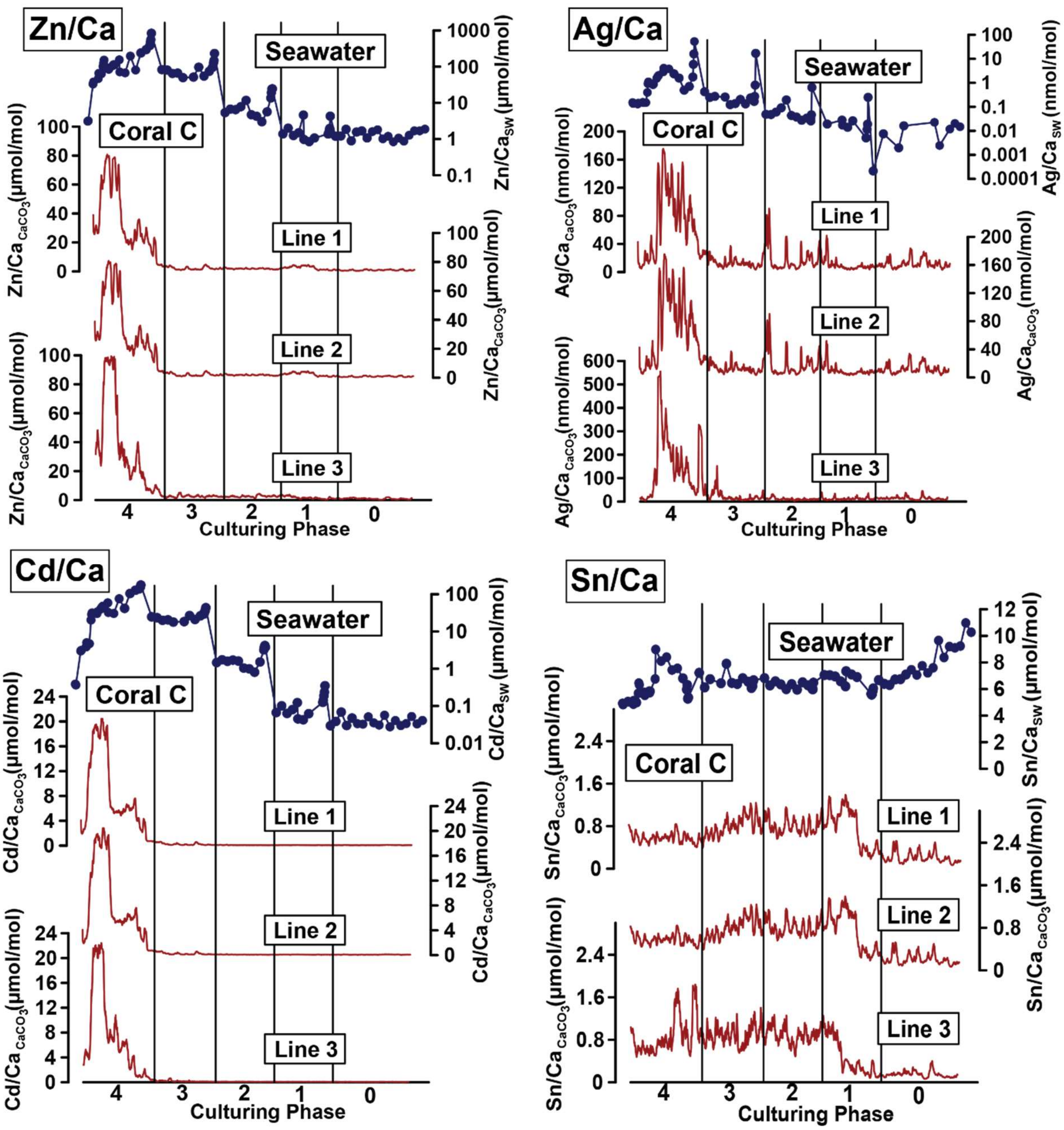
Zn/Ca
Seawater
Coral C
Line 1
Line 2
Line 3
Culturing Phase
Ag/Ca
Cd/Ca
Sn/Ca
4
3
2
1
0

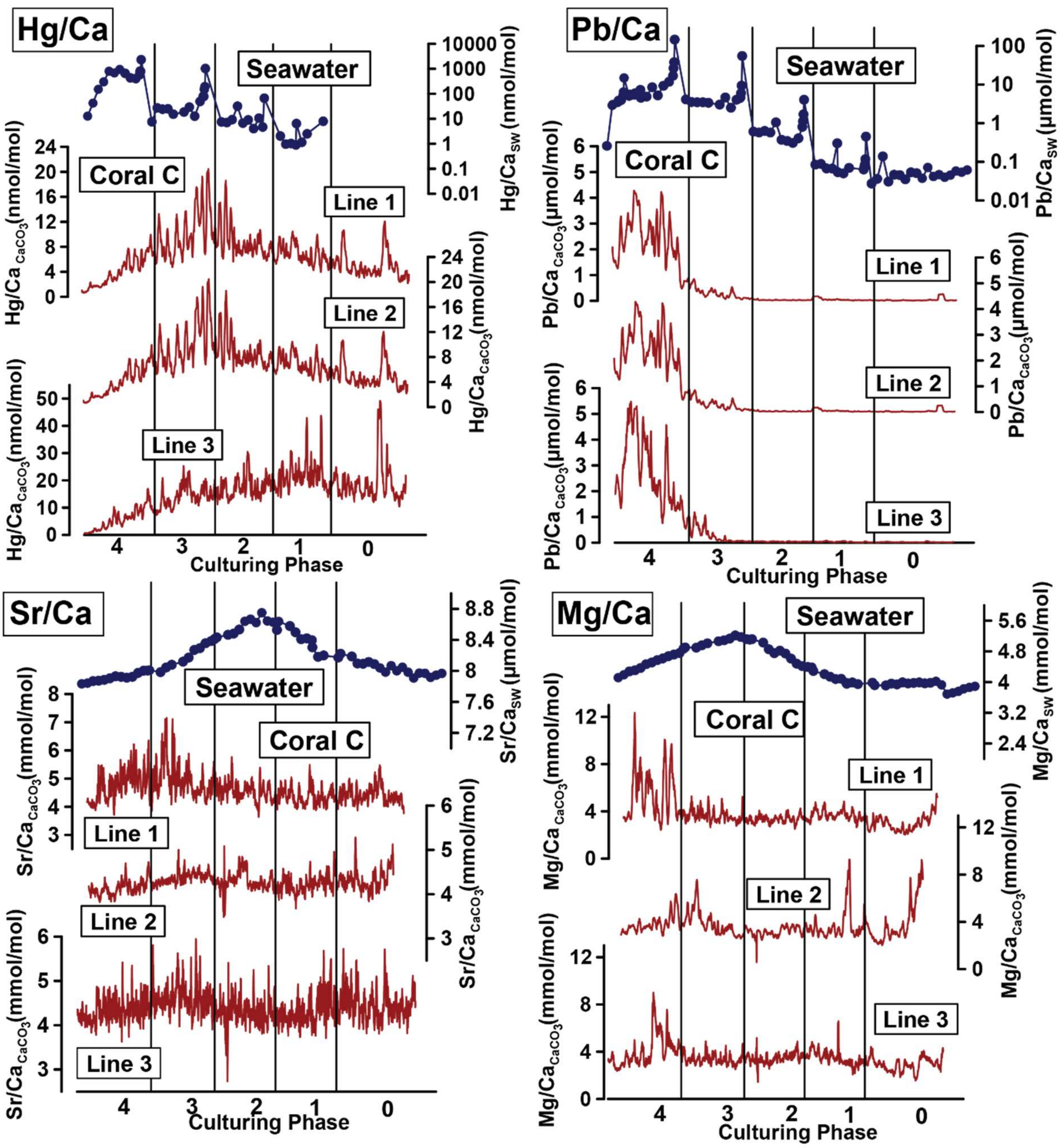

Figure A4.6: TE/Ca values of single lines on coral C cultured in the metal system measured by laser ablation ICP-MS (lower graphs) and corresponding TE/Ca values in the culturing medium (topmost graph). To facilitate a comparison, all coral and water lines were transformed to the same Y-scale and therefore, differences in growth rates cannot be seen in this figure (see Table 4.3 for growth rates). All elements but Cr, Cu, Sn, Sr and Mg are displayed with a logarithmic scale for the water measurements. All values can be found in Table 4.2 and Tables S4.1-S4.4 (available at PANGAEA = https://doi.pangaea.de/10.1594/PANGAEA.938748).

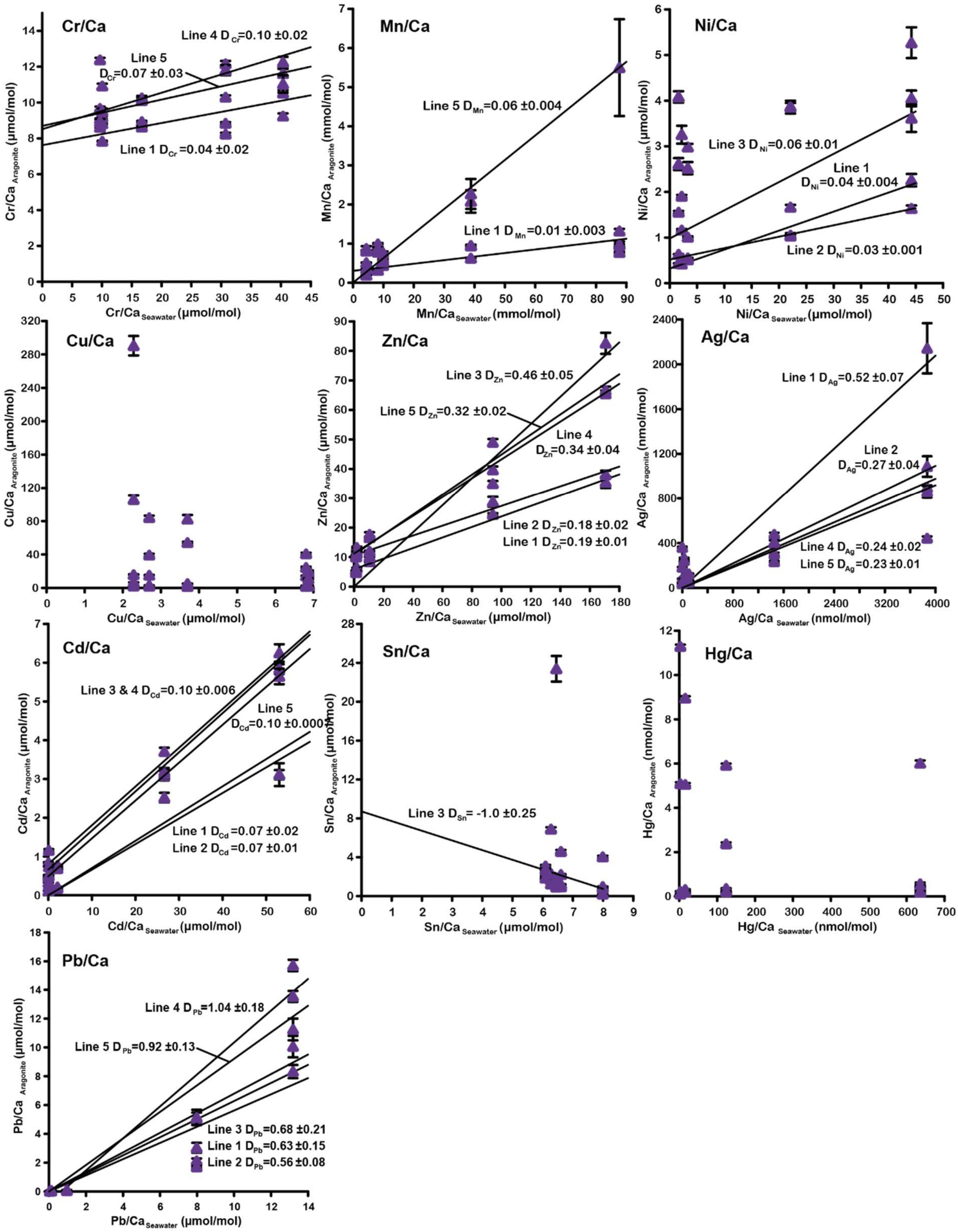

Figure A4.7: Comparison of TE/Ca values of different laser ablation lines of coral colony D. Mean TE/Ca in the coral aragonite versus the mean TE/Ca values in the corresponding culturing medium based on phase 0 to 4 of the metal system is shown. Each data point represents the mean value of laser ablation ICP-MS measurements calculated from the individual culturing phase plotted against the mean metal concentrations in the seawater averaged over the culturing phase (Table 4.2). Error bars symbolize the standard error of the mean (standard deviation σ/√n). Note that error bars are only given for the TE/Ca values of the coral aragonite as the metal concentration in the culturing medium was strongly varying (see Figure 4.2) due to the punctual input of the stock solution. This results in a disproportional high standard error, which in turn would make it impossible to see distinct features in the plot if it would be displayed. The linear regression line is given, when elements showed a significant correlation between seawater and aragonite. D_{TE} (±SE) values represent the slope of the regression line, which is partly forced through the origin. All values can be found in Table B4.4.

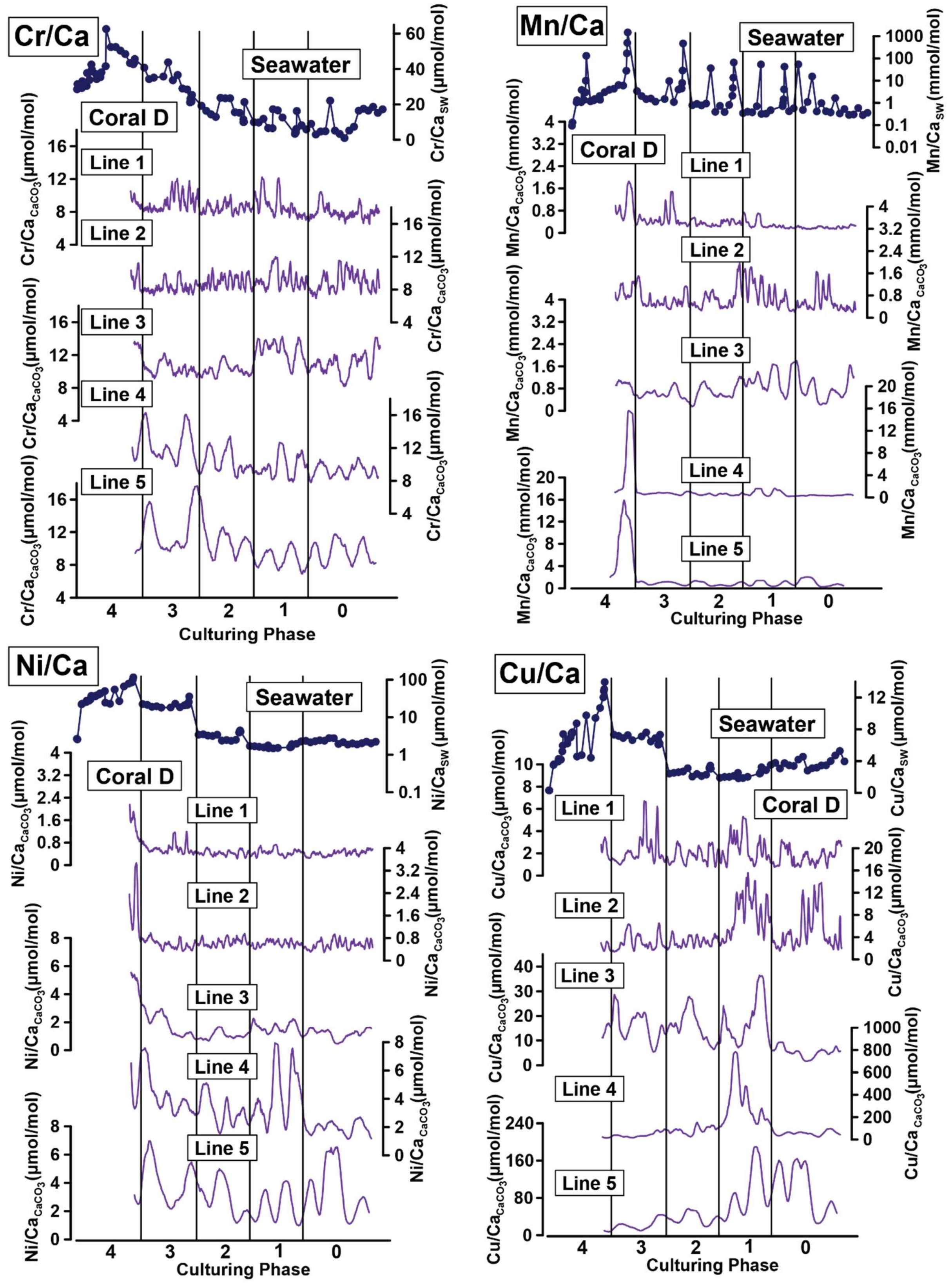
Cr/Ca
Seawater
Coral D
Line 1
Line 2
Line 3
Line 4
Line 5
Cr/Ca_{SW} (µmol/mol)
Cr/Ca_{CaCO_3}(µmol/mol)
Culturing Phase
Mn/Ca
Mn/Ca_{SW} (mmol/mol)
Mn/Ca_{CaCO_3}(mmol/mol)
Ni/Ca
Ni/Ca_{SW} (µmol/mol)
Ni/Ca_{CaCO_3}(µmol/mol)
Cu/Ca
Cu/Ca_{SW} (µmol/mol)
Cu/Ca_{CaCO_3}(µmol/mol)
4
3
2
1
0

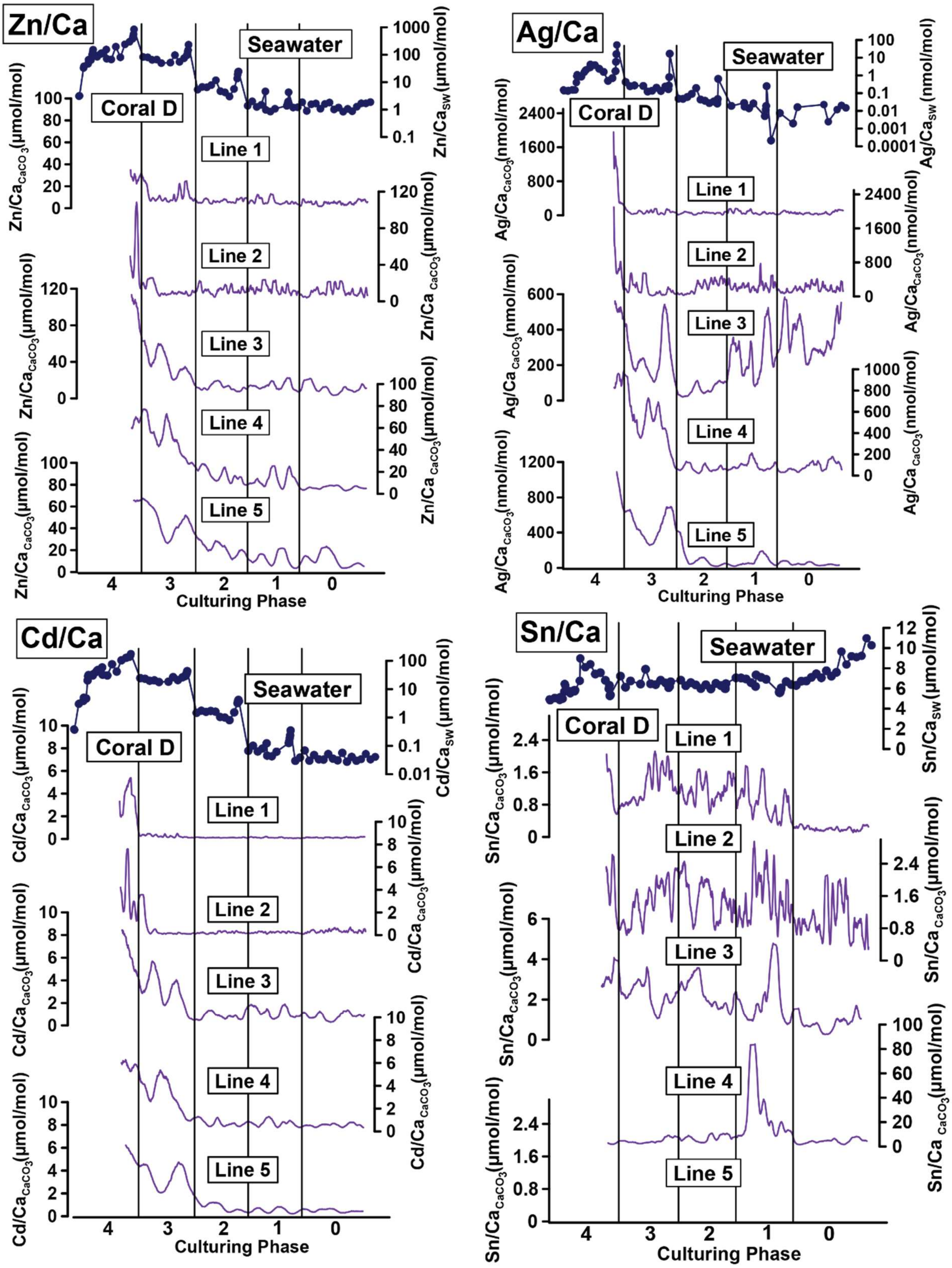

Zn/Ca
Seawater
Coral D
Line 1
Line 2
Line 3
Line 4
Line 5
Zn/Ca$_{CaCO_3}$(µmol/mol)
Zn/Ca$_{SW}$(µmol/mol)
Culturing Phase
Ag/Ca
Ag/Ca$_{CaCO_3}$(nmol/mol)
Ag/Ca$_{SW}$(nmol/mol)
Cd/Ca
Cd/Ca$_{CaCO_3}$(µmol/mol)
Cd/Ca$_{SW}$(µmol/mol)
Sn/Ca
Sn/Ca$_{CaCO_3}$(µmol/mol)
Sn/Ca$_{SW}$(µmol/mol)
4
3
2
1
0

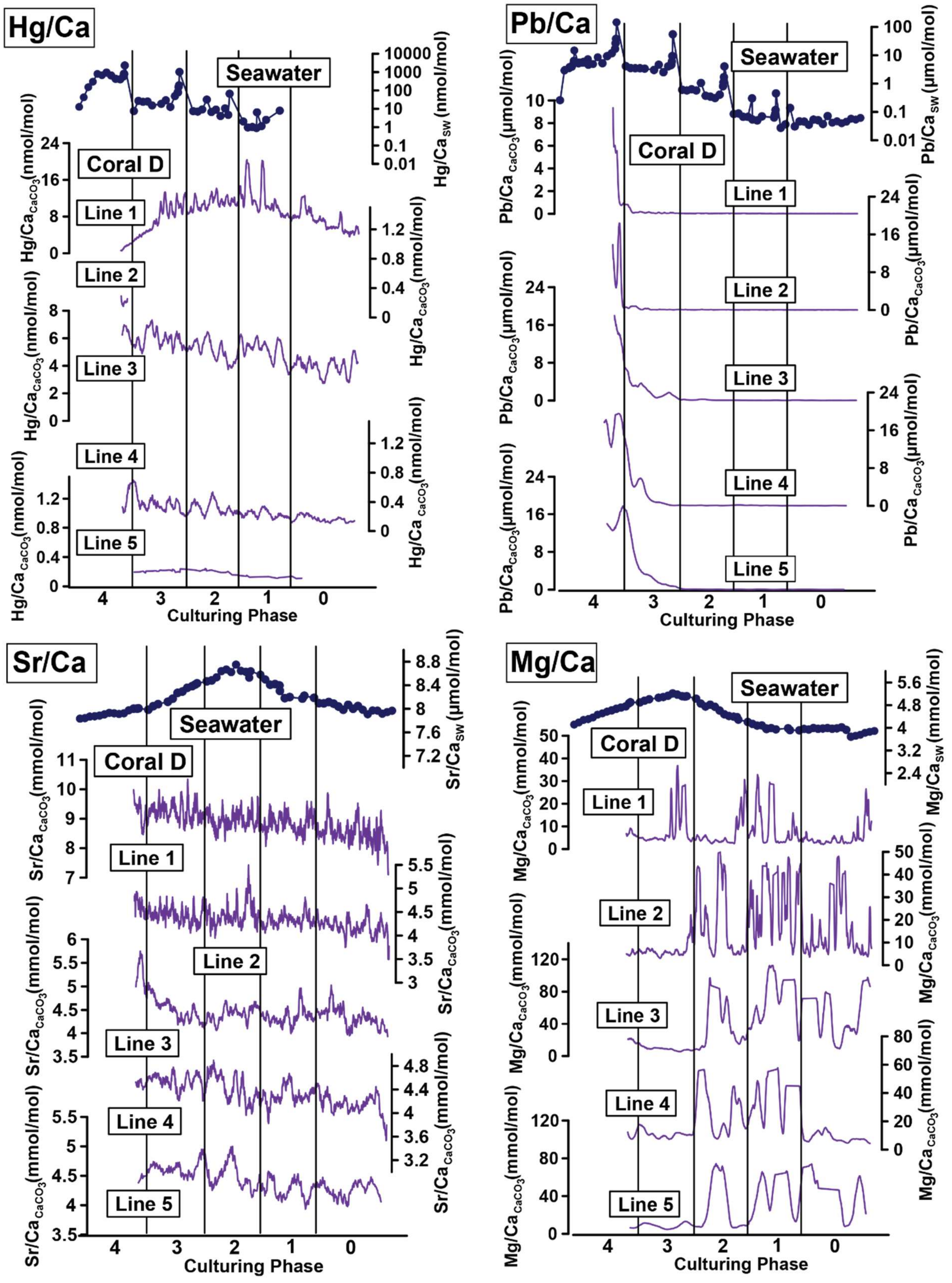

Figure A4.8: TE/Ca values of single lines on coral D cultured in the metal system measured by laser ablation ICP-MS (lower graphs) and corresponding TE/Ca values in the culturing medium (topmost graph). To facilitate a comparison, all coral and water lines were transformed to the same Y-scale and therefore, differences in growth rates cannot be seen in this figure (see Table 4.3 for growth rates). Note that coral D died at the beginning of phase 4 after approximately 2.5 weeks. In some cases, Sn (line 5) and Hg (line 2, Phase 0 to 3) were not detectable. All elements but Cr, Cu, Sn, Sr and Mg are displayed with a logarithmic scale for the water measurements. All values can be found in Table 4.2 and Tables S4.1-S4.4 (available at PANGAEA = https://doi.pangaea.de/10.1594/PANGAEA.938748).

4.6.2 Appendix B: Additional Tables

Table B4.1: Average concentration, RSD (1σ in %), literature values, accuracy in comparison to literature values and number of measurements of the reference materials SLRS-6, SLEW-3, in-house reference materials (South Atlantic surface water and South Atlantic Gyre water) and NASS-6 measured with ICP-MS. Average concentration, RSD and accuracy values displayed here are averaged from single measuring days. Cr values are analysed after dilution of the samples and all other elements were analyses after preconcentration with a SeaFAST system. NRCC-National Research Council Canada. *Values originated from 1:10 dilution of SLRS-6. See also Schmidt et al., 2021.

Reference Materials	Cr	Mn	Ni	Cu	Zn	Cd	Pb
SLRS-6	**nmol kg^{-1}**	**nmol kg^{-1}**	**nmol kg^{-1}**	**nmol kg^{-1}**	**nmol kg^{-1}**	**nmol kg^{-1}**	**nmol kg^{-1}**
Average conc.	4732	52956	9811	338014*	31391*	62	786
RSD%	3.5	3.9	6.0	1.7*	7.2*	12.8	0.8
Yeghicheyan et al., 2019	4509	38616	10496	376378*	26920*	56	820
Accuracy	0.96	0.74	1.08	1.11*	0.86*	0.90	1.04
Number	4	11	11	13*	13*	7	7
SLEW-3							
Average conc.		40007	17508	22907	4442	343	
RSD%		4.3	3.5	4.2	9.1	4.8	
Leonhard et al., 2002		29326	20958	24409	3074	427	
Accuracy		0.74	1.21	1.07	0.78	1.28	
Number		12	12	12	12	12	
South Atlantic Gyre water							
Average conc.		1615	2189	2649	5614		
RSD%		6.2	3.7	5.3	13.2		
Number		10	10	10	10		
South Atlantic surface water							
Average conc.		1959	2417	2646	39718		
RSD%		6.8	2.8	5.8	2.2		
Number		6	6	6	6		
NASS-6							
Average conc.	6747	11162	3557	5206	5158	169	
RSD%	15.9	5.2	3.2	3.0	25.3	7.0	
NRCC	2293	9654	5129	3528	3931	165	
Accuracy	0.34	0.87	0.76	0.35	0.81	0.98	
Number	9	11	11	11	11	2	

Table B4.2: Average concentration, RSD (1σ in %), literature values, accuracy in comparison to literature values and number of measurements of the reference materials NIST SRM 614, JCt-1, JCp-1, MACS-3 and ECRM752-1 measured with LA-ICP-MS. Please note that for the ECRM752-1 no reported values for the elements of interest are available, which is also the case for some elements in other reference materials. Please note further that the Hg/Ca values in the NIST glasses are not reliable as Hg is volatile and most likely volatilized during the glass formation. Average concentration, RSD and accuracy values displayed here are averaged from single measuring days.

Reference materials	**Cr/Ca**	**Mn/Ca**	**Ni/Ca**	**Cu/Ca**	**Zn/Ca**	**Ag/Ca**	**Cd/Ca**	**Sn/Ca**	**Hg/Ca**	**Pb/Ca**
NIST SRM 614	µmol mol^{-1}	µmol mol^{-1}	µmol mol^{-1}	µmol mol^{-1}	µmol mol^{-1}	µmol mol^{-1}	µmol mol^{-1}	µmol mol^{-1}	µmol mol^{-1}	µmol mol^{-1}
Mean value	14.30	10.93	9.74	10.22	85.88	1.82	3.13	6.05	0.28	5.70
RSD%	6.89	6.04	10.77	2.31	1.80	2.88	4.95	2.96	45.43	3.29
Jochum et al., 2011	10.78	12.18	8.83	10.16	20.11	1.83	2.35	6.67		5.28
Accuracy	0.79	1.12	0.93	0.99	0.23	1.01	0.79	1.11		0.93
Number of spots	24	24	24	24	24	24	24	24	12	24
MACS-3	mmol mol^{-1}	mmol mol^{-1}	mmol mol^{-1}	mmol mol^{-1}	mmol mol^{-1}	mmol mol^{-1}	mmol mol^{-1}	mmol mol^{-1}	µmol mol^{-1}	mmol mol^{-1}
Mean value	0.21	0.96	0.09	0.18	0.15	0.06	0.05	0.04	5.41	0.03
RSD%	1.08	1.39	1.28	1.27	1.96	4.51	2.53	2.05	11.41	2.51
Jochum et al., 2019	0.23	0.99	0.10	0.19	0.20	0.05	0.05	0.05	5.41	0.03
Accuracy	1.10	1.04	1.10	1.10	1.39	0.87	1.11	1.16	1.00	1.20
Number of spots	22	22	22	22	22	22	22	22	22	22
JCt-1NP	µmol mol^{-1}	µmol mol^{-1}	µmol mol^{-1}	µmol mol^{-1}	µmol mol^{-1}	µmol mol^{-1}	µmol mol^{-1}	µmol mol^{-1}	µmol mol^{-1}	µmol mol^{-1}
Mean value	8.70	0.78	0.61	1.19	1.95	0.003	0.08	0.01	0.20	0.07
RSD%	2.40	3.31	3.52	3.71	6.30	26.03	24.17	10.77	20.54	2.65
Jochum et al., 2019	0.93	1.01	1.03	1.48						0.06
Accuracy	0.03	0.55	0.33	1.20						0.71
Number of spots	38	38	38	38	38	36	38	38	29	38
JCp-1NP	µmol mol^{-1}	µmol mol^{-1}	µmol mol^{-1}	µmol mol^{-1}	µmol mol^{-1}	µmol mol^{-1}	µmol mol^{-1}	µmol mol^{-1}	µmol mol^{-1}	µmol mol^{-1}
Mean value	11.93	1.63	1.77	0.92	1.59	0.01	0.07	0.07	0.02	0.14
RSD%	6.30	5.22	6.39	4.42	5.21	12.29	12.56	10.49	14.81	4.85
Jochum et al., 2019	1.27	2.16	1.05	1.29	3.53					0.15
Accuracy	5.78	0.61	4.72	1.26	0.51					0.67
Number of spots	34	34	34	34	34	34	34	34	20	34
ECRM752-1	µmol mol^{-1}	µmol mol^{-1}	µmol mol^{-1}	µmol mol^{-1}	µmol mol^{-1}	µmol mol^{-1}	µmol mol^{-1}	µmol mol^{-1}	µmol mol^{-1}	µmol mol^{-1}
Mean value	162.31	4.77	2.75	10.60	0.005	0.59	0.06	0.05	0.92	0.92
RSD%	2.25	5.41	5.76	3.51	16.41	2.29	5.79	18.44	5.56	5.56
Number of spots	22	22	22	22	22	22	22	19	22	22

Table B4.3: Mg/Ca and Sr/Ca values in the culturing medium of the metal system. CL=Metal system, W=week, D=Day, Ph=Phase.

Sample ID	**Phase**	**Sampling Date**	**Mg/Ca**	**Sr/Ca**

Metal System			mmol/mol	µmol/mol
CL0 W2	0	16.8.19	3.89	7.97
CL0 W3	0	25.8.19	3.86	7.94
CL0 W4	0	29.8.19	3.83	7.92
CL0 W5	0	4.9.19	3.76	7.97
CL0 W6	0	9.9.19	3.72	7.97
CL0 W7	0	16.9.19	3.69	7.91
CL0 W8	0	23.9.19	3.93	7.98
CL0 W9	0	2.10.19	4.02	8.05
CL0 W10	0	7.10.19	3.98	8.00
CL0 W11	0	15.10.19	3.97	8.07
CL0 W12	0	21.10.19	3.99	7.98
CL0 W13	0	28.10.19	3.98	8.04
CL0 W14	0	4.11.19	3.96	8.09
CL0 W15	0	11.11.19	3.99	8.12
CL0 W16	0	21.11.19	3.94	8.09
CL0 W17	0	28.11.19	3.96	8.10
CL0 W18	0	5.12.19	3.91	8.19
CL0 W19	0	10.12.19	3.92	8.22
CL1 W1 D1	1	16.12.19	3.98	8.17
CL1 W1 D5	1	20.12.19	3.95	8.20
CL1 W4	1	6.1.20	3.99	8.18
CL1 W5	1	16.1.20	3.96	8.30
CL1 W6	1	23.1.20	3.98	8.40
CL1 W6 D2	1	24.1.20	4.08	8.42
CL1 W7	1	28.1.20	4.08	8.41
CL1 W8	1	6.2.20	4.14	8.50
CL1 W9	1	10.2.20	4.21	8.58
CL1 W10	1	18.2.20	4.29	8.64
CL2 W1 D1	2	24.2.20	4.38	8.53
CL2 W1 D4	2	27.2.20	4.39	8.63
CL2 W2	2	2.3.20	4.42	8.64
CL2 W3	2	9.3.20	4.48	8.75
CL2 W4	2	16.3.20	4.61	8.62
CL2 W5	2	26.3.20	4.74	8.67
CL2 W6	2	31.3.20	4.82	8.64
CL2 W7	2	7.4.20	4.75	8.53
CL2 W8	2	14.4.20	4.86	8.48
CL2 W9	2	23.4.20	5.03	8.47
CL2 W10	2	30.4.20	5.12	8.43
CL3 W1 D1	3	4.5.20	5.11	8.41
CL3 W1 D5	3	8.5.20	5.12	8.38
CL3 W2	3	12.5.20	5.17	8.36
CL3 W3	3	19.5.20	5.21	8.29
CL3 W4	3	26.5.20	5.13	8.27
CL3 W5	3	4.6.20	5.09	8.17
CL3 W6	3	11.6.20	5.06	8.12
CL3 W7	3	18.6.20	5.01	8.08

CL3 W8	3	25.6.20	4.96	8.04
CL3 W9	3	2.7.20	4.90	7.98
CL3 W10	3	9.7.20	4.90	8.01
CL4 W1 D1	4	15.7.20	4.87	8.00
CL4 W1 D4	4	17.7.20	4.76	8.00
CL4 W2	4	22.7.20	4.72	7.97
CL4 W3	4	27.7.20	4.67	7.92
CL4 W4	4	6.8.20	4.62	7.91
CL4 W5	4	13.8.20	4.57	7.92
CL4 W6	4	20.8.20	4.51	7.93
CL4 W7	4	25.8.20	4.47	7.90
CL4 W8	4	31.8.20	4.37	7.88
CL4 W9	4	7.9.20	4.31	7.87
CL4 W10	4	14.9.20	4.28	7.87
CL4 W11 D1	4	22.9.20	4.19	7.84
CL4 W12	4	28.9.20	4.11	7.83
CL4 W13 D1	4	5.10.20	4.00	7.82

Table B4.4*:* Mean heavy metal–to–calcium values of single lines and the composite line of the coral colonies A to D in the metal system. The mean heavy metal-to-calcium ratio per phase, the standard errors of the mean (standard deviation σ/√n) and the D_{TE} values calculated for single phases without any correlation are given. Furthermore, the D_{TE} values calculated with all phases, representing the slope of the linear regression line (OLS-Ordinary Least Squares) of all means, Pearson's correlation coefficient (R^2) and its significance (p) are given. Values marked in italic are outlier and were not considered for further calculations. Cases where the regression lines were forced through the origin are indicated. In cases when a regression did not show significant correlation, the D_{TE} range calculated separately from the individual phases is given. Ph = Phase, SD = Standard deviation. Values in Table S4.1-4.4 are the basis of all calculations (available at PANGAEA = https://doi.pangaea.de/10.1594/PANGAEA.938748).

	Ph	Cr/Ca	Mn/Ca	Ni/Ca	Cu/Ca	Zn/Ca	Ag/Ca	Cd/Ca	Sn/Ca	Hg/Ca	Pb/Ca
Coral A		**µmol/ mol**	**mmol/ mol**	**µmol/ mol**	**µmol/ mol**	**µmol/ mol**	**nmol/ mol**	**µmol/ mol**	**µmol/ mol**	**nmol/ mol**	**µmol/ mol**
Mean Metal											
Coral A, Line 1	0	6.75	0.26	0.29	1.31	5.97	6.92	0.16	0.17	0.39	0.01
Coral A, Line 1	1	6.74	0.24	0.28	1.61	3.97	6.32	0.13	0.22	0.47	0.01
Coral A, Line 1	2	7.14	0.35	0.23	0.95	7.26	8.52	0.15	0.97	0.56	0.07
Coral A, Line 1	3	7.27	0.50	0.39	0.81	20.08	108.38	1.21	0.77	0.55	1.24
Coral A, Line 1	4	7.05	0.67	0.68	0.88	38.42	103.05	4.78	0.52	0.42	1.67
Standard Error											
Coral A, Line 1	0	0.03	0.00	0.00	0.02	0.06	0.16	0.00	0.00	0.01	0.00
Coral A, Line 1	1	0.03	0.00	0.00	0.02	0.04	0.17	0.00	0.00	0.01	0.00
Coral A, Line 1	2	0.05	0.01	0.00	0.02	0.10	0.22	0.00	0.01	0.01	0.00
Coral A, Line 1	3	0.05	0.01	0.01	0.01	0.34	5.12	0.03	0.01	0.01	0.04
Coral A, Line 1	4	0.04	0.02	0.02	0.03	1.02	5.77	0.21	0.00	0.01	0.07
D_{TE} Single Phases											
Coral A, Line 1	0	0.67	0.06	0.13	0.35	4.41	*76.67*	3.98	0.02		0.25
Coral A, Line 1	1	0.70	0.03	0.17	0.70	2.12	0.22	1.08	0.03	0.17	0.09

Coral A, Line 1	2	0.43	0.04	0.07	0.35	0.69	0.08	0.07	0.15	0.04	0.07
Coral A, Line 1	3	0.24	0.01	0.02	0.12	0.21	0.07	0.05	0.12	0.004	0.15
Coral A, Line 1	4	0.17	0.01	0.02	0.13	0.23	0.03	0.09	0.09	0.001	0.13
D_{TE} ±SD		0.17- 0.70	0.005 ±0.001	0.008 ±0.001	0.12- 0.70	0.21 ±0.01	0.04 ±0.01	0.07 ±0.006	0.02- 0.15	0.001- 0.17	0.14 ±0.02
Correlation coefficient (R^2)			0.93	0.99		0.93	0.93	0.98			0.96
Significance (p)			0.008	0.001		0.001	0.01	0.002			0.01
Forced through origin		Single Points	No	No	Single Points	Yes	Yes	Yes	Single Points	Single Points	Yes
Mean Metal											
Coral A, Line 2	0	7.83	0.19	0.28	1.37	3.13	6.91	0.20	0.34	0.61	0.02
Coral A, Line 2	1	8.16	0.29	0.24	1.16	6.62	7.81	0.16	1.08	0.65	0.08
Coral A, Line 2	2	7.15	0.31	0.25	1.51	10.93	10.26	0.19	0.90	0.47	0.16
Coral A, Line 2	3	7.80	0.48	0.49	1.40	27.49	132.96	1.56	0.78	0.49	1.67
Coral A, Line 2	4	7.65	0.86	1.02	0.85	60.75	146.48	7.24	0.59	0.44	2.82
Standard Error											
Coral A, Line 2	0	0.06	0.00	0.00	0.03	0.05	0.18	0.00	0.01	0.02	0.00
Coral A, Line 2	1	0.07	0.01	0.00	0.03	0.09	0.21	0.00	0.01	0.02	0.00
Coral A, Line 2	2	0.04	0.01	0.00	0.04	0.12	0.29	0.00	0.01	0.01	0.00
Coral A, Line 2	3	0.06	0.01	0.01	0.04	0.68	6.25	0.06	0.01	0.01	0.06
Coral A, Line 2	4	0.07	0.02	0.02	0.02	1.05	6.84	0.21	0.01	0.01	0.07
D_{TE} Single Phases											
Coral A, Line 2	0	0.78	0.04	0.13	0.37	2.32	*76.62*	4.95	0.04		0.37
Coral A, Line 2	1	0.84	0.04	0.15	0.51	3.54	0.27	1.31	0.17	0.23	0.63
Coral A, Line 2	2	0.43	0.03	0.07	0.56	1.04	0.10	0.09	0.14	0.03	0.16
Coral A, Line 2	3	0.25	0.01	0.02	0.21	0.29	0.09	0.06	0.12	0.004	0.21
Coral A, Line 2	4	0.19	0.01	0.02	0.12	0.36	0.04	0.14	0.10	0.001	0.21
D_{TE} ±SD		0.19- 0.84	0.007 ±0.001	0.02 ±0.003	-0.13 ±0.01	0.28 ±0.04	0.04 ±0.003	0.1 ±0.02	0.04- 0.17	0.001- 0.23	0.19 ±0.02
Correlation coefficient (R^2)			0.97	0.9	0.96	0.93	0.98	0.91			0.97
Significance (p)			0.002	0.01	0.003	0.01	0.001	0.02			0.003
Forced through origin		Single Points	No	No	No	No	Yes	Yes	Single Points	Single Points	Yes
Mean Metal											
Coral A, Line 3	0	8.03	0.52	0.32	2.06	3.95	27.16	0.11	0.46		0.02
Coral A, Line 3	1	10.15	0.64	0.39	1.28	6.12	7.31	0.16	1.30		0.07
Coral A, Line 3	2	16.50	2.90	0.68	1.82	13.84	17.23	0.66	1.40		0.50
Coral A, Line 3	3	23.41	2.22	1.38	1.32	63.35	496.57	4.52	1.41		6.61
Coral A, Line 3	4	85.86	4.14	6.99	5.17	147.15	1112.58	14.20	2.35	0.73	17.31
Standard Error											
Coral A, Line 3	0	0.09	0.01	0.01	0.10	0.04	2.68	0.002	0.01		0.001
Coral A, Line 3	1	0.13	0.01	0.01	0.04	0.11	0.41	0.01	0.02		0.003
Coral A, Line 3	2	0.40	0.13	0.02	0.04	0.31	0.95	0.02	0.02		0.01
Coral A, Line 3	3	0.47	0.06	0.04	0.03	2.15	27.65	0.16	0.03		0.25
Coral A, Line 3	4	4.32	0.25	0.34	0.30	3.28	55.96	0.44	0.08	0.10	0.59
D_{TE} Single Phases											
Coral A, Line 3	0	0.80	0.12	0.14	0.56	2.92	*300.99*	2.87	0.06		0.48
Coral A, Line 3	1	1.05	0.08	0.24	0.56	3.27	0.26	1.25	0.20		0.60
Coral A, Line 3	2	0.99	0.29	0.20	0.68	1.32	0.17	0.31	0.22		0.52
Coral A, Line 3	3	0.76	0.06	0.06	0.19	0.67	0.34	0.17	0.21		0.83
Coral A, Line 3	4	2.13	0.05	0.16	0.75	0.86	0.29	0.27	0.39	0.001	1.31

D_{TE} ±SD		1.52 ±0.66	0.05-0.29	0.14 ±0.03	0.19-0.75	0.85 ±0.05	0.31 ±0.02	0.26 ±0.03	0.06-0.39	0.001*	1.23 ±0.15
Correlation coefficient (R^2)		0.84		0.93		0.99	0.99	0.98			0.97
Significance (p)		0.05		0.02		0.001	0.001	0.002			0.003
Forced through origin		Yes	Single Points	Yes	Single Points	Yes	Yes	Yes	Single Points	Single Points	Yes
Coral A Compositeline											
Coral A, Composite Line	0	7.48	0.33	0.30	1.57	4.28	12.23	0.21	0.40	0.50	0.02
Coral A, Composite Line	1	8.37	0.40	0.30	1.32	5.50	7.14	0.42	1.02	0.56	0.05
Coral A, Composite Line	2	10.25	1.19	0.39	1.41	10.78	11.19	0.58	0.99	0.51	0.25
Coral A, Composite Line	3	13.16	1.07	0.78	1.16	38.52	252.31	2.17	0.95	0.50	3.49
Coral A, Composite Line	4	33.02	1.88	2.99	2.25	83.60	492.12	6.49	1.21	0.44	7.49
Standard Error											
Coral A, Composite Line	0	0.04	0.003	0.002	0.04	0.03	0.93	0.00	0.01	0.02	0.0003
Coral A, Composite Line	1	0.05	0.005	0.003	0.02	0.05	0.14	0.01	0.02	0.01	0.001
Coral A, Composite Line	2	0.14	0.05	0.01	0.02	0.15	0.29	0.01	0.01	0.01	0.01
Coral A, Composite Line	3	0.20	0.02	0.02	0.02	1.04	12.26	0.07	0.01	0.01	0.13
Coral A, Composite Line	4	1.43	0.09	0.13	0.10	1.72	27.64	0.18	0.03	0.01	0.25
D_{TE} Single Phases											
Coral A, Composite Line	0	0.74	0.08	0.13	0.42	3.16	*135.58*	5.21	0.05		0.36
Coral A, Composite Line	1	0.86	0.05	0.19	0.58	2.94	0.25	3.38	0.16	0.20	0.43
Coral A, Composite Line	2	0.61	0.12	0.12	0.52	1.02	0.11	0.27	0.16	0.03	0.26
Coral A, Composite Line	3	0.43	0.03	0.04	0.17	0.41	0.17	0.08	0.14	0.004	0.44
Coral A, Composite Line	4	0.82	0.02	0.07	0.33	0.49	0.13	0.12	0.20	0.001	0.57
D_{TE} ±SD		0.68 ±0.21	0.02 ±0.005	0.06 ±0.01	0.17-0.58	0.47 ±0.03	0.13 ±0.01	0.11 ±0.01	-0.40 ±0.04	0.001-0.2	0.53 ±0.04
Correlation coefficient (R^2)		0.94	0.76	0.91		0.99	0.99	0.97	0.97		0.99
Significance (p)		0.04	0.05	0.01		0.001	0.001	0.004	0.002		0.001
Forced through origin		Yes	No	Yes	Single Points	Yes	Yes	Yes	No	Single Points	Yes
Coral B Mean Metal											
Coral B - Line 1	0	6.99	0.15	0.89	1.30	0.85	11.42	0.07	0.22	4.89	0.03
Coral B - Line 1	1	6.65	0.15	0.74	1.09	2.49	10.94	0.07	0.80	6.93	0.04
Coral B - Line 1	2	6.93	0.17	0.50	0.98	1.84	18.20	0.08	0.78	8.58	0.03
Coral B - Line 1	3	7.82	0.33	0.73	1.24	1.95	12.68	0.21	0.81	10.12	0.24

Coral B - Line 1	4	7.67	0.96	1.56	1.34	30.66	61.85	7.35	0.57	3.92	2.22
Standard Error											
Coral B - Line 1	0	0.05	0.002	0.01	0.02	0.01	0.24	0.001	0.004	0.06	0.001
Coral B - Line 1	1	0.04	0.003	0.01	0.02	0.04	0.35	0.001	0.01	0.06	0.001
Coral B - Line 1	2	0.05	0.004	0.01	0.02	0.02	0.74	0.001	0.01	0.10	0.0005
Coral B - Line 1	3	0.06	0.01	0.01	0.02	0.03	0.30	0.005	0.01	0.14	0.01
Coral B - Line 1	4	0.04	0.02	0.02	0.03	0.64	1.41	0.18	0.003	0.07	0.03
D_{TE} Single Phases											
Coral B - Line 1	0	0.69	0.03	0.41	0.35	0.63	*126.56*	1.86	0.03		0.50
Coral B - Line 1	1	0.69	0.02	0.45	0.48	1.33	0.38	0.60	0.12	2.42	0.36
Coral B - Line 1	2	0.42	0.02	0.15	0.36	0.18	0.18	0.04	0.12	0.55	0.03
Coral B - Line 1	3	0.25	0.01	0.03	0.18	0.02	0.01	0.01	0.12	0.08	0.03
Coral B - Line 1	4	0.19	0.01	0.04	0.19	0.18	0.02	0.14	0.09	0.01	0.17
D_{TE} ±SD		0.03 ±0.01	0.01 ±0.001	0.57 ±0.18	0.18-0.48	0.14 ±0.05	0.02 ±0.003	0.11 ±0.04	0.03-0.12	0.01-2.42	0.13 ±0.05
Correlation coefficient (R^2)		0.81	0.98	0.85		0.81	0.87	0.82			0.82
Significance (p)		0.04	0.003	0.04		0.05	0.03	0.05			0.05
Forced through origin		No	Yes	Yes	Single Points	Yes	Yes	Yes	Single Points	Single Points	Yes
Mean Metal											
Coral B - Line 2	0	7.10	0.58	0.79	0.99	0.84	10.06	0.07	0.14		0.02
Coral B - Line 2	1	6.66	0.52	0.70	0.85	2.78	9.71	0.07	0.62		0.03
Coral B - Line 2	2	6.77	0.48	0.49	0.69	2.04	8.08	0.08	0.59		0.02
Coral B - Line 2	3	7.23	0.56	0.57	0.86	2.22	10.05	0.24	0.59	0.32	0.20
Coral B - Line 2	4	6.95	1.19	1.31	0.79	38.53	41.02	8.47	0.43	0.26	1.74
Standard Error											
Coral B - Line 2	0	0.07	0.01	0.02	0.02	0.01	0.29	0.00	0.00		0.00
Coral B - Line 2	1	0.07	0.01	0.01	0.02	0.07	0.46	0.00	0.01		0.00
Coral B - Line 2	2	0.08	0.01	0.01	0.01	0.03	0.29	0.00	0.01		0.00
Coral B - Line 2	3	0.08	0.01	0.01	0.02	0.05	0.29	0.01	0.01	0.10	0.01
Coral B - Line 2	4	0.05	0.03	0.03	0.03	1.10	1.64	0.29	0.00	0.01	0.04
D_{TE} Single Phases											
Coral B - Line 2	0	0.71	0.13	0.36	0.27	0.62	*111.50*	1.74	0.02		0.40
Coral B - Line 2	1	0.69	0.06	0.43	0.37	1.49	0.34	0.58	0.10		0.25
Coral B - Line 2	2	0.41	0.05	0.15	0.26	0.19	0.08	0.04	0.09		0.02
Coral B - Line 2	3	0.24	0.01	0.03	0.13	0.02	0.01	0.01	0.09	0.003	0.02
Coral B - Line 2	4	0.17	0.01	0.03	0.11	0.23	0.01	0.16	0.07	0.0004	0.13
D_{TE} ±SD		0.17-0.71	0.01 ±0.002	0.03-0.43	0.11-0.37	0.18 ±0.06	0.01 ±0.002	0.13 ±0.04	0.02-0.10	0.0004 -0.003	0.10 ±0.04
Correlation coefficient (R^2)			0.85			0.81	0.88	0.82			0.82
Significance (p)			0.02			0.05	0.02	0.05			0.05
Forced through origin		Single Points	No	Single Points	Single Points	Yes	Yes	Yes	Single Points	Single Points	Yes
Mean Metal											
Coral B - Line 3	0	7.16	0.22	0.90	1.34	1.03	13.29	0.05	0.17	19.65	0.02
Coral B - Line 3	1	7.37	0.27	0.73	1.08	2.35	10.65	0.06	0.78	19.46	0.04
Coral B - Line 3	2	7.77	0.34	1.02	1.28	2.46	12.34	0.08	0.91	16.75	0.05
Coral B - Line 3	3	8.40	0.46	1.20	1.16	2.55	19.08	0.17	0.84	13.51	0.24
Coral B - Line 3	4	9.80	1.21	1.87	3.03	30.87	130.10	6.01	0.86	5.47	2.56
Standard Error											
Coral B - Line 3	0	0.04	0.002	0.01	0.02	0.01	0.22	0.001	0.003	0.21	0.0004

Coral B - Line 3	1	0.05	0.004	0.01	0.01	0.03	0.26	0.001	0.01	0.18	0.001
Coral B - Line 3	2	0.05	0.005	0.01	0.02	0.03	0.33	0.001	0.01	0.16	0.0007
Coral B - Line 3	3	0.05	0.01	0.03	0.02	0.03	0.62	0.003	0.01	0.16	0.01
Coral B - Line 3	4	0.06	0.02	0.02	0.08	0.88	3.73	0.18	0.01	0.11	0.04
D_{TE} Single Phases											
Coral B - Line 3	0	0.71	0.05	0.41	0.36	0.76	*147.32*	1.38	0.02		0.44
Coral B - Line 3	1	0.76	0.03	0.45	0.47	1.26	0.37	0.51	0.12	6.80	0.32
Coral B - Line 3	2	0.47	0.03	0.31	0.47	0.23	0.12	0.04	0.15	1.07	0.05
Coral B - Line 3	3	0.27	0.01	0.05	0.17	0.03	0.01	0.01	0.13	0.11	0.03
Coral B - Line 3	4	0.24	0.01	0.04	0.44	0.18	0.03	0.11	0.14	0.01	0.19
D_{TE} ±SD		0.08 ±0.01	0.01 ±0.001	0.05 ±0.003	0.17-0.47	0.15 ±0.05	0.03 ±0.006	0.09 ±0.03	0.02-0.15	-0.02 ±0.004	0.15 ±0.05
Correlation coefficient (R^2)		0.89	0.95	0.74		0.83	0.94	0.82		0.94	0.81
Significance (p)		0.02	0.004	0.01		0.05	0.01	0.05		0.03	0.05
Forced through origin		No	Yes	Yes	Single Points	Yes	Yes	Yes	Single Points	No	Yes
Mean Metal											
Coral B - Line 4	0	6.71	0.26	1.08	0.76	0.87	20.60	0.06	0.11	3.10	0.02
Coral B - Line 4	1	7.26	0.12	0.79	0.85	1.51	20.63	0.07	0.33	0.91	0.02
Coral B - Line 4	2	7.74	0.25	0.99	0.92	3.49	19.72	0.08	0.95	0.16	0.05
Coral B - Line 4	3	9.02	0.39	0.87	0.99	3.29	25.89	0.23	0.89		0.35
Coral B - Line 4	4	9.20	1.10	1.68	1.91	26.54	96.57	4.84	0.67	0.43	2.35
Standard Error											
Coral B - Line 4	0	0.03	0.01	0.01	0.01	0.01	0.15	0.001	0.001	0.02	0.0002
Coral B - Line 4	1	0.05	0.003	0.02	0.01	0.03	0.22	0.001	0.01	0.02	0.0004
Coral B - Line 4	2	0.05	0.01	0.02	0.01	0.05	0.25	0.001	0.01	0.04	0.001
Coral B - Line 4	3	0.06	0.01	0.01	0.02	0.06	0.66	0.01	0.01		0.02
Coral B - Line 4	4	0.05	0.03	0.03	0.04	0.65	3.41	0.14	0.01	0.03	0.05
D_{TE} Single Phases											
Coral B - Line 4	0	0.67	0.06	0.49	0.20	0.64	*228.24*	1.52	0.01		0.36
Coral B - Line 4	1	0.75	0.01	0.49	0.37	0.80	0.72	0.58	0.05	0.32	0.18
Coral B - Line 4	2	0.46	0.03	0.30	0.34	0.33	0.19	0.04	0.15	0.01	0.05
Coral B - Line 4	3	0.29	0.01	0.04	0.14	0.03	0.02	0.01	0.13		0.04
Coral B - Line 4	4	0.23	0.01	0.04	0.28	0.16	0.02	0.09	0.11	0.001	0.18
D_{TE} ±SD		0.08 ±0.01	0.01 ±0.002	0.04-0.49	0.14-0.37	0.13 ±0.04	0.02 ±0.003	0.07 ±0.02	0.01-0.15	0.001-0.32	0.14 ±0.04
Correlation coefficient (R^2)		0.92	0.95			0.86	0.89	0.83			0.85
Significance (p)		0.01	0.01			0.05	0.01	0.04			0.04
Forced through origin		No	Yes	Single Points	Single Points	Yes	Yes	Yes	Single Points	Single Points	Yes
Coral B Compositeline											
Coral B - Composite Line	0	7.10	0.32	0.85	1.20	0.90	11.56	0.07	0.18	12.24	0.02
Coral B - Composite Line	1	6.90	0.33	0.72	1.00	2.57	10.37	0.07	0.74	13.37	0.04
Coral B - Composite Line	2	7.06	0.34	0.67	0.96	2.10	12.67	0.08	0.76	12.31	0.03
Coral B - Composite Line	3	7.60	0.45	0.81	1.09	2.22	14.44	0.21	0.76	11.74	0.24
Coral B - Composite Line	4	7.94	1.13	1.61	1.71	34.92	75.43	7.62	0.63	4.57	2.16

Standard Error											
Coral B - Composite Line	0	0.04	0.003	0.01	0.01	0.01	0.13	0.0005	0.002	0.14	0.001
Coral B - Composite Line	1	0.04	0.003	0.005	0.01	0.04	0.18	0.001	0.010	0.12	0.001
Coral B - Composite Line	2	0.04	0.004	0.01	0.01	0.01	0.32	0.001	0.004	0.11	0.0005
Coral B - Composite Line	3	0.04	0.004	0.01	0.01	0.02	0.25	0.003	0.005	0.12	0.01
Coral B - Composite Line	4	0.04	0.02	0.02	0.04	0.85	2.26	0.22	0.01	0.10	0.03
D_{TE} Single Phases											
Coral B - Composite Line	0	0.71	0.07	0.39	0.32	0.66	*128.12*	1.65	0.02		0.44
Coral B - Composite Line	1	0.71	0.04	0.44	0.44	1.38	0.36	0.56	0.11	4.67	0.30
Coral B - Composite Line	2	0.42	0.03	0.20	0.36	0.20	0.12	0.04	0.12	0.78	0.04
Coral B - Composite Line	3	0.25	0.01	0.04	0.16	0.02	0.01	0.01	0.11	0.09	0.03
Coral B - Composite Line	4	0.20	0.01	0.04	0.25	0.20	0.02	0.14	0.10	0.01	0.16
D_{TE} ±SD		0.03 ±0.004	0.01 ±0.001	0.02 ±0.005	0.16-0.44	0.16 ±0.06	0.02 ±0.003	0.12 ±0.04	0.02-0.12	-0.01 ±0.001	0.13 ±0.04
Correlation coefficient (R^2)		0.95	0.94	0.81		0.82	0.92	0.82		0.99	0.82
Significance (p)		0.004	0.01	0.04		0.05	0.01	0.05		0.05	0.05
Forced through origin		No	No	No	Single Points	Yes	Yes	Yes	Single Points	No	Yes
Coral C											
Mean Metal											
Coral C - Line 1	0	8.45	0.17	0.49	1.01	8.93	4.79	0.05	0.57	0.48	0.03
Coral C - Line 1	1	9.31	0.23	0.50	2.22	13.37	10.64	0.08	0.90	0.69	0.04
Coral C - Line 1	2	10.08	0.22	0.56	2.99	19.14	20.83	0.13	0.99	0.77	0.09
Coral C - Line 1	3	12.55	0.40	0.74	1.10	47.22	123.02	1.34	0.91	1.41	1.81
Coral C - Line 1	4	19.93	1.15	2.28	1.69	141.18	640.17	8.65	1.06	3.74	7.36
Standard Error											
Coral C - Line 1	0	0.05	0.002	0.01	0.02	0.08	0.08	0.001	0.01	0.01	0.0003
Coral C - Line 1	1	0.09	0.01	0.01	0.06	0.21	0.27	0.001	0.01	0.01	0.001
Coral C - Line 1	2	0.08	0.004	0.01	0.12	0.28	0.49	0.003	0.01	0.02	0.003
Coral C - Line 1	3	0.12	0.01	0.01	0.02	0.97	4.70	0.04	0.01	0.03	0.06
Coral C - Line 1	4	0.24	0.02	0.04	0.03	1.88	18.87	0.18	0.02	0.09	0.16
D_{TE} Single Phases											
Coral C - Line 1	0	0.84	0.04	0.22	0.27	6.60	*53.07*	1.17	0.07		0.56
Coral C - Line 1	1	0.96	0.03	0.31	0.97	7.14	0.37	0.64	0.14	0.24	0.32
Coral C - Line 1	2	0.60	0.02	0.17	1.11	1.82	0.20	0.06	0.16	0.05	0.10
Coral C - Line 1	3	0.41	0.01	0.03	0.16	0.50	0.08	0.05	0.14	0.01	0.23
Coral C - Line 1	4	0.49	0.01	0.05	0.25	0.83	0.17	0.16	0.17	0.01	0.56
D_{TE} ±SD		0.32 ±0.07	0.01 ±0.001	0.04 ±0.01	0.16-1.11	0.76 ±0.12	0.16 ±0.02	0.14 ±0.03	-0.25 ±0.02	0.005 ±0.0002	0.47 ±0.11
Correlation coefficient (R^2)		0.87	0.97	0.88		0.95	0.97	0.90	0.98	0.99	0.91

Significance (p)		0.02	0.003	0.02		0.01	0.003	0.02	0.001	0.0001	0.02
Forced through origin		No	Yes	No	Single Points	Yes	Yes	Yes	No	No	Yes
Mean Metal											
Coral C - Line 2	0	7.98	0.27	0.76	2.08	10.10	18.78	0.03	0.71	0.51	0.07
Coral C - Line 2	1	7.54	0.34	0.51	1.29	11.89	9.33	0.04	0.80	0.40	0.06
Coral C - Line 2	2	7.31	0.20	0.35	1.39	14.52	10.61	0.12	0.68	0.38	0.12
Coral C - Line 2	3	8.19	0.56	0.71	1.72	38.81	93.30	1.08	0.53	0.35	1.24
Coral C - Line 2	4	10.10	0.99	1.26	1.08	94.22	162.22	8.33	0.53	0.57	2.83
Standard Error											
Coral C - Line 2	0	0.04	0.003	0.01	0.04	0.10	0.36	0.0005	0.01	0.01	0.001
Coral C - Line 2	1	0.05	0.005	0.011	0.03	0.15	0.23	0.001	0.01	0.01	0.001
Coral C - Line 2	2	0.05	0.00	0.00	0.03	0.19	0.28	0.01	0.00	0.01	0.00
Coral C - Line 2	3	0.05	0.01	0.03	0.04	0.56	2.74	0.02	0.01	0.01	0.04
Coral C - Line 2	4	0.07	0.02	0.02	0.02	1.05	4.82	0.18	0.00	0.01	0.04
D_{TE} Single Phases											
Coral C - Line 2	0	0.79	0.06	0.34	0.56	7.46	*208.17*	0.79	0.09		1.35
Coral C - Line 2	1	0.78	0.04	0.32	0.56	6.35	0.33	0.35	0.12	0.14	0.51
Coral C - Line 2	2	0.44	0.02	0.11	0.52	1.38	0.10	0.05	0.11	0.02	0.12
Coral C - Line 2	3	0.27	0.01	0.03	0.25	0.41	0.06	0.04	0.08	0.003	0.16
Coral C - Line 2	4	0.25	0.01	0.03	0.16	0.55	0.04	0.16	0.09	0.001	0.21
D_{TE} ±SD		0.25-0.79	0.01 ±0.001	0.03-0.34	0.16-0.56	0.53 ±0.07	0.05 ±0.002	0.13 ±0.03	0.08-0.12	0.001-0.14	0.2 ±0.03
Correlation coefficient (R^2)			0.99			0.96	0.98	0.89			0.96
Significance (p)			0.001			0.01	0.0003	0.02			0.01
Forced through origin		Single Points	No	Single Points	Single Points	Yes	Yes	Yes	Single Points	Single Points	Yes
Mean Metal											
Coral C - Line 3	0	7.81	0.22	0.60	0.88	8.90	5.77	0.03	0.52	0.33	0.03
Coral C - Line 3	1	7.55	0.27	0.42	1.18	10.26	7.58	0.04	0.72	0.32	0.03
Coral C - Line 3	2	8.00	0.27	0.44	1.71	18.18	18.40	0.07	0.80	0.36	0.06
Coral C - Line 3	3	8.70	0.43	0.52	1.05	33.55	62.78	0.71	0.66	0.39	0.80
Coral C - Line 3	4	9.90	1.04	1.25	0.82	99.39	194.50	7.37	0.62	0.53	3.06
Standard Error											
Coral C - Line 3	0	0.04	0.003	0.01	0.01	0.08	0.10	0.0004	0.01	0.01	0.0004
Coral C - Line 3	1	0.05	0.006	0.01	0.03	0.11	0.17	0.001	0.01	0.01	0.001
Coral C - Line 3	2	0.06	0.00	0.01	0.06	0.18	0.67	0.00	0.01	0.01	0.00
Coral C - Line 3	3	0.05	0.01	0.01	0.03	0.52	2.49	0.02	0.01	0.01	0.03
Coral C - Line 3	4	0.07	0.03	0.02	0.01	1.02	6.82	0.15	0.01	0.01	0.06
D_{TE} Single Phases											
Coral C - Line 3	0	0.78	0.05	0.27	0.24	6.58	*63.96*	0.83	0.06		0.64
Coral C - Line 3	1	0.78	0.03	0.26	0.52	5.48	0.27	0.32	0.11	0.11	0.26
Coral C - Line 3	2	0.48	0.03	0.13	0.63	1.73	0.18	0.03	0.13	0.02	0.06
Coral C - Line 3	3	0.28	0.01	0.02	0.15	0.36	0.04	0.03	0.10	0.003	0.10
Coral C - Line 3	4	0.25	0.01	0.03	0.12	0.58	0.05	0.14	0.10	0.001	0.23
D_{TE} ±SD		0.06 ±0.01	0.01 ±0.001	0.02 ±0.004	0.12-0.63	0.54 ±0.08	0.05 ±0.001	0.11 ±0.03	0.07-0.13	0.001-0.11	0.2 ±0.04
Correlation coefficient (R^2)		0.95	0.98	0.83		0.94	0.99	0.89			0.93
Significance (p)		0.005	0.001	0.03		0.01	<0.0001	0.02			0.01
Forced through origin		No	No	No	Single Points	Yes	Yes	Yes	Single Points	Single Points	Yes

Coral C Compositeline											
Coral C - Composite Line		7.85	0.24	0.67	1.44	9.45	12.89	0.03	0.62	0.44	0.05
Coral C - Composite Line		7.57	0.29	0.46	1.22	11.05	8.57	0.04	0.76	0.36	0.05
Coral C - Composite Line		7.66	0.23	0.39	1.46	16.29	14.16	0.09	0.75	0.37	0.09
Coral C - Composite Line		8.37	0.49	0.61	1.28	35.50	75.90	0.86	0.59	0.36	0.98
Coral C - Composite Line		10.05	1.26	1.29	0.98	99.04	231.79	8.25	0.57	0.57	3.16
Standard Error											
Coral C - Composite Line		0.03	0.002	0.01	0.02	0.06	0.22	0.0003	0.01	0.01	0.001
Coral C - Composite Line		0.04	0.004	0.01	0.02	0.10	0.15	0.0005	0.01	0.01	0.001
Coral C - Composite Line		0.03	0.003	0.003	0.02	0.13	0.33	0.004	0.01	0.01	0.002
Coral C - Composite Line		0.03	0.01	0.01	0.02	0.49	2.28	0.02	0.004	0.01	0.03
Coral C - Composite Line		0.05	0.03	0.01	0.01	0.93	5.32	0.16	0.004	0.01	0.04
D_{TE} Single Phases											
Coral C - Composite Line		0.78	0.06	0.30	0.39	6.98	*142.90*	0.81	0.08		0.99
Coral C - Composite Line		0.78	0.04	0.28	0.53	5.90	0.30	0.34	0.12	0.13	0.39
Coral C - Composite Line		0.46	0.02	0.12	0.54	1.55	0.14	0.04	0.12	0.02	0.09
Coral C - Composite Line		0.27	0.01	0.03	0.19	0.38	0.05	0.03	0.09	0.003	0.12
Coral C - Composite Line		0.25	0.01	0.03	0.14	0.58	0.06	0.16	0.09	0.001	0.24
D_{TE} ±SD		0.07 ±0.02	0.01 ±0.001	0.02 ±0.005	0.14-0.54	0.54 ±0.08	0.06 ±0.003	0.13 ±0.03	0.08-0.12	0.001-0.13	0.21 ±0.04
Correlation coefficient (R^2)		0.82	0.97	0.80		0.95	0.99	0.87			0.94
Significance (p)		0.03	0.003	0.04		0.01	0.0002	0.03			0.01
Forced through origin		No	No	No	Single Points	Yes	Yes	Yes	Single Points	Single Points	Yes
Coral D											
Mean Metal											
Coral D - Composite Linie (=Line 1)	0	7.84	0.19	0.42	1.64	4.72	53.17	0.11	0.21	6.74	0.01
Coral D - Composite Linie (=Line 1)	1	8.61	0.32	0.43	2.21	6.36	62.04	0.11	0.92	11.29	0.02
Coral D - Composite Linie (=Line 1)	2	8.93	0.44	0.51	2.06	8.41	61.98	0.21	1.25	8.95	0.07

Coral D - Composite Linie (=Line 1)	3	8.84	0.94	1.03	1.76	24.44	397.15	3.09	0.95	2.37	2.14
Coral D - Composite Linie (=Line 1)	4	10.52	0.99	2.26	2.84	35.51	2142.55	3.11	2.10	0.57	10.06
Standard Error											
Coral D - Composite Linie (=Line 1)	0	0.03	0.002	0.004	0.02	0.05	0.97	0.001	0.002	0.06	0.0001
Coral D - Composite Linie (=Line 1)	1	0.04	0.00	0.004	0.03	0.07	1.10	0.001	0.01	0.08	0.0003
Coral D - Composite Linie (=Line 1)	2	0.05	0.01	0.006	0.04	0.13	1.21	0.004	0.01	0.09	0.0013
Coral D - Composite Linie (=Line 1)	3	0.07	0.03	0.03	0.05	0.43	27.19	0.12	0.02	0.06	0.160
Coral D - Composite Linie (=Line 1)	4	0.16	0.07	0.14	0.17	1.97	224.11	0.30	0.07	0.05	0.75
D_{TE} Single Phases											
Coral D - Composite Linie (=Line 1)	0	0.78	0.04	0.19	0.44	3.49	*589.20*	2.88	0.03		0.22
Coral D - Composite Linie (=Line 1)	1	0.89	0.04	0.27	0.97	3.40	2.17	0.91	0.14	3.94	0.21
Coral D - Composite Linie (=Line 1)	2	0.54	0.04	0.15	0.77	0.80	0.61	0.10	0.20	0.57	0.07
Coral D - Composite Linie (=Line 1)	3	0.29	0.02	0.05	0.26	0.26	0.27	0.12	0.14	0.02	0.27
Coral D - Composite Linie (=Line 1)	4	0.26	0.01	0.05	0.41	0.21	0.55	0.06	0.35	0.001	0.76
D_{TE} ±SD		0.04 ±0.02	0.01 ±0.003	0.04 ±0.004	0.26-0.97	0.19 ±0.01	0.52 ±0.07	0.07 ±0.02	0.03-0.35	0.001-3.94	0.63 ±0.15
Correlation coefficient (R^2)		0.81	0.77	0.97		0.99	0.97	0.90			0.89
Significance (p)		0.04	0.05	0.002		0.0003	0.004	0.03			0.02
Forced through origin		No	No	No	Single Points	No	Yes	Yes	Single Points	Single Points	Yes
Mean Metal											
Coral D - Line 2	0	8.81	0.51	0.55	4.77	10.03	184.12	0.33	0.98		0.03
Coral D - Line 2	1	9.08	0.83	0.63	6.49	12.86	264.31	0.25	1.45		0.04
Coral D - Line 2	2	8.63	0.54	0.55	3.04	10.05	124.36	0.18	1.67		0.08
Coral D - Line 2	3	8.23	0.95	1.05	2.59	28.78	302.21	2.52	1.19	0.26	3.04
Coral D - Line 2	4	9.24	0.77	1.64	2.13	38.05	1086.80	3.11	1.85	0.22	8.33
Standard Error											
Coral D - Line 2	0	0.04	0.01	0.01	0.10	0.14	2.93	0.005	0.01		0.0003

Coral D - Line 2	1	0.04	0.01	0.01	0.13	0.14	4.92	0.003	0.02		0.0005
Coral D - Line 2	2	0.04	0.01	0.01	0.04	0.12	3.96	0.003	0.02		0.002
Coral D - Line 2	3	0.08	0.02	0.04	0.09	1.69	12.45	0.12	0.03	0.04	0.34
Coral D - Line 2	4	0.15	0.02	0.07	0.09	1.39	91.77	0.12	0.06	0.02	0.45
D_{TE} Single Phases											
Coral D - Line 2	0	0.88	0.12	0.25	1.29	7.41	*2040.40*	8.33	0.12		0.54
Coral D - Line 2	1	0.94	0.10	0.39	2.84	6.87	9.26	2.01	0.23		0.35
Coral D - Line 2	2	0.52	0.05	0.17	1.13	0.96	1.21	0.08	0.27		0.09
Coral D - Line 2	3	0.27	0.02	0.05	0.38	0.31	0.21	0.09	0.18		0.38
Coral D - Line 2	4	0.23	0.01	0.04	0.31	0.22	0.28	0.06	0.30	0.0004	0.63
D_{TE} ±SD		0.23- 0.94	0.01- 0.12	0.03 ±0.001	0.17 ±0.02	0.18 ±0.02	0.27 ±0.04	0.07 ±0.01	0.12- 0.30	0.0004 *	0.56 ±0.08
Correlation coefficient (R^2)				0.99		0.98	0.91	0.90			0.96
Significance (p)				0.004		0.002	0.01	0.01			0.01
Forced through origin		Single Points	Single Points	No	Single Points	No	Yes	Yes	Single Point	Single Point	Yes
Mean Metal											
Coral D - Line 3	0	10.92	0.81	1.16	5.10	10.25	360.45	0.84	0.83	3.93	0.03
Coral D - Line 3	1	12.38	0.99	1.55	15.88	13.27	242.66	1.16	1.83	5.09	0.03
Coral D - Line 3	2	10.19	0.55	1.01	15.18	11.98	62.26	0.77	2.31	5.06	0.11
Coral D - Line 3	3	10.30	0.63	1.67	14.38	35.00	232.60	3.20	2.21	5.92	1.70
Coral D - Line 3	4	11.63	0.96	4.05	17.54	82.59	443.13	6.25	3.09	6.01	11.24
Standard Error											
Coral D - Line 3	0	0.13	0.03	0.02	0.13	0.29	8.07	0.02	0.03	0.06	0.001
Coral D - Line 3	1	0.12	0.02	0.03	0.53	0.28	8.61	0.03	0.07	0.07	0.001
Coral D - Line 3	2	0.07	0.02	0.02	0.38	0.23	2.12	0.02	0.04	0.06	0.005
Coral D - Line 3	3	0.10	0.01	0.05	0.35	0.92	8.85	0.09	0.05	0.07	0.07
Coral D - Line 3	4	0.24	0.03	0.17	0.82	3.57	15.99	0.22	0.11	0.13	0.75
D_{TE} Single Phases											
Coral D - Line 3	0	1.09	0.18	0.53	1.38	7.58	*3994.50*	21.21	0.10		0.54
Coral D - Line 3	1	1.28	0.12	0.95	6.95	7.09	8.50	9.29	0.28	1.78	0.25
Coral D - Line 3	2	0.61	0.06	0.30	5.64	1.14	0.61	0.37	0.37	0.32	0.12
Coral D - Line 3	3	0.34	0.02	0.08	2.11	0.37	0.16	0.12	0.33	0.05	0.21
Coral D - Line 3	4	0.29	0.01	0.09	2.55	0.48	0.11	0.12	0.51	0.01	0.85
D_{TE} ±SD		0.29- 1.28	0.01- 0.18	0.06 ± 0.01	1.38- 6.95	0.46 ±0.05	0.11- 3994.50	0.10 ± 0.006	-1.0 ±0.25	0.01- 1.78	0.68 ±0.21
Correlation coefficient (R^2)				0.86		0.96		0.98	0.87		0.85
Significance (p)				0.02		0.004		0.001	0.03		0.04
Forced through origin		Single Points	Single Points	No	Single Points	Yes	Single Points	No	No	Single Points	Yes
Mean Metal											
Coral D - Line 4	0	9.16	0.35	1.90	54.21	5.44	79.77	0.52	4.04	0.16	0.04
Coral D - Line 4	1	9.67	0.78	4.08	290.45	12.51	92.05	0.74	23.39	0.23	0.09
Coral D - Line 4	2	10.25	0.60	2.98	84.10	16.55	65.83	0.77	6.88	0.31	0.07
Coral D - Line 4	3	12.16	2.08	3.87	40.75	49.01	477.25	3.71	4.59	0.36	5.08
Coral D - Line 4	4	12.25	1.32	5.27	19.99	65.45	896.41	5.84	2.71	0.47	15.72
Standard Error											
Coral D - Line 4	0	0.07	0.01	0.03	1.14	0.10	3.13	0.01	0.12	0.01	0.001
Coral D - Line 4	1	0.10	0.03	0.12	11.66	0.40	3.00	0.02	1.32	0.01	0.003
Coral D - Line 4	2	0.12	0.02	0.07	2.36	0.40	2.33	0.02	0.20	0.01	0.002
Coral D - Line 4	3	0.16	0.29	0.08	1.48	1.14	14.85	0.10	0.15	0.01	0.40

Coral D - Line 4	4	0.30	0.06	0.34	1.00	1.19	22.52	0.13	0.13	0.04	0.40
D_{TE} Single Phases											
Coral D - Line 4	0	0.91	0.08	0.87	14.66	4.02	*883.97*	13.11	0.51		0.69
Coral D - Line 4	1	1.00	0.10	2.51	*127.14*	6.68	3.23	5.91	3.62	0.08	0.73
Coral D - Line 4	2	0.61	0.06	0.90	31.22	1.57	0.64	0.37	1.10	0.02	0.08
Coral D - Line 4	3	0.40	0.05	0.18	5.98	0.52	0.33	0.14	0.69	0.003	0.64
Coral D - Line 4	4	0.30	0.02	0.12	2.91	0.38	0.23	0.11	0.44	0.001	1.19
D_{TE} ±SD		0.10 ±0.02	0.02-0.10	0.12-2.51	2.91-127.14	0.34 ±0.04	0.24 ±0.02	0.10 ±0.006	0.44-3.62	0.001-0.08	1.04 ±0.18
Correlation coefficient (R^2)		0.93				0.97	0.97	0.99			0.94
Significance (p)		0.01				0.003	0.001	0.0003			0.01
Forced through origin		No	Single Points	Single Points	Single Points	No	Yes	No	Single Points	Single Points	Yes
Mean Metal											
Coral D - Line 5	0	9.51	0.87	3.25	82.38	10.03	39.53	0.47		0.11	0.04
Coral D - Line 5	1	8.92	0.86	2.61	105.92	11.24	74.66	0.51		0.10	0.05
Coral D - Line 5	2	10.11	0.76	2.52	39.29	17.72	51.45	0.69		0.19	0.06
Coral D - Line 5	3	11.81	2.27	3.86	24.47	39.67	405.52	3.14		0.21	5.14
Coral D - Line 5	4	11.03	5.50	3.62	10.67	66.63	859.12	5.65		0.19	13.54
Standard Error											
Coral D - Line 5	0	0.16	0.06	0.20	4.95	0.64	1.54	0.01		0.02	0.001
Coral D - Line 5	1	0.17	0.04	0.13	4.91	0.62	5.68	0.02		0.02	0.002
Coral D - Line 5	2	0.21	0.04	0.13	1.62	0.70	3.65	0.03		0.05	0.00
Coral D - Line 5	3	0.28	0.38	0.14	0.96	1.18	18.48	0.12		0.03	0.53
Coral D - Line 5	4	0.49	1.24	0.30	0.82	1.28	52.32	0.20		0.05	0.38
D_{TE} Single Phases											
Coral D - Line 5	0	0.95	0.20	1.48	*22.28*	7.42	*438.09*	11.98			0.70
Coral D - Line 5	1	0.92	0.10	1.60	*46.36*	6.01	2.62	4.06		0.04	0.38
Coral D - Line 5	2	0.61	0.08	0.76	14.58	1.68	0.50	0.33		0.01	0.06
Coral D - Line 5	3	0.38	0.06	0.17	3.59	0.42	0.28	0.12		0.002	0.64
Coral D - Line 5	4	0.27	0.06	0.08	1.55	0.39	0.22	0.11		0.0003	1.03
D_{TE} ±SD		0.07 ±0.03	0.06 ±0.004	0.07-1.60	1.55-46.36	0.32 ±0.02	0.23 ±0.01	0.10 ±0.0007		0.0003 -0.03	0.92 ±0.13
Correlation coefficient (R^2)		0.74	0.99			0.99	0.98	0.99			0.96
Significance (p)		0.05	0.001			0.0002	0.0002	*			0.004
Forced through origin		Single Points	Single Points	Single Points	Single Points	No	Yes	No		Single Points	Yes
Metal - Mean of all colonies (composite lines)											
	Ph	**Cr/Ca**	**Mn/Ca**	**Ni/Ca**	**Cu/Ca**	**Zn/Ca**	**Ag/Ca**	**Cd/Ca**	**Sn/Ca**	**Hg/Ca**	**Pb/Ca**
D_{TE} ±SD		0.21 ±0.1	0.01 ±0.002	0.03 ±0.005	no correlation	0.35 ±0.05	0.18 ±0.06	0.11 ±0.01	-0.37 ±0.11	no correlation	0.37 ±0.07
Correlation coefficient (R^2)		0.47	0.65	0.71		0.79	0.44	0.85	0.39		0.70
Significance (p)		0.04	*	*		*	0.01	*	0.003		*
Forced through origin		No	No	No		Yes	Yes	Yes	No		Yes

*<0.0001

4.7 Supplementary Material

Table S4.1-S4.4: Time resolved trace element–to–calcium values of coral A to D in the metal system along the measured LA-ICP-MS scanning lines and values derived from the composite lines. Measurements were carried out from the top of the coral to the bottom and the distance starting from the top is indicated as “Elapse Time”. TE/Ca values are already processes as described in the main manuscript and outliers are rejected. Note that the composite line of coral D is identically with line 1 as this was the only measurement along the main growth axis. The dataset is available at PANGAEA (https://doi.pangaea.de/10.1594/PANGAEA.938748).

4.8 Data availability

All data generated or analysed during this study are either included in this article and its appendices. The supplementary material (Table S4.1-S4.4) is available at PANGAEA (https://doi.pangaea.de/10.1594/PANGAEA.938748).

4.9 Acknowledgements

We want to gratefully thank Florian Böhm for his help with words and deeds. Furthermore, he provided the host aquarium and took care of the experimental aquaria whenever his help was needed. Without him, we would not have been able to perform these culturing experiments. The association “Kieler Aquarienfreunde” gave important input on coral aquaria and helped with the organization of the coral colonies. The company Whitecorals provided the culturing system and were always open for questions. Claas Hiebenthal, KIMOCC, had helped with the system design and provided system parts as well as technical support. Marlene Wall helped with informative input and borrowed system parts. Clara Wichmanns and Anja Convents work as our student helpers is greatly acknowledged. Furthermore, Regina Surberg carried out the ICP-OES measurements, Ana Kolevica took care for the ICP-MS machine and Ulrike Westernströer set up and helped with the laser ablation measurements, which was vitally important for this manuscript. Sven Marquardt helped with the data handling.

4.10 References

Abdo, Safa Y.; Duliu, Octavian G.; Zinicovscaia, Inga; Sherif, Mohamed M.; Frontasyeva, Marina V. (2017): Epithermal neutron activation analysis of major and trace elements in Red Sea scleractinian corals. In: Journal of Radioanalytical and Nuclear Chemistry 314 (2), S. 1445–1452. DOI: 10.1007/s10967-017-5511-8.

Alibert, Chantal; Kinsley, Les; Fallon, Stewart J.; McCulloch, Malcolm T.; Berkelmans, Ray; McAllister, Felicity (2003): Source of trace element variability in Great Barrier Reef corals affected by the Burdekin flood plumes. In: Geochimica et Cosmochimica Acta 67 (2), S. 231–246. DOI: 10.1016/S0016-7037(02)01055-4.

Allemand, Denis; Ferrier-Pagès, Christine; Furla, Paola; Houlbrèque, Fanny; Puverel, Sandrine; Reynaud, Stéphanie et al. (2004): Biomineralisation in reef-building corals. From molecular mechanisms to environmental control. In: Comptes Rendus Palevol 3 (6-7), S. 453–467. DOI: 10.1016/j.crpv.2004.07.011.

Allemand, Denis; Tambutté, Éric; Zoccola, Didier; Tambutté, Sylvie (2011): Coral calcification, cells to reefs. In: Coral reefs: An Ecosystem in Transition, S. 119–150. DOI: 10.1007/978-94-007-0114-4_9.

Allison, Nicola; Cohen, Itay; Finch, Adrian A.; Erez, Jonathan; Tudhope, Alexander W. (2014): Corals concentrate dissolved inorganic carbon to facilitate calcification. In: Nature Communications 5 (1), S. 1–6. DOI: 10.1038/ncomms6741.

Allison, Nicola; Finch, Adrian A. (2004): High-resolution Sr/Ca records in modern Porites lobata corals. Effects of skeletal extension rate and architecture. In: Geochemistry, Geophysics, Geosystems 5 (5). DOI: 10.1029/2004GC000696.

Al-Rousan, Saber A.; Al-Shloul, Rashid N.; Al-Horani, Fuad A.; Abu-Hilal, Ahmad H. (2007): Heavy metal contents in growth bands of Porites corals. Record of anthropogenic and human developments from the Jordanian Gulf of Aqaba. In: Marine Pollution Bulletin 54 (12), S. 1912–1922. DOI: 10.1016/j.marpolbul.2007.08.014.

Altschul, Stephen F.; Gish, Warren; Miller, Webb; Myers, Eugene W.; Lipman, David J. (1990): Basic local alignment search tool. In: Journal of molecular biology 215 (3), S. 403–410. DOI: 10.1016/S0022-2836(05)80360-2.

Am Ali, Abdel-hamid; Hamed, Mohamed A.; Abd El-Azim, Hoda (2011): Heavy metals distribution in the coral reef ecosystems of the Northern Red Sea. In: Helgoland Marine Research 65 (1), S. 67–80. DOI: 10.1007/s10152-010-0202-7.

Amiel, Abraham J.; Friedman, Gerald M.; Miller, Donald S. (1973): Distribution and nature of incorporation of trace elements in modern aragonitic corals. In: Sedimentology 20 (1), S. 47–64. DOI: 10.1111/j.1365-3091.1973.tb01606.x.

Anthony, Kenneth R. N. (1999): A tank system for studying benthic aquatic organisms at predictable levels of turbidity and sedimentation. Case study examining coral growth. In: Limnology and Oceanography 44 (6), S. 1415–1422. DOI: 10.4319/lo.1999.44.6.1415.

Anu, G.; Kumar, N. C.; Jayalakshmi, Krishnan J.; Nair, Subadrah M. (2007): Monitoring of heavy metal partitioning in reef corals of Lakshadweep Archipelago, Indian Ocean. In: Environmental Monitoring and Assessment 128 (1), S. 195–208. DOI: 10.1007/s10661-006-9305-7.

Arumugam, Nithiya; Chelliapan, Shreeshivadasan; Thirugnana, Sathiabama T.; Jasni, Aida Batrisyia (2020): Optimisation of heavy metals uptake from Leachate using red seaweed Gracilaria changii. In: Journal of Environmental Treatment Techniques 8 (3), S. 1089–1092.

Barakat, S. A.; Al-Rousan, S.; Al-Trabeen, M. S. (2015): Use of scleractinian corals to indicate marine pollution in the northern Gulf of Aqaba, Jordan. In: Environmental Monitoring and Assessment 187 (2), S. 1–12. DOI: 10.1007/s10661-015-4275-2.

Batista, Daniela; Muricy, Guilherme; Rocha, Rafael Chávez; Miekeley, Norbert F. (2014): Marine sponges with contrasting life histories can be complementary biomonitors of heavy metal pollution in coastal ecosystems. In: Environmental Science and Pollution Research 21 (9), S. 5785–5794. DOI: 10.1007/s11356-014-2530-7.

Baudouin, M. F.; Scoppa, P. (1974): Acute toxicity of various metals to freshwater zooplankton. In: Bulletin of Environmental Contamination and Toxicology 12 (6), S. 745–751. DOI: 10.1007/BF01685925.

Besada, Victoria; Andrade, José Manuel; Schultze, Fernando; González, Juan José (2009): Heavy metals in edible seaweeds commercialised for human consumption. In: Journal of Marine Systems 75 (1-2), S. 305–313. DOI: 10.1016/j.jmarsys.2008.10.010.

Bilings, Gale K.; Ragland, Paul C. (1968): Geochemistry and mineralogy of the recent reef and lagoonal sediments south of Belize (British Honduras). In: Chemical Geology 3 (2), S. 135–153. DOI: 10.1016/0009-2541(68)90006-5.

Bjerrum, N. (1936): Bjerrum's Inorganic Chemistry, 3rd Danish ed. In: Heinemann, London.

Bosch, Adina C.; O'Neill, Bernadette; Sigge, Gunnar O.; Kerwath, Sven E.; Hoffman, Louwrens C. (2016): Heavy metals in marine fish meat and consumer health. A review. In: Journal of the Science of Food and Agriculture 96 (1), S. 32–48. DOI: 10.1002/jsfa.7360.

Brown, B. E.; Tudhope, A. W.; Le Tissier, M. D.A.; Scoffin, T. P. (1991): A novel mechanism for iron incorporation into coral skeletons. In: Coral Reefs 10 (4), S. 211–215. DOI: 10.1007/s00338-005-0013-5.

Cacciapaglia, C.; van Woesik, R. (2018): Marine species distribution modelling and the effects of genetic isolation under climate change. In: Journal of Biogeography 45 (1), S. 154–163. DOI: 10.1111/jbi.13115.

Capasso, Laura; Ganot, Philippe; Planas-Bielsa, Víctor; Tambutté, Sylvie; Zoccola, Didier (2021): Intracellular pH regulation. Characterization and functional investigation of H+ transporters in Stylophora pistillata. In: BMC Molecular and Cell Biology 22 (1), S. 1–19. DOI: 10.1186/s12860-021-00353-x.

Carriquiry, J. D.; Villaescusa, J. A. (2010): Coral Cd/Ca and Mn/Ca records of ENSO variability in the Gulf of California. In: Climate of the Past 6 (3), S. 401–410. DOI: 10.5194/cp-6-401-2010.

Carriquiry, José D.; Horta-Puga, Guillermo (2010): The Ba/Ca record of corals from the Southern Gulf of Mexico. Contributions from land-use changes, fluvial discharge and oil-drilling muds. In: Marine Pollution Bulletin 60 (9), S. 1625–1630. DOI: 10.1016/j.marpolbul.2010.06.007.

Cebrian, Emma; Uriz, María-J; Turon, Xavier (2007): Sponges as biomonitors of heavy metals in spatial and temporal surveys in northwestern Mediterranean. Multispecies comparison. In: Environmental Toxicology and Chemistry: An International Journal 26 (11), S. 2430–2439. DOI: 10.1897/07-292.1.

Chen, Tian-Ran; Yu, Ke-Fu; Li, Shu; Price, Gilbert J.; Shi, Qi; Wei, Gang-Jian (2010): Heavy metal pollution recorded in Porites corals from Daya Bay, northern South China Sea. In: Marine Environmental Research 70 (3-4), S. 318–326. DOI: 10.1016/j.marenvres.2010.06.004.

Clark, Tara R.; Zhao, Jian-Xin; Feng, Yue-xing; Done, Terry J.; Jupiter, Stacy; Lough, Janice; Pandolfi, John M. (2012): Spatial variability of initial 230Th/232Th in modern Porites from the inshore region of the Great Barrier Reef. In: Geochimica et Cosmochimica Acta 78, S. 99–118. DOI: 10.1016/j.gca.2011.11.032.

Cooper, Timothy F.; De'Ath, Glenn; Fabricius, Katharina E.; Lough, Janice M. (2008): Declining coral calcification in massive Porites in two nearshore regions of the northern Great Barrier Reef. In: Global Change Biology 14 (3), S. 529–538. DOI: 10.1111/j.1365-2486.2007.01520.x.

Correge, Thierry (2006): Monitoring of terrestrial input by massive corals. In: Journal of Geochemical Exploration 88 (1-3), S. 380–383. DOI: 10.1016/j.gexplo.2005.08.080.

Cuif, Jean-Pierre; Dauphin, Yannicke; Doucet, Jean; Salome, Murielle; Susini, Jean (2003): XANES mapping of organic sulfate in three scleractinian coral skeletons. In: Geochimica et Cosmochimica Acta 67 (1), S. 75–83. DOI: 10.1016/S0016-7037(02)01041-4.

Cuif, Jean-Pierre; Dauphin, Yannicke; Berthet, Patrick; Jegoudez, Jocelyne (2004): Associated water and organic compounds in coral skeletons. Quantitative thermogravimetry coupled to infrared absorption spectrometry. In: Geochemistry, Geophysics, Geosystems 5 (11). DOI: 10.1029/2004GC000783.

Cuif, J-P; Dauphin, Y.; Gautret, P. (1999): Compositional diversity of soluble mineralizing matrices in some recent coral skeletons compared to fine-scale growth structures of fibres. Discussion of consequences for biomineralization and diagenesis. In: International journal of earth sciences 88 (3), S. 582–592. DOI: 10.1007/s005310050286.

Dar, Mahmoud Abdel Radi; Soliman, Farouk Ahmed; Abd Allah, Ibrahem Mohamed (2018): The Contributions of Flashfloods on the Heavy Metals Incorporations Within the Coral Skeletons at Gulfs of Suez and Aqaba, Egypt. In: International Journal of Ecotoxicology and Ecobiology 3 (1), S. 11. DOI: 10.11648/j.ijee.20180301.13.

Darmono (2001): Lingkungan Hidup dan Pencemaran. In: Jakarta: UI Press.

David, C. P. (2003): Heavy metal concentrations in growth bands of corals. A record of mine tailings input through time (Marinduque Island, Philippines). In: Marine Pollution Bulletin 46 (2), S. 187–196. DOI: 10.1016/S0025-326X(02)00315-6.

Davis, T. A.; Volesky, B.; Vieira, RHSF (2000): Sargassum seaweed as biosorbent for heavy metals. In: Water Research 34 (17), S. 4270–4278. DOI: 10.1016/S0043-1354(00)00177-9.

D'Croz, Luis; Maté, Juan L.; Oke, JoAnne E. (2001): Responses to elevated sea water temperature and UV radiation in the coral Porites lobata from upwelling and non-upwelling environments on the Pacific coast of Panama. In: Bulletin of Marine Science 69 (1), S. 203–214.

Diagomanolin, V.; Farhang, M.; Ghazi-Khansari, M.; Jafarzadeh, N. (2004): Heavy metals (Ni, Cr, Cu) in the karoon waterway river, Iran. In: Toxicology Letters 151 (1), S. 63–67. DOI: 10.1016/j.toxlet.2004.02.018.

Edinger, Evan N.; Risk, Michael J. (2000): Effect of land-based pollution on central Java coral reefs. In: Journal of Coastal Development 3 (2), S. 593–613.

El-Sorogy, Abdelbaset S.; Mohamed, Mohamed A.; Nour, Hamdy E. (2012): Heavy metals contamination of the Quaternary coral reefs, Red Sea coast, Egypt. In: Environmental Earth Sciences 67 (3), S. 777–785. DOI: 10.1007/s12665-012-1535-.

Erez, J.; Braun, A. (2007): Calcification in hermatypic corals is based on direct seawater supply to the biomineralisation site. In: Geochimica et Cosmochimica Acta 71 (15), SA260.

Esslemont, Graeme (2000): Heavy metals in seawater, marine sediments and corals from the Townsville section, Great Barrier Reef Marine Park, Queensland. In: Marine Chemistry 71 (3-4), S. 215–231. DOI: 10.1016/S0304-4203(00)00050-5.

Fallon, Stewart J.; McCulloch, Malcolm T.; van Woesik, Robert; Sinclair, Daniel J. (1999): Corals at their latitudinal limits. Laser ablation trace element systematics in Porites from Shirigai Bay, Japan. In: Earth and Planetary Science Letters 172 (3-4), S. 221–238. DOI: 10.1016/S0012-821X(99)00200-9.

Finch, Adrian A.; Allison, Nicola (2008): Mg structural state in coral aragonite and implications for the paleoenvironmental proxy. In: Geophysical Research Letters 35 (8). DOI: 10.1029/2008GL033543.
Fleitmann, Dominik; Dunbar, Robert B.; McCulloch, Malcolm; Mudelsee, Manfred; Vuille, Mathias; McClanahan, Tim R. et al. (2007): East African soil erosion recorded in a 300 year old coral colony from Kenya. In: Geophysical Research Letters 34 (4). DOI: 10.1029/2006GL028525.
Forsman, Zac H.; Barshis, Daniel J.; Hunter, Cynthia L.; Toonen, Robert J. (2009): Shape-shifting corals. Molecular markers show morphology is evolutionarily plastic in Porites. In: BMC evolutionary biology 9 (1), S. 1–9. DOI: 10.1186/1471-2148-9-45.
Fricker, Mattias B.; Kutscher, Daniel; Aeschlimann, Beat; Frommer, Jakob; Dietiker, Rolf; Bettmer, Jörg; Günther, Detlef (2011): High spatial resolution trace element analysis by LA-ICP-MS using a novel ablation cell for multiple or large samples. In: International Journal of Mass Spectrometry 307 (1-3), S. 39–45. DOI: 10.1016/j.ijms.2011.01.008.
Frontalini, Fabrizio; Coccioni, Rodolfo (2008): Benthic foraminifera for heavy metal pollution monitoring. A case study from the central Adriatic Sea coast of Italy. In: Estuarine, Coastal and Shelf Science 76 (2), S. 404–417. DOI: 10.1016/j.ecss.2007.07.024.
Gagnon, Alexander C.; Adkins, Jess F.; Erez, Jonathan (2012): Seawater transport during coral biomineralization. In: Earth and Planetary Science Letters 329, S. 150–161. DOI: 10.1016/j.epsl.2012.03.005.
Garbe-Schönberg, Dieter; Müller, Samuel (2014): Nano-particulate pressed powder tablets for LA-ICP-MS. In: Journal of Analytical Atomic Spectrometry 29 (6), S. 990–1000. DOI: 10.1039/C4JA00007B.
Green, Daniel H.; Edmunds, Peter J.; Carpenter, Robert C. (2008): Increasing relative abundance of Porites astreoides on Caribbean reefs mediated by an overall decline in coral cover. In: Marine Ecology Progress Series 359, S. 1–10. DOI: 10.3354/meps07454.
Grottoli, Andréa G.; Matthews, Kathryn A.; Palardy, James E.; McDonough, William F. (2013): doi.org/10.1016/j.chemgeo.2013.08.024. Calibration and interpretation. In: Chemical Geology 356, S. 151–159. DOI: 10.1016/j.chemgeo.2013.08.024.
Guzman, Hector M.; Cortes, Jorge (1989): Growth rates of eight species of scleractinian corals in the eastern Pacific (Costa Rica). In: Bulletin of Marine Science 44 (3), S. 1186–1194.
Guzmán, Héctor M.; Garcıa, Elia M. (2002): Mercury levels in coral reefs along the Caribbean coast of Central America. In: Marine Pollution Bulletin 44 (12), S. 1415–1420. DOI: 10.1016/S0025-326X(02)00318-1.
Guzmán, Héctor M.; Jiménez, Carlos E. (1992): Contamination of coral reefs by heavy metals along the Caribbean coast of Central America (Costa Rica and Panama). In: Marine Pollution Bulletin 24 (11), S. 554–561. DOI: 10.1016/0025-326X(92)90708-E.
Hammer, Øyvind; Harper, David A. T.; Ryan, Paul D. (2001): PAST. Paleontological statistics software package for education and data analysis. In: Palaeontologia Electronica 4 (1), S. 9.
Hanna, R. G.; Muir, Glen L. (1990): Red Sea corals as biomonitors of trace metal pollution. In: Environmental Monitoring and Assessment 14 (2), S. 211–222. DOI: 10.1007/BF00677917.
Inoue, Mayuri; Nohara, Masato; Okai, Takashi; Suzuki, Atsushi; Kawahata, Hodaka (2004): Concentrations of trace elements in carbonate reference materials coral JCp-1 and giant

clam JCt-1 by inductively coupled plasma-mass spectrometry. In: Geostandards and Geoanalytical Research 28 (3), S. 411–416. DOI: 10.1111/j.1751-908X.2004.tb00759.x.

Jafarabadi, Ali Ranjbar; Bakhtiari, Alireza Riyahi; Maisano, Maria; Pereira, Patrícia; Cappello, Tiziana (2018): First record of bioaccumulation and bioconcentration of metals in Scleractinian corals and their algal symbionts from Kharg and Lark coral reefs (Persian Gulf, Iran). In: Science of the Total Environment 640, S. 1500–1511. DOI: 10.1016/j.scitotenv.2018.06.029.

Jiang, Wei; Yu, Kefu; Wang, Ning; Yang, Hua; Yang, Haodan; Xu, Shendong et al. (2020): Distribution coefficients of trace metals between modern coral-lattices and seawater in the northern South China Sea. Species and SST dependencies. In: Journal of Asian Earth Sciences 187, S. 104082. DOI: 10.1016/j.jseaes.2019.104082.

Jochum, Klaus Peter; Garbe-Schönberg, Dieter; Veter, Marina; Stoll, Brigitte; Weis, Ulrike; Weber, Michael et al. (2019): Nano-powdered calcium carbonate reference materials. Significant progress for microanalysis? In: Geostandards and Geoanalytical Research 43 (4), S. 595–609. DOI: 10.1111/ggr.12292.

Jochum, Klaus Peter; Weis, Ulrike; Stoll, Brigitte; Kuzmin, Dmitry; Yang, Qichao; Raczek, Ingrid et al. (2011): Determination of reference values for NIST SRM 610–617 glasses following ISO guidelines. In: Geostandards and Geoanalytical Research 35 (4), S. 397–429. DOI: 10.1111/j.1751-908X.2011.00120.x.

Jupiter, S. (2008): Coral rare earth element tracers of terrestrial exposure in nearshore corals of the Great Barrier Reef. In: Proc. 11th Int. Coral Reef Symposium 4, pp. 105–109.

Kaczmarsky, Longin; Richardson, Laurie L. (2007): Transmission of growth anomalies between Indo-Pacific Porites corals. In: Journal of Invertebrate Pathology 94 (3), S. 218–221. DOI: 10.1016/j.jip.2006.11.007.

Katoh, Kazutaka; Misawa, Kazuharu; Kuma, Kei-ichi; Miyata, Takashi (2002): MAFFT. A novel method for rapid multiple sequence alignment based on fast Fourier transform. In: Nucleic Acids Research 30 (14), S. 3059–3066. DOI: 10.1093/nar/gkf436.

Katoh, Kazutaka; Standley, Daron M. (2013): MAFFT multiple sequence alignment software version 7. Improvements in performance and usability. In: Molecular biology and evolution 30 (4), S. 772–780. DOI: 10.1093/molbev/mst010.

Kefu, Yu; Tegu, Chen; Dingcheng, Huang; Huanting, Zhao; Jinliang, Zhong; Dongsheng, Liu (2001): The high-resolution climate recorded in the δ18O of Porites lutea from the Nansha Islands of China. In: Chinese Science Bulletin 46 (24), S. 2097–2102. DOI: 10.1007/BF02901141.

Klein, R.; Loya, Y. (1991): Skeletal growth and density patterns of two Porites corals from the Gulf of Eilat, Red Sea. In: Marine Ecology Progress Series 77 (2), S. 253–259.

Kotov, S., & Paelike, H. (2018): QAnalySeries-a cross-platform time series tuning and analysis tool. In: In AGU Fall Meeting Abstracts (Vol. 2018, pp. PP53D-1230). DOI: 10.1002/essoar.10500226.1.

Kourandeh, Mehdi Bolouki; Nabavi, Seyed Mohammad Bagher; Shokri, Mohammad Reza; Ghanemi, Kamal; Feng, Yuexing (in review): Trace Metals Content in Annually-Banded Scleractinian Coral 'Porites Lobata' Across the Northern Persian Gulf. In: Environmental Science and Pollution Research, Epub ahead of print. PMID: 34165735. DOI: 10.1007/s11356-021-14938-8.

Kourandeh, Mehdi Bolouki; Nabavi, Seyed Mohammad Bagher; Shokri, Mohammad Reza; Ghanemi, Kamal; Feng, Yuexing (2021): Trace metal content in annually banded scleractinian coral 'Porites lobata'across the northern Persian Gulf. In: Environmental Science and Pollution Research, S. 1–13. DOI: 10.1007/s11356-021-14938-8.

Larocque, Adrienne C. L.; Rasmussen, Patricia E. (1998): An overview of trace metals in the environment, from mobilization to remediation. In: Environmental Geology 33 (2-3), S. 85–91. DOI: 10.1007/S002540050227.

Leonard, N. D.; Welsh, K. J.; Nguyen, Ai Duc; Sadler, J.; Pandolfi, John M.; Clark, Tara R. et al. (2019): High resolution geochemical analysis of massive Porites spp. corals from the Wet Tropics, Great Barrier Reef. Rare earth elements, yttrium and barium as indicators of terrigenous input. In: Marine Pollution Bulletin 149, S. 110634. DOI: 10.1016/j.marpolbul.2019.110634.

Lewis, S. E.; Brodie, J. E.; McCulloch, M. T.; Mallela, J.; Jupiter, S. D.; Williams, H. Stuart et al. (2012): An assessment of an environmental gradient using coral geochemical records, Whitsunday Islands, Great Barrier Reef, Australia. In: Marine Pollution Bulletin 65 (4-9), S. 306–319. DOI: 10.1016/j.marpolbul.2011.09.030.

Li, Tao; Cai, Guanqiang; Zhang, Muhui; Li, Sun; Nie, Xin (2021): The response of benthic foraminifera to heavy metals and grain sizes. A case study from Hainan Island, China. In: Marine Pollution Bulletin 167, S. 112328. DOI: 10.1016/j.marpolbul.2021.112328.

Linn, L. J.; Delaney, M. L.; Druffel, E. R.M. (1990): Trace metals in contemporary and seventeenth-century Galapagos coral. Records of seasonal and annual variations. In: Geochimica et Cosmochimica Acta 54 (2), S. 387–394. DOI: 10.1016/0016-7037(90)90327-H.

Liu, Qunqun; Wang, Feifei; Meng, Fanping; Jiang, Lei; Li, Guangjing; Zhou, Rongguang (2018): Assessment of metal contamination in estuarine surface sediments from Dongying City, China. Use of a modified ecological risk index. In: Marine Pollution Bulletin 126, S. 293–303. DOI: 10.1016/j.marpolbul.2017.11.017.

Livingston, H. D.; Thompson, Geoffrey (1971): Trace Element concentration in some modern corals. In: Limnology and Oceanography 16 (5), S. 786–796. DOI: 10.4319/lo.1971.16.5.0786.

Lord, Karina Scavo; Barcala, Anna; Aichelman, Hannah E.; Kriefall, Nicola G.; Brown, Chloe; Knasin, Lauren et al. (2021): Distinct Phenotypes Associated with Mangrove and Lagoon Habitats in Two Widespread Caribbean Corals, Porites astreoides and Porites divaricata. In: The Biological Bulletin 240 (3), S. 0. DOI: 10.1086/714047.

Lough, J. M.; Barnes, D. J.; Devereux, M. J.; Tobin, B. J.; Tobin, S. (1999): Variability in growth characteristics of massive Porites on the Great Barrier Reef. In: CRC Reef Research Technical Report No.28 Australian Institute of Marine Science, Townsville.

Lough, J. M.; Barnes, D. J.; Taylor, R. B. (1996): The potential of massive corals for the study of high-resolution climate variation in the past millennium. In: Climatic Variations and Forcing Mechanisms of the Last 2000 Years: Springer, S. 355–371.

Mansour, Abbas M.; Askalany, Mohamed S.; Madkour, Hashem A.; Assran, Bakheit B. (2013): Assessment and comparison of heavy-metal concentrations in marine sediments in view of tourism activities in Hurghada area, northern Red Sea, Egypt. In: The Egyptian Journal of Aquatic Research 39 (2), S. 91–103. DOI: 10.1016/j.ejar.2013.07.004.

Mass, Tali; Drake, Jeana L.; Heddleston, John M.; Falkowski, Paul G. (2017): Nanoscale visualization of biomineral formation in coral proto-polyps. In: Current Biology 27 (20), 3191-3196. e3. DOI: 10.1016/j.cub.2017.09.012.

McCulloch, Malcolm; Fallon, Stewart; Wyndham, Timothy; Hendy, Erica; Lough, Janice; Barnes, David (2003): Coral record of increased sediment flux to the inner Great Barrier Reef since European settlement. In: Nature 421 (6924), S. 727–730. DOI: 10.1038/nature01361.

Mieremet, Ben (1997): Report of the Middle East Seas Regional Strategy Workshop for the International Coral Reef Initiative: Aqaba, Jordan, 21-25 September 1997. In: Office of Oceanic and Coastal Resources Management, National Ocean and Atmospheric Administration.

Mohammed, Tarek Abdel-Aziz Ahmed; Dar, Mahmoud A. (2010): Ability of corals to accumulate heavy metals, Northern Red Sea, Egypt. In: Environmental Earth Sciences 59 (7), S. 1525–1534. DOI: 10.1007/s12665-009-0138-x.

Mokhtar, Mazlin Bin; Praveena, Sarva Mangala; Aris, Ahmad Zaharin; Yong, Ow Cher; Lim, Ai Phing (2012): Trace metal (Cd, Cu, Fe, Mn, Ni and Zn) accumulation in Scleractinian corals. A record for Sabah, Borneo. In: Marine Pollution Bulletin 64 (11), S. 2556–2563. DOI: 10.1016/j.marpolbul.2012.07.030.

Munsel, D.; Kramar, U.; Dissard, Delphine; Nehrke, Gernot; Berner, Z.; Bijma, Jelle et al. (2010): Heavy metal incorporation in foraminiferal calcite. Results from multi-element enrichment culture experiments with Ammonia tepida. In: Biogeosciences 7 (8), S. 2339–2350. DOI: 10.5194/bg-7-2339-2010.

Nardelli, Maria Pia; Malferrari, Daniele; Ferretti, Annalisa; Bartolini, A.; Sabbatini, Anna; Negri, Alessandra (2016): Zinc incorporation in the miliolid foraminifer Pseudotriloculina rotunda under laboratory conditions. In: Marine Micropaleontology 126, S. 42–49. DOI: 10.1016/j.marmicro.2016.06.001.

Nguyen, A. D.; Zhao, J. X.; Feng, Y. X.; Hu, W. P.; Yu, K. F.; Gasparon, Massimo et al. (2013): Impact of recent coastal development and human activities on Nha Trang Bay, Vietnam. Evidence from a Porites lutea geochemical record. In: Coral Reefs 32 (1), S. 181–193. DOI: 10.1007/s00338-012-0962-4.

Nguyen, Lam-Tung; Schmidt, Heiko A.; Haeseler, Arndt von; Minh, Bui Quang (2015): IQ-TREE. A fast and effective stochastic algorithm for estimating maximum-likelihood phylogenies. In: Molecular biology and evolution 32 (1), S. 268–274. DOI: 10.1093/molbev/msu300.

Nour, Hamdy El Sayed (2019): Assessment of heavy metals contamination in surface sediments of Sabratha, Northwest Libya. In: Arabian Journal of Geosciences 12 (6), S. 1–9. DOI: 10.1007/s12517-019-4343-y.

Nour, Hamdy El Sayed; Nouh, El Said (2020): Using coral skeletons for monitoring of heavy metals pollution in the Red Sea Coast, Egypt. In: Arabian Journal of Geosciences 13 (10), S. 1–12. DOI: 10.1007/s12517-020-05308-8.

Oron, Shai; Sadekov, Aleksey; Katz, Timor; Goodman-Tchernov, Beverly (2021): Benthic foraminifera geochemistry as a monitoring tool for heavy metal and phosphorus pollution—A post fish-farm removal case study. In: Marine Pollution Bulletin 168, S. 112443. DOI: 10.1016/j.marpolbul.2021.112443.

Pingitore Jr, Nicholas E.; Iglesias, Arturo; Bruce, Allison; Lytle, Farrel; Wellington, Gerard M. (2002): Valences of iron and copper in coral skeleton. X-ray absorption spectroscopy analysis. In: Microchemical Journal 71 (2-3), S. 205–210. DOI: 10.1016/S0026-265X(02)00012-7.

Prouty, N. G.; Hughen, K. A.; Carilli, J. (2008): Geochemical signature of land-based activities in Caribbean coral surface samples. In: Coral Reefs 27 (4), S. 727–742. DOI: 10.1007/s00338-008-0413-4.

Prouty, Nancy G.; Field, Michael E.; Stock, Jonathan D.; Jupiter, Stacy D.; McCulloch, Malcolm (2010): Coral Ba/Ca records of sediment input to the fringing reef of the southshore of Moloka'i, Hawai'i over the last several decades. In: Marine Pollution Bulletin 60 (10), S. 1822–1835. DOI: 10.1016/j.marpolbul.2010.05.024.

Readman, J. W.; Tolosa, I.; Law, A. T.; Bartocci, J.; Azemard, S.; Hamilton, T. et al. (1996): Discrete bands of petroleum hydrocarbons and molecular organic markers identified within massive coral skeletons. In: Marine Pollution Bulletin 32 (5), S. 437–443. DOI: 10.1016/0025-326X(96)83974-9.

Reichelt-Brushett, Amanda J.; Harrison, Peter L. (2005): The effect of selected trace metals on the fertilization success of several scleractinian coral species. In: Coral Reefs 24 (4), S. 524–534. DOI: 10.1007/s00338-005-0013-5.

Reyes-Bonilla, H. (1992): New records for hermatypic corals (Anthozoa Scleractinia) in the Gulf of California, Mexico, with an historical and biogeographical discussion. In: Journal of Natural History 26 (6), S. 1163–1175. DOI: 10.1080/00222939200770671.

Rodríguez, Gualberto Rosado; Morales, Ernesto Otero (2020): Assessment of heavy metal contamination at Tallaboa Bay (Puerto Rico) by marine sponges' bioaccumulation and fungal community composition. In: Marine Pollution Bulletin 161, S. 111803. DOI: 10.1016/j.marpolbul.2020.111803.

Saha, Narottam; Webb, Gregory E.; Zhao, Jian-Xin (2016): doi.org/10.1016/j.scitotenv.2016.05.066. In: Science of the Total Environment 566, S. 652–684. DOI: 10.1016/j.scitotenv.2016.05.066.

Santhanam, P. (2011): An investigation on heavy metals accumulation in water, sediment and small marine food chain (plankton and fish) from Coromandel Coast, Southeast Coast of India. In: Indian Journal Of Natural Sciences International Bimonthly ISSN 976, S. 997.

Sayers, E. W., Barrett, T., Benson, D. A., Bryant, S. H., Canese, K., Chetvernin, V., et al. (2009): Database resources of the National Center for Biotechnology Information. In: Nucleic Acids Research (37, D5–D15). DOI: 10.1093/nar/gkn741.

Schmidt, Sarina; Hathorne, Edmund Charles; Schönfeld, Joachim; Garbe-Schönberg, Dieter (2021): Heavy metal uptake of near-shore benthic foraminifera during multi-metal culturing experiments. In: Biogeosciences, [preprint], in review, 2021. DOI: 10.5194/bg-2021-158.

Schneider, R. C.; Smith, S. V. (1982): Skeletal Sr content and density in Porites spp. in relation to environmental factors. In: Marine Biology 66 (2), S. 121–131. DOI: 10.1007/BF00397185.

Séré, M. G.; Schleyer, M. H.; Quod, J. P.; Chabanet, Pascale (2012): Porites white patch syndrome. An unreported coral disease on Western Indian Ocean reefs. In: Coral Reefs 31 (3), S. 739. DOI: 10.1007/s00338-012-0897-9.

Shannon, Robert D. (1976): Revised effective ionic radii and systematic studies of interatomic distances in halides and chalcogenides. In: Acta Crystallographica Section A: crystal physics, diffraction, theoretical and general crystallography 32 (5), S. 751–767. DOI: 10.1107/S0567739476001551.

Shen, G. T. (1996): Rapid changes in the tropical ocean and the use of corals as monitoring systems. In: Berger A (ed) Geoindicator: assessing rapid environmental changes in earth systems. Brokfield, Rotterdam, pp 125–169.

Shen, G. T.; Sanford, C. L. (1990): Trace element indicators of climate variability in reef-building corals. In: Elsevier oceanography series, Bd. 52: Elsevier, S. 255–283.

Shen, Glen T. (1986): Lead and cadmium geochemistry of corals. Reconstruction of historic perturbations in the upper ocean. Massachusetts Institute of Technology.

Shen, Glen T.; Boyle, Edward A. (1987): Lead in corals. Reconstruction of historical industrial fluxes to the surface ocean. In: Earth and Planetary Science Letters 82 (3-4), S. 289–304. DOI: 10.1016/0012-821X(87)90203-2.

Shen, Glen T.; Boyle, Edward A. (1988): Determination of lead, cadmium and other trace metals in annually-banded corals. In: Chemical Geology 67 (1-2), S. 47–62. DOI: 10.1016/0009-2541(88)90005-8.

Shen, Glen T.; Campbell, Todd M.; Dunbar, Robert B.; Wellington, Gerard M.; Colgan, Mitchell W.; Glynn, Peter W. (1991): Paleochemistry of manganese in corals from the Galapagos Islands. In: Coral Reefs 10 (2), S. 91–100. DOI: 10.1007/BF00571827.pdf.

Smith, L. W.; Barshis, D.; Birkeland, C. (2007): Phenotypic plasticity for skeletal growth, density and calcification of Porites lobata in response to habitat type. In: Coral Reefs 26 (3), S. 559–567. DOI: 10.1007/s00338-007-0216-z.

Sonone, Swaroop S.; Jadhav, Swapnali; Sankhla, Mahipal Singh; Kumar, Rajeev (2020): Water contamination by heavy metals and their toxic effect on aquaculture and human health through food Chain. In: Letters in Applied NanoBioScience 10 (2), S. 2148–2166. DOI: 10.33263/LIANBS102.21482166.

Sowa, Kohki; Watanabe, Tsuyoshi; Kan, Hironobu; Yamano, Hiroya (2014): Influence of land development on Holocene Porites coral calcification at Nagura bay, Ishigaki island, Japan. In: PLoS One 9 (2), e88790. DOI: 10.1371/journal.pone.0088790.

St John, B. (1974): Heavy metals in the skeletal carbonate of scleractinian corals. In: Proc. 2ndInt. Coral Reef Symposium, pp. 461–469.

Sun, Chang-Yu; Stifler, Cayla A.; Chopdekar, Rajesh V.; Schmidt, Connor A.; Parida, Ganesh; Schoeppler, Vanessa et al. (2020): From particle attachment to space-filling coral skeletons. In: Proceedings of the National Academy of Sciences 117 (48), S. 30159–30170. DOI: 10.1073/pnas.2012025117.

Tambutté, Sylvie; Holcomb, Michael; Ferrier-Pagès, Christine; Reynaud, Stéphanie; Tambutté, Éric; Zoccola, Didier; Allemand, Denis (2011): Coral biomineralization. From the gene to the environment. In: Journal of Experimental Marine Biology and Ecology 408 (1-2), S. 58–78. DOI: 10.1016/j.jembe.2011.07.026.

Taubner, Isabelle; Böhm, Florian; Eisenhauer, Anton; Tambutté, Eric; Tambutté, Sylvie; Moldzio, Stephan; Bleich, Markus (2017): An improved approach investigating epithelial ion transport in scleractinian corals. In: Limnology and Oceanography: Methods 15 (9), S. 753–765. DOI: 10.1002/lom3.10194.

Terakado, Yasutaka; Masuda, Akimasa (1988): The coprecipitation of rare-earth elements with calcite and aragonite. In: Chemical Geology 69 (1-2), S. 103–110. DOI: 10.1016/0009-2541(88)90162-3.

Thornton, Iain (1995): Metals in the global environment. Facts and misconceptions: International Council on Metals and the Environment.

Tisthammer, Kaho H.; Richmond, Robert H. (2018): Corallite skeletal morphological variation in Hawaiian Porites lobata. In: Coral Reefs 37 (2), S. 445–456. DOI: 10.1007/s00338-018-1670-5.

Titelboim, Danna; Sadekov, Aleksey; Blumenfeld, Maya; Almogi-Labin, Ahuva; Herut, Barak; Halicz, Ludwik et al. (2021): Monitoring of heavy metals in seawater using single chamber foraminiferal sclerochronology. In: Ecological Indicators 120, S. 106931. DOI: 10.1016/j.ecolind.2020.106931.

Tortolero-Langarica, J. J.A.; Carricart-Ganivet, J. P.; Cupul-Magaña, A. L.; Rodríguez-Troncoso, A. P. (2017): Historical insights on growth rates of the reef-building corals Pavona gigantea and Porites panamensis from the Northeastern tropical Pacific. In: Marine Environmental Research 132, S. 23–32. DOI: 10.1016/j.marenvres.2017.10.004.

Tortolero-Langarica, J. J.A.; Rodríguez-Troncoso, A. P.; Carricart-Ganivet, J. P.; Cupul-Magaña, A. L. (2016): Skeletal extension, density and calcification rates of massive free-living coral Porites lobata Dana, 1846. In: Journal of Experimental Marine Biology and Ecology 478, S. 68–76. DOI: 10.1016/j.jembe.2016.02.005.

Veeh, H. Herbert; Turekian, Karl K. (1968): Cobalt, silver, and uranium concentrations of reef-building corals in the pacific ocean. In: Limnology and Oceanography 13 (2), S. 304–308. DOI: 10.4319/lo.1968.13.2.0304.

Venugopal, B.; Luckey, T. D. (1975): "Toxicology of nonradio-active heavy metals and their salts", in Heavy Metal Toxicity, Safety and Hormology, T. D. Luckey, B. Venugopal, D. Hutcheson (Eds.). In: George Thieme, Stuttgart.

Weis, Judith S. (2015): Marine pollution. What everyone needs to know: Oxford University Press Oxford University Press (273 P).

Williams, T. M.; Rees, J. G.; Setiapermana, D. (2000): Metals and trace organic compounds in sediments and waters of Jakarta Bay and the Pulau Seribu Complex, Indonesia. In: Marine Pollution Bulletin 40 (3), S. 277–285.

Wu, Yang; Fallon, Stewart J.; Cantin, Neal E.; Lough, Janice M. (2021): Surface ocean radiocarbon from a Porites coral record in the great barrier reef. 1945–2017. In: Radiocarbon, S. 1–11. DOI: 10.1017/RDC.2020.141.

Zhang, Jinfeng; Gao, Xuelu (2015): Heavy metals in surface sediments of the intertidal Laizhou Bay, Bohai Sea, China. Distributions, sources and contamination assessment. In: Marine Pollution Bulletin 98 (1-2), S. 320–327. DOI: 10.1016/j.marpolbul.2015.06.035.

5 Summary, Conclusion and Outlook

5.1 Summary and Conclusions

This thesis provides fundamental research on the uptake and incorporation of ten different heavy metals (Cr, Mn, Ni, Cu, Zn, Ag, Cd, Hg, Sn and Pb) into the calcium carbonate of three benthic foraminifera (*A. aomoriensis*, *A. batava* and *E. excavatum*) and two tropical coral species (*P. lichen* and *P. lobata*). Furthermore, the distribution of foraminiferal species and the connectivity between different environments in the North Sea was assessed by using the living fauna and dead foraminiferal assemblages.

Chapter 1 investigated the living fauna and dead foraminiferal assemblages along a transect from the supratidal Japsand up to Hallig Hooge. The most abundant species in both assemblages was *Ammonia batava*. *Elphidium selseyense* and *Elphidium williamsoni* were also common in the living fauna. The size distribution curves of the three most abundant species from the living fauna revealed that *Ammonia batava* and *Elphidium selseyense* reproduced recently, while *Elphidium williamsoni* had just started to reproduce. *Haynesina germanica* was rare in the living fauna but frequent in the dead assemblage. The dead assemblage yielded species that were not found in the living fauna from the area. Some of these species, e.g., *Bucella frigida*, were reworked from older sediments while others, e.g., *Jadammina macrescens*, originated from other areas of the North Sea or the North Atlantic and were transported to Japsand via tidal currents. *Haynesina germanica*, *Ammonia batava* and different *Elphidium* species from the living fauna depicted a close linkage between the open North Sea and marginal marine environments close to the mainland. These species behave opportunistic and are able to occupy a variety of environments. Hence, they well may cope with environmental changes in the future. The results of this study indicated that transport mechanisms were dominant environmental factors shaping in particular the dead foraminiferal assemblages in the Japsand area.

Chapter 2 assessed the heavy metal incorporation into the calcite of the foraminiferal species *Ammonia aomoriensis*, *Ammonia batava* and *Elphidium excavatum* and its dependency on the heavy metal concentration in the ambient seawater. Culturing experiments with a mixture of ten different metals over a wide concentration range revealed species-specific differences in the incorporation of heavy metals. All metals used in this study were incorporated into the foraminiferal calcite of all three species. Laser ablation ICP-MS analysis of the foraminiferal calcite of all three species exhibited a strong positive correlation with Pb and Ag concentrations in the culturing medium. *A. aomoriensis* further revealed a correlation with Mn and Cu, *A. batava* with Mn and Hg and *E. excavatum* with Cr and Ni. Zn, Sn and Cd showed no clear trends. D_{TE} values of Ni, Zn, Cd, Hg and Pb decreased with increasing heavy metal concentration in the seawater, which may point towards an early protective mechanism, prior to damage, reduced growth or death of the organism. The results of this study facilitate a reconstruction of the heavy metal concentration in seawater for those elements showing a correlation between TE/Ca ratios in calcite and seawater. The partition coefficients allow a quantification of metal concentrations in polluted or pristine areas.

The aim of **Chapter 3** was to examine whether the incorporation of heavy metals into the aragonitic skeleton of the scleractinian corals *Porites lobata* and *Porites lichen* is a direct function of their concentration in seawater. Culturing experiments exposed *P. lobata* and *P. lichen* to a mixture of ten dissolved metals. Laser ablation ICP-MS measurements of the coral aragonite precipitated during the culturing showed only minor, non-systematic interspecies differences in the trace metal concentrations. Intraspecies variations could be linked to measurements deviating from the maximum growth axis. A positive correlation between the TE/Ca values and the coral skeleton was found for Cr, Mn, Ni, Zn, Ag, Cd and Pb. The uptake of these metals therefore mainly depended on their concentration in seawater. The incorporation of the heavy metals into the coral skeleton was most likely performed by Ca^{2+} substitution or by adsorption to organic matter. Cu, Sn and Hg did not show any clear trend, which for Cu and Sn was caused by the low variability in the culturing medium. Hg concentration in seawater varied appropriately, but the Hg concentration in the coral skeleton was too low to interpret. The calibrations of this study and the D_{TE} values permit a determination of heavy metal concentrations in seawater, which provides a promising tool for ecosystem status assessments in the future.

Overall, this study provided new insights into the distribution patterns and ecological driving factors that are shaping the foraminiferal assemblages in the Japsand area in the German North Sea. Besides ecological insights, this study also provides new information concerning biomineralization processes of benthic foraminifera and tropical corals. Both were incorporating a variety of heavy metals into their skeleton or their test, of which the majority depended mainly on the heavy metal concentration of the water the organism grew in. Species-specific differences in the uptake of heavy metals emerged, which makes future research vitally important. Moreover, laser ablation ICP-MS has been proven as a useful method for analysing the heavy metal concentration in calcium carbonate archives like foraminiferal shells and coral skeletons. Major advantages of this method are a minimal destruction of the sample material, a high spatial resolution, minimal sample preparation and a high analysis output. This provides the opportunity to resolve seasonal profiles and to identify short-term events like the punctual introduction of contaminants into the environment, in particular for corals. Furthermore, foraminifera can be measured without dissolving their entire test. The specimens may be kept and curated as taxonomic references for future investigations. Suitable geological archives in combination with laser ablation ICP-MS analysis enable a reconstruction of the heavy metal concentration in seawater for both, ecosystem monitoring and reconstructions of heavy metal input in the past.

5.2 Outlook

This thesis answers basic questions addressing the heavy metal incorporation into the calcitic test of benthic foraminifera and into the aragonitic skeleton of tropical corals. Nevertheless, there are still uncertainties and unanswered questions, which deserve further research.

First of all, this study focussed on benthic foraminifera from temperate environments and tropical corals, that are restricted to near-shore environments. These areas are especially under threat by anthropogenic and natural heavy metal input, but other areas can also be influenced by elevated heavy metal concentrations. Therefore, it would be interesting to investigate the heavy metal concentration in the shell of foraminifera and corals that are living in different environments e.g., the continental shelf and the deep-sea, especially in the vicinity of cold and warm seeps, and submarine lava flows. Besides tropical corals, also cold-water corals like *Lophelia* could serve as an archive for the heavy metal concentration and isotopes in these deeper environments, in particular around mud volcanos (Little et al., 2021). Furthermore, the analysis of deep-sea corals could make such environments accessible and investigate the anthropogenic impact on the deep sea (Qu et al., 2021). In different environments, other coral and foraminiferal species need to be investigated. Ideally, culturing experiments with representative species for the specific environments should be carried out to analyse the sensitivity of different species to the heavy metal concentration in the ambient seawater, which varies between species. Some studies already approached the heavy metal concentration in tropical foraminifers (e.g., Titelboim et al., 2018 and 2021; Sagar et al., 2021a), but much more research is necessary, in particular on oceanic islands and comparing bioprovinces on the Pacific Ocean.

Besides the calcite or the aragonite of foraminifera or corals, other materials and organisms may also have the ability to serve as environmental archives for heavy metal contamination. It could for example be possible to analyse the TE/Ca values in the shell or skeletons of snails, sponges, brachiopods, ostracods, bryozoa or crabs to investigate environments on land, fresh water or marine environments that are lacking foraminifera and corals. For a reliable application of these organisms, culturing studies would be necessary to identify what is influencing the heavy metal concentration in the shell or skeleton.

Corals and foraminifera could also incorporate other pollutants like organic compounds, e.g., PAH (polycyclic aromatic hydrocarbons) and microplastic. A few studies are already addressing the uptake of such pollutants by foraminifera and corals (Hall et al., 2015; Han et al., 2020; Yang et al., 2020; Birarda et al., 2021). Culturing experiments that could provide a quantitative correlation between the compound in the water and in the test or skeleton are yet to be performed. A quantitative investigation could further reveal if corals and foraminifera in large reefs are possible sinks for environmental pollutants. This could in turn enable an application of them to remove elements from the seawater permanently and therefore serve as cleaning agents for the oceans.

Coral skeletons have a long history as archives for various environmental conditions including heavy metal concentration (e.g., Guzmán and Jiménez, 1992; Esslemont, 2000; Ali et al., 2011; Yang et al., 2020). However, so far no culturing studies investigated the uptake mechanism of these heavy metals in very detail and from a physiological aspect. The heavy metal concentration of the test of foraminifera on the other hand are less studied and most literature concerning the influence of heavy metals on foraminifera are based on assemblage analysis or surface sediment studies (e.g., Ferraro et al., 2006; Carnahan et al., 2008; Martins et al., 2013; Li et al., 2021). Therefore, down-core sediment records of TE/Ca values based on foraminifera are rare and more research on this topic is needed. The analysis of TE/Ca concentrations in the foraminiferal tests of high-resolution down-core records could provide insights into the historical development of the heavy metals in seawater (e.g., Rumolo et al., 2009).

Additional References

Akan, J. C., Abdulrahman, F. I., Sodipo, O. A., Ochanya, A. E., and Askira, Y. K.: Heavy metals in sediments from river Ngada, Maiduguri Metropolis, Borno state, Nigeria, Journal of Environmental Chemistry and Ecotoxicology, 2, 131–140, doi:10.5897/JECE.9000033, 2010.

Al-Horani, F. A., Al-Moghrabi, S. M., and Beer, D. de: The mechanism of calcification and its relation to photosynthesis and respiration in the scleractinian coral *Galaxea fascicularis*, Marine Biology, 142, 419–426, doi:10.1007/s00227-002-0981-8, 2003.

Ali, A. A.-h., Hamed, M. A., and Abd El-Azim, H.: Heavy metals distribution in the coral reef ecosystems of the Northern Red Sea, Helgoland Marine Research, 65, 67–80, doi:10.1007/s10152-010-0202-7, 2011.

Allemand, D., Tambutté, É., Zoccola, D., and Tambutté, S.: Coral calcification, cells to reefs, Coral reefs: An Ecosystem in Transition, 119–150, doi:10.1007/978-94-007-0114-4_9, 2011.

Allison, N. and Finch, A. A.: High temporal resolution Mg/Ca and Ba/Ca records in modern *Porites lobata* corals, Geochemistry, Geophysics, Geosystems, 8, doi:10.1029/2006GC001477, 2007.

Al-Rousan, S. A., Al-Shloul, R. N., Al-Horani, F. A., and Abu-Hilal, A. H.: Heavy metal contents in growth bands of *Porites* corals: Record of anthropogenic and human developments from the Jordanian Gulf of Aqaba, Marine Pollution Bulletin, 54, 1912–1922, doi:10.1007/s12665-012-1640-0, 2007.

Amiel, A. J., Friedman, G. M., and Miller, D. S.: Distribution and nature of incorporation of trace elements in modern aragonitic corals, Sedimentology, 20, 47–64, doi:10.1111/j.1365-3091.1973.tb01606.x, 1973a.

Amiel, A. J., Miller, D. S., and Friedman, G. M.: Incorporation of uranium in modern corals, Sedimentology, 20, 523–528, doi:10.1111/j.1365-3091.1973.tb01629.x, 1973b.

Angell, R. W.: Test morphogenesis (chamber formation) in the foraminifer *Spiroloculina hyalina* Schulze, The Journal of Foraminiferal Research, 10, 89–101, doi:10.2113/gsjfr.10.2.89, 1980.

Ansari, T. M., Marr, I. L., and Tariq, N.: Heavy metals in marine pollution perspective-a mini review, Journal of Applied Sciences, 4, 1–20, doi:10.3923/jas.2004.1.20, 2004.

Anu, G., Kumar, N. C., Jayalakshmi, K. J., and Nair, S. M.: Monitoring of heavy metal partitioning in reef corals of Lakshadweep Archipelago, Indian Ocean, Environmental Monitoring and Assessment, 128, 195–208, doi:10.1007/s10661-006-9305-7, 2007.

Banner, F. T., Sheehan, R., and Williams, E.: The organic skeletons of rotaline foraminifera; a review, The Journal of Foraminiferal Research, 3, 30–42, doi:10.2113/gsjfr.3.1.30, 1973.

Bennett, H.: Concise chemical and technical dictionary, Chemical Pub. Co, 1986.

Bentov, S., Brownlee, C., and Erez, J.: The role of seawater endocytosis in the biomineralization process in calcareous foraminifera, Proceedings of the National Academy of Sciences, 106, 21500–21504, doi:10.1073/pnas.0906636106, 2009.

Bentov, S. and Erez, J.: Impact of biomineralization processes on the Mg content of foraminiferal shells: A biological perspective, Geochemistry, Geophysics, Geosystems, 7, doi:10.1029/2005GC001015, 2006.

Bertlich, J., Nürnberg, D., Hathorne, E. C., Nooijer, L. J. d., Mezger, E. M., Kienast, M., Nordhausen, S., Reichart, G.-J., Schönfeld, J., and Bijma, J.: Salinity control on Na incorporation into calcite tests of the planktonic foraminifera *Trilobatus sacculifer*–evidence from culture experiments and surface sediments, Biogeosciences, 15, 5991–6018, doi:10.5194/bg-15-5991-2018, 2018.

Bertram, C. J., Elderfield, H., Shackleton, N. J., and MacDonald, J. A.: Cadmium/calcium and carbon isotope reconstructions of the glacial northeast Atlantic Ocean, Paleoceanography, 10, 563–578, doi:10.1029/94PA03058, 1995.

Bielmyer-Fraser, G. K., Patel, P., Capo, T., and Grosell, M.: Physiological responses of corals to ocean acidification and copper exposure, Marine Pollution Bulletin, 133, 781–790, doi:10.1016/j.marpolbul.2018.06.048, 2018.

Birarda, G., Buosi, C., Caridi, F., Casu, M. A., Giudici, G. de, Di Bella, L., Medas, D., Meneghini, C., Pierdomenico, M., and Sabbatini, A.: Plastics,(bio) polymers and their apparent biogeochemical cycle: An infrared spectroscopy study on foraminifera, Environmental Pollution, 279, 116912, doi:10.1016/j.envpol.2021.116912, 2021.

Boyle, E. A. and Keigwin, L. D.: Deep circulation of the North Atlantic over the last 200,000 years: Geochemical evidence, Science, 218, 784–787, doi:10.1126/science.218.4574.784, 1982.

Bradl, H.: Heavy metals in the environment: Origin, interaction and remediation, Elsevier, 2005.

Branson, O., Redfern, S. A. T., Tyliszczak, T., Sadekov, A., Langer, G., Kimoto, K., and Elderfield, H.: The coordination of Mg in foraminiferal calcite, Earth and Planetary Science Letters, 383, 134–141, doi:10.1016/j.epsl.2013.09.037, 2013.

Brown, B. E., Tudhope, A. W., Le Tissier, M. D.A., and Scoffin, T. P.: A novel mechanism for iron incorporation into coral skeletons, Coral Reefs, 10, 211–215, doi:10.1007/BF00336776, 1991.

Bryan, S. P. and Marchitto, T. M.: Testing the utility of paleonutrient proxies Cd/Ca and Zn/Ca in benthic foraminifera from thermocline waters, Geochemistry, Geophysics, Geosystems, 11, doi:10.1029/2009GC002780, 2010.

Cardini, U.: Dinitrogen fixation in coral reef ecosystems facing climate change, Staats-und Universitätsbibliothek Bremen, 2015.

Carnahan, E. A., Hoare, A. M., Hallock, P., Lidz, B. H., and Reich, C. D.: Distribution of heavy metals and foraminiferal assemblages in sediments of Biscayne Bay, Florida, USA, Journal of Coastal Research, 24, 159–169, doi:10.2112/06-0666.1, 2008.

Chevalier, J.-P.: Ordre des Scléractiniaires., Doumenc D (ed) Cnidaires Anthozoaires. Masson, Paris, pp 403–764, 1987.

Clarke, H., D'Olivo, J. P., Falter, J., Zinke, J., Lowe, R., and McCulloch, M.: Differential response of corals to regional mass-warming events as evident from skeletal Sr/Ca and Mg/Ca ratios, Geochemistry, Geophysics, Geosystems, 18, 1794–1809, doi:10.1002/2016GC006788, 2017.

Cohen, A. L. and McConnaughey, T. A.: Geochemical perspectives on coral mineralization, Reviews in Mineralogy and Geochemistry, 54, 151–187, doi:10.2113/0540151, 2003.

Cuif, J.-P. and Dauphin, Y.: The two-step mode of growth in the scleractinian coral skeletons from the micrometre to the overall scale, Journal of Structural Biology, 150, 319–331, doi:10.1016/j.jsb.2005.03.004, 2005.

Cuif, J.-P., Dauphin, Y., Berthet, P., and Jegoudez, J.: Associated water and organic compounds in coral skeletons: Quantitative thermogravimetry coupled to infrared absorption spectrometry, Geochemistry, Geophysics, Geosystems, 5, doi:10.1029/2004GC000783, 2004.

Darmono: Lingkungan Hidup dan Pencemaran., Jakarta: UI Press, 2001.

Das, S., Patnaik, S. C., Sahu, H. K., Chakraborty, A., Sudarshan, M., and Thatoi, H. N.: Heavy metal contamination, physico-chemical and microbial evaluation of water samples collected from chromite mine environment of Sukinda, India, Transactions of Nonferrous Metals Society of China, 23, 484–493, doi:10.1016/S1003-6326(13)62489-9, 2013.

David, C. P.: Heavy metal concentrations in growth bands of corals: A record of mine tailings input through time (Marinduque Island, Philippines), Marine Pollution Bulletin, 46, 187–196, doi:10.1016/S0025-326X(02)00315-6, 2003.

Delaney, M. L., Bé, A. W. H., and Boyle, E. A.: Li, Sr, Mg, and Na in foraminiferal calcite shells from laboratory culture, sediment traps, and sediment cores, Geochimica et Cosmochimica Acta, 49, 1327–1341, doi:10.1016/0016-7037(85)90284-4, 1985.

Diagomanolin, V., Farhang, M., Ghazi-Khansari, M., and Jafarzadeh, N.: Heavy metals (Ni, Cr, Cu) in the karoon waterway river, Iran, Toxicology Letters, 151, 63–67, doi:10.1016/j.toxlet.2004.02.018, 2004.

Duffus, J. H.: " Heavy metals" a meaningless term? (IUPAC Technical Report), Pure and Applied Chemistry, 74, 793–807, doi:10.1351/pac200274050793, 2002.

El-Sorogy, A. S., Mohamed, M. A., and Nour, H. E.: Heavy metals contamination of the Quaternary coral reefs, Red Sea coast, Egypt, Environmental Earth Sciences, 67, 777–785, doi:10.1007/s12665-012-1535-0, 2012.

Erez, J.: The source of ions for biomineralization in foraminifera and their implications for paleoceanographic proxies, Reviews in Mineralogy and Geochemistry, 54, 115–149, doi:10.2113/0540115, 2003.

Esslemont, G.: Heavy metals in corals from Heron Island and Darwin harbour, Australia, Marine Pollution Bulletin, 38, 1052–1054, doi:10.1016/S0025-326X(99)00183-6, 1999.

Esslemont, G.: Heavy metals in seawater, marine sediments and corals from the Townsville section, Great Barrier Reef Marine Park, Queensland, Marine Chemistry, 71, 215–231, doi:10.1016/S0304-4203(00)00050-5, 2000.

Fautin, D. G. and Mariscal, R.N.: Cnidaria: Anthozoa., Harrison FW, Westfall JA (eds) Placozoa, Porifera, Cnidaria, and Ctenophora. Wiley-Liss, New York, pp 267–358, 1991.

Ferraro, L., Sprovieri, M., Alberico, I., Lirer, F., Prevedello, L., and Marsella, E.: Benthic foraminifera and heavy metals distribution: A case study from the Naples Harbour (Tyrrhenian Sea, Southern Italy), Environmental Pollution, 142, 274–287, doi:10.1016/j.envpol.2005.10.026, 2006.

Filipsson, H. L., Bernhard, J. M., Lincoln, S. A., and McCorkle, D. C.: A culture-based calibration of benthic foraminiferal paleotemperature proxies: Δ^{18}O and Mg/Ca results, Biogeosciences, 7, 1335–1347, doi:10.5194/bg-7-1335-2010, 2010.

Gagnon, A. C., Adkins, J. F., and Erez, J.: Seawater transport during coral biomineralization, Earth and Planetary Science Letters, 329, 150–161, doi:10.1016/j.epsl.2012.03.005, 2012.

Galloway, S. B., Woodley, C. M., McLaughlin, S. M., Work, T. M., Bochsler, V. S., Meteyer, C. U., Sileo, L., Peters, E. C., Kramarsky-Winters, E., and Morado, J. F.: Coral disease and health workshop: Coral histopathology II, National Oceanic and Atmospheric Administration, 2007.

Geerken, E., Nooijer, L. J. de, Roepert, A., Polerecky, L., King, H. E., and Reichart, G. J.: Element banding and organic linings within chamber walls of two benthic foraminifera, Scientific Reports, 9, 1–15, doi:10.1038/s41598-019-40298-y, 2019.

Gervais, P.: Sur un point de la Physiologie des Foraminifères, Comptes rendus hebdomadaires de l'Académie des Sciences, 25, 467–468, 1847.

Glas, M. S., Langer, G., and Keul, N.: Calcification acidifies the microenvironment of a benthic foraminifer (*Ammonia sp.*), Journal of Experimental Marine Biology and Ecology, 424, 53–58, doi:10.1016/j.jembe.2012.05.006, 2012.

Goreau, T. J.: Coral skeletal chemistry: Physiological and environmental regulation of stable isotopes and trace metals in *Montastrea annularis*, Proceedings of the Royal Society of London. Series B. Biological Sciences, 196, 291–315, doi:10.1098/rspb.1977.0042, 1977.

Groeneveld, J. and Filipsson, H. L.: Mg/Ca and Mn/Ca ratios in benthic foraminifera: The potential to reconstruct past variations in temperature and hypoxia in shelf regions, Biogeosciences, 10, 5125–5138, doi:10.5194/bg-10-5125-2013, 2013.

Guo, X., Xu, B., Burnett, W. C., Yu, Z., Yang, S., Huang, X., Wang, F., Nan, H., Yao, P., and Sun, F.: A potential proxy for seasonal hypoxia: LA-ICP-MS Mn/Ca ratios in benthic foraminifera from the Yangtze River Estuary, Geochimica et Cosmochimica Acta, 245, 290–303, doi:10.1016/j.gca.2018.11.007, 2019.

Guzmán, H. M. and Jiménez, C. E.: Contamination of coral reefs by heavy metals along the Caribbean coast of Central America (Costa Rica and Panama), Marine Pollution Bulletin, 24, 554–561, doi:10.1016/0025-326X(92)90708-E, 1992.

Hall, N. M., Berry, K. L.E., Rintoul, L., and Hoogenboom, M. O.: Microplastic ingestion by scleractinian corals, Marine Biology, 162, 725–732, doi:10.1007/s00227-015-2619-7, 2015.

Han, M., Zhang, R., Yu, K., Li, A., Wang, Y., and Huang, X.: Polycyclic aromatic hydrocarbons (PAHs) in corals of the South China Sea: Occurrence, distribution, bioaccumulation, and considerable role of coral mucus, Journal of Hazardous Materials, 384, 121299, doi:10.1016/j.jhazmat.2019.121299, 2020.

Hanna, R. G. and Muir, G. L.: Red Sea corals as biomonitors of trace metal pollution, Environmental Monitoring and Assessment, 14, 211–222, doi:10.1007/BF00677917, 1990.

Hayward, B. W., Holzmann, M., Grenfell, H. R., Pawlowski, J., and Triggs, C. M.: Morphological distinction of molecular types in *Ammonia*–towards a taxonomic revision of the world's most commonly misidentified foraminifera, Marine Micropaleontology, 50, 237–271, doi:10.1016/S0377-8398(03)00074-4, 2004.

Heider, A. von: Die Gattung *Cladocora* Ehrenb., Ehrenb. Sber Akad Wiss Wien, 84:634–637, 1881.

Hemleben, C. H., Erson, O. R., Berthold, W., and Spindler, M.: Calcification and chamber formation in Foraminifera-a brief overview, Biomineralization in lower plants and animals

(BSC Leadbeater, R Riding, eds) Clarendon Press, Oxford, 237–249, doi:10.2307/1485304, 1986.

Hintz, C. J., Chandler, G. T., Bernhard, J. M., McCorkle, D. C., Havach, S. M., Blanks, J. K., and Shaw, T. J.: A physicochemically constrained seawater culturing system for production of benthic foraminifera, Limnology and Oceanography: Methods, 2, 160–170, doi:10.4319/lom.2004.2.160, 2004.

Inoue, M., Suzuki, A., Nohara, M., Kan, H., Edward, A., and Kawahata, H.: Coral skeletal tin and copper concentrations at Pohnpei, Micronesia: Possible index for marine pollution by toxic anti-biofouling paints, Environmental Pollution, 129, 399–407, doi:10.1016/j.envpol.2003.11.009, 2004.

Ishikawa, M. and Ichikuni, M.: Uptake of sodium and potassium by calcite, Chemical Geology, 42, 137–146, doi:10.1016/0009-2541(84)90010-X, 1984.

J. Falbe and M. Regitz (Eds.): Roempp Chemie-Lexikon, George Thieme, Weinheim, 1996.

Jaishankar, M., Tseten, T., Anbalagan, N., Mathew, B. B., and Beeregowda, K. N.: Toxicity, mechanism and health effects of some heavy metals, Interdisciplinary Toxicology, 7, 60, doi:10.2478/intox-2014-0009, 2014.

Jiang, W., Yu, K., Wang, N., Yang, H., Yang, H., Xu, S., Wei, C., Wang, S., and Wang, Y.: Distribution coefficients of trace metals between modern coral-lattices and seawater in the northern South China Sea: Species and SST dependencies, Journal of Asian Earth Sciences, 187, 104082, doi:10.1016/j.jseaes.2019.104082, 2020.

Kabata-Pendias, A. and Pendias, H.: Trace Elements in Soils and Plants, 3rd edn CRC Press: Boca Raton, 2001.

Kelly, A. E., Reuer, M. K., Goodkin, N. F., and Boyle, E. A.: Lead concentrations and isotopes in corals and water near Bermuda, 1780–2000, Earth and Planetary Science Letters, 283, 93–100, doi:10.1016/j.epsl.2009.03.045, 2009.

Koho, K. A., Nooijer, L. J. d., Fontanier, C., Toyofuku, T., Oguri, K., Kitazato, H., and Reichart, G.-J.: Benthic foraminiferal Mn/Ca ratios reflect microhabitat preferences, Biogeosciences, 14, 3067–3082, doi:10.5194/bg-14-3067-2017, 2017.

Kumar, S. K., Chandrasekar, N., and Seralathan, P.: Trace elements contamination in coral reef skeleton, Gulf of Mannar, India, Bulletin of Environmental Contamination and Toxicology, 84, 141, doi:10.1007/s00128-009-9905-3, 2010.

La Barnard, Macintyre, I. G., and Pierce, J. W.: Possible environmental index in tropical reef corals, Nature, 252, 219–220, doi:10.1038/252219a0, 1974.

Lea, D. W.: Trace elements in foraminiferal calcite, in: Modern foraminifera, Springer, 259–277, 1999.

Lewis, G. N.: Valence and the structure of atoms and molecules, The Chemical Catalog Company, Inc., New York, 1–172, 1923.

Lewis, S. E., Lough, J. M., Cantin, N. E., Matson, E. G., Kinsley, L., Bainbridge, Z. T., and Brodie, J. E.: A critical evaluation of coral Ba/Ca, Mn/Ca and Y/Ca ratios as indicators of terrestrial input: New data from the Great Barrier Reef, Australia, Geochimica et Cosmochimica Acta, 237, 131–154, doi:10.1016/j.gca.2018.06.017, 2018.

Li, T., Cai, G., Zhang, M., Li, S., and Nie, X.: The response of benthic foraminifera to heavy metals and grain sizes: A case study from Hainan Island, China, Marine Pollution Bulletin, 167, 112328, doi:10.1016/j.marpolbul.2021.112328, 2021.

Linshy, V. N., Rana, S. S., Kurtarkar, S., Saraswat, R., and Nigam, R.: Appraisal of laboratory culture experiments on benthic foraminifera to assess/develop paleoceanographic proxies, Indian Journal of Geo-Marine Sciences, 36(4):301-321, 2007.

Little, S. H., Wilson, D. J., Rehkämper, M., Adkins, J. F., Robinson, L. F., and van de Flierdt, T.: Cold-water corals as archives of seawater Zn and Cu isotopes, Chemical Geology, 578, 120304, doi:10.1016/j.chemgeo.2021.120304, 2021.

Marchitto, T. M. and Broecker, W. S.: Deep water mass geometry in the glacial Atlantic Ocean: A review of constraints from the paleonutrient proxy Cd/Ca, Geochemistry, Geophysics, Geosystems, 7, doi:10.1029/2006GC001323, 2006.

Marshall, J. F. and McCulloch, M. T.: An assessment of the Sr/Ca ratio in shallow water hermatypic corals as a proxy for sea surface temperature, Geochimica et Cosmochimica Acta, 66, 3263–3280, doi:10.1016/S0016-7037(02)00926-2, 2002.

Martins, V. A., Frontalini, F., Tramonte, K. M., Figueira, R. C. L., Miranda, P., Sequeira, C., Fernández-Fernández, S., Dias, J. A., Yamashita, C., and Renó, R.: Assessment of the health quality of Ria de Aveiro (Portugal): Heavy metals and benthic foraminifera, Marine Pollution Bulletin, 70, 18–33, doi:10.1016/j.marpolbul.2013.02.003, 2013.

Matthews, K. A., Grottoli, A. G., McDonough, W. F., and Palardy, J. E.: Upwelling, species, and depth effects on coral skeletal cadmium-to-calcium ratios (Cd/Ca), Geochimica et Cosmochimica Acta, 72, 4537–4550, doi:10.1016/j.gca.2008.05.064, 2008.

McGann, M.: High-resolution foraminiferal, isotopic, and trace element records from Holocene estuarine deposits of San Francisco Bay, California, Journal of Coastal Research, 24, 1092–1109, doi:10.2112/08A-0003.1, 2008.

McGeer, J. C., Szebedinszky, C., McDonald, D. G., and Wood, C. M.: Effects of chronic sublethal exposure to waterborne Cu, Cd or Zn in rainbow trout. 1: Iono-regulatory disturbance and metabolic costs, Aquatic Toxicology, 50, 231–243, doi:10.1016/S0166-445X(99)00105-8, 2000.

Mezger, E. M., Nooijer, L. J. de, Boer, W., Brummer, G. J.A., and Reichart, G. J.: Salinity controls on Na incorporation in Red Sea planktonic foraminifera, Paleoceanography, 31, 1562–1582, doi:10.1002/2016PA003052, 2016.

Mitterer, R. M.: Amino acid composition and metal binding capability of the skeletal protein of corals, Bulletin of Marine Science, 28, 173–180, 1978.

Moyer, R. P., Grottoli, A. G., and Olesik, J. W.: A multiproxy record of terrestrial inputs to the coastal ocean using minor and trace elements (Ba/Ca, Mn/Ca, Y/Ca) and carbon isotopes ($\delta^{13}C$, $\Delta^{14}C$) in a nearshore coral from Puerto Rico, Paleoceanography, 27, doi:10.1029/2011PA002249, 2012.

Murray, J. W.: Distribution and population dynamics of benthic foraminifera from the southern North Sea, Journal of Foraminiferal Research, 22, 114–128, doi:10.2113/gsjfr.22.2.114, 1992.

N. Bjerrum.: Bjerrum's Inorganic Chemistry, 3rd Danish ed., Heinemann, London, 1936.

Naser, H. A.: Assessment and management of heavy metal pollution in the marine environment of the Arabian Gulf: A review, Marine Pollution Bulletin, 72, 6–13, doi:10.1016/j.marpolbul.2013.04.030, 2013.

Natale, G. S., Basso, N. G., and Ronco, A. E.: Effect of Cr (VI) on early life stages of three species of hylid frogs (*Amphibia*, *Anura*) from South America, Environmental Toxicology:

An International Journal, 15, 509–512, doi:10.1002/1522-7278(2000)15:5<509:AID-TOX21>3.0.CO;2-S, 2000.

Nehrke, G., Keul, N., Langer, G., Nooijer, L. J. de, Bijma, J., and Meibom, A.: A new model for biomineralization and trace-element signatures of Foraminifera tests, Biogeosciences, 10, 6759–6767, doi:10.5194/bg-10-6759-2013, 2013.

Nooijer, L. J. de, Langer, G., Nehrke, G., and Bijma, J.: Physiological controls on seawater uptake and calcification in the benthic foraminifer *Ammonia tepida*, Biogeosciences, 6, 2669–2675, doi:10.5194/bg-6-2669-2009, 2009.

Nooijer, L. J. de, Toyofuku, T., Oguri, K., Nomaki, H., and Kitazato, H.: Intracellular pH distribution in foraminifera determined by the fluorescent probe HPTS, Limnology and Oceanography: Methods, 6, 610–618, doi:10.4319/lom.2008.6.610, 2008.

Nordberg, G. F., Nogawa, K., Nordberg, M., and Friedmann, J. M.: Cadmium. Handbook on the toxicology of metals, Amsterdam: Elsevier, 2007.

Nürnberg, D., Bijma, J., and Hemleben, C.: Assessing the reliability of magnesium in foraminiferal calcite as a proxy for water mass temperatures, Geochimica et Cosmochimica Acta, 60, 803–814, doi:10.1016/0016-7037(95)00446-7, 1996.

Okumura, M. and Kitano, Y.: Coprecipitation of alkali metal ions with calcium carbonate, Geochimica et Cosmochimica Acta, 50, 49–58, doi:10.1016/0016-7037(86)90047-5, 1986.

Passow, H., Rothstein, A., and Clarkson, T. W.: The general pharmacology of the heavy metals, Pharmacological Reviews, 13, 1961.

Pingitore Jr, N. E., Iglesias, A., Bruce, A., Lytle, F., and Wellington, G. M.: Valences of iron and copper in coral skeleton: X-ray absorption spectroscopy analysis, Microchemical Journal, 71, 205–210, doi:10.1016/S0026-265X(02)00012-7, 2002.

Pourret, O.: On the necessity of banning the term “heavy metal” from the scientific literature, Sustainability, 10, 2879, doi:10.3390/su10082879, 2018.

Pretet, C., Reynaud, S., Ferrier-Pages, C., Gattuso, J.-P., Kamber, B. S., and Samankassou, E.: Effect of salinity on the skeletal chemistry of cultured scleractinian zooxanthellate corals: Cd/Ca ratio as a potential proxy for salinity reconstruction, Coral Reefs, 33, 169–180, doi:10.1007/s00338-013-1098-x, 2014.

Prothro, M. G.: Office of Water policy and technical guidance on interpretation and implementation of aquatic life metals criteria, United States Environmental Protection Agency., 1993.

Puverel, S., Tambutte, E., Zoccola, D., Domart-Coulon, I., Bouchot, A., Lotto, S., Allemand, D., and Tambutte, S.: Antibodies against the organic matrix in scleractinians: A new tool to study coral biomineralization, Coral Reefs, 24, 149–156, doi:10.1007/s00338-004-0456-0, 2005.

Qu, Y., Xu, K., Li, T., Wang, M., Zhong, H., and Chen, T.: Deep-sea coral evidence for dissolved mercury evolution in the deep North Pacific Ocean over the last 700 years, Journal of Oceanology and Limnology, 39, 1622–1633, doi:10.1007/s00343-021-0474-6, 2021.

Ramos, A. A., Inoue, Y., and Ohde, S.: Metal contents in *Porites* corals: Anthropogenic input of river run-off into a coral reef from an urbanized area, Okinawa, Marine Pollution Bulletin, 48, 281–294, doi:10.1016/j.marpolbul.2003.08.003, 2004.

Rand, G. M., Wells, P. G., and McCarty, L. S.: Introduction to aquatic toxicology, Fundamentals of aquatic toxicology effects, environmental fate, and risk assessment. Taylor and Francis Publishers, North Palm Beach, Florida, USA, 3–67, doi:10.1201/9781003075363, 1995.

Reichelt-Brushett, A. J. and McOrist, G.: Trace metals in the living and nonliving components of scleractinian corals, Marine Pollution Bulletin, 46, 1573–1582, doi:10.1016/S0025-326X(03)00323-0, 2003.

Reiss, Z.E.E.V.: The *Bilamellidea*, nov. superfam., and remarks on Cretaceous *globorotaliids*, Cushman Foundation Foraminifreal Research Contribution, 8, 127–145, 1957.

Reuer, M. K., Boyle, E. A., and Cole, J. E.: A mid-twentieth century reduction in tropical upwelling inferred from coralline trace element proxies, Earth and Planetary Science Letters, 210, 437–452, doi:10.1016/S0012-821X(03)00162-6, 2003.

Richir, J. and Gobert, S.: Trace elements in marine environments: Occurrence, threats and monitoring with special focus on the Costal Mediterranean, Journal of Environmental and Analytical Toxicology, 6, doi:10.4172/2161-0525.1000349, 2016.

Rieuwerts, J. H.: Coal Mining on the Peak District's Eastern Uplands during the 16th to Early-20th Centuries, Mining History, 19, 1–49, 2015.

Rosenthal, Y., Boyle, E. A., and Labeyrie, L.: Last glacial maximum paleochemistry and deepwater circulation in the Southern Ocean: Evidence from foraminiferal cadmium, Paleoceanography, 12, 787–796, doi:10.1029/97PA02508, 1997.

Rumolo, P., Manta, D. S., Sprovieri, M., Coccioni, R., Ferraro, L., and Marsella, E.: Heavy metals in benthic foraminifera from the highly polluted sediments of the Naples harbour (Southern Tyrrhenian Sea, Italy), Science of the Total Environment, 407, 5795–5802, doi:10.1016/j.scitotenv.2009.06.050, 2009.

Sagar, N., Sadekov, A., Jenner, T., Chapuis, L., Scott, P., Choudhary, M., and McCulloch, M.: Heavy metal incorporation in foraminiferal calcite under variable environmental and acute level seawater pollution: Multi-element culture experiments for *Amphisorus hemprichii*, Environmental Science and Pollution Research, 1–14, doi:10.1007/s11356-021-15913-z, 2021a.

Sagar, N., Sadekov, A., Scott, P., Jenner, T., Vadiveloo, A., Moheimani, N. R., and McCulloch, M.: Geochemistry of large benthic foraminifera *Amphisorus hemprichii* as a high-resolution proxy for lead pollution in coastal environments, Marine Pollution Bulletin, 162, 111918, doi:10.1016/j.marpolbul.2020.111918, 2021b.

Saha, N., Webb, G. E., and Zhao, J.-X.: Coral skeletal geochemistry as a monitor of inshore water quality, Science of the Total Environment, 566, 652–684, doi:10.1016/j.scitotenv.2016.05.066, 2016.

Sayani, H. R., Thompson, D. M., Carilli, J. E., Marchitto, T. M., Chapman, A. U., and Cobb, K. M.: Reproducibility of Coral Mn/Ca-Based Wind Reconstructions at Kiritimati Island and Butaritari Atoll, Geochemistry, Geophysics, Geosystems, 22, e2020GC009398, doi:10.1029/2020GC009398, 2021.

Schultze, M.: Beobachtungen uber die Fortpflanzung der Polythalamien, Archiv für Anatomie und Physiologie., 165–173, 1856.

Shah, S. B.: Heavy Metals in Scleractinian Corals, Springer Nature, 2021.

Shannon, R. D.: Revised effective ionic radii and systematic studies of interatomic distances in halides and chalcogenides, Acta Crystallographica Section A: crystal physics, diffraction, theoretical and general crystallography, 32, 751–767, 1976.

Shen, C.-C., Lee, T., Chen, C.-Y., Wang, C.-H., Dai, C.-F., and Li, L.-A.: The calibration of D [Sr/Ca] versus sea surface temperature relationship for *Porites* corals, Geochimica et Cosmochimica Acta, 60, 3849–3858, doi:10.1016/0016-7037(96)00205-0, 1996.

Shen, G. T.: Rapid changes in the tropical ocean and the use of corals as monitoring systems., Berger A (ed) Geoindicator: assessing rapid environmental changes in earth systems. Brokfield, Rotterdam, pp 125–169, 1996.

Shen, G. T. and Boyle, E. A.: Lead in corals: Reconstruction of historical industrial fluxes to the surface ocean, Earth and Planetary Science Letters, 82, 289–304, doi:10.1016/0012-821X(87)90203-2, 1987.

Shen, G. T. and Boyle, E. A.: Determination of lead, cadmium and other trace metals in annually-banded corals, Chemical Geology, 67, 47–62, doi:10.1016/0009-2541(88)90005-8, 1988.

Shen, G. T., Boyle, E. A., and Lea, D. W.: Cadmium in corals as a tracer of historical upwelling and industrial fallout, Nature, 328, 794–796, doi:10.1038/328794a0, 1987.

Shen, G. T., Campbell, T. M., Dunbar, R. B., Wellington, G. M., Colgan, M. W., and Glynn, P. W.: Paleochemistry of manganese in corals from the Galapagos Islands, Coral Reefs, 10, 91–100, 1991.

Smith, C. W., Fehrenbacher, J. S., and Goldstein, S. T.: Incorporation of heavy metals in experimentally grown foraminifera from Sapelo Island, Georgia and Little Duck Key, Florida, USA, Marine Micropaleontology, 156, 101854, doi:10.1016/j.marmicro.2020.101854, 2020.

Stolarski, J.: Three-dimensional micro-and nanostructural characteristics of the scleractinian coral skeleton: A biocalcification proxy, Acta Palaeontologica Polonica, 48, 2003.

Tachikawa, K. and Elderfield, H.: Microhabitat effects on Cd/Ca and $\delta^{13}C$ of benthic foraminifera, Earth and Planetary Science Letters, 202, 607–624, doi:10.1016/S0012-821X(02)00796-3, 2002.

Tambutté, E., Tambutté, S., Segonds, N., Zoccola, D., Venn, A., Erez, J., and Allemand, D.: Calcein labelling and electrophysiology: Insights on coral tissue permeability and calcification, Proceedings of the Royal Society B: Biological Sciences, 279, 19–27, doi:10.1098/rspb.2011.0733, 2012.

Tambutté, S., Holcomb, M., Ferrier-Pagès, C., Reynaud, S., Tambutté, É., Zoccola, D., and Allemand, D.: Coral biomineralization: From the gene to the environment, Journal of Experimental Marine Biology and Ecology, 408, 58–78, doi:10.1016/j.jembe.2011.07.026, 2011.

Ter Kuile, B. and Erez, J.: The size and function of the internal inorganic carbon pool of the foraminifer *Amphistegina lobifera*, Marine Biology, 99, 481–487, doi:10.1007/BF00392555, 1988.

Titelboim, D., Sadekov, A., Blumenfeld, M., Almogi-Labin, A., Herut, B., Halicz, L., Benaltabet, T., Torfstein, A., Kucera, M., and Abramovich, S.: Monitoring of heavy metals in seawater using single chamber foraminiferal sclerochronology, Ecological Indicators, 120, 106931, doi:10.1016/j.ecolind.2020.106931, 2021.

Titelboim, D., Sadekov, A., Hyams-Kaphzan, O., Almogi-Labin, A., Herut, B., Kucera, M., and Abramovich, S.: Foraminiferal single chamber analyses of heavy metals as a tool for monitoring permanent and short term anthropogenic footprints, Marine Pollution Bulletin, 128, 65–71, doi:10.1016/j.marpolbul.2018.01.002, 2018.

Toyofuku, T., Matsuo, M. Y., Nooijer, L. J. de, Nagai, Y., Kawada, S., Fujita, K., Reichart, G.-J., Nomaki, H., Tsuchiya, M., and Sakaguchi, H.: Proton pumping accompanies calcification in foraminifera, Nature Communications, 8, 1–6, doi:10.1038/ncomms14145, 2017.

Wefer, G.: Umwelt, Produktion und Sedimentation benthischer Foraminiferen in der westlichen Ostsee, Reports Sonderforschungsbereich 95 Wechselwirkung Meer - Meeresboden, 14, 1–103, 1976.

Weil, S. M., Buddemeier, R. W., Smith, S. V., and Kroopnick, P. M.: The stable isotopic composition of coral skeletons: Control by environmental variables, Geochimica et Cosmochimica Acta, 45, 1147–1153, doi:10.1016/0016-7037(81)90138-1, 1981.

Wit, J. C., Nooijer, L. J. de, Wolthers, M., and Reichart, G.-J.: A novel salinity proxy based on Na incorporation into foraminiferal calcite, Biogeosciences, 10, 6375–6387, doi:10.5194/bg-10-6375-2013, 2013.

Wolf-Gladrow, D. A., Bijma, J., and Zeebe, R. E.: Model simulation of the carbonate chemistry in the microenvironment of symbiont bearing foraminifera, Marine Chemistry, 64, 181–198, doi:10.1016/S0304-4203(98)00074-7, 1999.

Woodruff, S. D., Diaz, H. F., Worley, S. J., Reynolds, R. W., and Lubker, S. J.: Early ship observational data and ICOADS, Climatic Change, 73, 169–194, doi:10.1007/s10584-005-3456-3, 2005.

Xiang, R., Yang, Z., Saito, Y., Fan, D., Chen, M., Guo, Z., and Chen, Z.: Paleoenvironmental changes during the last 8400 years in the southern Yellow Sea: Benthic foraminiferal and stable isotopic evidence, Marine Micropaleontology, 67, 104–119, doi:10.1016/j.marmicro.2007.11.002, 2008.

Yang, T., Diao, X., Cheng, H., Wang, H., Zhou, H., Zhao, H., and Chen, C. M.: Comparative study of polycyclic aromatic hydrocarbons (PAHs) and heavy metals (HMs) in corals, sediments and seawater from coral reefs of Hainan, China, Environmental Pollution, 264, 114719, doi:10.1016/j.envpol.2020.114719, 2020.

Zeebe, R. E. and Sanyal, A.: Comparison of two potential strategies of planktonic foraminifera for house building: Mg^{2+} or H^+ removal?, Geochimica et Cosmochimica Acta, 66, 1159–1169, doi:10.1016/S0016-7037(01)00852-3, 2002.

Danksagung

Zu allererst möchte ich mich bei meinen Betreuern Joachim Schönfeld, Ed Hathorne und Martin Frank bedanken. Herr Schönfeld, Sie hatten von Anfang an ein offenes Ohr, haben mir stets mit Rat und Tat zur Seite gestanden und ohne Sie wäre ich auf keinen Fall so weit gekommen. Die Zusammenarbeit mit Ihnen hat unglaublich viel Spaß gemacht und ich habe sehr viel von Ihnen gelernt. Auch die gemeinsamen Exkursionen möchte ich auf keinen Fall missen. Ed, dir möchte ich besonders für deine vielen Ideen und Einfälle und für deinen wissenschaftlichen Input danken. Du hast mich vor allem bei dem Generieren der Daten und auch bei deren Aufarbeitung maßgeblich unterstützt. Martin, dir möchte ich dafür danken, dass du dir immer Zeit genommen hast und stets versucht hast alles möglich zu machen, auch wenn du sicherlich mehr als genug anderes zu tun hättest.

Ein ganz besonderer Dank geht an Florian. Danke, dass du mich in die Welt der Aquaristik eingeführt hast und mir so viel mit dem Kultivieren der Korallen geholfen hast. Ohne dich hätten die Korallen und ich meine Zeit am GEOMAR sicherlich nicht überlebt. Die Gespräche mit dir haben mir immer den Tag versüßt und du hattest immer einen guten Rat, wenn mal etwas schiefgegangen ist.

Danke Jutta und Siggie für eure tatkräftige Unterstützung im Labor. Ihr habt immer versucht, alles möglich zu machen und habt euch kreative Lösungen für auftretende Probleme überlegt. Ohne euch wären wir im Labor auf jeden Fall verloren gewesen.

Außerdem möchte ich meinen HIWIs und Praktikanten Mats, Clara, Antina, Lena und Anja für ihre Unterstützung danken! Nadine und Dirk, vielen Dank, dass ich euer Labor für die Aufreinigung meiner Proben nutzen konnte. Jan und Matthias, danke, dass ihr mir bei den Lasermessungen am GEOMAR geholfen habt. Ana, danke, dass ich in deinem Clean Lab arbeiten durfte, als unseres geschlossen war und danke, dass wir an deiner Maschine messen durften. Regina, danke für die Messungen an der OES. Kati, danke für die Hg Messungen.

Danke auch an die Mitarbeiter der Uni Kiel. Danke Ulrike, Dieter, Karen und Angela für eure Hilfe bei den Laser Messungen und danke Wolfgang, Julia und Sebastian dafür, dass ich euer Mikroskop nutzen durfte und eine so tolle Einweisung bekommen habe. Danke Nina, dass du mich immer mit auf Ausfahrt genommen hast und mich überhaupt erst motiviert hast, mich auf diese Doktorarbeit zu bewerben.

Ein großer Dank geht an meine Kollegen, ohne die die Zeit am GEOMAR sicher langweilig geworden wäre. Vor allem die Menschen aus dem wunderbaren Flur 8C haben mich immer unterstützt und mit Klönschnack zwischendurch aufgeheitert. Vielen Dank Jacky, Steini, Lisa, Katriina, Nina, Lara, Guillaume, Peer, Timo, Yang, Georgi, Kristin, Eleni, Sascha, Meike, Steffen und Zhouling.

Danke Wiebe fürs Korrekturlesen.

Zu guter Letzt möchte ich mich bei meinen Freunden und meiner Familie bedanken. Ohne euch wäre ich nichts. Ihr seid mein Anker und seid stets zur Stelle, wann immer ich euch brauche. Ihr gebt mir Kraft und Stärke, wann immer ich sie benötige. Die Doktorzeit war weiß Gott nicht immer einfach für mich und ich musste sowohl privat also auch beruflich erhebliche Rückschläge einstecken, doch ihr habt mich immer wieder aufgefangen und mich wieder zusammengesetzt. Ein besonderer Dank gilt dabei meinen beiden besten Freunden Lara und Ivo, meinem Freund Danny, meiner Mutter Rosita, meinen Brüdern Heiko und Marco, und meinem Vater Rainer.